Bioprocess optimisation improves identity and potency of olfactory ensheathing cells for neurologic regeneration

Rachael Claire Wood

Department of Biochemical Engineering

University College London

Thesis submitted for degree of

Doctor of Philosophy

January 2018

I, Rachael C Wood, confirm that the work presented in this thesis is my own. Where information has been derived from other sources, I confirm that this has been indicated in the thesis.

Acknowledgements

I would like to take this opportunity to thank my primary supervisor Professor Ivan Wall for his assistance in helping to develop this project and for his constant advice. I would also like to thank Dr Melanie Georgiou for training me in the lab as well as her advice throughout my first year. In addition I would like to thank the Regenerative Medicine group at UCL, in particular Rana Khalife, Patricia Pérez Esteban, Gerardo Santiago Toledo and Ivano Colao for their input and companionship in the lab. I hope we sufficiently bemused anyone that walked past our lab with our crazy questions, mad dancing and office jousting competitions.

To my friends and family, both here and in New Zealand, and to the members of my hockey team, thanks for listening to my problems, complaints, celebrations and excitement over what I'm sure were the strangest things. Without my ability to rant out over these things and your amazing support, I would never be in a fit mental state to write this.

To my parents, well, what to say? Thanks for encouraging me, for sparking my curiosity, for allowing me to pursue whatever caught my imagination at the time, for visiting and taking me on adventures when I was so far away from home and of course for always letting me talk to my dog Zara on skype when it had been a long day.

Thanks have to go to ReNeuron for their permission to use their synthetic drug 4-hydroxy-tamoxifen which aids in the proliferation and ongoing immortality of the human mucosal cells. I take this opportunity to express gratitude to UCL and NZFGW for the funding that allows me to be here, carry out this research and enjoy such an incredible learning experience.

Abstract

The potential application of olfactory ensheathing cells (OECs) to spinal cord injury has been the focus of a lot of research over the past ten years. Currently there are many challenges associated with the use of these cells as a therapy. These include the inherent plasticity of the cells and the fact they are challenging to sustain in culture for prolonged periods due to poor survival and proliferation. They possess unique properties as they are able to support neuronal survival and facilitate the regeneration of severed axons and therefore overcoming these challenges would be a step towards developing a cell therapy for spinal cord injury.

Initially rat models were used to determine culture conditions that enhance the protein expression of key OEC markers p75NTR and S100β. An increase in p75NTR expression was achieved by co-culturing the primary rat OECs with a conditionally immortalised immobilised human mucosal fibroblast cell line feeder layer. OECs cultured on feeders were found to adopt a more spindle-like appearance compared with cells cultured on laminin which adopted an enlarged morphology. This morphological change is significant as spindle-shaped OECs are associated with neural regeneration function. Conditioned media collected from the human feeders resulted in an increase in Thy1.1 protein expression, an undesirable marker, with no increase in p75NTR expression and co-culture of primary OECs with mouse feeders (Ms3T3) gave similar results to co-culture with human feeders. It was determined that OECs benefit from the cell to cell contact and not necessarily trophic factors present in the media. The best culture conditions for primary rat OECs were found to be Ms3T3 feeders with DMEM/F12 Glutamax media. Testing with conditionally immortalised human OEC cell lines found contrasting results where an increase in S100β was observed when cells were cultured on laminin and lower levels of expression observed during feeder co-culture. Similarly to primary rat OECs, conditioned media from human mucosal fibroblasts was detrimental to S100β expression. The best culture conditions for human OECs were found to be laminin coated wells with DMEM/F12 Glutamax media. These data sets show that care has to be taken when translating animal models to studies with human cells as the data does not always correlate.

Studies continued to characterise optimum culture conditions for the conditionally immortalised human OEC cell line. MACS purification technology was used to remove Thy1 positive cells from the polyclonal population. Although this removal was successful, it was

found that the complete removal of Thy1 from the population does not ensure Thy1 is not present in the future population. After 5 days in culture Thy1 was being expressed in the Thy1 negative population. Time point staining determined that Thy1 turns on and off during time in culture and the removal of Triton X from the staining protocol is vital to visualising the presence of this protein. This time point study also revealed p75NTR is not a stable marker for OECs as turns off over time in culture. Further study towards understanding the role Thy1 and p75NTR take in OEC function would be beneficial to development of an OEC cell therapy for spinal cord injury.

After the identification of optimum culture conditions for enhanced p75NTR and S100β expression, co-culture with neurons was carried out in order to determine if these conditions would link to an improvement in functional support. Neurite length was measured after 5 days of co-culture and was normalised against the number of neurites and neurons, which is an established method of relating the behaviour of the neurons to functional response after implantation. It was found that conditions that related to higher expression of p75NTR and S100β (laminin coated wells, standard media, shorter time in culture) led to longer and more numerous neurites. From this it can be established that levels of p75NTR and S100β expression are good predictive tools for the extent to which OECs can support neural regeneration in culture. The next step would be to relate the expression of these markers to the myelination of neurons. Thy1 expression was not found to be related to neurite extension and purified populations of negative and positive Thy1 OECs resulted in longer neurites than the original mixed population. This could be due to lateral inhibition but further work is required to confirm this theory.

Results described in this thesis have demonstrated that caution needs to be applied when scaling rat studies to human cell work. It has also shown that the method and timing of detecting protein expression can be vital to the results observed. These are key aspects that need to be considered in order to fully characterise cell populations, especially one as variable as OECs. The methods used in this work showed an increase in p75NTR and S100β expression led to longer neurites extended from neurons. Further work should be carried out in order to fully understand the interaction between OECs and neurons and to explain the potential lateral inhibition pattern observed.

Contents

Acknowledgements 3

Abstract 4

List of Figures 9

List of Tables 12

Abbreviations 13

1.0 Introduction 15

1.1 Regenerative Medicine 15

1.1.1 Regenerative Medicine and Cell Therapy 15

1.1.2 Autologous and Allogeneic Cell Therapy 15

1.2 Spinal Cord Injury 16

1.2.1 The Spinal Cord 16

1.2.2 Anatomy of the Spinal Cord 18

1.2.3 Causes of Spinal Cord Injury 19

1.2.4 Mechanism of Spinal Cord Injury 19

1.2.5 The Glial Scar 20

1.2.6 Neural Regeneration 22

1.2.7 Axonal Myelination 23

1.2.8 Current Treatment of Spinal Cord Injury 24

1.2.9 Previous Research of Cell Therapy Options 24

1.3 Olfactory Ensheathing Cells 26

1.3.1 Olfactory Ensheathing Cells 26

1.3.2 The Olfactory Mucosa and the Olfactory Bulb 28

1.3.3 Characterisation of Olfactory Ensheathing Cells 29

1.3.4 Application of Olfactory Ensheathing Cells to Spinal Cord Injury 33

1.3.5 Successful Case Studies using Olfactory Ensheathing Cells 34

1.3.6 Challenges associated with using OECs towards Spinal Cord Repair 37

1.3.7 Aims of Study and Thesis Outline 38

2.0 Materials and Methods 40

2.1 Cell culture 40

2.1.1 Isolation of OECs from Rat 40

2.1.2 Culture of HuG418 41

2.1.3 Culture of Ms3T3 44

2.1.4 Culture of PA5 and PA7 44
2.1.5 Culture of NG108-15 45
2.2 MACS Purification 45
2.3 Cell Characterisation Techniques 46
2.3.1 Immunocytochemistry 46
2.3.2 Circularity Analysis 48
2.3.3 Flow Cytometry 48
2.4 Statistical Analysis 49
3.0 Co-culture of Olfactory Ensheathing Cells 51
3.1 Introduction 51
3.2 Aim and Hypothesis 53
3.3 Results 54
3.3.1 Rat OECs co-cultured with HuG418 OFs 54
3.3.2 Rat OECs co-cultured with conditioned media from HuG418 63
3.3.3 Rat OECs cultured with HuG418 and Ms3T3 70
3.3.4 Human PA7 co-cultured with Ms3T3 and conditioned media from HuG418 77
3.3.5 Human PA5 co-cultured with Ms3T3 and conditioned media from HuG418 82
3.4 Conclusions 87
4.0 Identity Markers and Purification of Human Olfactory Ensheathing Cell Populations 89
4.1 Introduction 89
4.2 Aim and Hypothesis 91
4.3 Results 92
4.3.1 Characterisation of PA5 Purified Populations 92
4.3.2 Expression of Identity Markers up to 48 hours in culture and under different processing techniques 100
4.3.3 Expression of Identity Markers after six days in culture 104
4.3.4 Characterisation of Purified PA5 cells after six days in culture 112
4.4 Conclusions 119
5.0 The impact of different bioprocess parameters on OEC support of neuronal function 121
5.1 Introduction 121
5.2 Aim and Hypothesis 122

5.3 Results 123
5.3.1 Functional responses of neuronal cells to OECs when cultured with difference ECM and culture media conditions 123
5.3.2 Functional response of neuronal cells to OECs with different time-dependent p75NTR expression levels 130
5.3.3 Functional response of neuronal cells to OECs with different Thy1 expression levels 136
5.3.4 Functional response of NG108-15 neurons co-cultured with OECs and conditioned media collected during high and low p75NTR expression 143
5.4 Conclusions 151
6.0 Conclusions and Future Work 153
6.1 Concluding Remarks 153
6.2 Recommendations for Future Work 155
7.0 References 159
8.0 Appendix One 175
8.1 Circularity Macro 175
8.2 Flow cytometry for LD column 175

List of Figures

Figure 1.1: MRI of the spine and spinal cord segments. 17
Figure 1.2: Schematic of the spinal cord after SCI. 21
Figure 1.3: Central and Peripheral nervous system neurons and myelination mechanism. 23
Figure 1.4: Schematic of the olfactory nervous system and location in the human body. 27
Figure 2.1: Rat mucosa dissection and treatment. 41
Figure 2.2: Overview of c-MycER^{TAM} technology. 42
Figure 3.1: Human layer characterisation. 55
Figure 3.2: Identification of OEC^{R} cells in culture. 55
Figure 3.3: Fluorescent micrographs of a cell population derived from rat olfactory mucosa cultured on laminin and a human feeder layer. 57
Figure 3.4: Yield of cells from feeder and feeder free conditions. 57
Figure 3.5: Assembled fluorescent micrograph of a cell population derived from rat olfactory mucosa cultured on a human feeder layer of olfactory fibroblasts. 59
Figure 3.6: Input and output of ImageJ using the circularity macro. 61
Figure 3.7: Circularity analysis on S100β positive cells when OEC^{R}s were cultured on laminin and feeders. 62
Figure 3.8: Identification of OEC^{R} cells culture in conditioned media. 64
Figure 3.9: Fluorescent micrographs of a cell population from rat olfactory mucosa cultured on laminin and a human feeder layer with and without HuG418 CM. 66
Figure 3.10: S100β fluorescent micrographs of a cell population from rat olfactory mucosa cultured on laminin and a human feeder layer with and without HuG418 CM. 67
Figure 3.11: Cell counts conducted on wells stained with p75NTR/Thy1.1 and S100β/α-SMA in the presence of CM. 67
Figure 3.12: Circularity of S100β positive cells cultured on laminin with CM (A), laminin (B), feeders with CM (C) and feeders (D). 69
Figure 3.13: Mouse feeder (Ms3T3) layer characterisation. 71
Figure 3.14: Identification of OEC^{R} cells in feeder culture. 71
Figure 3.15: Fluorescent micrographs of a cell population derived from rat olfactory mucosa cultured on HuG418 and Ms3T3. 74
Figure 3.16: Purity and yield of cells grown on human and mouse feeders. 74
Figure 3.17: Comparison of S100β antibodies. 75
Figure 3.18: Circularity analysis on S100β positive cells when OEC^{R}s were cultured on human and mouse feeders. 76
Figure 3.19: Bright field micrographs of PA7 cells plated on Ms3T3 feeders, PLL and laminin. 79
Figure 3.20: Fluorescent micrographs of PA7 cells cultured on laminin, PLL and Ms3T3 feeders with either standard media (+/- NT-3) or CM (+/- NT-3). 81
Figure 3.21: PA7 cell counts conducted on wells stained for S100β on different matrices under different media conditions. 82
Figure 3.22: Bright field micrographs of PA5 cells plated on Ms3T3 feeders, PLL and laminin. 84
Figure 3.23: Fluorescent micrographs of PA5 cells cultured on laminin, PLL and Ms3T3 feeders with either standard media (+/- NT-3) or CM (+/- NT-3). 86

Figure 3.24: PA5 cell counts conducted on wells stained for S100β on different matrices under different media conditions. 87
Figure 4.1: MACS purification process. 93
Figure 4.2: Flow cytometry graph output from BD Accuri™ C6 flow cytometer. 95
Figure 4.3: Fluorescent micrographs characterising of pre- and post- purification populations. 97
Figure 4.4: Quantification of MACS purification characterisation. 98
Figure 4.5: p75NTR circularity of MACS purification populations. 99
Figure 4.6: Fluorescent micrographs of the time point staining of PA5 cell population. 103
Figure 4.7: Quantification of p75NTR protein expression. 103
Figure 4.8: Quantification of Thy1 protein expression. 104
Figure 4.9: Fluorescent micrographs of time point staining of PA5 cell population after MACS purification. 107
Figure 4.10: Quantification of time point characterisation of MACS purified PA5 population protein expression. 108
Figure 4.11: Quantification of time point characterisation of purified PA5 population yield. 109
Figure 4.12: p75NTR circularity of time point MACS purification populations. 111
Figure 4.13: Fluorescent micrographs of extended time point staining of PA5 cell population after MACS purification. 115
Figure 4.14: Quantification of extended time point p75NTR staining of MACS PA5 purification. 116
Figure 4.15: Quantification of extended time point Thy1 staining of MACS PA5 purification. 117
Figure 4.16: Quantification of extended time point S100β staining of MACS PA5 purification. 117
Figure 4.17: Cell circularity of MACS purified populations during extended culture. 119
Figure 5.1: Fluorescent micrographs of OECs cultured in isolation for 5 days. 124
Figure 5.2: Quantification of S100β positive cells at day 5 on OEC only conditions. 124
Figure 5.3: Phase contrast images of OECs and NG108-15s cultured in different matrix and media conditions 125
Figure 5.4: Fluorescent micrographs of NG108-15 cells grown on laminin and Ms3T3 feeders with either standard media or conditioned media. 127
Figure 5.5: Quantification of neurites and neurons in OEC co-culture on laminin and Ms3T3 feeders with standard and CM. 128
Figure 5.6: Fluorescent micrographs validating p75NTR expression over time. 131
Figure 5.7: Quantification of p75NTR positive cells at 24 hours and 5 days for OEC only conditions. 131
Figure 5.8: Phase contrast images of OECs and NG108-15s cultured at different levels of p75NTR expression. 132
Figure 5.9: Fluorescent micrographs of NG108-15 cells grown on OECs at different levels of p75NTR expression. 134
Figure 5.10: Quantification of NG108-15 neurites and neuron number cultured on OECs at different levels of p75NTR expression. 135
Figure 5.11: Fluorescent micrographs validating the MACS purification process. 138

Figure 5.12: Quantification of Thy1 staining before and after MACS purification. 138
Figure 5.13: Phase contrast images of OECs and NG108-15s cultured on OECs before and after purification process. 139
Figure 5.14: Fluorescent micrographs of NG108-15 cells grown on OECs before and after purification process. 141
Figure 5.15: Quantification of NG108-15 cells cultured on OECs before and after purification process. 142
Figure 5.16: Fluorescent micrographs validating p75NTR expression over time. 144
Figure 5.17: Quantification of p75NTR positive cells at 24 hours and day 5 on OEC only conditions. 145
Figure 5.18: Phase contrast images of OECs and NG108-15s cultured at different levels of p75NTR expression in different media conditions. 146
Figure 5.19: Fluorescent micrographs of NG108-15 cells grown on OECs at different levels of p75NTR expression in different media conditions. 148
Figure 5.20: Quantification of NG108-15 neurites and neuron number cultured on OECs at different levels of p75NTR expression in different media conditions. 149
Figure A8.1: Flow cytometry graph output from BD Accuri™ C6 flow cytometer from purification with LD column. 176

List of Tables

Table 1-1: Summary of commonly used OEC markers. 29
Table 2-1: Specificity of primary antibodies 47

Abbreviations

4-OHT	4-hydroxy-tamoxifen
A	Area
α	Significance level (statistical tests)
α-SMA	Smooth muscle actin
ASIA	American Spinal Injury Association
BBB	Basso Beattie Breshnahan Score (measure of locomotor behaviour)
BDNF	Brain Derived Neurotrophic Factor
CM	Conditioned Media
CNS	Central Nervous System
DAPI	4',6-diamidino-2-phenylindole
DMEM	Dulbecco's Modified Eagles Medium
DMSO	Dimethyl sulfoxide
E	Eluted (Thy1.1 negative) fraction from MACS purification process
ECM	Extracellular Matrix
EDTA	Ethylenediaminetetra acetic acid
FBS	Fetal Bovine Serum
FGF2	Fibroblast growth factor 2
Fn	Fibronectin
GFAP	Glial Fibrillary Acidic Protein
HBSS	Hanks Balanced Salt Solution
hES	Human Embryonic stem cells
hMSCs	Human Mesenchymal Stem Cells
HuG418	Olfactory fibroblast cell line derived from the human mucosa
ICC	Immunocytochemistry
M	Molar
MACS	Magnetic Activated Cell Sorting
mES	Mouse embryonic stem cells
MMC	Mitomycin C
MRI	Magnetic Resonance Image
Ms3T3	Embryonically derived mouse fibroblast cell line
NGF	Nerve Growth Factor
NSCs	Neural Stem Cells

NT-3	Neurotrophin-3
NTR	Neurotrophin Receptor
OB	Olfactory Bulb
OB-OECs	Olfactory Ensheathing Cells isolated from the olfactory bulb
OECs	Olfactory Ensheathing Cells
OEC^{H}	Human Olfactory Ensheathing Cells
OEC^{R}	Rat Olfactory Ensheathing Cells
OFs	Olfactory Fibroblasts
OM	Olfactory Mucosa
OM-OECs	Olfactory Ensheathing Cells isolated from the olfactory mucosa
OPs	Oligodendrocyte Progenitors
P	Perimeter
PA5	Olfactory ensheathing cell line derived from the human mucosa
PA7	Olfactory ensheathing cell line derived from the human mucosa
PBS	Phosphate Buffered Saline
PLGA	poly(D,L-lactide-co-glycolide)
PLL	Poly-L-lysine
PFA	Paraformaldehyde
PNS	Peripheral Nervous System
PP	Pre-purification fraction in the MACS purification process
P/S	Penicillin/Streptomycin
R	Retained (Thy1.1 positive) fraction from MACS purification process
RT	Room temperature
SCs	Schwann Cells
SCI	Spinal Cord Injury
SEM	Standard Error of the Mean
Std	Standard Media (DMEM/F12, GlutaMAX^{TM}-I, 2%FBS, 1% P/S)
T25	Tissue culture flask with 25cm^2 surface area
T75	Tissue culture flask with 75cm^2 surface area
TE	Trypsin/EDTA solution
Thy1	Thymocyte antigen
Thy1.1	Thymocyte antigen subtype 1

1.0 Introduction

1.1 Regenerative Medicine

1.1.1 Regenerative Medicine and Cell Therapy

Regenerative medicine is an emerging discipline in the field of biomedicine. It is defined as 'using human genes, proteins and cells to regrow, restore or provide mechanical replacements for tissues that have been injured by trauma, damaged by disease or worn by time' (Mironov et al., 2004). It provides a platform that allows scientists to direct tissue healing processes (Holzapfel et al., 2016). Cells are taken from a donor/patient and treated with appropriate biological processes to ensure the cells can carry out the appropriate function in the body. These fully functioning cells are transplanted into patients and help the body repair damage (Mironov et al., 2004).

1.1.2 Autologous and Allogeneic Cell Therapy

Cell therapy comes in two varieties; autologous and allogeneic. Autologous cell therapy is a treatment method where cells are biopsied from and implanted into the same patient. As the patients' own cells are used, immunosuppression is not required. Cells can be taken from the patient, treated as necessary and expanded before implantation. This is only a viable option when time is not a limiting factor and there is a low variability in the cell sample (Dodson and Levine, 2015). These conditions are necessary as time is needed to biopsy, treat and expand the cells before implantation. A high variability in cell sample results in a lower cell yield of desirable cells and therefore a longer expansion time is required and potentially more purification steps. Variability in the yield of desirable cells has a significant impact on the commercial potential of a cell therapy and can prevent it reaching the clinic (Dodson and Levine, 2015).

Allogeneic cell therapy occurs when the implanted cells come from a different donor. This comes with immunosuppression requirements, but still allows the body to heal itself. It is normally a precursor therapy to autologous therapy as further research and work can allow an autologous therapy to be developed. Allogeneic therapy is more likely to be used when

time is critical and the cells are not able to proliferate sufficiently within the necessary time frame (Dodson and Levine, 2015).

In order to achieve a successful cell therapy transfer to the clinic, the cells need to be obtained in sufficient numbers for transplantation to the patient. This can be more of a challenge in autologous therapy as only one patient sample can be taken and there can be variability in patient sampling. The method of obtaining the cells must be safe, reliable and reproducible (Barnett and Riddell, 2004). These are key challenges that need to be addressed.

This thesis uses the principles of regenerative medicine towards developing an allogeneic cell therapy for spinal cord repair.

1.2 Spinal Cord Injury

1.2.1 The Spinal Cord

The spinal cord is formed of long, thin bundles of nervous tissue and support cells that extend from the brain to the lumbar, but not as far as the coccyx (Figure 1.1). This is due to the vertebral column growing faster than the spinal cord. The spinal cord segments have the same names as the vertebrae (cervical, thoracic, sacrum, lumbar and coccyx); however, they do not line up with the equivalent vertebrae due to this length difference (Watson et al., 2008).

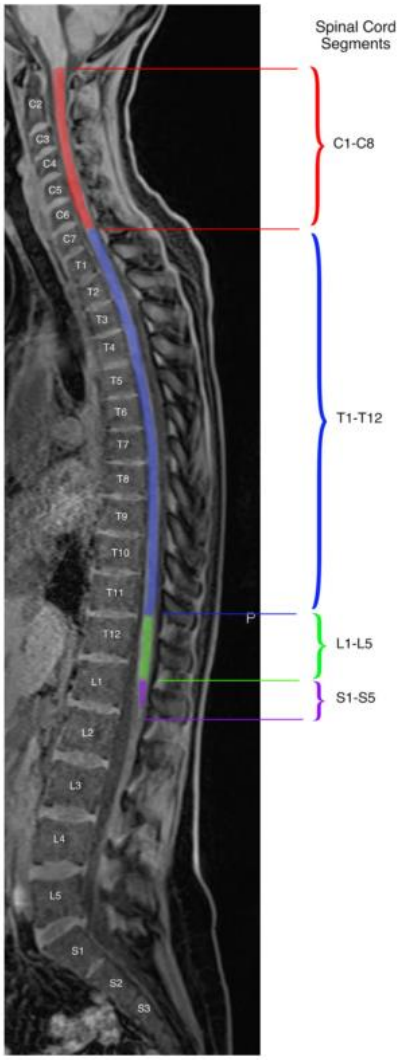

Figure 1.1: MRI of the spine and spinal cord segments. This figure shows the length of the spinal cord compared to the spinal column. Although the spinal cord and column have the same segments, these do not line up with each other due to the differences in growth speeds. C - cervical, T - thoracic, L- lumbar, S - sacrum. Image credit: Diaz and Morales, 2016.

Along with the brain, the spinal cord makes up the central nervous system (CNS), which is responsible for the transmission of nerve signals throughout the body. It is enclosed by the vertebrae which protects the fragile spinal cord from injury (Watson et al., 2008, O'Malley et al., 2014). The spinal nerves transmit sensory information from the target organs to the CNS and sends motor commands from the CNS to muscles and target organs. This information can be anything from movement commands to the awareness of touch and pain. The nerve rootlets that emerge from the spinal cord are bundled together so that each segment of the spinal cord releases a pair of spinal nerves into the peripheral nervous system (PNS) (Watson et al., 2008).

1.2.2 Anatomy of the Spinal Cord

There are 31 pairs of spinal nerves in the spinal cord and each segment (with the exception of C1, as seen in Figure 1.1) has ventral and dorsal nerve roots. The fundamental difference between the two roots is that ventral roots contain motor fibres and the dorsal roots contain sensory fibres. These spinal nerves leave the spinal cord and enter the PNS to communicate with the body (Watson et al., 2008).

The spinal cord is made up of white and grey matter. Neurons in the white matter are surrounded by myelin sheaths and fat which gives it its name. Grey matter on the other hand does not have this surrounding support, hence why it is a different colour. The white and grey matter can be divided anatomically or functionally (Diaz and Morales, 2016).

Functionally, the white matter comprises of ascending, descending and propriospinal pathways (Diaz and Morales, 2016) and is made up of axons, blood vessels, neuronal cell bodies, dendrites and glial cells (Watson et al., 2008). A pathway is a group of tracts with related functions, and a tract is a term given to nerve fibre bundles that have the same origin, course, terminations and function (Watson et al., 2008). The propriospinal pathway contains a significant part of the white matter (Diaz and Morales, 2016) and connects the spinal cord segments together (Watson et al., 2008). The descending tracts include the corticospinal, vestibulospinal, tectospinal and reticulospinal tracts. The largest of these is the corticospinal tract, which is made up of over one million axons. The ascending tracts include the spinothalamic, spinocerebellar and spinotectal tracts. They also include the posterior and anterolateral columns which are responsible for conveying proprioceptive, tactile and vibratory information. The most clinically relevant ascending tract is the spinothalamic tract, which conveys non-discriminative touch and pressure sensations (ventral) and pain and temperature sensations (dorsal) (Diaz and Morales, 2016).

The grey matter is made up of neuronal cell bodies, dendrites, axons and glial cells (Watson et al., 2008). It is divided into dorsal and ventral horns with an intermediate grey layer. The grey matter comprises of 10 cell layers in humans. This starts with the dorsal apex (Lamina 1) and goes up to the ventral apex (Lamina 10) (Diaz and Morales, 2016). The ventral horn carries motor information, the dorsal carries sensory information and the intermediate grey layer is responsible for autonomic functions (Diaz and Morales, 2016).

1.2.3 Causes of Spinal Cord Injury

1,200 people are diagnosed with a new spinal cord injury (SCI) in the United Kingdom each year, which translates to someone becoming paralysed every eight hours (Apparelyzed, 2015). SCI is most commonly caused by motor accidents (37%), awkward falls (42%) and violent injuries (National Spinal Cord Injury Center, 2006, Apparelyzed, 2015, Barnett and Riddell, 2007) and the majority of patients will suffer partial or complete paralysis (Willerth and Sakiyama-Elbert, 2008). 55% of SCI incidents in the UK occur in 18-30 year olds and 80% of sufferers are male (Apparelyzed, 2015).

Paralysis extends further than the ability to move limbs. It can affect the ability to breathe if the spinal cord is severed above the third cervical segment which can interrupt the continuity of the bulbospinal respiratory pathways. This means assisted ventilation is required for the rest of the patient's life, which can have a serious effect on quality of life (Li et al., 2003a). Additionally, patients can suffer from chronic neuropathic pain syndromes which can include depression, drug abuse and self-harm (Gwak et al., 2012).

1.2.4 Mechanism of Spinal Cord Injury

SCI normally occurs when the spinal column suffers impact that produces a contusion injury. The mechanism is a very complex process. Pressure from broken bones, fragments and swelling forces the spinal column to become displaced (Watson et al., 2008). SCI occurs in a biphasic pattern, comprising of primary and secondary damage mechanisms that remain active from days to weeks after the initial injury (Bramlett and Dietrich, 2007, Ahuja et al., 2017).

Primary damage consists of the initial impact, the continual compression, and shear damage in the injury area (Bramlett and Dietrich, 2007, Sekhon and Fehlings, 2001). Cells die at the injury site including neurons, astrocytes, oligodendrocytes and endothelial cells. This results in haemorrhaging, which disrupts the oxygen and nutrient supply to the damaged area which hampers repair (Hagg and Oudega, 2006, Franssen et al., 2007). The initial damage is followed by secondary damage, which can last months and even years after the injury (Bramlett and Dietrich, 2007). This secondary damage is an expansion of the haemorrhage front which leads to an expanding wave of further degeneration and cell death (Hagg and Oudega, 2006, Ramer et al., 2005). Due to the cellular membrane damage,

metabolic abnormalities and a shift in electrolyte ions occur. In addition, free radicals and edemas are formed. This leads to the destruction of grey and white matter around the injury site (Bramlett and Dietrich, 2007, Ahuja et al., 2017). This wave of secondary damage spreads radially and longitudinally around the injury site, so the ability to tackle the damage as early as possible is vital.

After a CNS injury, the axons attempt to regrow and reconnect, but are largely unsuccessful in finding their targets (Fraher, 2000). This is attributed to the presence of the glial scar. Even if a reconnection is made, it is difficult to determine whether the regrowing axons are truly regenerating axons, spared axons or collated sprouts from spared tracts unless the spinal cord was completely transected (Franssen et al., 2007).

1.2.5 The Glial Scar

The trauma that causes the injury in SCI breaches the barrier between the CNS and the rest of the body, as well as injuring cells and inducing swelling. The injured cells release toxins, which cause the cells above and below the injury to become apoptotic. The CNS breach eventually heals and the scar that forms is called the glial scar. This scar is the main impediment to spontaneous regeneration as the axons that do sprout and re-grow are unable to path-find through the scar to reach their target (Fawcett and Asher, 1999, Ronaghi et al., 2010, Kigerl et al., 2014, Yang et al., 2014, Fraher, 2000).

The glial scar is formed by an immune response. Its primary function is to restore the blood-CNS barrier and is mainly comprised of reactive astrocytes (Carwardine et al., 2016). When the CNS barrier is breached, cells that are normally excluded, enter the CNS and the presence of these 'foreign' cells triggers an immune response (Ronaghi et al., 2010, Ge et al., 2016). As part of this response, astrocytes in the lesion site proliferate in order to restore the CNS barrier (Ronaghi et al., 2010, Kigerl et al., 2014), which is a life-saving response to prevent further damage from the invading cells (Wu et al., 2013b, Boyd et al., 2005). This comes at the price of irreversible damage to the spinal cord (Ronaghi et al., 2010, Rodriguez et al., 2014, Raisman and Li, 2007) and is visualised in Figure 1.2 (Thuret et al., 2006). The glial scar prevents any resprouting from reaching its intended target (Thuret et al., 2006).

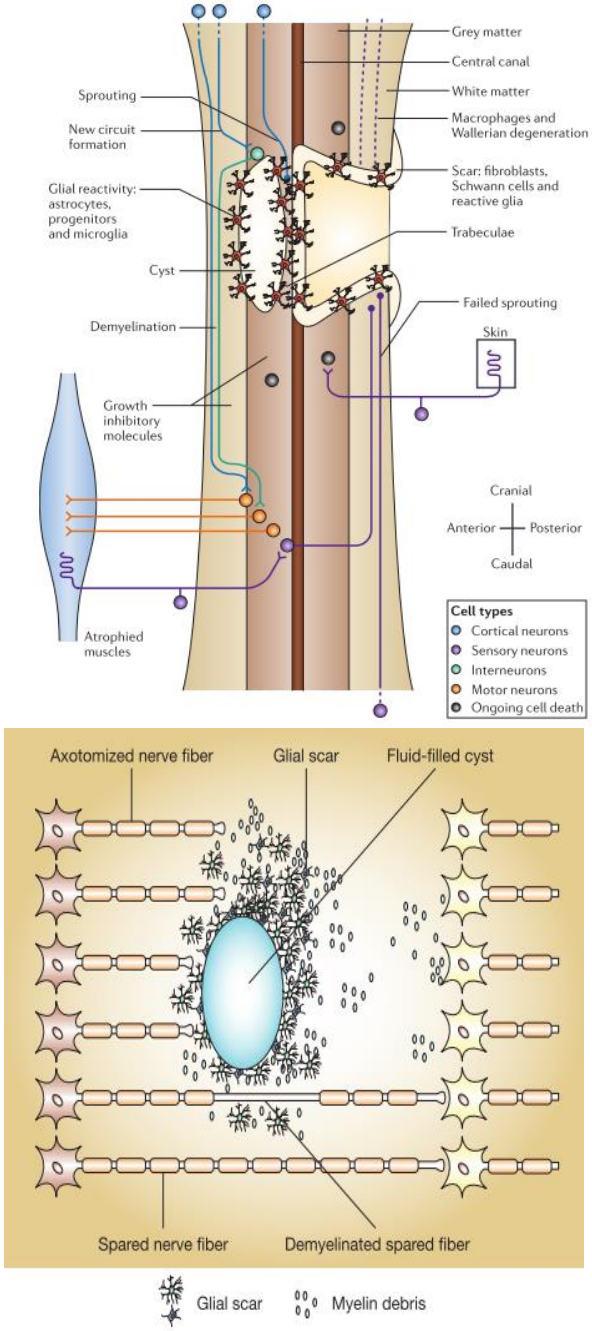

Figure 1.2: Schematic of the spinal cord after SCI. The glial scar is shown and demonstrates how it prevents resprouting. Some resprouting can occur but the glial scar prevents any neurons from getting through to their target. Image credit: (Thuret et al., 2006, Barnett and Riddell, 2007).

Studies have been conducted to determine the role of dysfunctional astrocytes, which are the main cell type that makes up the glial scar. It has been demonstrated that, when the astrocytes were unable to respond to the CNS injury, there was a significant increase in leukocytes, a failure to repair the blood-CNS barrier, and an increase in demyelination (Bush et al., 1999, Sofroniew, 2005). An increase in demyelination is undesirable because the myelin protects the nerve fibres and allows for the transmission of nerve signals (Bush

et al., 1999). Although the reactive astrocytes are able to restore the barrier, they do so at the expense of nerve regeneration. Reactive astrocytes have been shown to generate molecules with cytotoxic potential (reactive oxygen species), which damages local neural cells. However, they have also been shown to regulate inflammation after CNS injury (Bush et al., 1999). The factors that prompts them to become 'reactive' and whether they express beneficial or harmful signals is not fully understood (Sofroniew, 2005). Until their action can be understood, preventing astrocytes from forming the glial scar is not recommended as a course of action for spinal cord repair.

In addition to the barrier provided by the glial scar, it is postulated that the environment is unfavourable for nerve regeneration. Not only is the environment full of inhibitory molecules from the myelin debris, including necrosis and apoptosis signalling (Barnett and Riddell, 2007, Ramer et al., 2005, Carwardine et al., 2016, Ahuja et al., 2017), there is also a lack of sufficient blood supply that is required to provide nutrients to the injury site and enable the clearance of debris (Franssen et al., 2007). It is possible that if this environment is able to be changed, for example by introducing a cell type that expresses neurotrophic factors or stimulate regeneration, regeneration may be able to occur (Ramer et al., 2005).

Regenerating the CNS is a complex process (Barnett and Chang, 2004, Jin et al., 2002). Uninjured neurons must be present in the spinal cord that are capable of proliferation and therefore regeneration. Secondly, the damaged axons must be able to regenerate and reach their original neuronal target. Finally, these axons must be re-myelinated and able to re-establish the functional synapses (Yang et al., 2014).

1.2.6 Neural Regeneration

When nerves are severed they extend axons to reconnect to their original targets. In the PNS, this process is successfully aided by Schwann cells and function is normally restored (Hao and Collins, 2017). In the case of the CNS, the glial scar prevents any reconnection from occurring (Raisman and Li, 2007, Sakamoto and Kadomatsu).

Under normal conditions, neurons extend long axons to connect with their targets (Doron-Mandel et al., 2015). The axons of a neuron are therefore the most vulnerable point as any injury to the axon can silence the function of the neuron (Hao and Collins, 2017). In the PNS, when the axon suffers an injury, the neurons revert back to a regenerative state in

order to re-connect to their targets (Doron-Mandel et al., 2015). In the case of the CNS this regenerative state is vastly reduced and the physical barrier of the glial scar prevents any attempts at regeneration from connecting to their original target (Sakamoto and Kadomatsu, 2017).

1.2.7 Axonal Myelination

Axons are formed from the neurite extensions sent out from the main neuron body. The myelin sheath is fundamental for axonal function. It surrounds axons in the nervous system and insulates the neuron cytoplasm from the extracellular fluid. This allows electrical currents to flow across the plasma membrane. By protecting and insulating the axons, electrical transmissions can be sent along the axons. This leads to motor function (Franssen et al., 2007, Levitan and Kaczmarek, 2015).

In the PNS, Schwann cells form the myelin sheaths by tightly wrapping their membrane around the axon (Levitan and Kaczmarek, 2015). In the CNS, this role is carried out by oligodendrocytes (Figure 1.3). It is postulated that Olfactory Ensheathing Cells (OECs) can carry out the same role in the CNS (Blumenthal et al., 2013, Li et al., 1997). This will be discussed in Section 1.3.

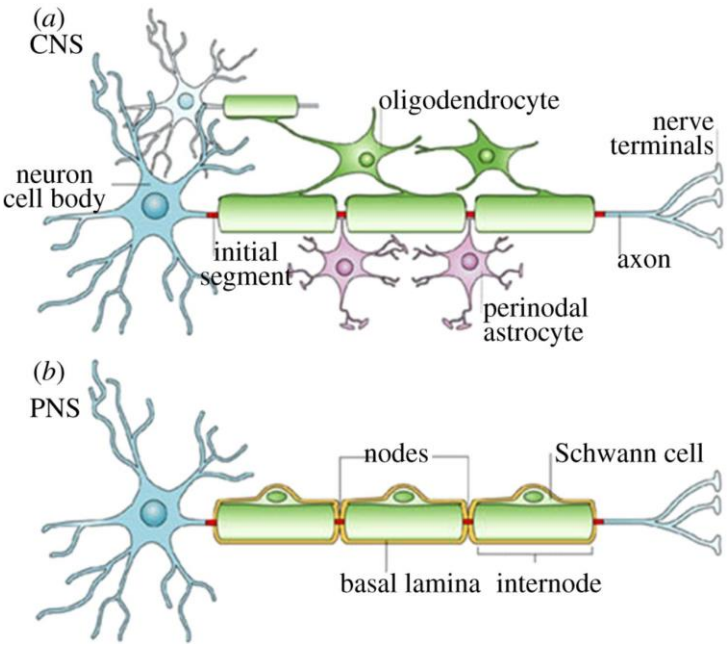

Figure 1.3: Central and Peripheral nervous system neurons and myelination mechanism. Neurons from the central (a) and peripheral nervous system (b) have the same configuration in respect to axon elongation from the main body. The axon is myelinated by oligodendrocytes in the CNS and Schwann cells in the PNS. Figure credit: (Siddique and Thakor, 2014)

1.2.8 Current Treatment of Spinal Cord Injury

There is currently no curative treatment for SCI. Patients who may have suffered a SCI are treated as if an SCI has occurred until proven otherwise. This ensures that patients do not suffer further damage to their spinal cord and some therefore only suffer short term symptoms that are abated after appropriate treatment such as physiotherapy and surgery (Ge et al., 2016, Watson et al., 2008).

1.2.9 Previous Research of Cell Therapy Options

Cell therapy treatments for SCI have been the focus of a lot of research and there have been many different cell types which have been investigated to try and determine an option that is able to traverse the glial scar and allow for function to be restored. Schwann cells have been investigated to determine if they could have a role in spinal cord regeneration cell therapy. On top of this, oligodendrocyte progenitors (OPs), human mesenchymal stem cells (hMSCs), neural stem cells (NSCs) and bone marrow stromal stem cells have been investigated in the past. This section will summarise previous findings and any shortcomings of these cells types to demonstrate why they have been found unsuitable so far.

Schwann cells (a glial cell from the PNS) have been the major focus of a lot of investigation. Glial cells are non-neuronal cells that provide support and protection for neurons in the CNS and PNS (Garcia-Segura and Melcangi, 2006). The PNS, unlike the CNS, retains its capacity for spontaneous nerve regeneration throughout life. This is due to the presence of Schwann cells (Frostick et al., 1998). After a peripheral nerve injury, Schwann cells proliferate and undergo phenotypic changes. They migrate from the nerve stumps and form a tissue bridge over the gap. This bridge guides the axons back, and the Schwann cells ensheath the regenerating axons to maintain the electric current required for nerve impulses (Torigoe et al., 1996). Their natural role in aiding axon regeneration has made them a popular candidate for SCI cell therapy. Despite their ability to support axon regeneration in the PNS, they lack critical regeneration properties for the CNS as they do not permit axons to re-enter the spinal cord (Tetzlaff et al., 2011), do not interact with the astrocyte dense glial scar (Yang et al., 2014) or reconnect the CNS (Raisman, 2007). Despite this, there is ongoing research using SCs to heal SCI and a group in Miami are currently in

the first stage of clinical trials using autologous Schwann cell transplants (Anderson et al., 2017).

OPs have been transplanted into the CNS of mice and rats but did not survive (Faulkner and Keirstead, 2005). This failure to survive was attributed to a lack of necessary survival factors as factors for OP proliferation are tightly regulated by the body for the expected number of cells. Any significant increase in this number of cells would not be able to be supported by the body and they would not survive (O'Leary and Blakemore, 1997, Franklin, 2002). Human embryonic stem cell (hESC) derived OPs were transplanted into chronic SCI in rats and assessed using GFP tracing; they survived and were integrated into the host tissue. Despite their survival, they did not remyelinate any spared axons and therefore were not able to restore the CNS (Faulkner and Keirstead, 2005).

Human mesenchymal stem cells (hMSCs) have also been considered as an alternative for cell therapy. hMSCs were seeded onto poly(D,L-lactide-co-glycolide acid) (PLGA) scaffolds and traced using the PKH67 Fluorescent Cell Linker Kit (Kang et al., 2012). The PLGA scaffold was implanted into a cavity at the T8-T9 vertebrae in rats. Rats that received the hMSC PLGA scaffold showed improvement in the eight weeks following surgery. This improvement was shown in a higher Basso Beattie Breshnahan (BBB) score (an assessment of locomotor behaviour) and an ability to regain hindlimb function (Kang et al., 2012). In addition to this, skin derived hMSCs were implanted into rat spinal injuries at T11 and, after 60 days, animals that had received the transplant showed an improvement in BBB score (Melo et al., 2017). Several studies have been carried out using hMSCs (from the dermal skin layer and adipose tissue) that have shown an improvement in function in rats (Zhou et al., 2016, Kang et al., 2012, Melo et al., 2017, Menezes et al., 2014, Park et al., 2010). These results are promising, and work continues in this field as a viable option for cell therapy in SCI. In terms of progress, the main studies showing the benefit of using hMSCs have all been published in the last ten years, which indicates that this work is still in the early stages.

Bone marrow stromal cells have also been researched alongside hMSCs. These cells are easy to obtain and are able to migrate to the injury site. It is thought that they aid recovery by providing neurotrophic factors, which assist the development of neurons and reduce the size of the glial scar (Namiki et al., 2000). Bone marrow cells have been genetically modified

to produce factors (NT-3, NGF and BDNF), which aid injury recovery. However, no functional recovery was observed in these studies (Yoshihara et al., 2006, Lu, 2005, Lu, 2007). Despite this, the genetically modified stromal cells allowed axons to regenerate past the glial scar, which demonstrates that it can be penetrated (Lu, 2005, Lu, 2007), therefore showing that the effects of the glial scar can be reversed. Recently a study by Raynald et al. (2016) delivered human bone marrow stromal stem cells to the rat spinal cord using a hyaluronic acid scaffold. They showed that the cells survived 8 weeks post injury and resulted in an increase in BBB score for transplanted animals (Raynald et al., 2016). These cells have potential, but the early work conducted showing a lack of functional recovery may indicate that they require specific conditions in order to aid SCI.

Finally, NSCs derived from rat tissue have been investigated as they convey the proliferative properties required for achieving desired cell numbers, yet are committed to a neural fate. This means that a more limited range of target cell products can be derived that are specific for neural regeneration, and they are therefore one step ahead of hMSCs (Willerth and Sakiyama-Elbert, 2008). In addition to this, they are capable of extensive, precise migration (Imitola et al., 2004). NSCs from adult rats have been modified to enhance derivation of neurons and oligodendrocytes; however, results have been variable with successful functional restoration and unsuccessful results (Lu et al., 2003, Ishii et al., 2006, Setoguchi et al., 2004). Key challenges that need to be overcome include long term survival of NSCs after transplantation and the issue that the majority of transplanted NSCs differentiate into astrocytes not neurons (Setoguchi et al., 2004, Mothe and Tator, 2013, Li et al., 2016, Liu et al., 2015).

1.3 Olfactory Ensheathing Cells

1.3.1 Olfactory Ensheathing Cells

Olfactory Ensheathing Cells (OECs) are specialised glial cells that are found in both the CNS and PNS. OECs form part of the primary olfactory system which belongs to the mammalian nervous system, able to regenerate neurons throughout life (Ramón-Cueto et al., 2000). The capacity of the olfactory system to regenerate throughout life is credited to the presence of the OECs (first identified by Golgi and Blanes in 1875) (Yang et al., 2014, Higginson and Barnett, 2011). They also can have a range of morphologies from bi-polar

spindly to flattened irregular, the significance of which is not fully understood yet (Ramón-Cueto et al., 2000).

OECs display a unique combination of phenotypic features of both Schwann cells and astrocytes (Doucette, 1990, Doucette and Devon, 1995, Oprych et al., 2016). This is significant because Schwann cells are responsible for nerve repair in the PNS. The weakness of Schwann cells as a spinal cord repair cell therapy is their inability to interact with astrocytes, which is the main cell type found in the glial scar. OECs on the other hand intermix with astrocytes in their role in the body and therefore have a significant advantage over Schwann cells (Franssen et al., 2007, Barnett and Riddell, 2004).

Within the olfactory system, OECs are found in the olfactory bulb and the nasal olfactory mucosa. The location of OECs in the body is shown in Figure 1.4 (Thuret et al., 2006). The olfactory bulb is located in the brain and the mucosa is inside the lining of the nose. Ensheathing glia wrap the axons as they make their way into the bulb (CNS) through the cribriform plate (Thuret et al., 2006). This protects the axons from coming into contact with other cell types and it is thought that this provides the environment required for axon regeneration (Ramón-Cueto and Avila, 1998). The ability to form new neurons from a compartment of stem cells has been maintained in mammals because many mammalian species are dependent on the sensory perception of smell to survive (Franssen et al., 2007).

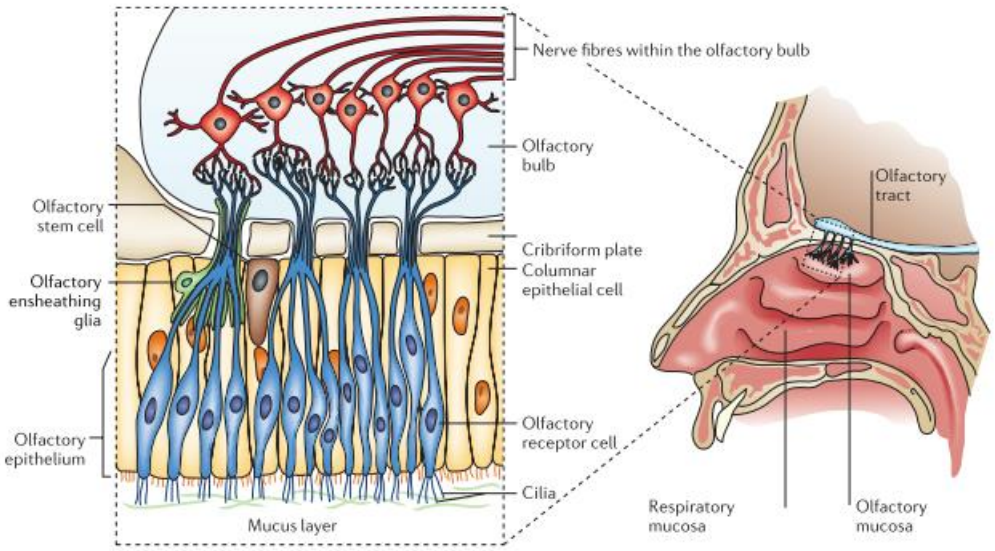

Figure 1.4: Schematic of the olfactory nervous system and location in the human body. The olfactory nerves connect the bulb (CNS) and the mucosa (PNS). The ensheathing glia wrap the axons as they make their way from the PNS to the CNS. Image credit: (Thuret et al., 2006).

1.3.2 The Olfactory Mucosa and the Olfactory Bulb

As reported in Section 1.3.1 and visualised in Figure 1.4, OECs are found in both the olfactory mucosa (OM) and the olfactory bulb (OB). It has been postulated that OECs from the OB and OM are separate sub-populations that carry out different functions. Any difference in the function between these two areas has not yet been identified (Chen et al., 2014, Hayat et al., 2003); although it has been postulated by Guerout et al that co-transplantation of OB-OECs and OM-OECs works better than either individually, as the two populations play different roles in nerve regeneration. Their research group transplanted OB-OECs, OM-OECs and various combinations of both into transected rat spinal cords. They found, using functional testing and electromyography of muscular activity, that a combination of OB-OECs and OM-OECs gave better functional recovery than pure populations (Guerout et al., 2011). The location of the cells has immediate implications for isolation.

Minimally invasive surgery is required to remove OECs from the nasal mucosa, which can be seen from Figure 1.4, as they can be accessed through the nose. This is important because the ability to remove the required cells with minimal risk allows them to be good candidates for cell therapy. The difficulty with this method is that the distribution of the OM is heterogeneous and therefore it cannot be distinguished from the respiratory mucosa (Ge et al., 2016, Chen et al., 2014). This increases the probability of contaminating cell types being present and more complicated purification methods are required. The OM is made up of three components: the epithelium, the basement membrane and the lamina propria. The basement membrane is found beneath the epithelium and the lamina propria is found on the other side of the membrane. Within these three areas, there are several key cell types that are found including OECs, olfactory receptor neurons (ORNs), sustentacular cells, Schwann cells, Bowman gland cells and basal cells which carry out a range of functions, for example ORNs are specialised for detecting odours (Chen et al., 2014). These are all potentially impurities that can be present in OM culture.

Removal of OECs from the olfactory bulb requires a craniotomy, which has serious risks and complications such as cerebrospinal fluid leakage, meningitis and loss of smell (Kachramanoglou et al., 2013, Wu et al., 2013b). These issues make the nasal mucosa a better option from a risk perspective. Cells from the OB have been shown to be more proliferative (Yui et al., 2011) which provides an argument for using a higher risk isolation

method. Most animal studies use OB cells for this reason and the fact that fewer contaminating cells are present in the OB (Blumenthal et al., 2013, Cao et al., 2004, Chuah and Au, 1993, Granger et al., 2014).

1.3.3 Characterisation of Olfactory Ensheathing Cells

1.3.3.1 Challenges

A key challenge of previous research using OECs is the lack of a definitive marker (Chen et al., 2014). Literature generally uses p75NTR and GFAP, however, neither of these markers exclusively define OECs and can mark contaminating cell types such as fibroblasts, Schwann cells and astrocytes (Orbay et al., 2015, Tong et al., 2010, Niapour et al., 2010, Wen et al., 2012, Mahapatra et al., 2009, Kawaja et al., 2009). In addition to this, S100β is often used as well. Traditionally Thy1.1 and Fibronectin (Fn) have been used as markers for contaminating fibroblasts. Fn is the main extracellular product from fibroblasts, however, like OECs, neither of these markers are exclusive to fibroblasts (Wu et al., 2013b, Ebel et al., 2013). For example Thy1.1 is a recognised stem cell antigen (Hu et al., 2010, Eslaminejad et al., 2007, Wu et al., 2013a). This further complicates the process of characterisation as the contaminants are not able to be fully characterised, together with the intrinsic difficulty characterising the desired population entails. S100β is a glial cell marker so although it can mark OECs due to the glial nature of the cells, it is also the marker used to identify Schwann cells, one of the contaminating cells present in the olfactory system (Chen et al., 2014). The markers and the cell types they are used for are summarised in Table 1-1.

Table 1-1: Summary of commonly used OEC markers.

	OECs	Fibroblasts	Schwann Cells
p75NTR	√	X	√
S100β	√	X	√
Thy1	√	√	X
Fn	√	√	X

A lack of specific marker would not be such an important issue if isolation of the cells was a straight forward process. Isolation from the rat mucosa comprises of fewer contaminating cell types compared with the bulb and other animal mucosae as the rat mucosa is yellow in

colour and can be easily excised from the nasal cavity (Bianco et al., 2004, Chen et al., 2014). This being said, dissection is incapable of separating out peripheral nerves and Schwann cells, so there will always be a degree of contamination (Kawaja et al., 2009). The most common contaminating cells are fibroblasts and Schwann cells but there can also be cells such as astrocytes and other respiratory tissue cells present in this area (Bianco et al., 2004, Kawaja et al., 2009). Although astrocytes have a distinct morphology, the morphology of OECs is plastic and this makes the isolation challenges more difficult to overcome (Chuah and Au, 1993, Barnett and Riddell, 2004).

OECs are known to adopt two morphologies. One is spindle shaped, the other is a flattened morphology. These two morphologies are considered to have different antigenic characteristics, with the spindle shaped cells expressing p75NTR and flattened cells expressing GFAP (Sonigra et al., 1999, Barnett and Riddell, 2004, Ebel et al., 2013, Boyd et al., 2003, van den Pol and Santarelli, 2003). These cells are plastic and are capable of changing between the two morphologies in under an hour (van den Pol and Santarelli, 2003, Vincent et al., 2005, Ebel et al., 2013). This means that the studies that have taken place using different methods of antibody purification may have been studying different parts of the OEC population as opposed to the whole population.

1.3.3.2 p75NTR

p75NTR is a neurotrophic receptor that can induce neurite outgrowth and cellular survival. It is also able to induce cell apoptosis through signal transduction pathways (Chen et al., 2009). It binds to NGF and other members of the neurotrophin family such as brain derived neurotrophic factor (BDNF), neurotrophic factor 3 (NT-3) and neurotrophic factors 4/5 (NT-4/5). The mechanism of p75NTR and how it relates to neurons and glia is still not fully understood (Chen et al., 2009, Ramer et al., 2005, Oprych et al., 2016). p75NTR is expressed in the rodent olfactory epithelium when neurogenesis is accelerated, and it is postulated that olfactory epithelium samples from adult humans are in a more active state of regeneration hence why p75NTR is expressed in humans through to adulthood (Hahn et al., 2005).

A study conducted by Radtke et al (2010), found that primary OB-OECs reduced their expression of p75NTR during time in culture. After one week in culture, the population was strongly positive for p75NTR whereas after six weeks *in vitro*, immunocytochemistry (ICC)

and fluorescent activated cell sorting (FACs) analysis determined significantly reduced p75NTR expression (Radtke et al., 2010). These older cells also showed a lack of myelination ability that was present in the cells cultured for 1-2 week despite the fact these cells remained viable (Radtke et al., 2010). This raises the concern that assessing a healthy OEC culture needs more analysis than simply assessing morphology and viability. Other studies have determined that p75NTR expression is linked to cell cycle and an increase in cell density leads to a downregulation of p75NTR expression (Kendall et al., 2002, Erck et al., 1998). This time dependence could explain some of the variation in published studies, and questions whether at least part of the variability in improved functional observations could be due to the OECs losing some of their key traits before transplantation.

p75NTR is the main marker used to identify positive populations of OECS (Franssen et al., 2007, Barnett and Riddell, 2004, Boyd et al., 2003, Guerout et al., 2011, Pellitteri et al., 2010, Sonigra et al., 1999). The issue is that the use of p75NTR does not eliminate the possibility of Schwann cell contamination. This can cause complications in interpreting results as the myelination of cells after implantation cannot be attributed to OECs over Schwann cells if this is the only marker used (Kawaja et al., 2009). The most common method of identifying Schwann cells is co-culturing populations with astrocytes. The OECs grow among the astrocytes whereas the Schwann cells have a distinct, separate population in culture (Barnett and Riddell, 2004).

1.3.3.3 S100β

S100β is a calcium binding protein that influences cellular responses along calcium related signal transduction pathways (Chong, 2016, Jin et al., 2014). Due to its relation to calcium signalling, it acts in a dose dependent manner (Sandrin and Cosset, 2006, Steiner et al., 2007). It is mainly expressed in the cytoplasm of astrocytes in the CNS, but is also expressed in the nucleus, and its biological role has been closely associated with neuroprotection and neurotoxicity (Chong, 2016, Jin et al., 2014), as well as cell cycle and differentiation (Gilquin et al., 2010). S100β is expressed in OECS, oligodendrocytes, neural progenitor cells and Schwann cells (Chong, 2016). It is Schwann cells in particular that have the most relevance in this study as Schwann cells are one of the potential contaminating cell types present in the olfactory mucosa. As reported in Section 1.3.3.2, Schwann cells also express p75NTR and therefore differentiating between the two cells types that also share morphological similarities (Kawaja et al., 2009) adds a significant challenge.

1.3.3.4 Thy1

Thy1 is a recognised stem cell antigen (Hu et al., 2010, Eslaminejad et al., 2007, Wu et al., 2013a), and is commonly used to characterise fibroblast presence in OEC culture (Wu et al., 2013b, Ebel et al., 2013). Thy1 is an extracellular receptor for the leukocyte integrin Mac-1 and therefore serves an important role in the adhesion and transmigration of neurotrophils and monocytes to sites of inflammation (Saalbach et al., 2005, Kisselbach et al., 2009). It is characterised as an activation-associated cell adhesion molecule and is expressed by fibroblasts, neuronal cells, blood stem cells and other cell types in the human adult (Saalbach et al., 2005).

The key problem with using Thy1 as a contamination marker is research groups have identified that OECs are also capable of expressing Thy1 and therefore there is no way to determine the cell type present if this is the only method applied (Sonigra et al., 1999, Nash et al., 2001, Nash et al., 2002, Hayat et al., 2003). This links to the issue of whether the studies previously carried out have actually studied the whole of the OEC population, or just a subset as the removal of populations with certain markers may actually be removing part of the OEC population.

Thy1.1 and Thy1.2 are subtypes of Thy1 which are found in rodents (Hayat et al., 2003). For the rat cells used in this study, Thy1.1 was used to identify fibroblasts present in the culture which is consistent with what is used in literature (Kawaja et al., 2009).

1.3.3.5 Fibronectin

Fn is an extracellular matrix protein that is implicated in many biological processes including axon regeneration in mature white matter, neuron outgrowth, cell adhesion and maintenance of shape (Wang and Ni, 2016, Tom et al., 2004, Liu et al., 2010, Ramón-Cueto and Nieto-Sampedro, 1992). Fn is produced in monomeric form and polymerised at the cell boundary to create a fibril. This fibril form is found in the intracellular space but is most commonly used to mark fibroblasts, which has been its main role in OEC studies (Keyvan-Fouladi et al., 2003, Li et al., 2003b, Krudewig et al., 2006). There is evidence, however, that it is also expressed by OECs (Ramon-Cueto et al., 1993, Kawaja et al., 2009). It is not unexpected that it is found in the olfactory system considering that it has been shown to have a role in wound healing, inflammation and the adhesion and migration of neurons (Zollinger and Smith, 2016, Liu et al., 2010, Gong and Shipley, 1996).

1.3.3.6 α-SMA

α-smooth muscle actin (α-SMA) is a cytoskeletal actin binding protein (Jahed et al., 2007) that is localised to stem and precursor cells (Hosoya et al., 2006) and fibroblasts (Skalli et al., 1989). It has also been reported to have an important role in cell division (Rockey et al., 2013). One group has reported that it is expressed in OECs but not in Schwann cells (Jahed et al., 2007). This would potentially allow for any Schwann cells present as impurities to be detected in OEC cultures, although olfactory fibroblasts in the culture would still react positively.

1.3.3.7 βIII-tubulin

As the name suggests, βIII-tubulin is a class three β-tubulin neuronal marker. It is a neuron specific isotype which is expressed during early neuronal development (Lee et al., 1990, Ambrogini et al., 2004). It is thought to have a role in neuronal differentiation and neurite outgrowth (Lee et al., 1990). βIII-tubulin was used as a neuronal marker during the functional studies (Section 5.0) to determine the presence of neurons and neurites.

1.3.4 Application of Olfactory Ensheathing Cells to Spinal Cord Injury

Schwann cells, another type of glial cell, have been researched extensively about their potential to help SCI. The main issue discovered was that Schwann cells do not associate with astrocytes, the main component of the glial scar. This is most likely due to them existing in strictly separate areas at the peripheral and central nervous system interface (Franssen et al., 2007, Barnett and Riddell, 2004). This means that Schwann cells have a significantly decreased ability to assist the nerves through the glial scar. OECs on the other hand, intermingle naturally with astrocytes at the border of the olfactory nerve layer in the OB and therefore have an advantage over Schwann cells (Ramer et al., 2004, Franssen et al., 2007). The full advantage of this has not been completely realised, as the mechanism by which OECs promote axon growth, is not fully understood (Ruitenberg et al., 2006, Keyvan-Fouladi et al., 2002).

What is known is that after damage to the olfactory nerves, OECs provide channels for the nerves to grow from the injury point back to the bulb. The channels formed by the OECs

protect the nerve fibres and allow them to grow (Raisman and Li, 2007). The concept is that after a SCI, OECs would be transplanted into the spinal cord and form similar channels to protect the nerve, so it can grow and reconnect with the severed end.

Their natural role in the body, as well as their ability to interact with astrocytes, are not the only strengths that OECs possess as a potential cell therapy candidate. Their unique capacity to permit axonal growth across the PNS-CNS interface is also critical to the success of neuronal regeneration in the spinal cord (Ramer et al., 2005). Generally glia do not co-exist in both the PNS and CNS, and therefore OECs have important characteristics that allow them to transverse this area (Mackay-Sim and Chuah, 2000).

1.3.5 Successful Case Studies using Olfactory Ensheathing Cells

1.3.5.1 Spinal cord repair in rats

The potential of using OECs to treat SCI was first shown in rats. In 1994, OECs that expressed p75NTR and fibronectin were transplanted into rats. The corticospinal tract in the upper cervical was removed (Li and Raisman, 1994) and OECs were transplanted into the lesion space (Li et al., 1998). Axons were labelled with biotin dextran and were observed to enlarge in diameter upon contact with the OECs. From the biotin dextran anterograde labelling, axons were observed to regenerate, forming parallel bundles and passing through the injury site. Three weeks after transplantation, the axons were ensheathed with myelin. Functional testing established that forepaw reaching function was restored. The transplanted OECs were still expressing p75NTR three months after the transplantation occurred (Li et al., 1998).

This research was followed up in 2000 by Imazumi et al. who investigated whether there was any difference in the number of regenerating axons when OECs were transplanted into the injury site. Rats had their spinal cord severed at T11. Neonatal OECs from rats were injected into the injury site. Control rats received DMEM and others received adult Schwann cells. Success was determined by electrophysiological analysis of axonal conduction, which was carried out 5-6 weeks after the cell transplantation. The conduction velocity of regenerated axons was higher when OECs were transplanted. This means that axons were regenerating and were myelinated. No electrical activity could be recorded in the control group. As with the study in 1998, biotin dextran was used to track axons; this

method showed a small number of labelled axons traversed and extended past the lesion when OECs were transplanted (Imaizumi et al., 1998).

In the same year, Ramón-Cueto et al. looked at long term functional recovery when OECs are transplanted. The spinal cord of the rats was severed at T8/T9, which paralysed the hind limbs. After two months, three of the OEC transplanted rats (total n=9), showed extensive movement of the knee, ankle and hip joints determined by weekly climbing tests with four difficulty levels. The remainder showed slight improvements in these joint areas. Control rats which received no transplant did not experience this improvement. After seven months, transplanted animals all passed at least the easiest level of the climbing test and 22% achieved the highest level. None of the non-transplanted animals achieved the easiest level. Histology carried out by tracking biotin dextran showed all transplanted animals exhibited some level of repair at the microscopic and macroscopic level (Ramón-Cueto et al., 2000).

1.3.5.2 Spinal cord repair in larger mammals

After the successes in rats, OEC studies were carried out in dogs to determine if canine OECs behaved in a similar manner. The canine spinal cord is of a similar length to the human spinal cord and therefore it has more relevance in terms of translation to the clinic (Roloff et al., 2013, Techangamsuwan et al., 2009, Ziege et al., 2013). There are concerns regarding the use of rats in previous studies because the rat system is very different from human clinically relevant cases, which questions whether the data collected from rat studies can be extrapolated to the human system. For example, a study conducted by Wewetzer et al. (2011) found that canine OECs differed from their rodent counterpart in aspects including *in vitro* growth, spontaneous immortalisation and morphology (Wewetzer et al., 2011). How these differences modify the ability of the OECs to remyelinate in different species is currently unknown.

Canine OECs from the OB were initially transplanted into rats. Animals that received canine OEC transplantation showed widespread remyelination throughout the lesion, observed by ultrastructural analysis (Smith et al., 2002). In 2012, small dogs (< 20kg) who were in the chronic phase of a SCI were treated using OEC transplantation. Animals were only accepted if they had complete paralysis (quadriplegia) and at least three months had passed since the injury. Using animals in the chronic phase of their injury allowed any progression to be

reliably attributed to the treatment. Animals were assessed monthly (up to six months) on locomotor performance on a treadmill, somatosensory-evoked potential, transcranial magnetic motor-evoked potential recordings and urodynamic assessments. From this study, animals who had received OEC transplantation (mixed OEC/fibroblast population from the mucosa) experienced improved forelimb-hindlimb coordination (Granger et al., 2012, Roloff et al., 2013).

1.3.5.3 Spinal cord repair in humans and primates

In a study that took place in 2004, transgenic porcine OB-OECs were transplanted into African green monkeys. The pigs had been transgenically modified to express human complement inhibitor CD59 (Radtke et al., 2004), which has been shown to support axonal regeneration and remyelination in rodent spinal cords (Imaizumi et al., 2000). Demyelinating lesions were made at T7 or T9, and porcine OB-OECs (98% pure using p75NTR, S100β and GFAP) were injected to the injury site and histologically assessed using p75NTR at four weeks. Remyelination occurred in 62.5% of lesions (Radtke et al., 2004). A positive result in primates is promising for human work.

Trials began in humans in 2006 (Lima et al., 2006). In one of the first studies, autologous olfactory mucosal transplantation was carried out seven patients, six of whom experienced an increase in their motor and sensory function. Two regained bladder sensation and another patient regained voluntary anal sphincter control. This was carried out with minimal parallel physiotherapy treatments. All patients received physiotherapy following the surgery for an unspecified length of time (Lima et al., 2006). In 2013, research carried out in Wroclaw Medical University, Poland, successfully transplanted OECs and fibroblasts into a patient who suffered an 8 mm transection injury at T9 due to a knife crime. A co-culture of autologous fibroblasts and OECs from the OB was transplanted into the injury site. The OECs were transplanted on either side of the spinal cord stumps. There was still a 2 mm thick spur of tissue connecting the stumps. The patient regained feeling below the injury site five months after surgery (Tabakow et al., 2013) and is now able to walk with assistance (Tabakow et al., 2014).

Alongside this patient, the same treatment was performed on two other patients (OECs from the OM) who had compression injuries from car accidents. All three patients were subjected to extensive pre and post-operative physiotherapy. This was carried out for three

control patients in parallel. Physiotherapy was carried out for 4-5 hours a day and 3-5 days per week. Neurological functional improvement was reported in all three patients with OEC transplantations. Their results showed an improvement in the spinal cord transmission and the activity of the lower extremity muscles compared to the control patients who only received physiotherapy. Only the patient with a transection injury and olfactory bulb OECs experienced functional recovery. No neurological deterioration, neuropathic pain, neuro-infection or tumorigenesis occurred as a result of OEC transplantation (Tabakow et al., 2013).

1.3.6 Challenges associated with using OECs towards Spinal Cord Repair

It is important that any treatment developed not only gives functional recovery, but is also financially viable and will reach as many patients as possible. The main challenge that has been identified so far in this Literature Review is the glial scar. This is because it is the physical barrier to axon regeneration. In order for axon regeneration to occur, the axons must be able to penetrate the scar so they can reach their original targets (Blesch and Tuszynski, 2003, Novikova et al., 2011).

The proliferation of OECs at the transplant site comprises of a challenge on its own, and it is being targeted in this thesis. Previous research indicates that the survival rate of OECs is low after injected to the lesion site. This results in a significant loss in cell numbers (Blumenthal et al., 2013). In addition, biopsies from hOM have a low yield (one study found that 48% of human mucosa biopsies had a yield of less than 5%) (Kachramanoglou et al., 2013). There are significant difficulties in obtaining enough OECs in biopsy material to culture and use as a consistent and reproducible autologous approach (Kachramanoglou et al., 2013). This leads to the prospect of creating an allogenic cell line. A 48% ‘failure’ rate is too high and it means that autologous treatment would not be wide reaching until the factors affecting failure could be mapped and addressed. These factors may never be fully understood and the technologies available should be utilised to help patients’ and their family’s suffering, even if that comes at the cost of lifetime immunosuppression.

In terms of purification, a challenge that has been explained in this Literature Review, is the lack of a cell specific marker for both OECs and olfactory fibroblasts (OFs) (Ulrich et al., 2014). In the lamina propria (part of the OM), there are contaminating cells such as

Schwann cells and endothelial cells (Chen et al., 2014). Not only can OECs and OFs not be reliably distinguished from each other, it is also difficult to differentiate OECs from cells such as Schwann cells as they share many immunological similarities (Babiarz et al., 2011). Additionally, in the human system, there is no clear delineation between the olfactory and respiratory regions in the nasal cavity and the mucosa is not identifiable at the macroscopic level, which increases the chance of contaminating cells being present (Morrison and Costanzo, 1992, Kachramanoglou et al., 2013).

Cell proliferation and yield of OECs is highly variable. Wu et al. (2013) conducted research on human OECs derived from the olfactory mucosa. OECs were classified as any cell that was labelled positive for both p75NTR and GFAP antibodies. From seven patients, the OEC yield ranged from 9.2%-73.2% (Wu et al., 2013b). This high variability indicates that allogenic treatment may be more appropriate. Autologous treatment would not be an appropriate line to follow if the yield of cells able to be obtained is so low and variable.

In another study, biopsies taken from 43 human mucosal biopsies confirmed that the critical parameters for ensuring a high yield and quality of OECs remain unknown. The factors explored include age, sex, past medical and surgical history, presenting complaint, drug history, allergies and smoking status. It was thought that key factors included age, smoking and the presence of any mucosal disease; however, the results obtained were not definitive (Kachramanoglou et al., 2013).

A successful cell therapy for SCI using OECs will not be a viable option until these challenges are addressed and overcome. This thesis aims to examine some of the challenges identified and provide further understanding of OECs and their neuro-regenerative effects.

1.3.7 Aims of Study and Thesis Outline

After reviewing the current literature on the use of OECs for spinal cord repair, it is evident that there is a need to fully characterise the OEC population and identify optimum conditions for the expression of protein marker p75NTR.

One of the initial objectives for this PhD was to investigate the use of a fibroblastic feeder layer to support OEC proliferation and encourage p75NTR expression. To achieve this objective, primary rat OECs were isolated and cultured with human and mouse fibroblasts.

Further to this, a human OEC cell line was developed in the laboratory and cultured in the conditions used for rat OECs. The results of this analysis are presented in Chapter Three.

Another objective of this thesis was to further understand the protein expression patterns of OECs in culture. p75NTR is normally used as a putative marker for OECs , although its expression does not confirm OEC identity (Franssen et al., 2007, Barnett and Riddell, 2004, Boyd et al., 2003, Guerout et al., 2011, Pellitteri et al., 2010, Sonigra et al., 1999). The objective was to determine the stability of p75NTR expression in culture and to determine whether immune-depletion of contaminating marker Thy1 could enrich p75NTR cells. The results of this analysis are presented in Chapter Four.

Finally this thesis aimed to identify whether a positively correlated relationship existed between cells with high p75NTR expression and neurite extension. OECs with a variety of p75NTR and Thy1 expression were co-cultured with neurons and the behaviour of the neurons and their neurites was examined after five days of co-culture. The results of this analysis are presented in Chapter Five.

Hopefully the information provided in this thesis will increase the knowledge of OECs, their markers, and their neural regenerative properties. This will help future research into the development of cell based therapies and ultimately a clinical cure for spinal cord injury.

2.0 Materials and Methods

2.1 Cell culture

2.1.1 Isolation of OECs from Rat

Mucosae were dissected from three adult female Sprague-Dawley 200-250g rats, which were euthanized by carbon dioxide asphyxiation (Schedule 1 method (Great Britain and Office, 2000)) according to the UK Animals (Scientific Procedures) Act 1986. Each rat provided two mucosae. Each mucosa was placed in DMEM/F12 media to be transported to the laboratory. The mucosae were placed in Hanks Balanced Salt Solution (HBSS, Gibco Life Technologies) with 1% P/S (10,000 units penicillin, 10mg streptomycin/ml) in a petri dish and washed by gently wiping each mucosa across a spatula. After washing, the mucosae were placed on a petri dish and cut up into small pieces and then placed in 5ml dispase II (2.4units/ml, Sigma-Aldrich, UK) solution for 45 minutes at 37°C in order to enzymatically digest the tissue.

The mucosa and dispase solution were placed in the centrifuge which was run for 5 minutes at 400g. The supernatant was discarded and the cells and tissue were re-suspended in 5 ml collagenase (Type I solution, 0.05%, Sigma-Aldrich) for 15 minutes at 37°C. Every 5 minutes the collagenase was taken out of the incubator and mechanically triturated briefly before being placed back in the incubator. At the 15 minute point the collagenase suspension was placed in the centrifuge for 5 minutes at 400g. The cells were re-suspended in 7ml DMEM/F12 media (2%FBS, 1% P/S) in a T25 flask at 37°C in 5% CO_2 for 24 hours. All cell culture, unless stated otherwise, was carried out at 37°C and 5% CO_2.

The cells were placed in a tissue culture flask for 24 hours as a differential adhesion step. The purpose of this step was to decrease the amount of contaminating fibroblasts in the culture. Fibroblasts have a faster adhesion time than OECs. After 24 hours most fibroblasts will adhere to the tissue culture plastic whereas OECs will still be in suspension (Georgiou et al., 2017). After 24 hours, the suspension was replated onto laminin (20 µg/ml, Sigma-Aldrich, UK) coated wells. The wells were coated for four hours at 37°C, the laminin was then removed and the cells were plated while the matrix was still wet. The isolation process is shown in Figure 2.1.

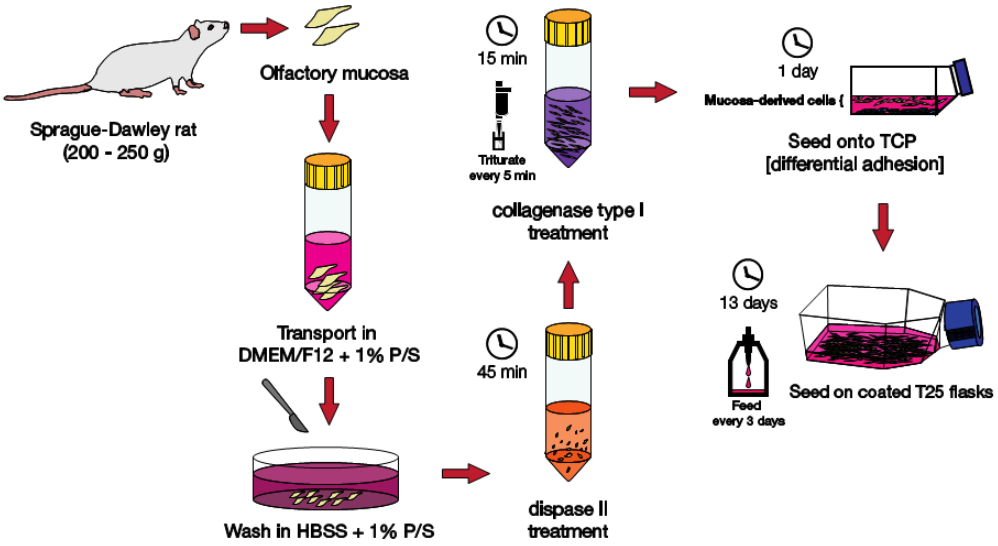

Figure 2.1: Rat mucosa dissection and treatment. This figure depicts the protocol from the dissection of the mucosa to re-plating after the differential adhesion step to final culture time. Figure credit: Gerardo Santiago Toledo, UCL.

2.1.2 Culture of HuG418

HuG418 was the name of the human mucosal fibroblast line that was used a feeder layer to support OEC proliferation and protein expression.

2.1.2.1 Creation and Immortalisation of HuG418

The feeder layer was prepared from cells isolated from the human olfactory mucosa. The cells used were thawed from a pre-existing cell line prepared by Dr Melanie Georgiou (UCL). The protocol followed by Dr Melanie Georgiou is summarised in the paper by (Pollock et al., 2006). The cells were immortalised using a retrovirus that contains the c-MycER fusion protein. This fusion protein has a modified oestrogen receptor. The synthetic drug 4-hydroxy-tamoxifen (4OHT) binds to the modified receptor which promotes cell proliferation, as shown in Figure 2.2. Immortalisation is halted when the cells are cultured without 4OHT. This allows the cells to be rapidly expanded *in vitro* but safely implanted *in vivo* (Pollock et al., 2006). This is a mixed population of cells due to the variety of cells present in the mucosa, however, due to the high proliferation of fibroblasts it is assumed that the majority of them are fibroblasts. For the remainder of this report, this cell population will be referred to as HuG418.

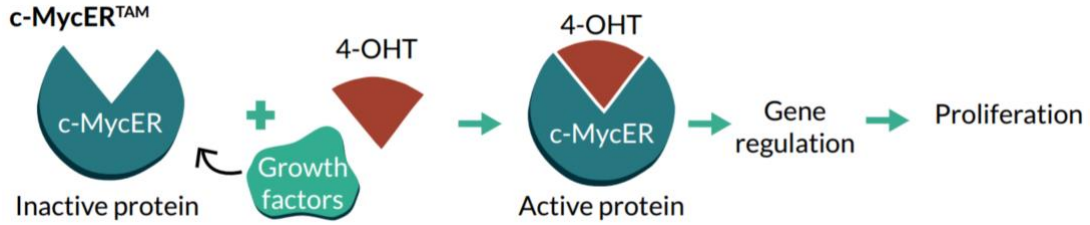

Figure 2.2: Overview of c-MycER^{TAM} technology. In the presence of 4-OHT, the genetically modified cells proliferate. Without 4-OHT, the cells revert to their normal phenotype and can be safely implanted into patients. Figure credit: (Wall et al., 2016).

2.1.2.2 Expansion of HuG418

HuG418 were cultured in DMEM/F12 media (GlutaMAX^{TM}-I, 2% FBS v/v, 1% P/S v/v, from now on referred to as DMEM/F12 media) in poly-l-lysine (PLL, 0.1 mg/ml, Sigma-Aldrich, UK) coated T75 flasks at 37°C and 5% CO_2. 3 ml of PLL was added to the T75 flask and allowed to coat for 30 minutes at room temperature (RT). PLL was removed and flasks were allowed to dry for at least 30 minutes at RT before cells were added. Media was changed every 2-3 days with 1 µL 4-hydroxy-tamoxifen (4-OHT) added per 10ml media.

Cells were passaged when they reached 70-80% confluency. All the media was removed from the flask and 5 ml of trypsin/EDTA (0.25% TE) was added to the flask and incubated for 5 minutes at 37°C. Detachment of cells was confirmed by microscope observation. If the cells did not appear to have detached, TE was left on for a maximum of seven minutes and the flask was hit once to encourage the cells to detach. TE was deactivated by adding 10ml of DMEM/F12 media and washing thoroughly over the surface. The solution was added to a centrifuge tube and spun at 400g for 5 minutes at 21°C. The supernatant was removed and cells were re-suspended in up to 4ml media. An 8 µL sample was taken and a cell count was carried out using a haemocytometer. Cells were seeded at a density of 5000 cells/cm^2.

2.1.2.3 Thawing of HuG418

Original vials of HuG418 were supplied by Dr Melanie Georgiou. These were stored at -196°C in liquid nitrogen with 0.5million cells/ml. Cells were transported from liquid nitrogen storage to the lab in dry ice. Vials were thawed rapidly in the water bath (37°C). Once the cell suspension was completely thawed, it was added dropwise to DMEM/F12 media and centrifuged at 400g for 5 minutes. This was done in order to remove the DMSO

from the cell solution. The supernatant was discarded and the cells resuspended in 10 ml DMEM/F12 media, plated in a PLL coated T75 flask (as explained in Section 2.1.2.2) and placed in the incubator.

2.1.2.4 Cryopreservation of HuG418

A bank of HuG418 cells was created from the original vials supplied by Dr Melanie Georgiou. Cells were treated with TE to detach them from the flask and spun down as in passaging (see Section 2.1.2.2). Cells were counted via haemocytometry and re-suspended in 90% FBS v/v, 10% DMSO v/v with 0.5 million cells added per ml. Vials were placed in a Mr. Frosty container at -80°C, which allowed for the controlled cooling of the cells at approximate rate of -1°C/min. After 24 hours the vials were transferred to the liquid nitrogen at -196°C for long term storage.

2.1.2.5 Preparation of HuG418 feeder layer

Feeder layers were prepared by removing the media from the T75 flask and replacing with 4ml of mitomycin C (MMC) (Sigma-Aldrich, UK) for 2 hours at 37°C to inactivate the cells. MMC acts by covalently crosslinking DNA which inhibits DNA synthesis and cell proliferation (Sigma-Aldrich, UK). After 2 hours the MMC was removed from the cells and the cells were washed with PBS (Lonza). The cells were removed from the flask following the same protocol as passaging (see Section 2.1.2.2) and placed in the centrifuge for 5 minutes at 400g. After discarding the supernatant, cells were re-suspended in DMEM/F12 and plated up at $12x10^3$ cells/cm^2. This density was used as it gave a good coverage of the well whilst allowing space for the OECs on the well surface. Feeders remained in the incubator for two days before any cells were plated on them.

2.1.2.6 Preparation of HuG418 Conditioned Media

Conditioned media from HuG418 was used in some experimental work (Section 3.3.2, 3.3.4-3.3.5 and 5.3.1). Media was collected from HuG418 culture after two days of conditioning. The media was spun at 400g for 5 minutes to remove any cell debris in the media. The supernatant was collected and added to fresh media at a 1:1 ratio. Fresh media was added to ensure that there were plenty of nutrients available for the cells to grow.

2.1.3 Culture of Ms3T3

A T25 flask of Ms3T3 fibroblasts was kindly gifted by Dr Victoria Tovell from the UCL Institute of Ophthalmology. The Ms3T3 cell line was developed in 1962 from mouse embryonic tissue. The cells were grown following a 3T3 culturing process, which means cells were transferred (passaged) every three days and plated at a density of $3x10^5$ cells/T25 flask. The Ms3T3-L1 clone was carried through for further testing and the cells obtained from the UCL Institute of Ophthalmology descended from this clone (Todaro and Green, 1963).

Ms3T3 cells were cultured with DMEM/F12 media (GlutaMAX^{TM}-I, 10% FBS v/v, 1% P/S) on tissue culture plastic. Media was changed every 2-3 days and cells were passaged at 70-80% confluency. Ms3T3 were seeded at 5000 cells/cm^2 and passaged, thawed and cryopreserved following the same protocol as HuG418 cells (see Section 2.1.2). Feeder layers made with Ms3T3 were prepared in the same way as HuG418 as explained in Section 2.1.2.5.

2.1.4 Culture of PA5 and PA7

2.1.4.1 Isolation and immortalisation of PA5 and PA7

The PA5 and PA7 cell lines were isolated by Dr David Choi from the human olfactory mucosa. They were conditionally immortalised by Dr Melanie Georgiou following a similar method as used for HuG418 (Section 2.1.2.1). In order to isolate the OECs as opposed to the fibroblasts, the cells were immortalised at day 6. This was done after the initial 24 hour differential adhesion step (as explained in Section 2.1.1) to ensure that fibroblasts were not contaminating the culture, and a further 5 days to allow the cells to attach.

In certain experiments, NT-3 (Sigma-Aldrich, UK) was added at a concentration of 50 ng/ml. NT-3 was added from the beginning of the experiment and replaced with every media change.

2.1.4.2 Expansion of PA5 and PA7

PA5 and PA7 cells were cultured with DMEM/F12 (GlutaMAX^{TM}-I, 2% FBS v/v) media on PLL coated flasks. PLL coating was carried as with culture for HuG418. The seeding density, passaging, thawing and cryopreservation were the same as for HuG418 (see Section 2.1.2).

2.1.5 Culture of NG108-15

The NG108-15 neuronal cell line was purchased from Sigma-Aldrich, UK. It is a hybrid cell line created by the fusion of mouse neuroblastoma and rat glioma (Klee and Nirenberg, 1974). NG108-15 cells were cultured with DMEM/F12 media on PLL coated flasks as instructed by the supplier (Sigma-Aldrich, UK). Media changes were carried out daily and the seeding density used for passaging was 5000 cells/cm^2. Contrary to the other cell lines used, trypsin was not used for passaging. As the cells only lightly attach to the culture surface, passaging was carried out by gently knocking the flask until the cells had detached. The supernatant was then centrifuged as normal, re-suspended and plated onto PLL coated flasks.

2.2 MACS Purification

Cells were purified using MACS Miltenyi Biotec microbead technology. Thy1.1 microbeads and LS columns were used for the purification. The buffer solution was made up of PBS with 0.5% v/v FBS and 2mM EDTA.

Cells were removed from the flask using the same protocol as passaging (see Section 2.1.2.2). An 8 µL sample was taken to determine the cell number. If a pre-purification sample was needed, this was taken at this point. Cells were then centrifuged at 300g for 10 minutes. The supernatant was discarded and cells were re-suspended in 60 µL of buffer and 40 µL of microbeads (per 10^7 total cells) to label Thy1.1 positive cells. This cell suspension was well mixed and incubated at 4°C for 15 minutes in the dark. When a fluorescent antibody was added for flow cytometry, it was added at this point. 10 µL of anti-mouse (Vector DyLight IgG 488, green) was added to the cell suspension and incubated for 5 minutes at 4°C. Cells were washed with 3 ml buffer per 10^7 cells and centrifuged at 300g for 10 minutes.

The supernatant was discarded and cells were re-suspended in 1ml buffer. The LS column was placed in the MidiMACS^{TM} separator and rinsed with 3ml buffer. A collection container was placed below the column and the cell suspension was applied to the column. Four washes (3 ml each) were applied to the column to allow unlabelled cells to wash through.

A new container was placed below the column and the column was removed from the MACS separator. 5ml of buffer was flushed through the column with the aid of the plunger. The two fractions were labelled as appropriate, spun at 400g for 5 minutes and used for experiments.

2.3 Cell Characterisation Techniques

2.3.1 Immunocytochemistry

Cells were fixed with 4% paraformaldehyde w/v (PFA, Sigma-Aldrich, UK) for 20 minutes at RT. The amount of PFA added depended on the well size. The volumes of solutions for immunocytochemistry (ICC) used were the volumes required to cover the surface of the well (100 µL in a 48 well plate, for example). PFA was removed and the cells washed three times with PBS. Three washes with PBS were carried out in between every step of the immuno-staining in order to remove and dilute any traces of the previous chemical. One wash was defined as filling the well with PBS and leaving for 5 minutes. 0.25% v/v Triton X (Sigma-Aldrich, UK) was added to each well and left for 30 minutes at RT. All solutions were made up in PBS.

5% v/v goat serum solution (Dako) was used as the blocking solution for 30 minutes at RT. The primary and The primary and secondary antibodies used depended on the experiment. Primary antibodies were prepared antibodies were prepared at a dilution of 1:200 and added for 90 minutes at RT. The primary antibodies, their primary antibodies, their specificity and the company they were purchased from are shown in in

Table 2-1. Negative controls were used for these experiments. The negative control was subject to the same treatment as other wells, the exception being the exclusion of the primary antibody. This ensured that there was no interaction between the secondary antibodies and any reactive sites on the cell surface. The secondary antibodies were prepared at 1:200 and Hoechst (Sigma-Aldrich, UK) was used to stain the nucleus of the cells and used at 1:1000. This solution was added for 45 minutes at RT. Plates were

wrapped in foil during this step as the secondary antibodies are light sensitive. After the PBS wash, the cells were sealed with parafilm and left overnight at 4°C in PBS. Fluorescent imaging was carried out in the following days on an EVOS FL microscope (Life Technologies).

5 images were taken per well and were taken in a cross formation around the centre of the well. 2-3 wells were stained per condition. After imaging, each channel was examined to assess whether the images taken were representative of the well. Brightness and shutter speed were set by identifying a cell that was determined to be positive and ensuring the background was dark to prevent overexposure of the cells. These settings were held constant between images for an experiment to ensure the images could be directly compared.

Images were analysed using ImageJ. A colour threshold was set to identify a positive cell and only cells that were identified to be above this threshold were counted as positive. This prevented bias from entering the interpretation of results. Positive cells were counted and results were calculated as a proportion of cells positive for the marker and the yield of positive cells over the imaged area.

Table 2-1: Specificity of primary antibodies

Specificity	Species	Target	Dilution	Company
p75NTR	Rabbit	Rat, Human	1:200	Millipore
Thy1.1	Mouse	Human	1:200	Sigma-Aldrich
Thy1.1	Mouse	Rat	1:200	Millipore
S100β	Rabbit	Rat, Human, Mouse	1:200	Dako
S100β	Mouse	Rat, Human, Mouse	1:200	BD Transduction Laboratories
Fn	Mouse	Human, Mouse	1:200	Sigma-Aldrich
GFAP	Rabbit	Rat, Human, Mouse	1:200	Dako
βIII tubulin	Mouse	Rat, Human	1:200	Sigma-Aldrich
α-SMA	Rabbit	Rat, Human, Mouse	1:200	Abcam

2.3.2 Circularity Analysis

A macro was written in ImageJ in order to analyse the morphology of the cells. Circularity was used as the defining value. The macro was written in JavaScript to automate a calculation method that already exists in ImageJ. The "adjust threshold" window opens automatically when the macro is run and can be adjusted to select the area of interest. Any cell that was larger than a set threshold (this value can be adjusted depending on whether the nucleus or the whole cell is being analysed) was discarded to prevent cell clusters being included in the calculation. In addition to this, any cells on the boundary of the image were discarded so they did not contribute to false readings. The circularity was calculated as in Equation 1 where A is the area (pixels^2) and P is the perimeter (pixels).

$$Circularity = \frac{4A\pi}{P^2} \qquad (1)$$

A circularity of 1 indicates a perfect circle and a circularity of 0 indicates a straight line. When the macro was run, a print out of the desired property (such as circularity or area) was displayed along with counts, mean and standard deviation. This data was exported to Excel and plotted as a histogram.

2.3.3 Flow Cytometry

2.3.3.1 Live Staining

Live staining of cells for flow cytometry was carried out on ice. 5% v/v goat serum solution (Dako) was used as the blocking solution for 15 minutes. In between each step, the cells were spun at 400g for 5 minutes. The primary antibody (mouse anti-Thy1.1, Thermo Scientific) was prepared at 1:200 and added for 30 minutes. A negative control was made up by excluding the primary antibody. The secondary antibody (Vector DyLight IgG 488, green) was prepared at 1:200 and added for 20 minutes. After the last spin, the cells were run immediately through the flow cytometer.

2.3.3.2 Flow cytometry

Flow Cytometry was carried out using the BD Accuri™ C6 flow cytometer from BD Biosciences. The cytometer was turned on and a backflush was run to remove any fluid from the system. The wash solution was run for 20 minutes with fast fluidics to remove any contaminants. 6 bead and 8 bead solutions were then run through the system according to the BD Accuri™ C6 manual in order to calibrate the machine.

Samples were run for 10,000 events with fast fluidics. Each sample was run twice. The secondary antibody used was anti-mouse (Vector DyLight IgG 488, green). Samples were gated according to the isotype and negative control, and analysed using the FL-1 channel.

2.4 Statistical Analysis

Data are presented as mean ± standard error of the mean (SEM). The SEM was used as the number of experimental repeats (n) was always 3 or more, and SEM is more appropriate for biological studies due to the inferential nature compared with standard deviation (Cumming et al., 2007). For the majority of the data one way ANOVA was used to determine statistically significant differences, and the Bonferroni correction was carried out using Origin software to calculate p-values. The Bonferroni correction was used as it is a conservative test, which reduces the chance of obtaining a false positive response (Shaffer, 1995). When there were only two sets of data to compare, the Shapiro-Wilk test was used to test for normality. When data was normally distributed when comparing two sets of data (as determined by the Shapiro-Wilk test), the Tukey test was used to test for significance. When data was not normally distributed, the Kruskal-Wallis test was used. The Bonferroni correction was not used for sets of data that only compares two conditions as there was no need to correct for multiple comparisons. For the comparison of histograms, the Kolmogorov-Smirnov test was carried out.

In this work, one experimental repeat (n) was defined as cells taken from different flasks/groups of animals. As only one source was available per cell line, these can never be true biological repeats. Care was taken to ensure that the flasks used had been cultured for at least two passages apart from cells in other repeats.

All tests were carried out with a confidence level of 95% (α=0.05) on raw data only. The α level is the probability of rejecting the null hypothesis when the null hypothesis is true. Unless stated otherwise, the null hypothesis was the means of all levels are equal. If the null hypothesis is rejected, it indicates that the population means are significantly different.

Statistics are only reported in the text when there are significant differences at the α=0.05 level. In all figures, a single asterisk (*) indicates p<0.05, two asterisks (**) indicate p<0.01, and three asterisks (***) indicate p<0.001.

3.0 Co-culture of Olfactory Ensheathing Cells

In this chapter, the behaviour of OECs in response to different types of feeders and conditioned media was examined. The goal was to determine whether OECs require physical or paracrine signals from fibroblasts to support their persistence in culture. Experiments were performed using OECs from rat and human. Initially cells derived from the rat mucosa were cultured on laminin versus human feeders obtained from the olfactory system (Section 3.3.1). Cell markers in OECs were examined in response to fibroblast-conditioned media in the presence and absence of feeders to determine the influence of paracrine signals (Section 3.3.2). This led on to studies comparing human feeders to commercial mouse embryonic 3T3 feeders, as the latter are available at GMP grade (Section 3.3.3). Finally experiments using a matrix of feeder and conditioned media parameters were performed using a conditionally immortalised human OEC line to assess the translatability of results obtained in rat to the human system (Section 3.3.4-5).

3.1 Introduction

OECs are notoriously difficult to grow (Barnett and Chang, 2004, Boyd et al., 2003, Lima et al., 2006, Gudino-Cabrera and Nieto-Sampedro, 1996) and one key question raised is whether OECs would better survive, grow and function if cultured with an underlying feeder layer. This is a common technique used for the culture of stem cells to either support the prolonged undifferentiated state or to encourage differentiation to a desired lineage (Richards et al., 2002, Simon et al., 2005, Fong and Bongso, 2006). Co-culture is used as a technique where cells are dependent on, or have enhanced function in the presence of other cells. Two or more cell types are grown together so the products of one cell type can be used to help the other, or have mutual benefits. This mirrors physiologic tissue where cells interact with each other and invoke dynamic signalling pathways (Bisson et al., 2015).

Fibroblasts support a range of tissues throughout the body, normally connective tissue (Petersen et al., 1995), and in the olfactory apparatus they form close interactions with OECs (García-Escudero et al., 2012). Pre-clinical transplant models have reported that the OEC function in SCI is dependent on the interaction between OECs and olfactory fibroblasts (OFs) (Keyvan-Fouladi et al., 2003, Ramón-Cueto et al., 2000, Raisman and Li, 2007, Teng et

al., 2008). Unlike OECs, there is no reported difference between fibroblasts obtained from the olfactory bulb as opposed to the olfactory mucosa (Yui et al., 2011). OFs are also thought to express NT-3 which enhances OEC growth (Ishihara et al., 2014).

In the olfactory system, it is thought that OECs and fibroblasts interact to help long distance axon regeneration (Li et al., 2005, Yui et al., 2011). It has been postulated previously by Jani and Raisman (2004), that olfactory fibroblasts are an essential support cell that enhances OEC function (Jani and Raisman, 2004). Whether this interaction is chemically (fibroblasts secreting growth factors) or physically (fibroblasts creating a biological scaffold for OECs) based, remains a point of argument (Yui et al., 2011). In addition to this, when OECs are completely purified, their ability to remyelinate axons is decreased (Blumenthal et al., 2013, Lakatos et al., 2003, Tabakow et al., 2014), indicating that another cell type is required which assists the OECs (Blumenthal et al., 2013). Fibroblasts are postulated to be this essential component which is required to promote axon regeneration in the spinal cord (Tabakow et al., 2014).

Fibroblasts are typically characterised using fibronectin, which is the major extracellular product from fibroblasts (McTigue et al., 1998). The cell surface antigen Thymocyte antigen 1 (Thy1.1) and Fibroblast Growth Factor (FGF2) (Wu et al., 2013b, Ebel et al., 2013) are also used to characterise fibroblast populations. However none of these markers are exclusive to fibroblasts and Thy1.1 is a recognised stem cell antigen (Hu et al., 2010, Eslaminejad et al., 2007, Wu et al., 2013a). Similar to OECs, this makes characterisation of a singular fibroblast population challenging.

Fibroblasts have been used extensively as feeders for epithelial cells (Kim et al., 2004, Lu et al., 2012). This layer is produced by inactivating the fibroblast monolayer with mitomycin c (MMC) for two hours at 37.5°C (Kim et al., 2004). This allows cell viability to be conserved but prevents proliferation. After this step, trypsin is used to remove the cells from the flask and the fibroblasts are plated at the desired cell density (Kim et al., 2004, Lu et al., 2012).

The first use of conditioned media to enhance the proliferation of cells was in 1966 where conditioned media from large populations of chick embryos was added to enhance the survival and proliferation of small populations of chick embryo cells (Rubin, 1966). As

reported in the previous section, fibroblasts have been used extensively as feeders to enhance the establishment of epithelial cells in culture (Yu et al., 2014). Studies have shown that the presence of feeders or conditioned media is enough to lend the necessary support to hES and mES to prevent differentiation. This indicates that fibroblasts secrete trophic factors that can have benefits such as long term proliferation and maintenance of pluripotency (Prowse et al., 2007).

3.2 Aim and Hypothesis

Previous research has shown that OEC survival and proliferation is diminished when OECs are grown at 100% purity (as defined by p75NTR staining), compared to when they are cultured as a mixed population (Blumenthal et al., 2013, Lakatos et al., 2003, Tabakow et al., 2014, Kachramanoglou et al., 2013, Li et al., 2003a). Therefore the initial aim of this chapter was to determine whether co-culture of OECs with fibroblast feeders enhances their activity. We hypothesised that olfactory fibroblasts would enhance the proliferation and survival of OECs.

Building on this initial aim, we wanted to determine whether conditioned media alone is sufficient to enhance OEC activity and if this occurs via paracrine signalling. We also wanted to determine if physical interaction between the two cell types is necessary which was carried out by using a commercial cell line, Ms3T3 cells as a substitute for human olfactory fibroblasts as a feeder. We hypothesised that olfactory fibroblasts would provide better support to the OECs due to its relevant anatomical origin.

In order to determine if these secreted factors are the reason that feeders have a positive influence of p75NTR expression and cell morphology, conditioned media was collected from the feeders and given to the OECs. If the trophic factors were responsible, it is expected that cells exposed to conditioned media would behave similar to those with feeders.

3.3 Results

3.3.1 Rat OECs co-cultured with HuG418 OFs

Primary rat OECs were co-cultured with immobilised HuG418 fibroblasts isolated from the human mucosa or cultured on laminin coated wells. The aim of this experiment was to determine if fibroblast feeders were required for rat OEC function.

3.3.1.1 Experimental Overview

In the first co-culture experiment rat OECs (OEC^Rs) were cultured on growth-inactivated HuG418 cells or laminin. This initial experiment was to determine whether feeders derived from the same anatomical location could positively impact OEC^Rs proliferation and survival. HuG418 feeders were immobilised using MMC for 2 hours at 37°C on day 0. Olfactory mucosa tissue from female Sprague-Dawley rats was isolated as described in Section 2.2.1 on day 1. Mucosal tissue from three rats was isolated per experimental repeat and four experimental repeats (n=4) were carried out.

After tissue digestion, dissociated mucosal cells were plated overnight to remove fast adhering fibroblasts from the culture through means of differential adhesion. On day 3, the supernatant containing non-adhered cells was plated evenly between the feeders and the feeder free condition in a total of 24 wells in two 24 well plates (3 wells per condition). Media changes were performed on days 7, 10 and 13. Cells were fixed on day 15 and stained using ICC techniques. Cells were stained for a panel of rat OMC markers; mouse and rabbit anti-S100β (BD Transduction Laboratories and Dako respectively), mouse and rabbit anti-p75NTR (Abcam and Millipore respectively), mouse anti-Thy1.1 (Millipore) and rabbit anti-α-SMA (Abcam). The secondary antibodies used were anti-mouse (Vector DyLight IgG 594, red) and anti-rabbit (Vector DyLight IgG 488, green) and the Hoechst used was from Sigma-Aldrich, UK.

3.3.1.2 Results and Discussion

First the feeder layer was characterised using antibodies against p75NTR, S100β, Fn, Thy1.1 and α-SMA. If and α-SMA. If OEC^R markers were positive in the absence of OEC^Rs, positive staining obtained in experiments obtained in experiments would not be able to be attributed to the OEC^Rs. The ICC shows that Fn was the only

that Fn was the only antibody that interacts positively with the HuG418 cells (Figure 3.1). This means that any positive cells for the other markers in these experiments can be attributed to the OEC^{R}s. Although Thy1.1 is a fibroblast marker, the antibody used had no reactivity with human cells (Section 2.3.1,

Table 2-1) and therefore the absence of positive staining was not of concern.

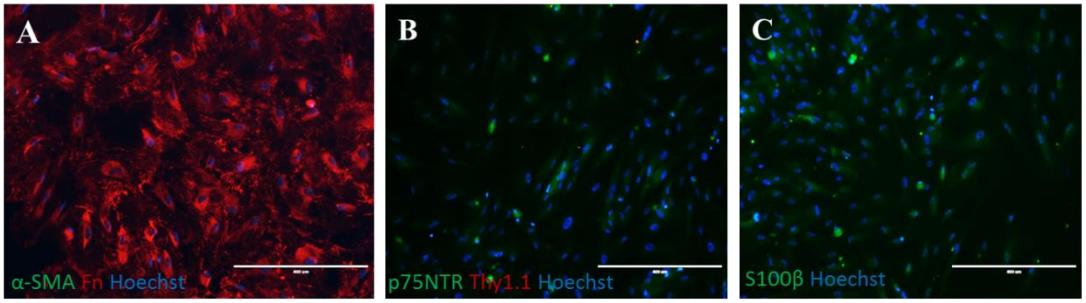

Figure 3.1: Human layer characterisation. Fluorescent micrographs of immunostaining carried out on the feeder layer without the presence of OEC^{R}s. Cells were fixed and stained to detect A) Fn (red), α-SMA (green), B) p75NTR (green), Thy1.1 (red) and C) S100β (Dako, green). All conditions were labelled with Hoechst to identify the nuclei of the cells. From this staining it can be seen that the markers used to characterise the OEC^{R}s did not cross react with the feeder cells. Additionally, the cells can be characterised as fibroblasts due to the positive labelling of the cells with fibronectin. The scale bar represents 400µm.

Next, OEC^R morphology was assessed at day 13 post-seeding using phase contrast microscopy (Figure 3.2). From these images it can be confirmed that the primary cells were able to survive on both laminin and the human feeder condition.

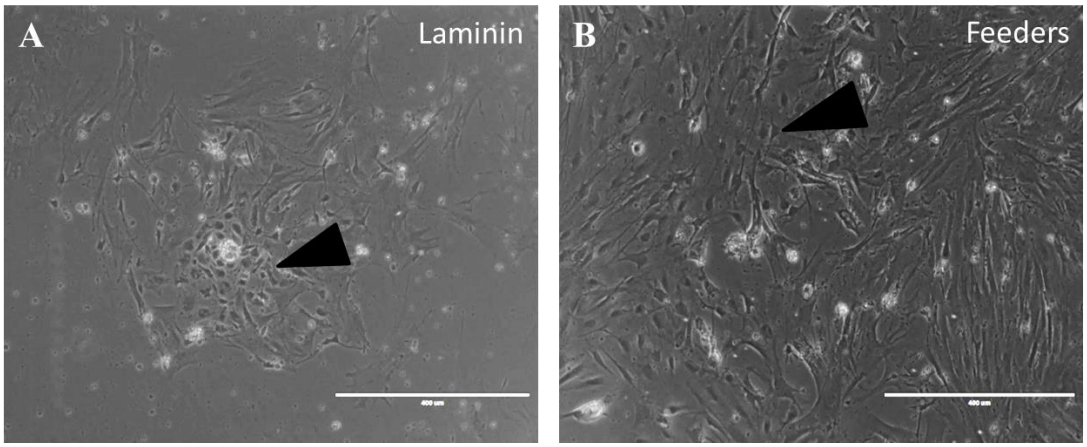

Figure 3.2: Identification of OEC^R cells in culture. Bright field micrographs of OEC^{R}s growing on laminin (A) and human feeders (B). Arrows point to OEC^{R}s populations which can be identified by their spindle shape. Images were taken on day 13. The scale bar represents 400µm.

Immunofluorescent labelling revealed that in the presence of OFs, expression of p75NTR in OEC^{R}s was enhanced. From the images obtained from the ICC (Figure 3.3) it can be determined that there was an increase in p75NTR expression (A, E) when OECs were

cultured on feeders. This was reflected in the quantitative analysis (Figure 3.4) where a significantly higher yield of p75NTR positive cells was measured on feeders (11.5±2.4 cells/mm^2) versus laminin (3.1±3.1 cells/mm^2, one-way ANOVA, Kruskal-Wallis post hoc, p=0.01). The ICC was quantified using yield (positive cells per mm^2) but not purity, as the presence of the feeders would make any assessment of purity misleading. There did not appear to be any visual differences with any of the other markers although there was potentially an increase in Thy1.1 expression (Figure 3.3E, F) although this is not as noticeable in Figure 3.3A and B. In literature, p75NTR expression has been observed to increase in relation to the expression of fibroblast growth factor 2 (FGF2) (Yan et al., 2001, Erck et al., 1998). The improvement in p75NTR expression could be due to the increase in FGF2 expression.

For Thy1.1 there appeared to be a tendency towards a higher expression in the presence of feeders, (17.9±9.6 cells/mm^2 on feeders, 3.5±1.1 cells/mm^2 on laminin) although there was no statistical significance (Figure 3.4). This tendency could imply that the HuG418 feeder cells are also giving some support to fibroblast impurities present in the OEC^R culture. Fibroblasts are known to communicate with each other via paracrine signalling loops to coordinate their actions (Wojtowicz et al., 2014). In addition to this, the particular extracellular matrix they excrete influences the neighbouring cells to behave in a similar way (Alberts et al., 2002). It is possible that although the fibroblasts are from different species, the extracellular matrix and paracrine signalling is still effective.

S100β staining in Figure 3.3D and H (mouse anti-S100β, Abcam) was not consistent with the S100β staining in Figure 3.3B and F (rabbit anti-S100β, Dako). On feeders the yield was 7.7±4.8 cells/mm^2 with rabbit anti-S100β and 34.2±9.3 cells/mm^2 with mouse anti-S100β. It is suspected that the mouse anti-S100β was unreliable due to less consistent staining occurring between repeats and this will be monitored in future experiments. Antibody unreliability is a known issue. This can occur due to different lots being produced in different animals. Numerous studies have been carried out validating the lack of specific staining and differences that occur in between lot numbers (Egelhofer et al., 2011, Bordeaux et al., 2010, Michel et al., 2009). Although antibodies are used frequently in biological studies, there are no universal guidelines or standardised methods (Bordeaux et al., 2010). This leads to variability and the assumption that Abcam and Dako follow different guidelines which could explain the differences observed.

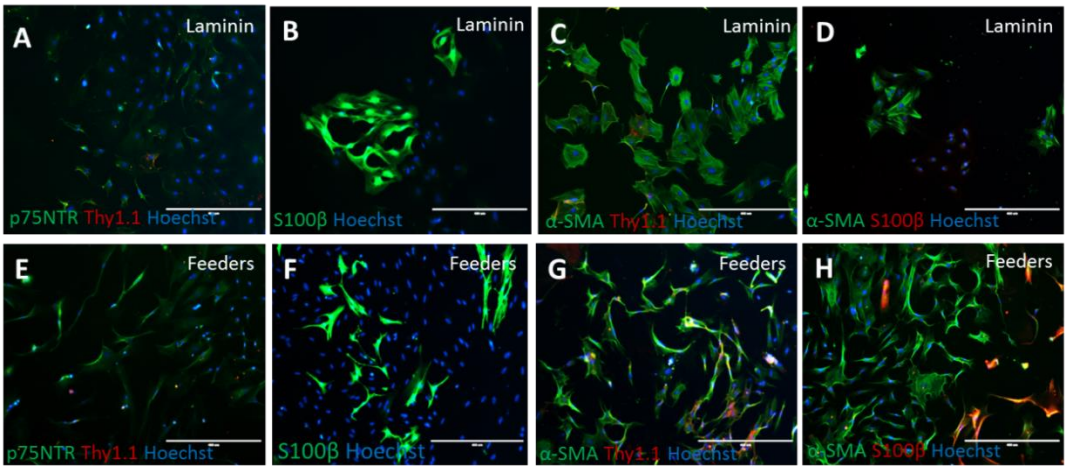

Figure 3.3: Fluorescent micrographs of a cell population derived from rat olfactory mucosa cultured on laminin and a human feeder layer. From images A and E it can be observed that p75NTR was more prevalent when feeders were present. Thy1.1 did not appear to have different levels of expression between the two conditions (A, C, E and G). The level of expression for other markers did not appear to change significantly between conditions. Comparing the feeder free system (A, B, C and D) to the feeder system (E, F, G and H), it was observed there was a change in morphology between the two conditions. When cultured in the feeder free system, the cells have a rounded morphology whereas cells grown on feeders can be seen to have adopted a more elongated morphology. The scale bar represents 400µm.

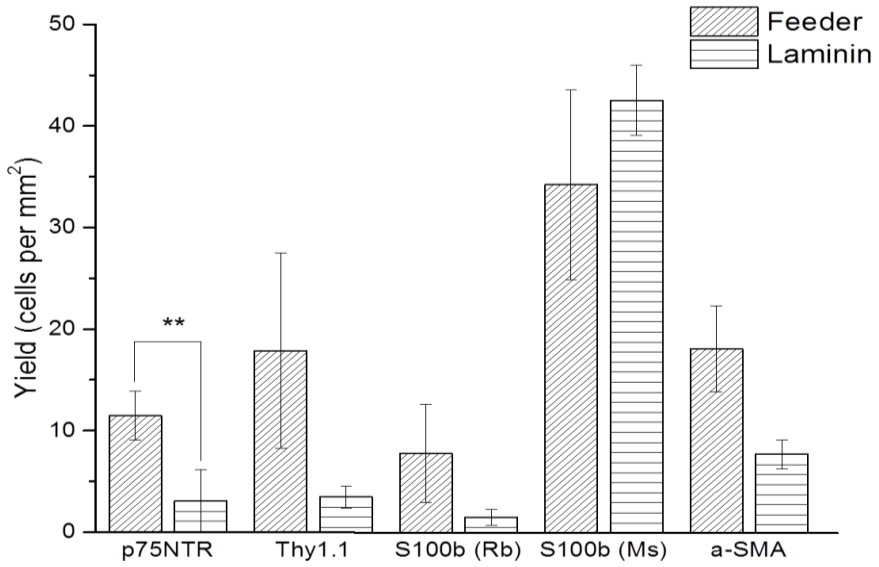

Figure 3.4: Yield of cells from feeder and feeder free conditions. From these results it can be seen that culturing cells on feeders results in significantly more p75NTR positive cells (Kruskal-Wallis test, *p*=0.01). Labelling with Thy1.1, both S100β antibodies and α-SMA did not show any significant results although there appear to be more Thy1.1 positive cells in the feeder condition. Two different antibodies were used for quantifying S100β and it can be seen that these antibodies were not equivalent in values. It is postulated that this occurred as one of the antibodies was not reliable and it was tested in the next set of experiments to determine its reliability. Data are means ± SEM, n=4.

It is very challenging to culture primary OECs, which leads to a wide variability in outcomes. This can be seen from the large error bars obtained in Figure 3.4 and has also been reported by others (Orbay et al., 2015, Tong et al., 2010, Niapour et al., 2010, Wen et al.,

2012, Mahapatra et al., 2009, Kawaja et al., 2009). This variability occurs in part due to a lack of robust markers by which OECs can be defined and isolated together with the heterogeneity of the cell types that make up the olfactory mucosa. Other cell types that may be present include basal horizontal cells, schwann cells, bowmans ducts and glands, sustentacular cells, olfactory fibroblasts, astrocytes and epithelial cells (Gomez et al., 2003, Choi et al., 2008, Barnett and Riddell, 2004, Boyd et al., 2003, Gorrie et al., 2010). In addition to this, there is no clear delineation between olfactory and respiratory tissues and therefore contamination with respiratory cell types is likely (Bianco et al., 2004, Ge et al., 2016).

Even though a differential adhesion step was used to remove rapidly adherent cells, leaving the slow attaching OECs in culture, the primary culture can still harbour contaminating cell types. This is demonstrated in Figure 3.5, where an entire well of OEC^{R}s on feeders was imaged at 10x objective magnification (EVOS Life Technologies AMF4300) and the resulting images merged together using *PanoramaPro2* in order to gain an understanding of the culture as a whole. It was observed that there are distinct areas of Thy1.1 positive colonies. When images were taken for counting, these images could yield data from 100% p75NTR positive to 0% p75NTR positive. This wide range of values results in a large standard deviation and therefore a large standard error of the mean across independent experiments (seen in Figure 3.4). These large errors are due to stochastic variability in the cultures due to different cell subsets present and these different cells can predominate in different regions of a single dish. This accounts for the dispersion of markers seen in Figure 3.5. From a cell manufacturing perspective, this again creates a significant challenge for creating a robust and well-characterised product.

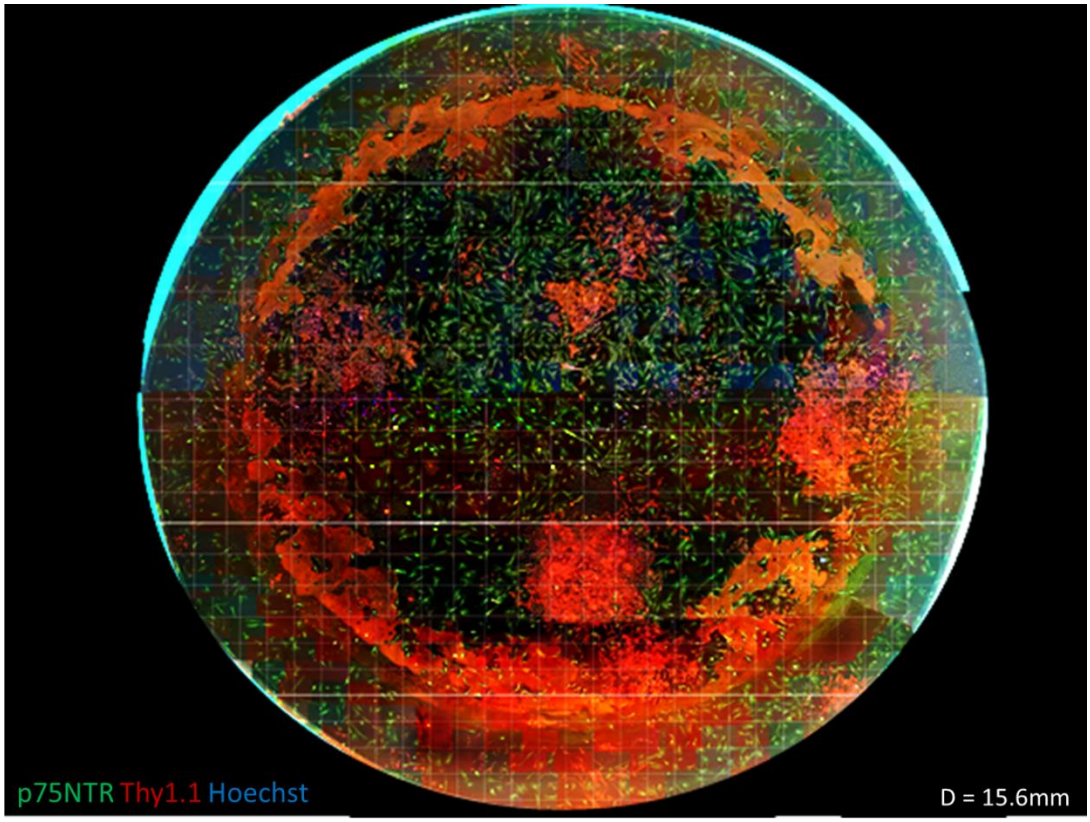

Figure 3.5: Assembled fluorescent micrograph of a cell population derived from rat olfactory mucosa cultured on a human feeder layer of olfactory fibroblasts. Images were taken at 10x magnification in a 24 well plate (diameter=15.6mm) and stitched together using *PanoramaPro2*. It can be observed in this stitched image that there are discrete cell populations present in the well plate. There are distinct areas of Thy1.1 (red) which do not appear to be indispersed with the more evenly distributed p75NTR positive cells (green). This variety in present populations explains the large error bars found in the cell counts. When multiple views were taken for counting, the purity ranged from 0-100% which resulted in a large standard deviation.

After staining, there was also a red/yellow ring around the peiphery of the plate that is not associated with any positive cells. On close inspection of the well plates used, it was found that the bottom of the wells was rarely smooth and often there were circular scratches, presumably as a result of the manufacturing process. It is postulated that the antibody interacted with this non smooth surface or was trapped in ECM deposited as a consequence of cell responses to the surface scratches and gave the circular staining (Stephens et al., 1997). This pattern was observed in several images; however, it was not until the full well was imaged that it was noticed that it made a complete circle.

OEC^Rs cultured on feeders adoped an elongated spindle shape whereas the cells cultured on laminin were found to be more cobblestone-like and enlarged (Figure 3.3). The distinct morphology of OEC^Rs cultured on feeders compared with those on laminin are not surprising, as distinct OEC morphologies have been reported in the literature. It is accepted

that OECs adopt one of two distinct morphologies. One morphology is enlarged, similar to that of an astrocyte, and the other more spindle shaped like Schwann cells (Kawaja et al., 2009, Omar et al., 2011, Oprych et al., 2016, Ramon-Cueto et al., 1993, Doucette, 1993). It has been claimed that this morphology can be controlled by adjusting culture conditions (Barnett and Roskams, 2008). However, it has also been seen that a cell with a spindle shaped morphology can produce enlarged daughter cells and vice versa (van den Pol and Santarelli, 2003). How this difference in morphology affects function is still debated but it is generally accepted that the spindle shaped morphology is more indicative of a phenotype that aids regeneration (Kawaja et al., 2009, Pellitteri et al., 2010, Fraher, 2000, Alexander et al., 2002). It is therefore possible that feeders could be used to control OEC morphology and associated function.

In order to quantify the morphology differences, a macro was written in ImageJ (as outlined in Section 2.3.3). The macro analysed the shape of the cells and returned a value of circularity, which is a ratio between the cell area and perimeter. The programme gave a visual output of the original image with cell outlines so it was possible to identify how accurately the programme had isolated and measured the circularity values. An example of input and output images is shown in Figure 3.6. As previously reported in Section 2.3.3, any cells that touched the border of the image were not measured as part of the area and perimeter were missing and therefore an accurate calculation could not be carried out.

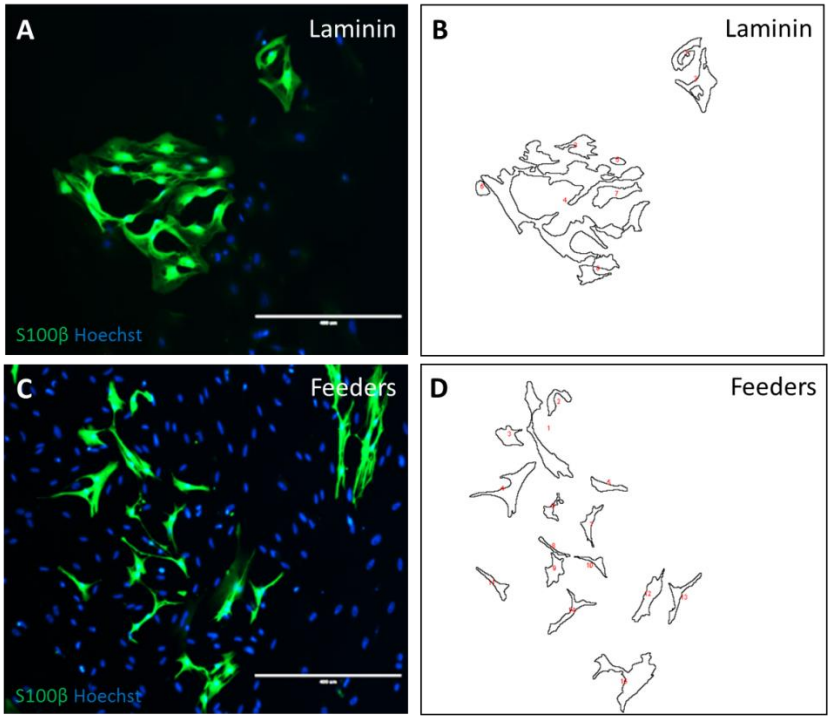

Figure 3.6: Input and output of ImageJ using the circularity macro. Fluorescent micrograph image showing candidate OECs at day 14 on laminin (A) and feeders (C) that were input to the circularity macro in Image J. S100β is shown in green and Hoechst in blue. B and D were the output from ImageJ when A and C were the input. Any cells that were touching the edge of the image were discarded and not counted in the calculation. Cells were selected, outlined and numbered according to the output data. Circularity was calculated as $4A\pi/P^2$ where A is the area of the cell and P is the perimeter. Outlines in images B and D can be seen to be a good match to the input image and therefore the circularity output can be trusted. The scale bar represents 400µm.

The circularity of every S100β (Dako) positive cell was analysed as they were present in comparably high numbers in both conditions. In addition to this, the nature of the marker expression meant that a full cell shape was easy to obtain, as opposed to α-SMA which stains in an incomplete pattern on laminin (Figure 3.3E) and also labels fibroblasts. This raw data was collated and presented in histograms which are shown in Figure 3.7.

From these histograms it can be seen that the distribution for OEC^Rs grown on feeders is shifted to the left, indicating more spindle shape cells are present whereas the distribution for laminin is more centred. This is backed up by the skew values which are 0.8 and 0.2 for the feeders and laminin respectively. A skew of zero indicates a distribution with perfect symmetry. From the skew numbers it can be determined that although both distributions have a left shift, this is more pronounced in the feeder condition. The flattened distribution of the laminin condition is quantified with the kurtosis value which is -0.8. A positive value indicates a peaked distribution and a negative value, a flat distribution. For comparison, a normal distribution has a kurtosis of zero using this calculation method. The feeder

distribution is only slightly less peaked than a normal distribution with a kurtosis value of -0.2. The Kolmogorov-Smirnov test was used to compare these distributions using the raw data and it was found that these distributions were significantly different from each other (p=0.04). This test compares the maximum vertical distance between the empirical cumulative distribution functions of the two samples (Noe, 1972, Bubeliny, 2013). As significance was found between these two distributions, this indicates that the presence of feeders had a significant effect on the morphology of the OEC^R population. Previously it was reported that changing culture conditions such as the serum concentration and inactivating the guanosine triphosphate RhoA resulted in changes in morphology. An absence of serum encouraged a process bearing morphology and more enlarged cells were encountered when RhoA was inactivated (Vincent et al., 2005). The results obtained here indicate that the presence of feeders, whether through paracrine or physical means, encouraged more spindle shaped OEC^{R}s.

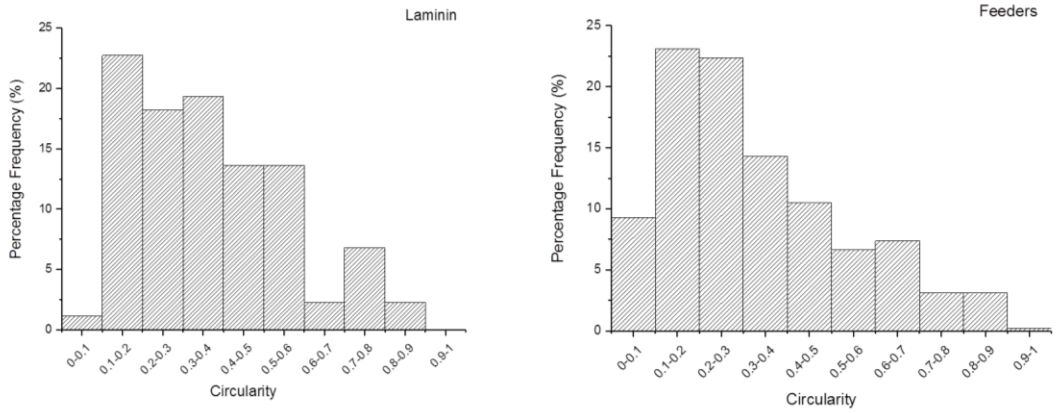

Figure 3.7: Circularity analysis on S100β positive cells when OEC^{R}s were cultured on laminin and feeders. From these distributions it can be seen that the circularity of OEC^{R}s on feeders tended towards 0.1-0.3 which is indicative of a spindle morphology. Compared to this, the distribution for cells on the feeder free system showed a more uniform distribution from 0.1-0.6. The feeder condition had a kurtosis value close to zero (-0.2) which shows that the peak is similar to that of a normal distribution. In feeder free, the kurtosis value is negative at -0.8 which quantifies the distribution as less peaked and more flattened. Statistical testing with the Kolmogorov-Smirnov test showed there was significant difference (p=0.04) between the distribution on laminin and the distribution on feeders. This data was analysed at n=4.

From this work it can concluded that the presence of feeders significantly upregulates the expression of p75NTR. This could be due to the increase of FGF2 expression which has been observed to upregulate p75NTR expression (Erck et al., 1998, Yan et al., 2001). Culturing OEC^{R}s on feeders also altered morphology leading to significantly more elongated cells compared with the culture on laminin. From this work, although a benefit is seen in the presence of human feeders, the interaction between the feeders and the OEC^{R}s was not

characterised. To further understand this relationship, it was decided to examine whether conditioned media from HuG418 feeders could modify p75NTR expression and cell morphology.

3.3.2 Rat OECs co-cultured with conditioned media from HuG418

After determining that fibroblast feeders influenced OEC^R morphology and p75NTR expression, the next experiments investigated whether the positive effects were due to physical presence of feeders, or secreted paracrine signals. To do this, OEC^Rs were cultured on feeders or laminin and in the presence or absence of HuG418-conditioned media.

3.3.2.1 Experimental Overview

To understand the influence of paracrine signalling independent of the physical presence of feeders, OEC^Rs were cultured in a feeder free system (on laminin) in the presence of conditioned media (CM) from HuG418. CM was added at a 1:1 ratio with fresh media to ensure cells received nutrients from fresh media as well as any soluble paracrine factors provided by HuG418. Conditioned media has been used in this way to influence the differentiation and proliferation of different cell types. For example, in oligodendrocytes, conditioned media from optic nerve cultures can enhance survival. This effect can be mimicked by adding a cocktail of factors to the media indicating that soluble factors present in the media are responsible for the increased survival rate (Cheng et al., 1998) and conditioned media has been found to contain relevant factors (Ge et al., 2016). It is postulated that similar to the oligodendrocytes, the OEC^Rs would benefit from soluble paracrine factors in the media from the HuG418 cell line.

The matrix of experimental conditions included feeders versus laminin and conditioned media versus standard media. It was hypothesised that if CM provided necessary soluble factors, then laminin with CM would perform as well as the feeders with standard media. This experiment was carried out to three experimental repeats (n=3).

3.3.2.2 Results and Discussion

Cells were cultured for 10 days and representative phase contrast images are shown in Figure 3.8. As with previous phase contrast images for these conditions (Figure 3.2), it can

be determined that the primary cells were surviving in all conditions. Although the feeder conditions look more confluent, this cannot be accurately determined due to the presence of the feeder cells. In both laminin conditions, there was no observable difference in the OEC^Rs morphology. OEC^Rs in feeder conditions are identified in the images with black arrows (Figure 3.1). Due to the close interaction between the feeders and OEC^Rs, it was not possible to determine any morphological difference in these images.

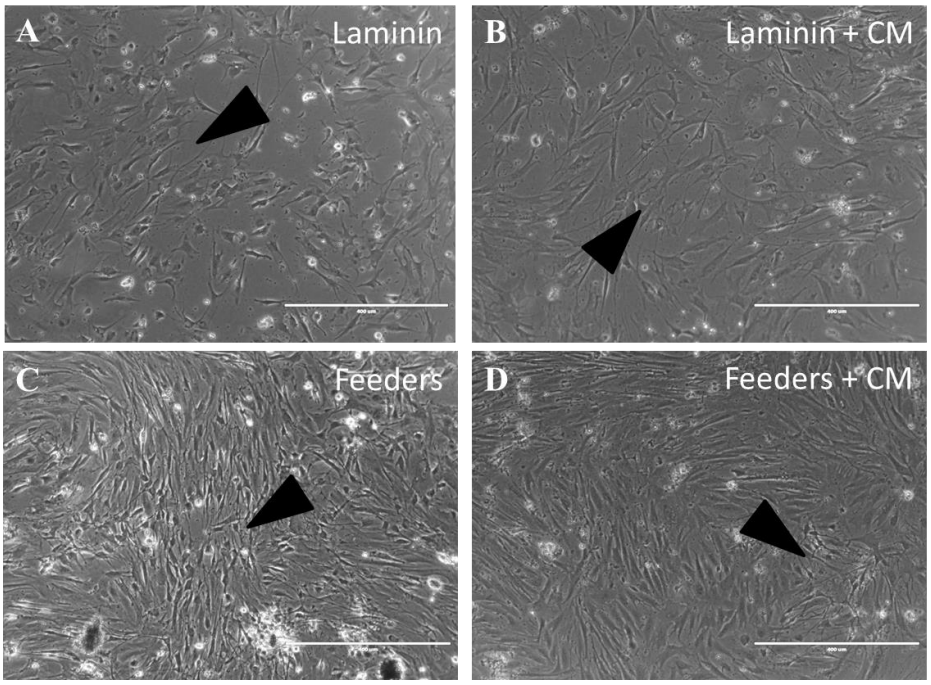

Figure 3.8: Identification of OEC^R cells culture in conditioned media. Bright field micrographs of OEC^Rs growing on laminin (A), laminin with conditioned media (B), human feeders (C) and human feeders with conditioned media (D) after 10 days in culture. Arrows point to OEC^R populations which can be identified by their spindle shape. From the phase contrast images it can be determined that there were OEC^Rs growing in all conditions. Cells appear to be more confluent in feeder conditions although this may not be significant as the presence of the feeders increases the number of cells present in the frame. The scale bar represents 400µm.

The ICC images from this experiment are shown in Figure 3.9 and Figure 3.10. Yield was the only measurement considered for the same reasons as previously reported in Section 3.4.1.2. The percentage of positive cells would be a misleading value due to the presence of negative feeder cells which would distort any purity count. The cell counts are shown in Figure 3.11. No significant difference was observed in α-SMA and S100β (Dako) staining.

It can be observed from Figure 3.9-Figure 3.11 that the addition of CM significantly increases the expression of Thy1.1. When CM was added to OEC^Rs cultured on feeders, an increase in Thy1.1 over and above the higher expression induced by feeders with standard media was observed (25.7±12.4 cells/mm^2 on feeders with CM from 14.5±4.8 cells/mm^2 on

feeders with standard media). The increase in Thy1.1 expression observed on laminin with CM (45.9±9.0 cells/mm^2) indicates that HuG418-derived CM affects Thy1.1 expression more when the feeders themselves were not present. This could be due to the feeders supporting themselves. Where feeders are present, those cells could uptake some of the soluble factors present in the CM, leaving a lower concentration of soluble factors for the OECs. This would mean that there are more soluble factors in the media when the feeders are not present. Fibroblasts participate in paracrine signalling (Alberts et al., 2002, Wojtowicz et al., 2014) and therefore it follows that if they are not present to receive the factors, the factors present can significantly assist other cells present.

p75NTR was present in all conditions at a similar level with the exception of laminin with standard media which was significantly lower at 4.0±0.8 cells/mm^2. The presence of CM increased the expression of p75NTR on laminin (19.7±7.6 cells/mm^2). An increase in p75NTR expression without the presence of the feeders would imply that there is some form of paracrine signalling going on. Whether this is due to FGF2 expression or a combination of other factors would require a deeper examination of the components in the CM. CM with laminin would be promising to take forward if it were not for the higher expression of Thy1.1. Thy1.1, historically an undesirable marker of fibroblast phenotype in the OEC field, negates the positive effect of the increase in putative OEC marker p75NTR as it implies a higher level of fibroblast impurities that would need to be removed from the culture.

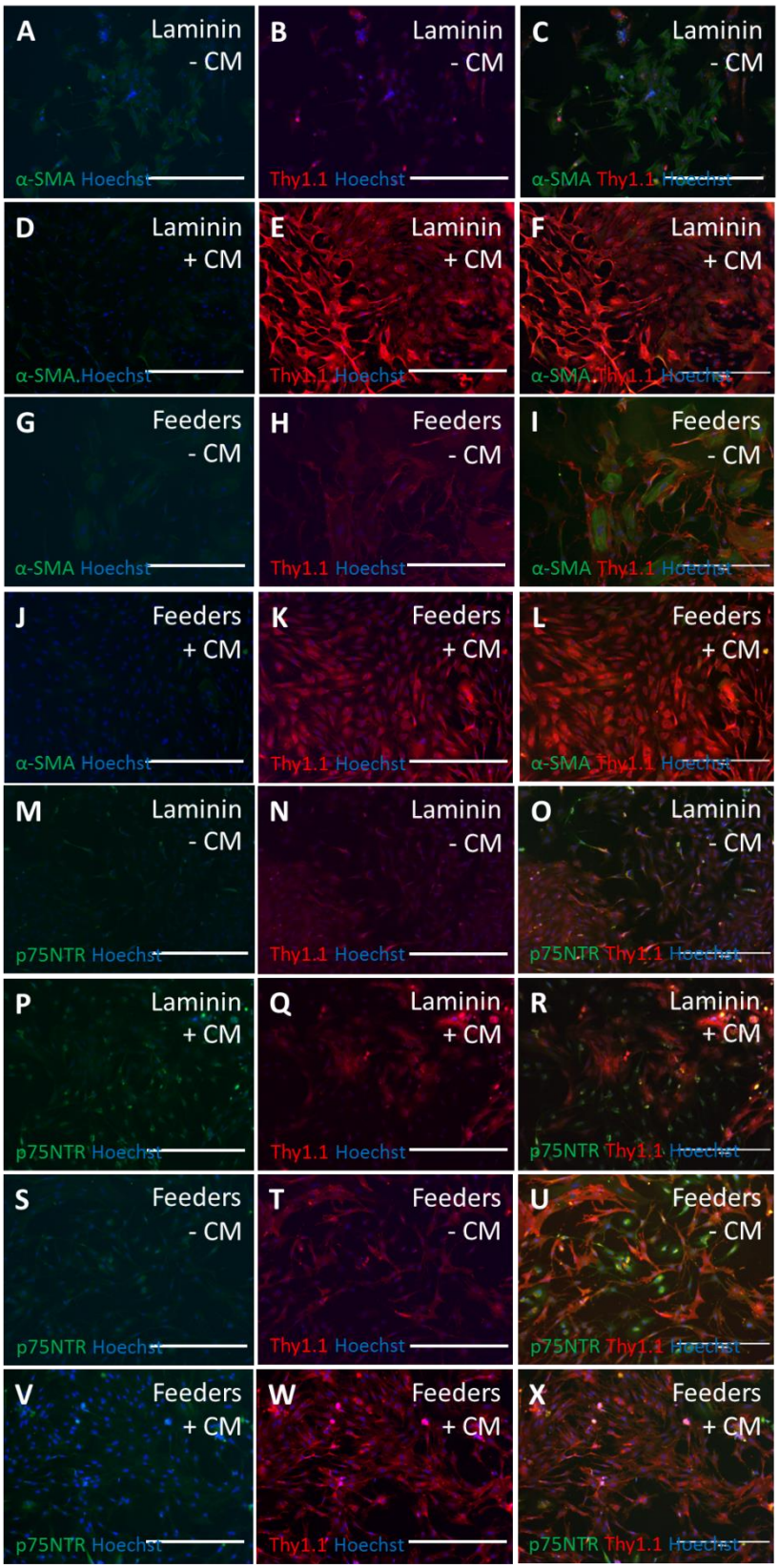

Figure 3.9: Fluorescent micrographs of a cell population from rat olfactory mucosa cultured on laminin and a human feeder layer with and without HuG418 CM. OEC^{R}s were stained on laminin (A-C, M-O), laminin with CM (D-F, P-R), human feeders (G-I, S-U) and human feeders with CM (J-L, V-X). Cells were fixed and stained at day 15 to detect α-SMA, Thy1.1, p75NTR and Hoechst. From these images it can be observed that the presence of CM significantly upregulated the expression of Thy1.1 (A-X). The scale bar represents 400µm.

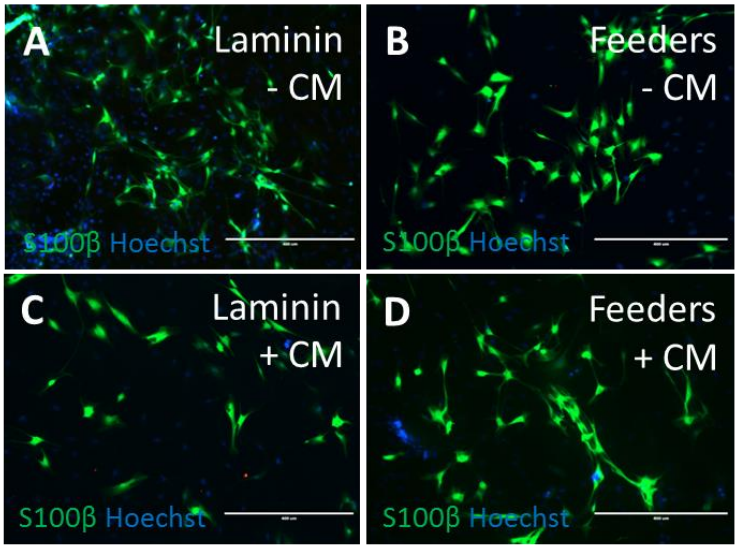

Figure 3.10: S100β fluorescent micrographs of a cell population from rat olfactory mucosa cultured on laminin and a human feeder layer with and without HuG418 CM. OEC^{R}s were stained on laminin (A), human feeders (B), laminin with CM (C) and human feeders with CM (D). Cells were fixed and stained at day 15 to detect S100β and Hoechst. From these images it can be seen that CM did not change the pattern of S100β staining. The scale bar represents 400µm.

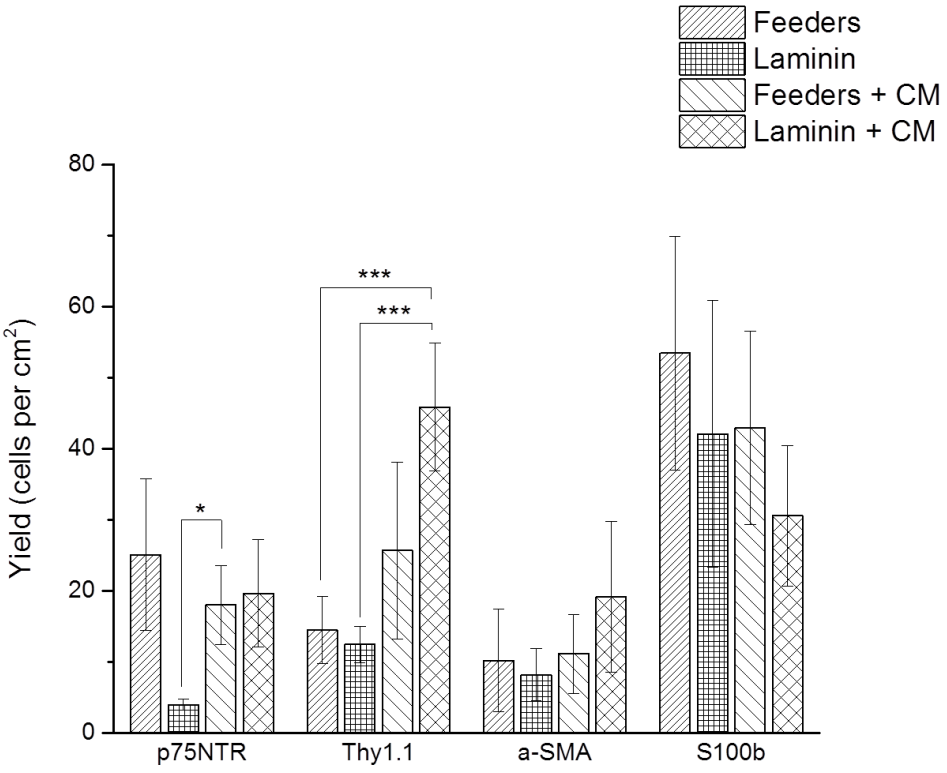

Figure 3.11: Cell counts conducted on wells stained with p75NTR/Thy1.1 and S100β/α-SMA in the presence of CM. This quantification validates what was observed in Figure 3.9-3.10. CM resulted in a significant upregulation of Thy1.1, especially when the cells were cultured on laminin (one-way ANOVA, Bonferroni post-hoc, p<0.001). The use of feeders enhanced p75NTR expression, however, the presence of CM also increased p75NTR expression on laminin. Data are means ± SEM, n=3.

Morphology of S100β positive cells was analysed in the same way as in the previous work (Section 3.4.1.2, using the macro detailed in Section 2.3.3). From the ICC in Figure 3.9, there was no obvious difference in cell morphology between conditions. Cells cultured on laminin with CM appeared to be more enlarged. Once the morphology was analysed in ImageJ, it was plotted and is visualised in Figure 3.12. Numerical analysis revealed that there was no significant difference between the distributions for feeders versus feeders with CM, and both conditions had a left skew (skew=0.4 and 0.5 respectively). The laminin condition with standard media remained similar to what was previously observed (skew=0.3, kurtosis=-0.8). This result validates the previous experimental work. When CM was added to the laminin condition, the distribution was significantly different to the standard laminin condition (one-way ANOVA, Bonferroni post-hoc, p=0.01). The distribution with CM had a less flattened distribution (kurt=-0.3 compared to -0.8) and a more pronounced left shift (skew=0.7 compared to 0.3). This is a stronger shift than the feeder conditions. This is significant as this was the condition with the most Thy1.1 positive cells. The most likely option is that spindle shaped OECs were also expressing Thy1.1 as well as S100β. Co-labelling of these antibodies was not been carried out in this study due to the lack of consistency experienced with the S100β antibody which meant the Thy1.1 and S100β antibodies used were raised in the same species. In Figure 3.9 co-labelling of p75NTR and Thy1.1 in OEC^Rs was observed. Literature has indicated that it is possible that OECs do co-express p75NTR and Thy1.1 (Hayat et al., 2003, Nash et al., 2001, Nash et al., 2002, Sonigra et al., 1999) and Thy1.1 and GFAP (Nash et al., 2001) so the assumption that Thy1.1 is a contaminating cell marker may need to be re-examined. Due to the lack of putative OEC markers (Ulrich et al., 2014, Barbacid, 1994), these cells are poorly characterised and this presents one of the major challenges of OEC research.

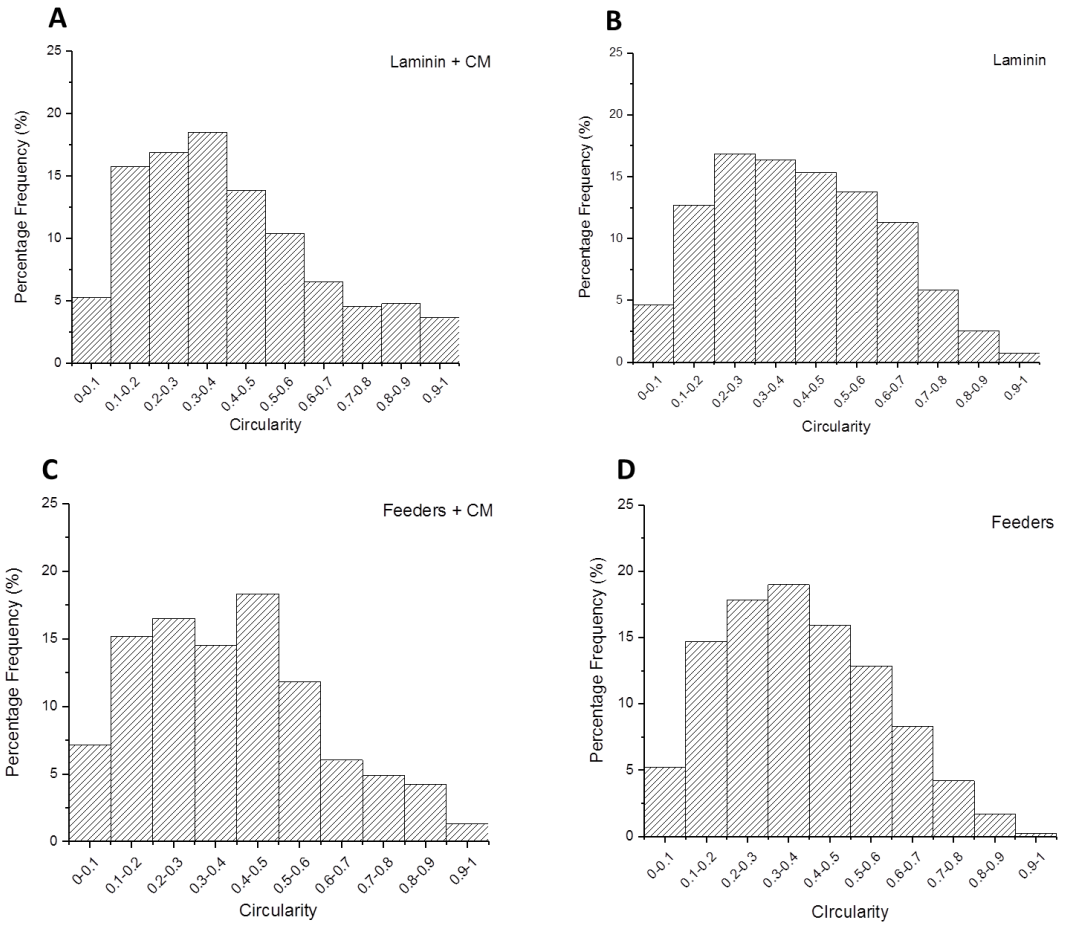

Figure 3.12: Circularity of S100β positive cells cultured on laminin with CM (A), laminin (B), feeders with CM (C) and feeders (D). The distribution for cells cultured on laminin does not have a sharp peak (kurt=-0.76) and is slightly skewed (skew=0.28). Feeders with CM show similar skew and kurt values as feeders alone (skew=0.45, kurt=0.46) and there was no significant difference between these two distributions. OECs grown on laminin with CM was significantly different to laminin with standard media (Kolmogorov-Smirnov test, *p*=0.01). This data was analysed at n=4.

From this experiment it could be determined from these results that although the presence of CM increases p75NTR expression by OEC^{R}s on laminin, it also results in a significant upregulation of Thy1.1, which has been historically regarded as an undesirable cell marker. However, the morphological analysis indicates that Thy1.1 may not be the undesirable cell marker it has been assumed to be. In the majority of the literature, Thy1.1 has always been treated as a marker of contaminating fibroblasts (Richter et al., 2005, Yang et al., 2014, Kueh et al., 2011, Vincent et al., 2005). It was found that a stronger shift to a more elongated cell shape occurred in the condition with the highest Thy1.1 yield. This is significant as the elongated cell shape is associated with regenerative properties (Pellitteri et al., 2010, Kawaja et al., 2009) and this would indicate that Thy1.1 was not necessarily having an adverse impact on OEC^{R}s morphology and functional properties. There is evidence that Thy1.1 is expressed by OECs (Ulrich et al., 2014, Nash et al., 2001, Sonigra et

al., 1999) and therefore it would appear that care needs to be taken when using Thy1.1 in isolation as a contaminating cell marker.

3.3.3 Rat OECs cultured with HuG418 and Ms3T3

CM was found to upregulate Thy1.1. To investigate whether the OECs response to feeders was specific to HuG418 cells or whether general fibroblasts would suffice, primary OECs were cultured with the original HuG518 cells or a mouse fibroblast line (Ms3T3) which is available as a GMP quality cell line. The aim of this experiment was to determine if the benefits found with feeder co-culture was specific to the HuG418 cell line or whether benefits could be seen with off the shelf GMP quality cell lines.

3.3.3.1 Experimental Overview

After showing that HuG418 feeders from the same anatomical locations as OECs could influence their characteristics, the next experiment sought to determine whether this is specific to anatomically matched fibroblasts or whether the response to feeders is generic enough that commercial GMP ready feeders could be used. HuG418 were isolated from the human mucosa whereas Ms3T3 are mouse embryonically derived cells. It was expected that if simple cell-to-cell contact was the only requirement, then Ms3T3 cells would support OECs as well as HuG418 cells.

Ms3T3 feeders were prepared the same as HuG418 feeders (detailed in Section 2.1.2.5) and the same panel of markers was used to characterise suitability of the feeders as a support layer. No feeder free condition was used as this was a straight comparison between two different feeder methods. Four experimental repeats were carried out following the 14 day protocol described in Section 3.3.1.1. Ms3T3 are a preferable option for a feeder layer as they are readily available to buy off the shelf as a GMP cell line (Waisman Biomanufacturing). This work was carried out with the help of an MSc student (Pelin Durali, UCL).

3.3.3.2 Results and Discussion

Characterisation of the feeders revealed that Ms3T3 cells stained positive for Fn, S100β and p75NTR (Figure 3.13). This reactivity has also been seen by other research groups (Hosoya

et al., 2006, Galow et al., 2017, Pugdee et al., 2007). The significance here is that care needs to be taken when assigning expression of these markers to OEC^{R}s.

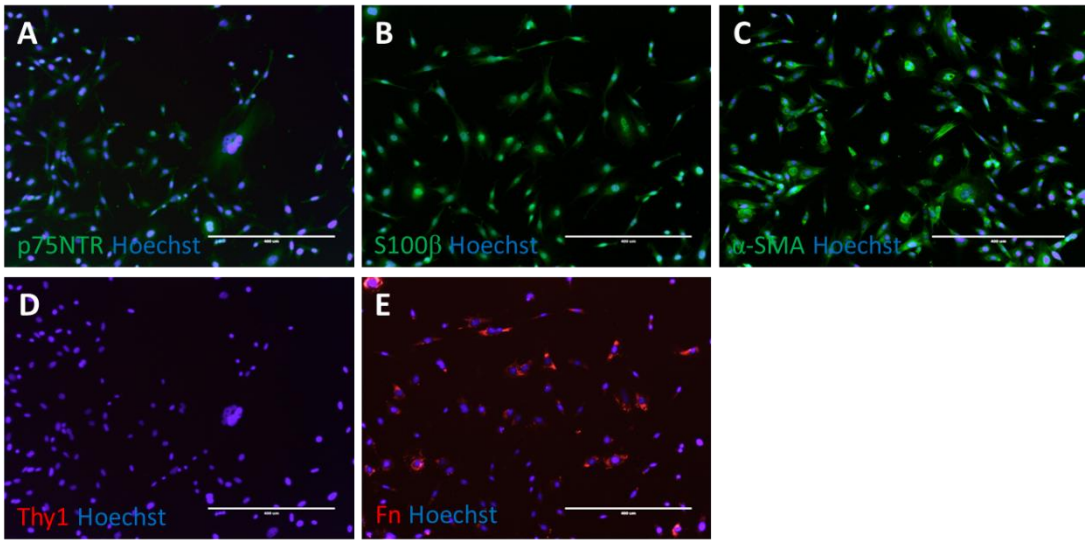

Figure 3.13: Mouse feeder (Ms3T3) layer characterisation. Fluorescent micrographs of immunostaining carried out on the feeder layer without the presence of OEC^{R}s. Cells were fixed and stained to detect A) p75NTR, B) S100β, C) α-SMA D) Thy1 and E) Fn. All conditions were stained with Hoechst to identify the nuclei of the cells. From this staining it can be seen that the markers used to characterise the OEC^{R}s stain the mouse feeder layer for S100β, Fn and α-SMA. The scale bar represents 400µm.

There appears to fewer attached cells in the Ms3T3 condition as determined by phase contrast images taken at day 7 (Figure 3.14). However, in spite of the unattached cells, surviving OEC^{R}s were observed on both types of feeders.

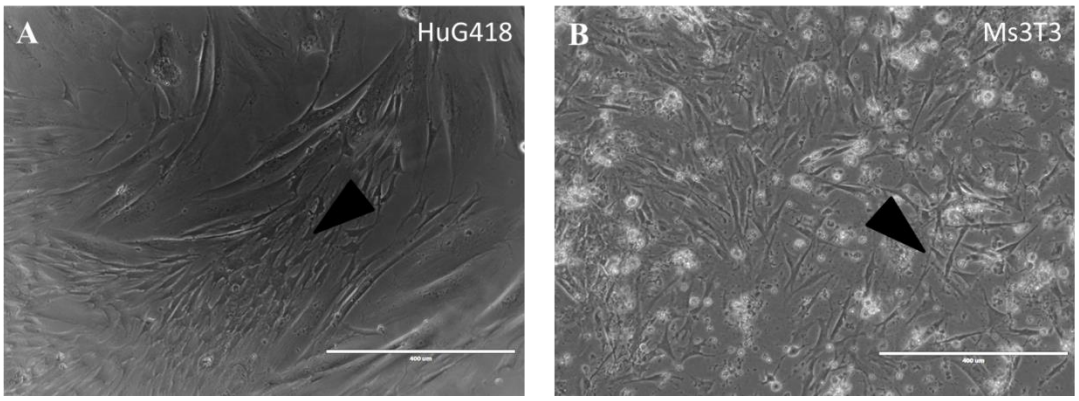

Figure 3.14: Identification of OEC^{R} cells in feeder culture. Bright field micrographs of OEC^{R}s growing on human (A) and mouse feeders (B). OEC^{R}s were plated on immobilised feeders and cultured for 14 days. These images were taken at day 7 and no difference between culture conditions was observed. Arrows point to OEC^{R} populations which can be identified by their spindle shape. The scale bar represents 400µm. Image credit: Pelin Durali, UCL.

One striking observation in the S100β (detecting OEC^{R}s) and Fn (fibroblasts) staining condition (Figure 3.15) was that the OEC^{R}s do not appear to grow directly over the feeder layer. Instead they grow close to the fibroblasts (Figure 3.15C and F). This placement makes sense if the cells are gaining benefits from cell to cell contact. If paracrine factors were involved, the OEC^{R}s would not necessarily border the fibroblasts so closely (Li et al., 2003b).

The ICC staining in Figure 3.15 was quantified using both purity and yield and the results from this are presented in Figure 3.16. Purity was used as a method to quantify the OEC^{R}s on the assumption that both feeder layers were plated at the same density and therefore there were equal numbers of negative feeders in each well and on average each image. Although this is not a perfect assumption, when it is considered alongside yield, it is justifiable. Purity was not used previously during quantification, as the presence of feeders in some conditions and not others meant any percentage value based on positively labelled cells would be distorted as there would always be negative feeders in the feeder conditions that would contribute to a lower percentage value being obtained.

From the ICC images (Figure 3.15A, D) and quantification (Figure 3.16), it was observed that α-SMA was more prevalent in the HuG418 culture (9.3±3.8% versus 2.0±0.8%). α-SMA is an actin binding protein in smooth muscle (Jahed et al., 2007) and is indicative of undifferentiated or immature cells (Hosoya et al., 2006). A higher level of α-SMA could therefore indicate that these cells are pre-cursors to an OEC sub-population. Alternatively, α-SMA has a role in cell division (Rockey et al., 2013) and therefore the cells plated on HuG418s are a more active proliferating culture.

No differences in p75NTR expression were observed on the different feeder layers (Figure 3.15C, D, and Figure 3.16) with purities of 4.9±2.0% and 9.7±4.4% on Ms3T3 and HuG418 respectively. This may indicate that the OEC^{R}s were benefitting from general cell-to-cell contact, not specifically to anatomically matched HuG418 cells. However, as both lines were comprised of fibroblasts, there could also be a common paracrine factor involved. OECs have been well documented to grow poorly in isolation and when a low yield is obtained, they do not proliferate (Lakatos et al., 2003, Blumenthal et al., 2013, Kachramanoglou et al., 2013). Additionally, they have been observed to survive better in a culture with a mixed population (normally OECs and OFs) (Keyvan-Fouladi et al., 2003, Tabakow et al., 2014, Teng et al., 2008, Ramón-Cueto et al., 2000, Raisman and Li, 2007).

This would also explain why the HuG418 CM did not have the anticipated beneficial impact on OEC^Rs p75TNR expression as hoped as the cells themselves may be required. In the literature, it has been observed that there is a close relationship between OECs and OFs. However it does appear that this relationship is due to the physical contact as opposed to any paracrine factors present (Jani and Raisman, 2004).

Thy1.1 expression was found to be significantly different between the two feeders (Kruskal-Wallis, p=0.01). As observed in the ICC images and quantification, the presence of Ms3T3 downregulated the expression of Thy1.1 (yield of 14.6±4.1 cells/mm^2 on HuG418 down to 4.8±2.1 cells/mm^2 on Ms3T3). This is important, as it indicates that the Ms3T3 feeders are superior to the HuG418 when it comes to supporting OEC^R growth and expression of p75NTR. OEC^Rs appear to be supported by cell to cell contact and from the results obtained in Section 3.3.2, do not gain any benefit from paracrine factors. These results suggest Ms3T3 feeders are superior to HuG418 cells as they result in fewer Thy1.1 positive cells whilst maintaining similar p75NTR expression levels.

In the ICC imaging and quantification, the difference between the Abcam and Dako S100β antibody was observed (Figure 3.15A, C, D and F). To confirm the unreliability of the Abcam antibody, OECs were labelled with both S100β antibodies for comparison (Figure 3.17). It was found that the Dako S100β resulted in brighter, more consistent labelling than those labelled with the Abcam S100β. The Dako antibody had clear labelling of the cells whereas the Abcam antibody, although faint labelling can be observed for most of the same cells, does not allow the same level of confidence of labelling to be obtained. Therefore, only the Dako antibody was used for subsequent experiments where S100β was characterised.

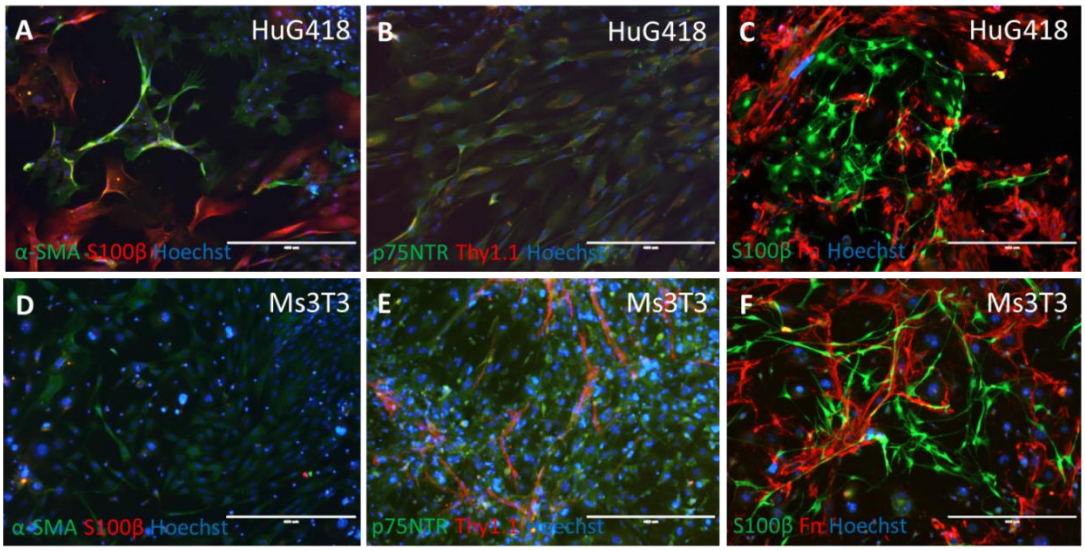

Figure 3.15: Fluorescent micrographs of a cell population derived from rat olfactory mucosa cultured on HuG418 and Ms3T3. From these images it was observed that the Abcam anti mouse S100β (A, D) did not produce the same results as the Dako anti rabbit S100β (C, F). There did not appear to be any significant increase in p75NTR (B, E) although Thy1.1 appeared to be more prevalent in the HuG418 condition. In terms of the successful S100β staining, it seemed the OEC^{R}s formed populations around the edges of the feeder layer as opposed to growing over top of the feeders (C, F). The S100β strands were mostly localised in between the positive Fn staining as opposed to clustering over the top. The scale bar represents 400µm.

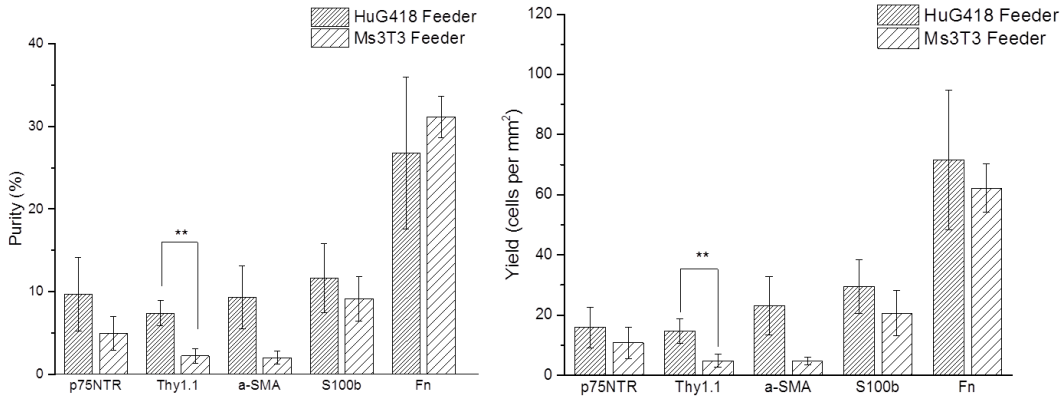

Figure 3.16: Purity and yield of cells grown on human and mouse feeders. These results have relatively large error bars due to the distinct populations present in the well plate. The only condition that exhibited any significance was Thy1.1 for both in purity and yield (Kruskal-Wallis, p<0.05). In the presence of HuG418 feeders the cells significantly upregulated Thy1.1 (Kruskal-Wallis, p<0.01). Although p75NTR shows higher expression in the presence of HuG418 feeders, this was not significant and not beneficial due to the upregulation of Thy1.1, an undesirable marker. Data are means ± SEM, n=4.

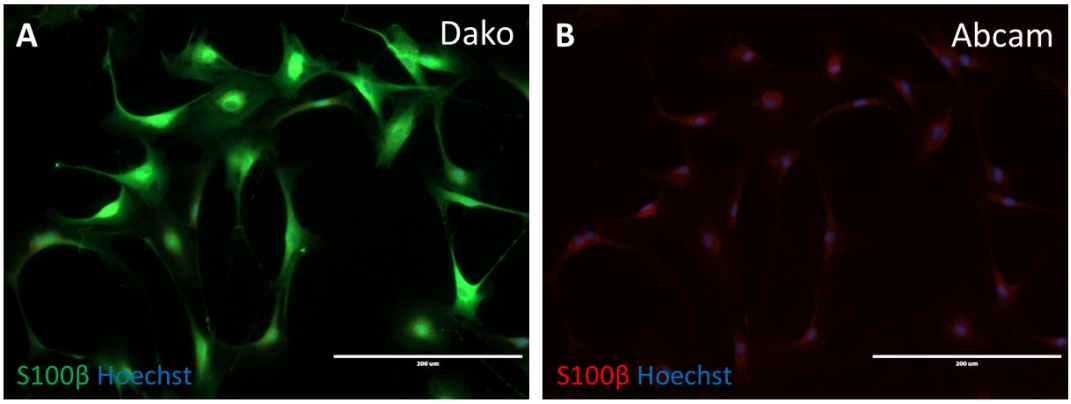

Figure 3.17: Comparison of S100β antibodies. The Dako antibody can be observed to label expression of S100β clearly. The Abcam antibody in comparison had weaker labelling. The differences shown here help explain why the labelling was not consistent between the two markers. From this point onwards, only the Dako antibody was used to ensure clear and consistent labelling was obtained. The scale bar represents 200µm.

The influence of the different feeder layers on cell morphology was also examined and the circularity analysis histograms are shown in Figure 3.18. The circularity analysis of S100β positive cells on HuG418 was consistent with what was observed for OEC^Rs on laminin and feeders (Figure 3.7 and Figure 3.12). Morphology of S100β positive cells on Ms3T3 also had a left shift (skew=0.54) towards a spindle shaped cell, although it was not as pronounced as that obtained on HuG418 feeders (skew=0.91). The shift obtained on Ms3T3 was also stronger than that of cells cultured on laminin (skew values around 0.20). This indicates that the mouse cells create a feeder layer that is functionally almost the same to the human fibroblast layer. Although the cells do not attain the same level of spindle morphology, they retain the same level of p75NTR expression while downregulating the fibroblastic marker Thy1.1.

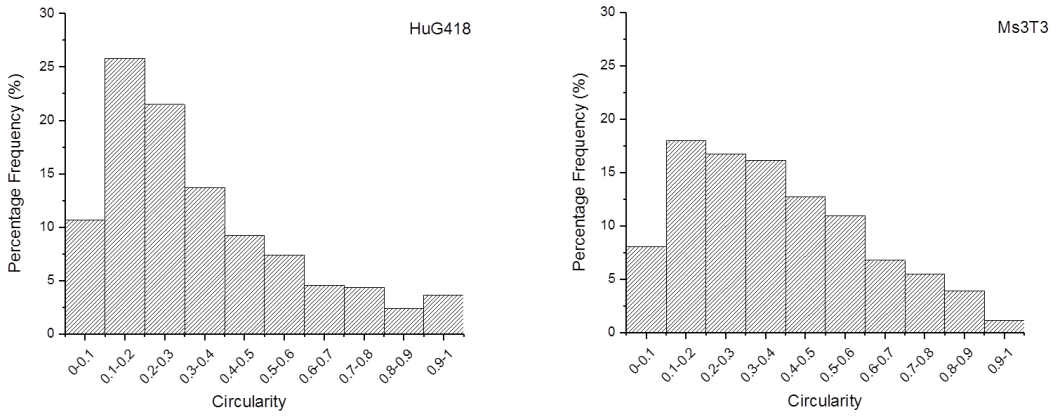

Figure 3.18: Circularity analysis on S100β positive cells when OEC^{R}s were cultured on human and mouse feeders. From these distributions it can be seen that there was a more defined peak obtained with HuG418. The kurtosis value remains low at 0.03 whereas the Ms3T3 distribution had a kurtosis of -0.54 which quantifies the peak strength. The skew value for HuG418 remains high at 0.91 showing the shift to the left in the distribution. The Ms3T3 distribution had a skew value of 0.54 which shows a less defined left shift. These distributions are significantly different according to the Kolmogorov-Smirnov test (p<0.05). This data was analysed at n=4.

These results, together with the results obtained with CM, indicate that OECs benefit from cell to cell contact rather than paracrine signalling by HuG418 cells. Ms3T3 cells are commercially available as a GMP cell line (Sigma-Aldrich, UK). Therefore their application as a feeder layer to enhance OEC phenotype during scalable manufacture is attractive to advance OECs towards clinic. Potential safety concerns around purity of the final clinical preparation could be addressed by purifying OECs with affinity-based removal of the mouse feeders. From this initial work with primary OEC^{R}s, it was found that OEC^{R}s have more promising regenerative function when cultured with feeders. However, there was no difference between human olfactory mucosa-derived feeders and mouse 3T3 cells in their ability to support OEC marker expression.

During this initial investigation into the behaviour of primary OEC^{R}s, work was ongoing in the lab to produce a conditionally immortalised human OEC cell line (as described in Section 2.1.4). Therefore the insight from these rat studies was applied to these candidate human cell lines in order to determine how translatable rat studies were. There are concerns that OECs in different animals behave differently (Wewetzer et al., 2011, Li et al., 2003a, Hahn et al., 2005). This is especially important when the length of the injury is considered. The gap to be bridged by the neurons is a lot smaller on a rat compared to a human (Li et al., 2003a) and the ability of OECs to support neurons over this small distance may not be relevant on human scale.

3.3.4 Human PA7 co-cultured with Ms3T3 and conditioned media from HuG418

Studies in small animals are important to generate pre-clinical data and to gain an understanding of responses in physiologic systems before moving to human. However, animal cells and tissue do not accurately reflect function or behaviour of human material and so human cells need to be studied. Therefore, the aim of the next experiment was to determine whether the responses of human OEC lines to feeders and feeder-conditioned media were the same for rat.

3.3.4.1 Experimental Overview

PA7 was the first human cell line that was expanded and used in experiments in the Regenerative Medicine laboratory at UCL. The PA7 cells were isolated from the human mucosa and after a differential adhesion step and 5 days in culture, immortalised with a retrovirus. The full details of the PA7 cell line creation is described in Section 2.1.4.1. Experiments were initially carried out using rat cells to determine the suitability of experimental methods and optimise pre-clinical work. Once protocols were established and the cell line technology was established, work began with human cells.

In order to determine the best culturing conditions and how these conditions relate to what was found with OEC^Rs, a variety of matrices and media conditions were tested. The matrix conditions were laminin, poly-l-lysine (PLL) and Ms3T3. Initially the PA7 cell line was expanded on PLL as this is the most commonly used matrix for OEC cultures (Alexander et al., 2002, Cao et al., 2007, Richter et al., 2005, Smith et al., 2002). The effect of PLL on glia is not well documented, although it has been observed to increase the rate of attachment of fetal neural cells to tissue culture plastic (TCP) flasks (Kozak et al., 1978). It is thought that PLL increases cell attachment due to nonspecific adhesion, where the polycationic polymer reduces the repulsive forces between the polyanionic surfaces of the cells and flask (Kozak et al., 1978).

OECs express laminin which promotes adhesion of many cell types and is typically used to culture stem cells (Goodman et al., 1987, Ramón-Cueto and Avila, 1998). Laminin has also been shown to support Schwann cell migration, differentiation and myelination and is upregulated during PNS injury (Wallquist et al., 2002). Therefore, laminin may be an ideal matrix for culture of OECs.

The media conditions used were standard media, standard media + NT-3, 1:1 standard media : CM, 1:1 standard media : CM + NT-3. From this matrix of 12 conditions, the goal was to identify optimal culture conditions for PA7. Three experimental repeats were carried out. Cells were cultured for 5 days with media changes occurring at day 3.

3.3.4.2 Results and Discussion

The PA7 cells gained a higher confluency when cultured on PLL and laminin as opposed to Ms3T3 feeders (Figure 3.19). In order to gain an understanding of the cell identity, ICC staining was carried out using S100β and Fn (Figure 3.20). p75NTR was not used for identification for this set of experiments due to issues with the reliability of a human p75NTR marker in the laboratory at this time. S100β is a suitable replacement as it is also a glial marker and is often used in conjunction with p75NTR as an OEC marker. The issue with using S100β is that it can also label Schwann cells which also may be present. Although these cells may be present, they are not expected to be present in high numbers. Studies carried out co-labelling rat and human OECs for human natural killer (HNK1), glial fibrillary acidic protein (GFAP) and p75NTR found fewer than 7% were positive for p75NTR, GFAP and HNK1, the combination attributed to Schwann cells (Gorrie et al., 2010, Feron et al., 2005, Bianco et al., 2004). S100β is consistently used in literature (Kawaja et al., 2009).

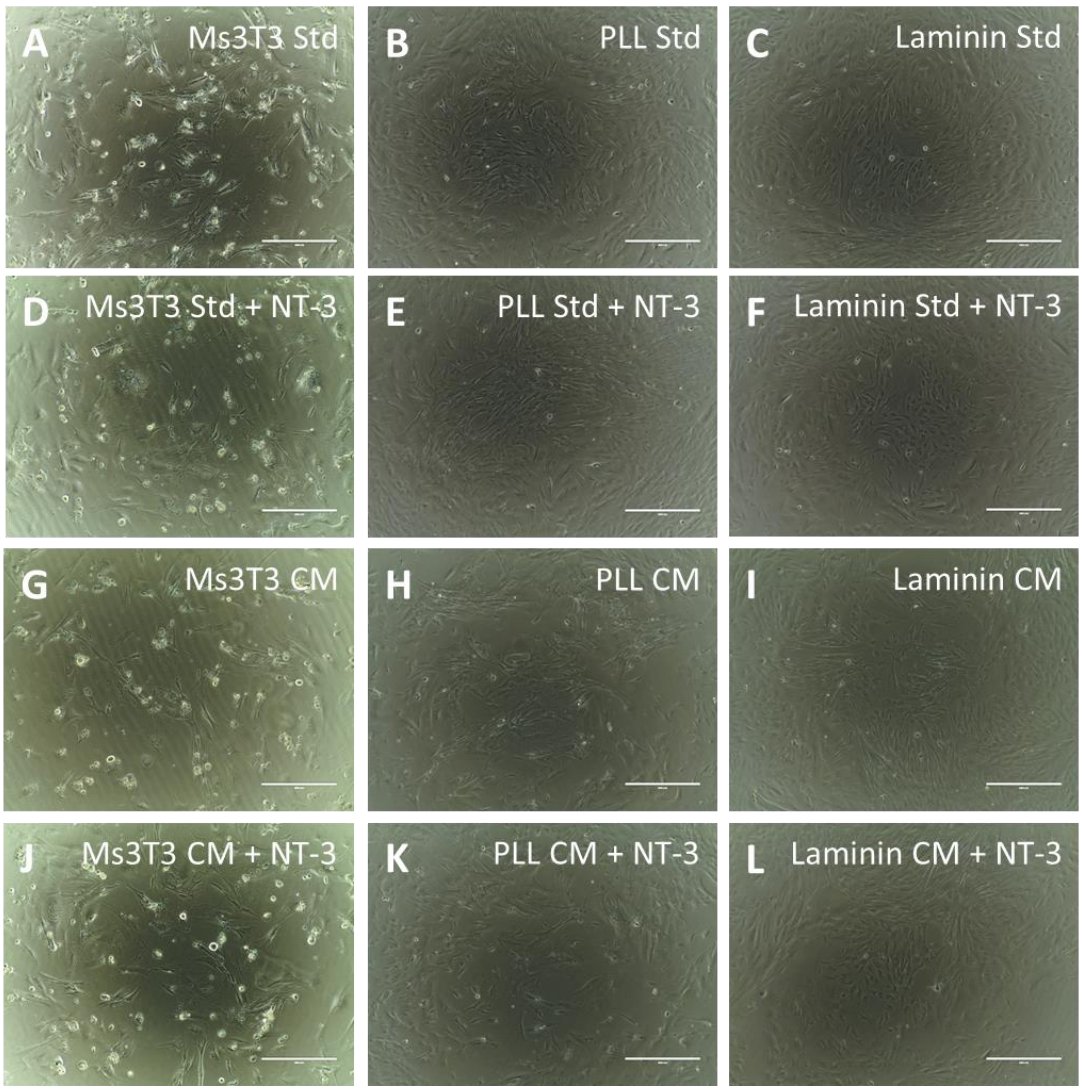

Figure 3.19: Bright field micrographs of PA7 cells plated on Ms3T3 feeders, PLL and laminin. These images were taken after 5 days in culture. It can be observed that a higher confluency was attained by the cells cultured on PLL and laminin (B, C, E, F, H, I, K and L) compared with cells cultured on feeders (A, D, G and J). It was difficult to determine the whether CM affects the confluency, although the cells with CM on laminin and PLL (H, I, K and L) seemed to be less confluent than those cultured with standard media (B, C, E and F). The scale bar represents 1000μm.

ICC micrographs revealed that Fn staining on laminin occurs in a completely different pattern to the other matrix conditions (Figure 3.20). In Ms3T3 and PLL conditions, the Fn deposition could be more easily traced back to the individual cells producing it. In contrast, on laminin, the staining pattern was more widely distributed. These distinct differences in the pattern were unexpected. Due to this staining pattern, cell counts and yield were not carried out for Fn due to the inaccuracy of determining the original cell responsible for the Fn. The reason for the different staining pattern on laminin is not known and no references to similar occurrences could be found in the literature. Cell counts and yield for S100β can be found in Figure 3.21.

S100β expression appeared to be more prominent in conditions with NT-3 compared with those conditions cultured in its absence (Figure 3.20). CM did not have any positive impact on S100β expression as confirmed in the quantification (Figure 3.21). When NT-3 was added alongside CM, an increase in S100β expression was observed compared to CM without NT-3. From the three matrix conditions, it was found the presence of Ms3T3 feeders was less beneficial for glial marker expression compared with PLL and laminin, which contrasts what was observed for OEC^Rs (yield of 64.7±22.0 cells/mm^2 on Ms3T3 with standard media compared to 79.8±21.1 cells/mm^2 and 98.6±18.4 cells/mm^2 for PLL and laminin with standard media respectively). This was not necessarily surprising as it has been found there are several differences between the rat and human olfactory system (Krudewig et al., 2006) including in vitro growth, spontaneous immortalisation and morphology (Omar et al., 2013, Rubio et al., 2008). Additionally, in terms of implantation and isolation, the OM in rats is yellow whereas in humans it cannot be discerned from the respiratory tissue (Bianco et al., 2004). This leads to a higher level of non-OECs being present in the implant which may or may not assist in regeneration. It does cause concern that any previous work that has been carried out in rat is not translatable to human scale up (Wewetzer et al., 2011, Ahuja et al., 2017).

Another difference between the rat and human OECs, is that the human OECs do not appear to benefit from the presence of NT-3. Although the study was not carried out as part of this thesis, other studies carried out in the laboratory at UCL have shown that NT-3 significantly increased the expression of glial markers in rat cells (Georgiou et al., 2017). For PA7, the presence of NT-3 seemed to slightly increase the purity of glial cell markers (Figure 3.21), and increase the level of expression (Figure 3.20), but none of these values were significant.

From the ICC and subsequent quantification (Figure 3.21), the best conditions for S100β expression in PA7 cells were identified as laminin coating and standard media.

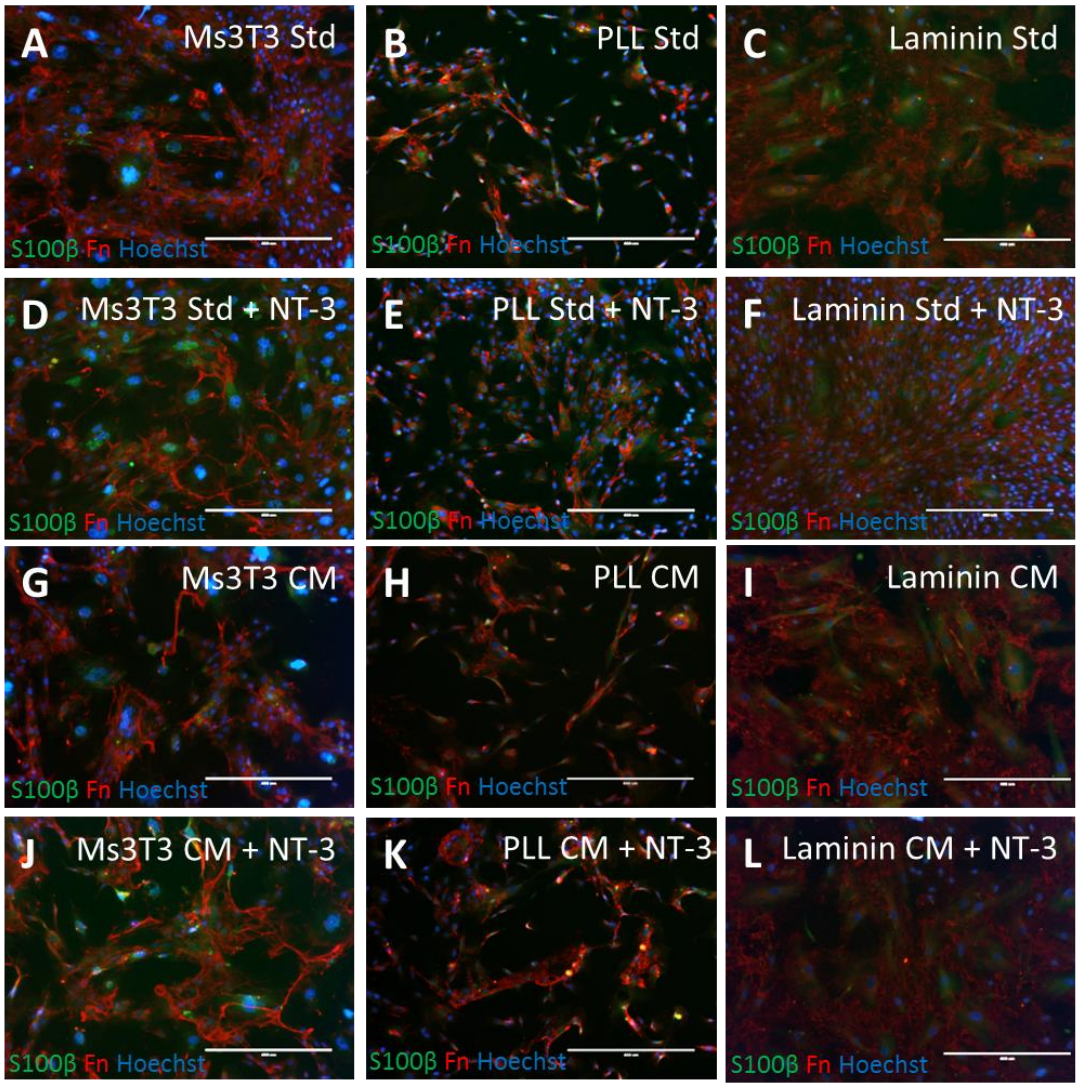

Figure 3.20: Fluorescent micrographs of PA7 cells cultured on laminin, PLL and Ms3T3 feeders with either standard media (+/- NT-3) or CM (+/- NT-3). Cells were fixed and stained for S100β (green) and Fn (red). Hoechst was used as a nuclear stain. It can be seen that the Fn staining pattern was distinctly different in conditions cultured on laminin (C, F, I and L). CM appeared to have a negative impact on S100β expression as it was more prominent in the standard media conditions (A, B, C, D, E and F). Additionally, NT-3 seemed to enhance S100β expression (D, E, F, J, K, and L). The scale bar represents 400µm.

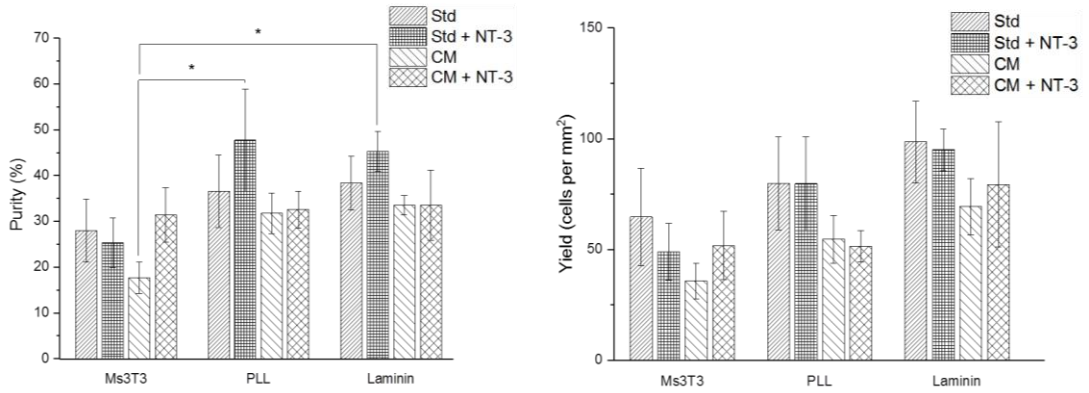

Figure 3.21: PA7 cell counts conducted on wells stained for S100β on different matrices under different media conditions. Culturing PA7 cells on Ms3T3 feeders produced the lowest purity and yield compared with the equivalent media conditions with PLL and laminin. In each matrices group it was observed that in general, CM led to a decrease in yield and the purity of S100β positive cells. NT-3 did not have a significant influence on S100β expression. Data are means ± SEM, n=3.

The differences that occur between rat and human OECs in regards to neurotrophic factors and matrix preference show that more in depth study and understanding of human OECs is necessary to be able to predict cell behaviour. It also indicates that care needs to be taken when translating results from rat to human OECs. Only one human cell line was investigated at this point, so some of these differences may be due to natural variability in human samples. To this end, a second candidate human cell line (PA5) was investigated using the same conditions to determine how species specific these results were.

3.3.5 Human PA5 co-cultured with Ms3T3 and conditioned media from HuG418

OECs obtained from human tissue are highly variable in their yield and behaviour (Wu et al., 2013a, Kachramanoglou et al., 2013). Therefore, the aim of this work was to repeat the experiment performed for PA7, using a second candidate cell line, PA5, to determine if the same expression patterns persist.

3.3.5.1 Experimental Overview

The experiments shown in Section 3.3.4 were repeated with PA5 to determine if the same trends were present and if any difference between the patient samples could be observed, or whether this variation was negligible in terms of human cell behaviour. The same media and matrix conditions were tested (n=3). In order to directly compare the experiments,

S100β was quantified for the different conditions, whereas the pattern of Fn was simply observed.

Due to the supply of antibodies in the laboratory at the time of this experiment, the secondary antibodies used were anti-rabbit (Vector DyLight IgG 594, red) and anti-mouse (Vector DyLight IgG 488, green). The implication of this is that the colours identifying S100β and Fn have been reversed from previous experiments.

3.3.5.2 Results and Discussion

Phase contrast imaging at day 5 revealed that cells cultured on Ms3T3 feeders appeared to reach a lower confluency than those cultured on PLL and laminin (Figure 3.22), similar to that seen with PA7 (Figure 3.19). Despite this, the differences between the feeders and PLL/laminin appeared to be less noticeable. When NT-3 was present, it seemed to have a promoting effect on cell proliferation under conditioned media conditions.

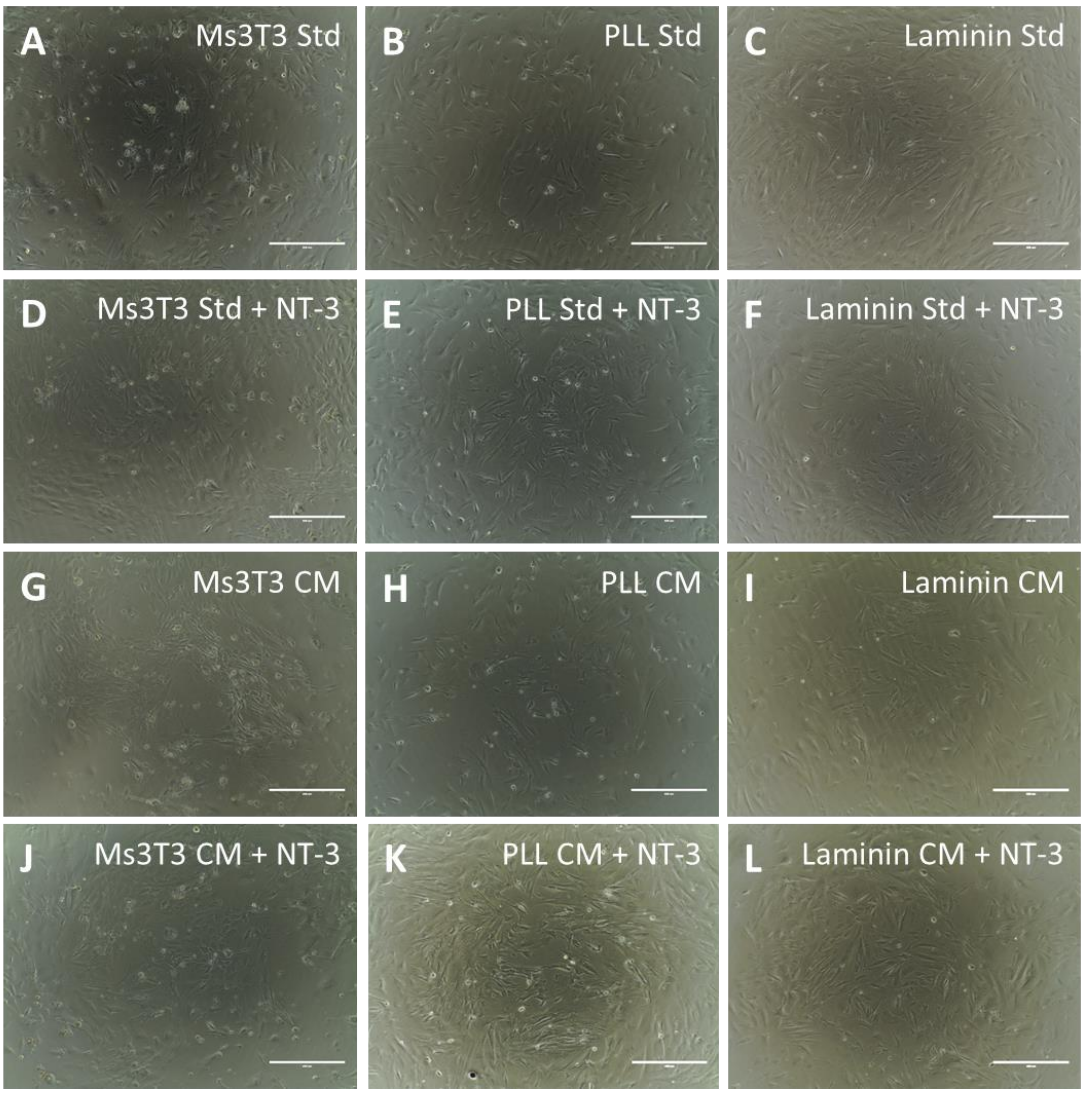

Figure 3.22: Bright field micrographs of PA5 cells plated on Ms3T3 feeders, PLL and laminin. These images were taken after 5 days in culture. It was difficult to determine any pattern from these phase contrast images in relation to the variables. NT-3 conditions may be encouraging higher confluency (D-F and J-L compared with A-C and G-I). It was difficult to determine whether CM influenced confluency from these images (G-L compared with A-F). The scale bar represents 400µm.

From the ICC micrographs and quantification in Figure 3.23 and Figure 3.24, it can be observed that laminin encourages stronger S100β expression (yield of 235.9±31.0 cells/mm^2 with standard media compared with 133.7±24.0 cells/mm^2 and 184.8±27.7 cells/mm^2 with standard media on Ms3T3 feeders and PLL respectively). In terms of purity, laminin with NT-3 had significantly higher purity of S100β cells compared with most of the Ms3T3 conditions (one-way ANOVA, Bonferroni post-hoc, $^{**}p<0.01$, $^{***}p<0.001$). Care needs to be taken looking at this measurement as the presence of the feeders that do not express S100β means the purity value obtained for Ms3T3 is actually lower than reality.

S100β expression was further enhanced with the presence of NT-3 (59.0±4.8% on laminin with NT-3 compared with 48.9±43% on laminin with standard media). As observed with the PA7s (Figure 3.20), conditioned media resulted in lower levels of S100β expression (48.9±4.3% on laminin with standard media compared with 44.4±4.1% on laminin with conditioned media). The presence of Ms3T3 feeders did not have a positive effect on the glial marker expression. Although PA5s on PLL showed evidence of S100β expression, this was not to the same extent as those cultured on laminin. In general, these images showed the same trends as those observed with the PA7 cell line.

Laminin with NT-3 was the highest performing condition in terms of yield and was significantly higher than most of the conditions with CM (one way ANOVA, Bonferroni post-hoc, *p<0.05, **p<0.01, ***p<0.001). This reaffirms the idea that CM does not have a beneficial effect on the expression of glial markers in the OEC population. This is in line with not only what was found with PA7 but also with primary rat cells.

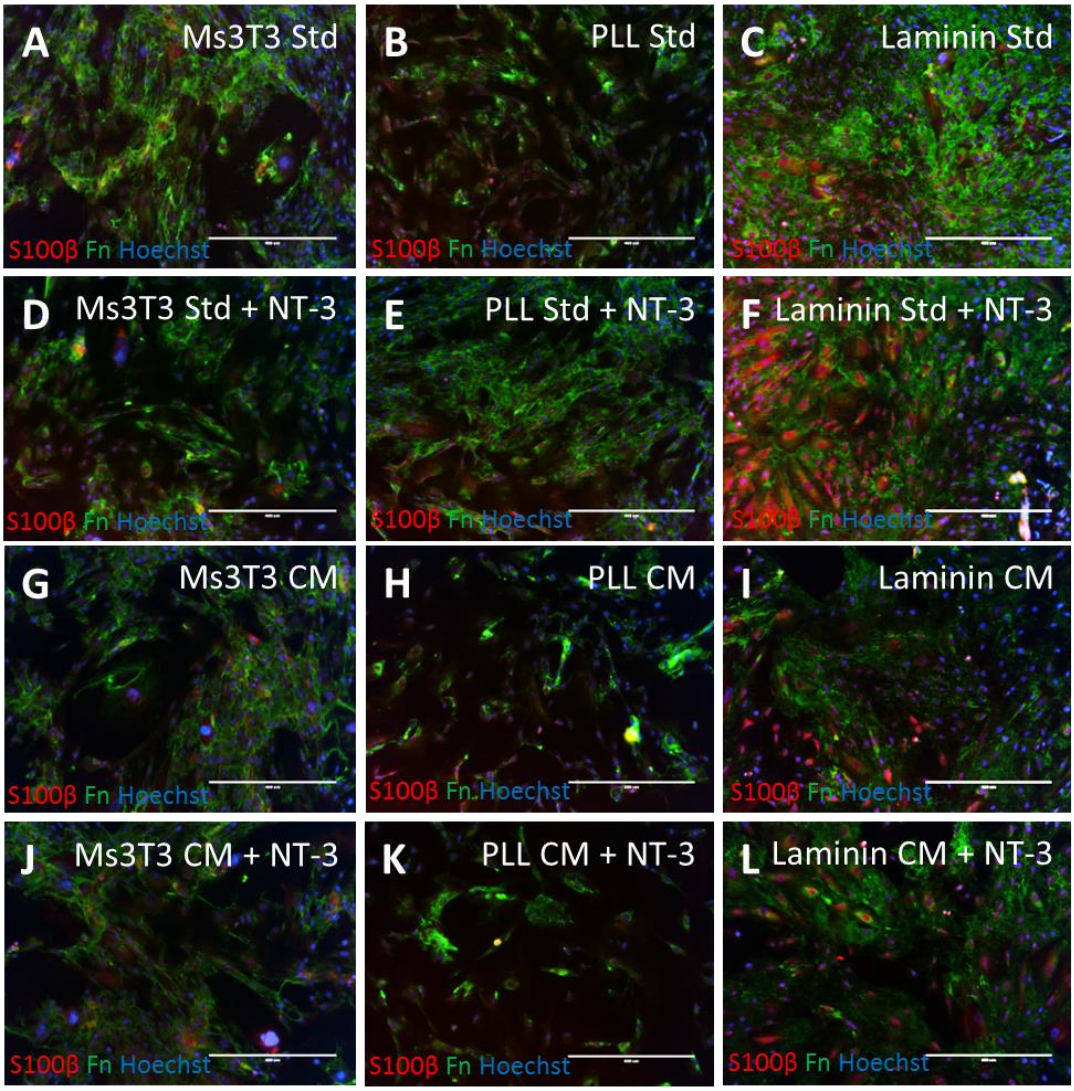

Figure 3.23: Fluorescent micrographs of PA5 cells cultured on laminin, PLL and Ms3T3 feeders with either standard media (+/- NT-3) or CM (+/- NT-3). Cells were fixed and stained for S100β (red) and Fn (green). Hoechst was used as a nuclear stain. It can be seen that as with the PA7 cell line, the Fn staining pattern was distinctly different in conditions cultured on laminin (C, F, I and L). CM appeared to have a negative relationship with S100β as it was more prominently expressed in standard media conditions (A-F). NT-3 increased the level of S100β expression. The S100β staining was brightest in the conditions with laminin and NT-3 (F and L). The scale bar represents 400μm.

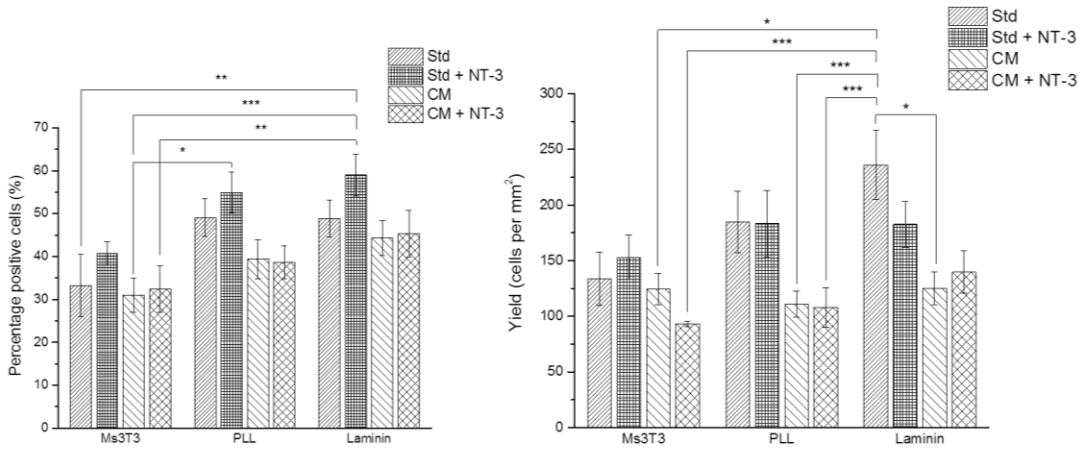

Figure 3.24: PA5 cell counts conducted on wells stained for S100β on different matrices under different media conditions. The PA5 cells followed a similar pattern to that exhibited by the PA7 cell line under the same conditions. For both cell lines, the addition of CM lowered both yield and purity. The addition of NT-3 increased purity for all matrix conditions although this did not necessarily translate to an obvious increase in the yield. The best performing matrix was laminin with both cell lines and the worst matrix condition was the Ms3T3 feeders. Data are means ± SEM, n=3.

The least ideal matrix for PA7 and PA5 was Ms3T3 feeders, which was in direct contrast to what was determined for OEC^{R}s. These observations collectively show that there are few similarities between rat and human OEC populations and research cannot be reliably translated between the two species (Dietz and Curt, 2006, Raisman et al., 2011, Wewetzer et al., 2011, Roloff et al., 2013, Techangamsuwan et al., 2009, Ziege et al., 2013). From these studies, it was determined to progress with the human cells.

3.4 Conclusions

From the OEC^{R}s work, it can be concluded that the optimum conditions for culturing are Ms3T3 feeders with standard media. These conditions resulted in the highest level of p75NTR expression with the lowest Thy1.1 expression. Although initially OEC^{R}s were cultured with feeders that also originated from the mucosa, it was found that the improvement they provided in terms of p75NTR expression was not cell line specific. It was determined that OEC^{R}s benefitted from cell to cell contact to enhance survival and the presence of soluble factors from OFs had a negative impact on marker expression, in particular Thy1.1, which was significantly upregulated. Thy1.1 is an undesired marker hence why CM and therefore paracrine factors are not thought to have a positive influence on the culture of OEC^{R}s.

The next phase of work moved to human candidate OEC lines. Two OEC^H cell lines were investigated to determine if they followed similar patterns to those obtained by the rat cells. It was found that feeders did not support OEC^Hs as well as ECM coating. CM was also detrimental to glial marker expression by OECs. The optimum conditions for growing OEC^Hs was found to be standard media with NT-3 on laminin coated flasks which was not the same as what was found for OEC^Rs. Therefore OEC^Rs are not suitable for undertaking studies of expected human cell behaviour.

Limitations in this study included the natural variability in OECs from the rat samples. The variability that exists between biological samples increases the standard error of the mean. This could be overcome by increasing the number of experimental repeats, however, the number of repeats required to identify outliers is expected to be high. In addition to this, not every type of coating and media was explored and therefore the conditions identified may not be the optimum for these cells due to the potential increased benefit of an unexplored variable.

4.0 Identity Markers and Purification of Human Olfactory Ensheathing Cell Populations

In this chapter, identity marker expression in OECs was examined using a human candidate cell line (derived in the Regenerative Medicine laboratory, see Section 2.1.4). Magnetic activated cell sorting (MACS) technology was used to immuno-deplete Thy1 positive cells from the OEC^H population, based on the reported observation that Thy1 cells are contaminating fibroblasts (Wu et al., 2013b, Ebel et al., 2013). The resulting sub-populations were then characterised using flow cytometry and ICC (Section 4.3.1). The expression of p75NTR and Thy1 in OEC^Hs was monitored over time (Section 4.3.2) to assess whether expression of markers is transient. The knowledge gained from this work was applied to the characterisation of the MACS purified fractions (Section 4.3.3). Finally, these purified fractions were cultured for six days to examine how the identity marker expression in these fractions changed over time (Section 4.3.4).

4.1 Introduction

As reported in Section 1.3.3, characterisation of OECs is challenging. This is because there are no definitive markers (Orbay et al., 2015, Tong et al., 2010, Niapour et al., 2010, Wen et al., 2012, Mahapatra et al., 2009, Kawaja et al., 2009) and the cells exhibit phenotypic plasticity and therefore do not express robust identity markers in a consistent fashion (van den Pol and Santarelli, 2003, Vincent et al., 2005, Ebel et al., 2013). One study found that mouse OECs were able to change from a rounded to a spindle shaped morphology in less than an hour using time lapse technology (van den Pol and Santarelli, 2003, Ebel et al., 2013). In addition to this, it was found that flattened cells could produce spindle shaped daughter cells and vice versa, independent of culture conditions (van den Pol and Santarelli, 2003).

OECs in the mucosa (where the PA5 cell line was isolated from) do not grow in isolation so there is potential for cell impurities including olfactory fibroblasts to be present in the PA5 OEC cell line. We sought to reduce this impurity risk by performing a 24 hour adhesion step, which removes rapidly adherent cells, leaving slow (~5 day) adhering OECs in culture. Therefore most anchorage-dependent cell impurities were assumed to be removed during

this differential adhesion stage. However, there is the risk that the process was not 100% effective.

It has been postulated in literature that there are two sub populations of OECs. These populations may have different functions that may involve both promotion and limitation of axon growth (Hayat et al., 2003, Ramón-Cueto and Nieto-Sampedro, 1992). Care needs to be taken when analysing purified or enriched populations, as interaction between the two sub populations may be required for functional operation.

p75NTR is widely reported in the literature as an identity marker of OECs (Section 1.3.3.2). Previous work in our laboratory (by Dr Melanie Georgiou, PDRA) attempted to utilise FACS to purify human OECs (PA5, PA7) using anti-p75NTR. However, cells did not survive the FACS purification process. This may be due to the p75NTR positive cells being sensitive to the shear stress during flow through the capillaries. Alternatively, as p75NTR is implicated in cell attachment and proliferation (Chen et al., 2009), the antibody may restrict the receptor's binding site activity, preventing attachment and proliferation. In order to circumvent this issue, Thy1 was used for MACs purification. MACS exposes the cells to lower shear stress and immuno-depleting Thy1 positive cells, rather than targeting p75NTR removes risk of compromising its binding site. In addition, any potential contaminating fibroblasts that had evaded the differential adhesion step would be removed from the culture.

p75NTR is reported to have an on/off switch mechanism (Gong et al., 1994, Vickland et al., 1991). Some attempts to isolate OECs from the olfactory mucosa and bulb have led to the observation of GFAP but not p75NTR expression (Franceschini and Barnett, 1996, Pixley, 1992, Huang et al., 2008, Franklin and Barnett, 1997) which raises questions on the identity of these cells and whether they are OECs that do not have p75NTR activated, or another type of cell. If p75NTR is not a consistent marker, it increases the difficulty of confidently identifying OECs in culture and questions whether another marker should be used as the identifying marker (Kawaja et al., 2009).

NT-3 has been reported to increase expression of p75NTR (Bradbury et al., 1999, Bregman et al., 1997, Xu et al., 1995, Ramer et al., 2005). Therefore, NT-3 was added as a neurotrophic factor to the media in some experiments. NT-3 was first described in 1986 by

Martin-Zanca (Martin-Zanca et al., 1986) and is a neurotrophin which is expressed by OECs (Bradbury et al., 1999). It acts through the Trk receptor (Barbacid, 1994) in order to promote remyelination and recovery of neuronal function (Zhang et al., 2017).

4.2 Aim and Hypothesis

The overall aim of this Chapter was to determine the stability of p75NTR in expression in culture. The specific objectives were to determine whether p75NTR and Thy1 were transient or constitutive markers for the PA5 cell line. In addition to this, we wanted to assess whether immune-depletion of Thy1 positive cells could enrich p75NTR positive cells.

4.3 Results

4.3.1 Characterisation of PA5 Purified Populations

PA5 cells were selected using MACS technology to immune-deplete Thy1 cells. The aim of this experiment was to characterise the unselected population and the retained (Thy1 positive) and eluted (Thy1 negative) fractions in order to determine whether p75NTR was enriched in the absence of Thy1.

4.3.1.1 Experimental Overview

The PA5 population was immuno-depleted for Thy1 using MACS technology with an LS column. LS columns are recommended for positive selection, where the magnetic beads attach to the cells of interest and LD columns are used for depletion, where the beads attach to cells needing removal from the process (Miltenyi et al., 1990). Initially LD columns were used for the purification as the aim was to deplete Thy1 from the population, however the flow cytometry results obtained showed no form of purification taking place (data shown in Appendix One). When LS columns were used, a change in Thy1 positivity could be observed in the population. Therefore, LS columns were used in this study.

The process of MACS purification is outlined in Figure 4.1. The magnetic beads are coated with Thy1 antibody, and therefore Thy1 positive cells attach to these beads. Cells are run through the column inside a magnetic field. Any cell that binds to a bead is retained inside the column as the magnetic field holds it in place. Thy1 negative cells are allowed to flow through the column and multiple column volumes are washed through the column to ensure all negative cells have left the column. After the Thy1 negative cells (eluted) have been collected, the column is removed from the magnetic field and the positive cell fraction (retained) can be collected (Miltenyi et al., 1990). These cells can then be cultured and differences in behaviour observed. The beads are biodegradable and do not persist in the culture after 72 hours (Miltenyi et al., 1990).

In this chapter, 'PP' refers to the ***pre-purified*** fraction. This was an unselected cell population that was taken from the cell culture before MACS was performed. 'E' refers to the ***eluted*** fraction which comprises of Thy1 negative cells. 'R' refers to the ***retained***

fraction which is the population that bound to the beads and was therefore positive for Thy1 at the time of purification.

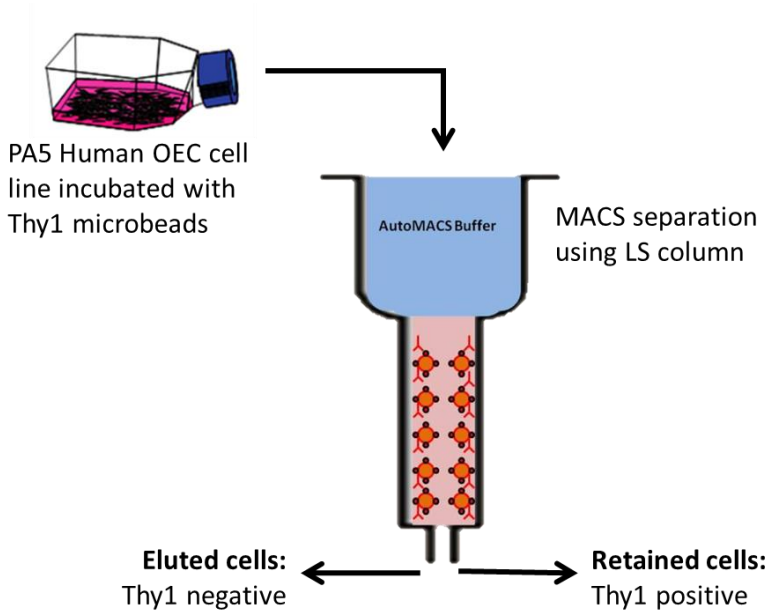

Figure 4.1: MACS purification process. Cells are incubated with microbeads that are coated with anti-Thy1 antibody. Cells that are positive for Thy1 attach to these magnetic beads. The cells are then put through a column in a magnetic field. Cells that are negative for Thy1 flow straight through (eluted cells) as the magnetic field does not affect them. Once the column is removed from the magnetic field, the cells that are positive for Thy1 are able to leave the column (retained fraction).

The efficiency of the MACS purification was assessed using flow cytometry and ICC. A sample was taken from the PA5 population before purification and plated at 12,000 cells/cm^2 in a 96 well plate. Samples from retained and eluted fractions were plated at the same density. All cells were fixed at 24 hours and labelled using ICC with Triton X permeabilisation. Flow cytometry was carried out immediately after purification (which included incubation with a fluorescent secondary antibody) and the pre-purified cell sample was live-stained in parallel and characterised using the BD Accuri™ C6 flow cytometer. An isotype control was run (IgG1 FITC, BD Biosciences) to compensate for any non-specific binding.

As the process aimed to remove Thy1 cells, the expected results were two distinct cell populations, one Thy1 depleted and the other Thy1 enriched. Antibodies were targeted against cell identity markers p75NTR (Millipore), S100β (Dako), Fn (Sigma-Aldrich, UK), Thy1 (Sigma-Aldrich, UK) and α-SMA (Abcam) to characterise the populations. The secondary

antibodies used were anti-rabbit (Vector DyLight IgG 594, red) and anti-mouse (Vector DyLight IgG 488, green).

4.3.1.2 Results and Discussion

In Figure 4.2, the flow cytometry graphs are displayed. M1 represents the Thy1 positive fraction and M2 represents the Thy1 negative fraction. The pre-purified fraction was mostly comprised of Thy1 positive cells (83.9% Thy1 positive, Figure 4.2B). The eluted fraction (Figure 4.2C) was mostly Thy1 negative (93.0% Thy1 negative) which confirms purification had taken place. In contrast, the retained fraction (Figure 4.2D), can be seen to have a split population with some Thy1 negative cells still present, but generally high levels of Thy1 positive cells (78.7% Thy1 positive). The Thy1 positive fraction had proportionally fewer Thy1 positive cells than the original population. This is may be due to the difficulties that occur when dealing with a population which is already highly pure (Miltenyi et al., 1990) or the plasticity of the cells in regards to protein expression (Sonigra et al., 1999, Barnett and Riddell, 2004, Ebel et al., 2013, Boyd et al., 2003, van den Pol and Santarelli, 2003). This was not regarded as a key issue as the eluted fraction was the key population of interest and the flow cytometry results indicated that the purification was successful.

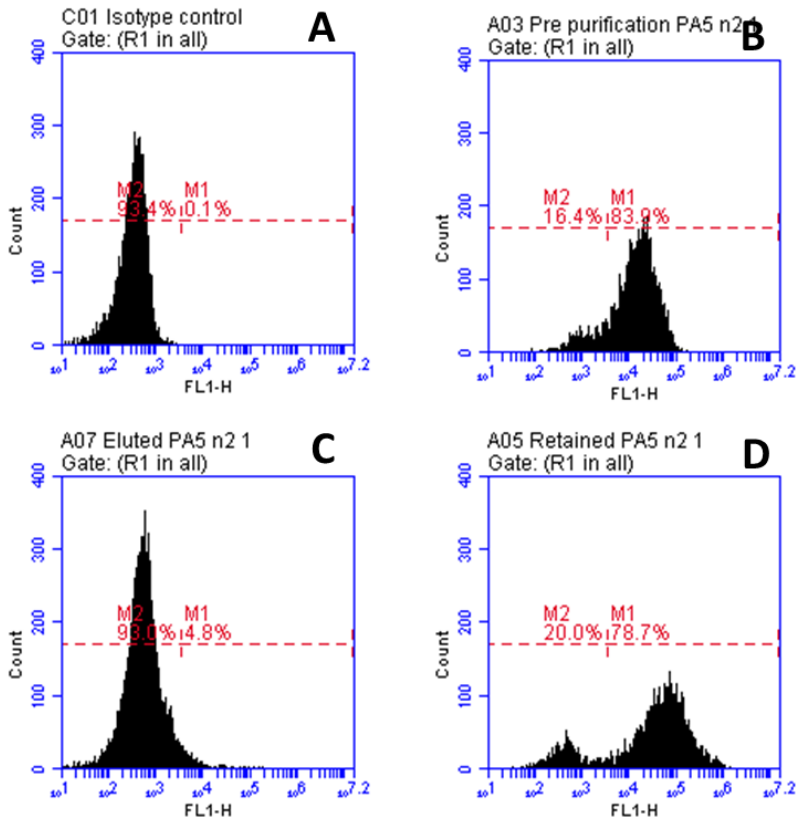

Figure 4.2: Flow cytometry graph output from BD Accuri™ C6 flow cytometer. Cells were purified using MACS technology to separate Thy1 positive cells from the rest of the population. The M1 bracket on the graphs indicates cells that are positive for Thy1 and the M2 bracket indicates cells that are negative for Thy1. The isotype control and pre-purification fractions were run using live staining and the eluted and retained fractions were stained by binding the secondary antibody to the MACS beads present.

ICC was carried out (Figure 4.3) and quantified (Figure 4.4) to characterise the populations for a variety of markers (p75NTR, Thy1 S100β, Fn and α-SMA). The only markers that were observed to change between populations were Thy1 and α-SMA.

Thy1 was present in significantly lower values in the eluted fraction (18.6±7.2%, one-way ANOVA, Bonferroni correction post-hoc, $p<0.01$). The pre-purified and retained fractions were 47.4±12.4% and 51.0±8.1% positive for Thy1 with ICC compared with 83.9% and 78.7% quantified as positive with the flow cytometer. This may be due to the different levels of detection between ImageJ and the BD Accuri™ C6 flow cytometer. Generally flow cytometry has higher levels of detection than ICC (Becton, 2015).

α-SMA was observed to be present in lower levels in the pre-purified fraction compared with the retained and eluted fractions (69.1±8.3% compared with 87.6±3.7% and 86.2±1.5%). α-SMA was used as it has been reported it is expressed by OECs but not

Schwann cells (Jahed et al., 2007). α-SMA identifies stem and pre-cursor cells which have been found in various tissue during repair and regeneration (Hosoya et al., 2006). It could be that when the population is split, more cells exhibit stem cell like behaviour as the population adapts. The differences in α-SMA expression are quantified in Figure 4.4.

Although all cells appear to express S100β and Fn (Figure 4.3), S100β expression was seen to be brighter and more cytoplasmic in the pre-purified and retained fractions compared to the eluted fraction where the expression remains very nuclear. S100β is associated with cell cycle and differentiation (Gilquin et al., 2010). It could be that the cell population in the pre-purified and retained fractions are proliferating more rapidly than those in the eluted fraction and this explains the difference in expression. S100β has been observed to act in a dose dependent manner (Sandrin and Cosset, 2006, Steiner et al., 2007) and therefore this could be what is occurring in these populations and the populations have been imaged at different stages of dosing.

There was no significant difference in p75NTR expression between the retained and eluted fractions. The hypothesis of this experiment was that depleting Thy1 may enrich p75NTR which was not what was observed in this work. The presence or absence of Thy1 expression was found to have no relation to the expression of key OEC marker p75NTR. This would indicate that OECs co-express Thy1 and p75NTR but can express only p75NTR which may explain the different opinions about expression in the literature (Hayat et al., 2003, Nash et al., 2001, Nash et al., 2002, Sonigra et al., 1999). It also agrees with the idea that methods of enrichment have to be used carefully as without a full understanding of the cells, functional parts of the population may be unintentionally removed (Kawaja et al., 2009).

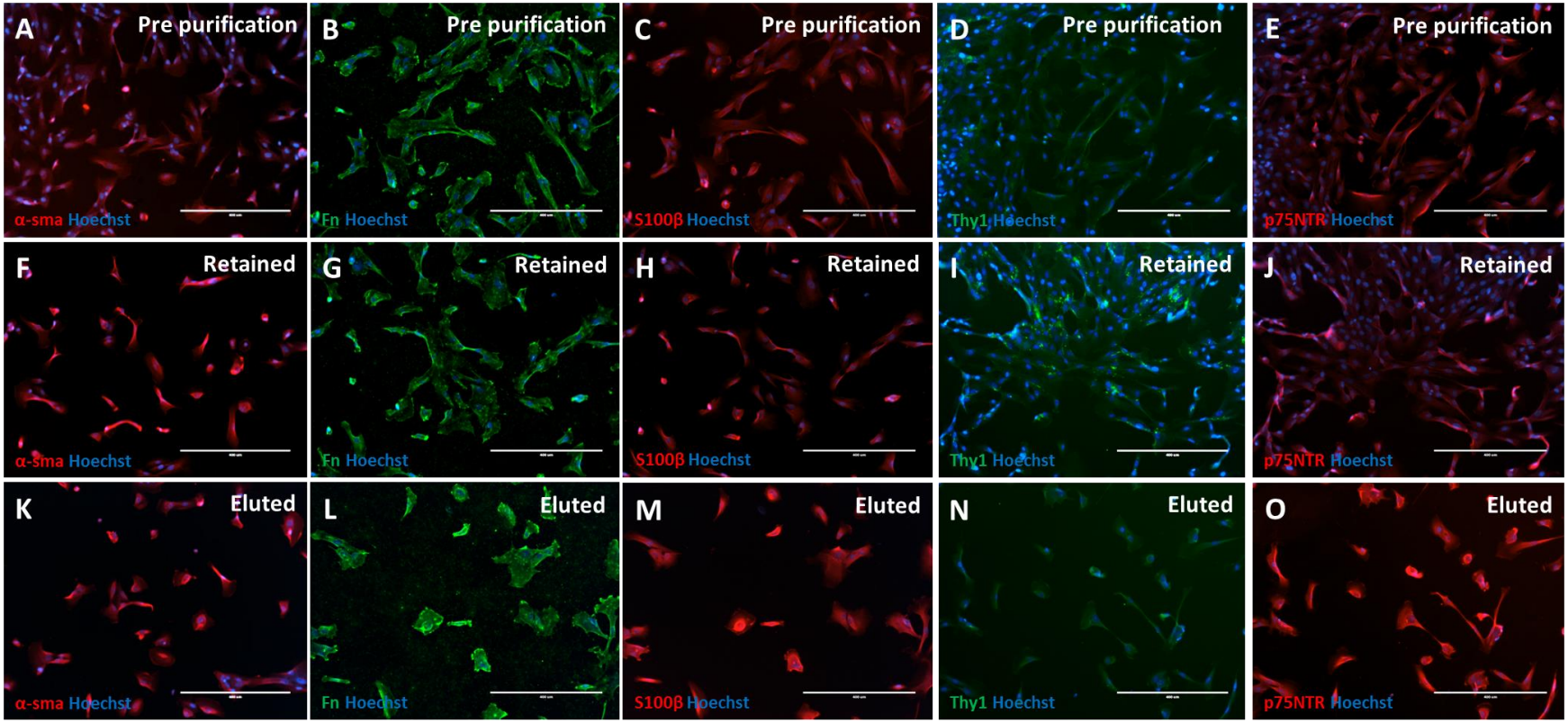

Figure 4.3: Fluorescent micrographs characterising of pre- and post- purification populations. Cells from the pre-purified (A-E), retained (F-J) and eluted (K-O) populations were fixed after 24 hours and characterised using α-SMA, S100β, Fn, p75NTR and Thy1, all with Triton X permeabilisation. Hoechst was used as a nuclear stain. Both the pre-purified (D) and retained (I) fractions had positive Thy1 staining whereas the eluted (N) fraction was completely negative. The scale bar represents 400μm.

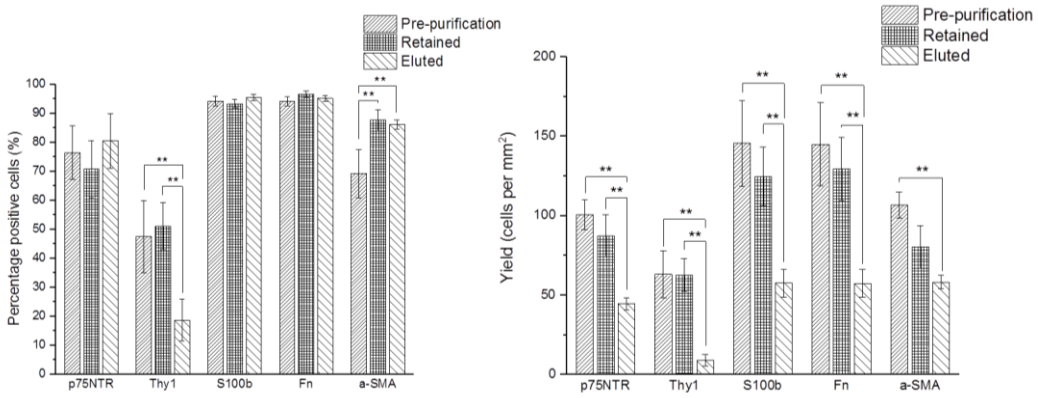

Figure 4.4: Quantification of MACS purification characterisation. Cells from the pre-purified, retained and eluted fractions were fixed and stained for p75NTR, Thy1, S100β, Fn and α-SMA. This staining was quantified using the percentage of positive cells present (A) and the total yield (B) for each marker. There was a significant difference for Thy1 between the pre-purified and retained fractions compared with the eluted fraction (one-way ANOVA, Bonferroni post-hoc, $p<0.01$). When yield was considered, in all conditions the eluted fraction was almost always significantly lower than the pre-purified and retained fractions (one-way ANOVA, Bonferroni post-hoc, $p<0.01$). Data are means ± SEM, n=3.

Another observation from the ICC micrographs in Figure 4.3 was the differences in morphology between the different populations, especially the more enlarged morphology in the eluted fraction. It was expected that the cells in the Thy1 negative fraction would assume more elongated cell morphologies. Instead the eluted cells were more enlarged than those in the Thy1 positive and pre-purified fraction. These differences in morphology were quantified using p75NTR positive staining and the ImageJ macro used in Chapter 3 and described in Section 2.3.3.

From the circularity graphs in Figure 4.5it can be observed that the distributions of the pre-purified and retained fractions were similar. They had a skew value of 1.1 and 1.2 respectively, although the retained fraction had a kurtosis value of 1.0 against the pre-purified value of 0.4, indicating a sharper peak. The difference in kurtosis values was due to the second minor peak in the pre-purified fraction at 0.8-0.9. The second peak could correlate to the eluted fraction cells as they produce a much flatter and wider distribution as shown by their skew and kurtosis values of 0.6 and -0.6 respectively. Cells in the eluted exhibited a more enlarged morphology than those in the other fractions. This could be due to this population taking longer to attach without Thy1 present and therefore retaining their larger morphology. Alternatively, the separation may be isolating a sub-population of OECs that is responsible for the enlarged morphology that has been observed in literature (Sonigra et al., 1999, Barnett and Riddell, 2004, Ebel et al., 2013, Boyd et al., 2003, van den

Pol and Santarelli, 2003, Vincent et al., 2005). This is important for functionality as it is the spindle shaped morphology that is accepted in literature to have the desired regenerative properties (Kawaja et al., 2009, Pellitteri et al., 2010, Fraher, 2000, Alexander et al., 2002). *In vivo*, OECs which exhibit the spindle shape have been observed to express desirable markers p75NTR and GFAP and allow neural regeneration. In contrast, OECs which were negative for these markers did not exhibit any regeneration during neuron co-culture (Alexander et al., 2002, Pellitteri et al., 2010). A population with a less spindle shaped morphology is thought to be less likely to possess these regenerative properties and is therefore an undesirable characteristic to observe in culture.

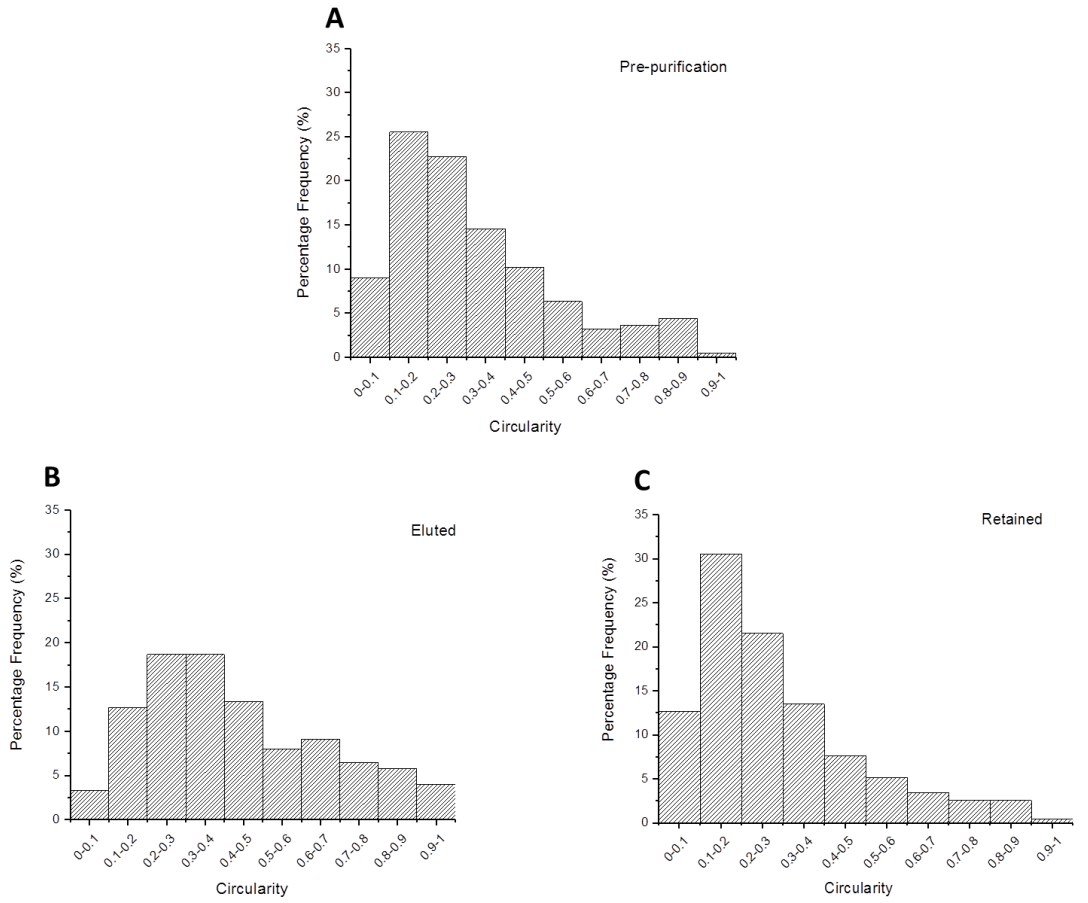

Figure 4.5: p75NTR circularity of MACS purification populations. Cells that were positive for p75NTR in each purified fraction were analysed for circularity by using the ImageJ macro. This data was organised and graphed as a distribution for percentage frequency in each interval. It can be determined that the pre-purification (A) and retained (C) fraction followed similar morphology patterns with shifts to the left and a peak at a circularity of 0.1-0.2. The eluted fraction (B) on the other hand followed a more uniform distribution with the most common circularity value lying between 0.2-0.4 and a skew value of 0.6. This data was analysed at n=3.

MACS is an efficient tool to separate Thy1 from the OEC population. It can be determined from this work that the presence of Thy1 does not affect p75NTR and S100β expression. This indicates the separation process may separate subpopulations of OECs rather than remove contaminating fibroblasts from the heterogeneous population. Differences were observed in the morphology of the cells in the different populations, although this may be due to the population isolated in the eluted fraction needing longer to fully adhere and proliferate.

4.3.2 Expression of Identity Markers up to 48 hours in culture and under different processing techniques

p75NTR is commonly used as a putative marker for OECs (Franssen et al., 2007, Barnett and Riddell, 2004, Boyd et al., 2003, Guerout et al., 2011, Pellitteri et al., 2010, Sonigra et al., 1999). The aim of the next experiment was to determine whether p75NTR is stably expressed by OEC^Hs over time in culture or whether expression changes with time or ICC processing method. This characterisation also examined expression of Thy1 which is normally used as a fibroblast marker (Wu et al., 2013b, Ebel et al., 2013).

4.3.2.1 Experimental Overview

Cells were plated at 12,000 cells/cm^2 on laminin coated 96 well plates. At the set time points 8, 12, 24 and 48 hours the cells were fixed and stained. Staining was carried out with or without a permeabilisation step using Triton X detergent. This allowed the differences in surface and intracellular expression to be observed. Three experimental repeats were carried out (n=3).

4.3.2.2 Results and Discussion

The first observation from the ICC and quantification (Figure 4.6-Figure 4.7) was that p75NTR turns off over time in culture (Figure 4.6A, E, I, M). For the first 24 hours, p75NTR was expressed strongly by the cells (95.9±1.1% at 24 hours with Triton X permeabilisation), however, by 48 hours this signal had significantly decreased (16.3±2.0% at 48 hours with Triton X permeabilisation). p75NTR has previously been reported to decrease with increased cell density (Kendall et al., 2002, Erck et al., 1998). The cells were plated at a high seeding density (12,000 cells/cm^2) and as the cells proliferate and become confluent this

may downregulate p75NTR as further proliferation is undesirable. This would also explain why p75NTR expression turns back on when the cells are plated on new surfaces as the cell density decreases.

It was found that in the absence of Triton X, p75NTR expression remained detectable (Figure 4.6B, F, J and N). This indicates that p75NTR was being expressed both on the surface and intracellularly, in agreeance with the literature (Krudewig et al., 2006). The distribution between the cell surface and the cytoplasmic compartment occur as proteins are constantly internalised and recycled to the surface when required (Prasad et al., 2010).

p75NTR may be turning off in culture as it may be a part of a subpopulation of OECs (Chen et al., 2014, Hayat et al., 2003). The culture was set up without any function required from the OECs which may result in unintentional selection for one of these subpopulations that do not take the leading role in assisting neural regeneration. Populations of OECs isolated from the same area have been observed to display different combinations of p75NTR and GFAP expression (Kawaja et al., 2009). The decrease observed in p75NTR expression may be linked to one of these subpopulations.

Alternatively, as reported in Section 1.3.3.2, p75NTR is associated with the cell cycle and proliferative neural populations (Kendall et al., 2002). When the proliferation decreases and the cell density increases, a decrease in p75NTR expression is observed (Erck et al., 1998). It could be that the decrease in p75NTR expression observed in Figure 4.7 is not related to subpopulations and is simply responding to the increased cell to cell contact. In astrocytes and SCs, p75NTR is upregulated after injury or stress to the cells, therefore this could also be what has been observed here (Cosgaya et al., 2002). Trypsinising the cells and removing them from the tissue culture surface may result in an upregulation of p75NTR.

In the absence of Triton X, higher levels of Thy1 expression were detected (64.3±2.2% at 8 hours without Triton X permeabilisation compared with 2.7±0.5 at 8 hours with Triton X permeabilisation, Figure 4.8). In the images with Triton X (Figure 4.6A, E, I and M), there was almost no Thy1 expression observed, however, cells from the same population are shown to strongly express Thy1 when the cell membrane remains intact (Figure 4.6B, F, J and N). Chemically breaking up the cell membrane decreased the ability to detect Thy1 expression. Triton X permeabilisation may cause damage to the transmembrane domain of

Thy1, preventing binding of the antibody. In the literature, both processing methods have been used prior to detecting Thy1, although the use of 0.1-0.25% Triton X is most commonly used (Kueh et al., 2011, Tome et al., 2007, Wu et al., 2013a, Ishihara et al., 2014, Lu, 2005, Jahed et al., 2007, Nash et al., 2001). This may explain why OECs are often characterised as Thy1 negative (Wu et al., 2013b, Ebel et al., 2013), Triton X permeabilisation may prevent its detection.

Unlike p75NTR, Thy1 was not observed to have a decreased signal over time. Instead, it was observed to be strongly expressed at 8 hours and 24 hours (64.3±2.2% and 78.9±4.3% respectively, with standard media and without Triton X permeabilisation) with lower expression levels observed at 12 and 48 hours (49.5±4.4% and 51.1±3.6% respectively, in standard media and without Triton X permeabilisation). This indicates that Thy1 expression changes over time. Therefore, caution is needed when labelling and characterising cells using Thy1 as a period of low expression may be captured but a higher expression can take place 12 hours later. Thy1 is associated with cell adhesion and transmigration (Saalbach et al., 2005). Therefore, the level of expression could be related to the proliferation rate. Over time the cells attach and show higher Thy1 expression, whereas when the cells are dividing slowly, the expression decreases.

NT-3 was added to the culture media (50ng/ml) in order to determine its relation to p75NTR expression. It was found from this study that NT-3 did not change the duration of p75NTR expression. In Figure 4.6A, E, I, M, p75NTR had a decreased signal by 48 hours in culture. When NT-3 was added to the culture media Figure 4.6C, G, K, O, the same pattern was observed and confirmed by the quantification (Figure 4.7). There was no extension of signal observed in NT-3 culture conditions (expression at 48 hours in standard media with Triton X permeabilisation was 16.3±2.0% without NT-3, and 13.9±1.1% with NT-3). NT-3 has been well documented to assist in remyelination (Bradbury et al., 1999, Bregman et al., 1997, Xu et al., 1995, Ramer et al., 2005), so it may be that NT-3 was not observed to increase p75NTR expression because the myelination abilities of the OECs were not being functionally tested in this work.

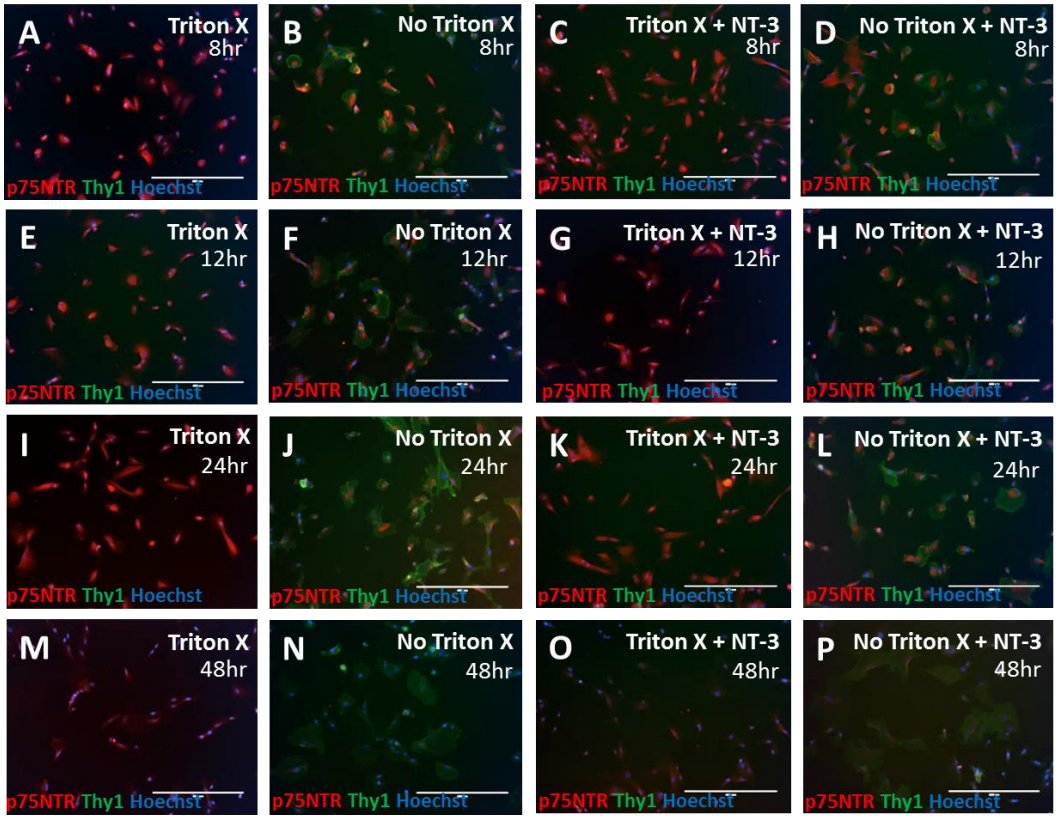

Figure 4.6: Fluorescent micrographs of the time point staining of PA5 cell population. Cells were fixed and stained at 8 (A-D), 12 (E-H), 24 (I-L) and 48 (M-P) hours. This staining was carried out with and without Triton X permeabilisation. Over time the expression of p75NTR decreased (A, E, I, M, C, G, K and O). The presence of p75NTR and Thy1 was observed to change depending on whether Triton X had been used. When Triton X was used, Thy1 was absent (A, E, I, M, C, G, K, O), however when Triton X was not used, a clear outline of the cells can be seen showing the expression of Thy1 (B, F, J, N, D, H, L and P). Thy1. is time dependent with the highest level of expression occurring at 8 and 24 hours (B, J, D and L) and lower levels occurring at 12 and 48 hours (F, N, H and P). NT-3 did not make a difference to p75NTR expression. The scale bar represents 400µm.

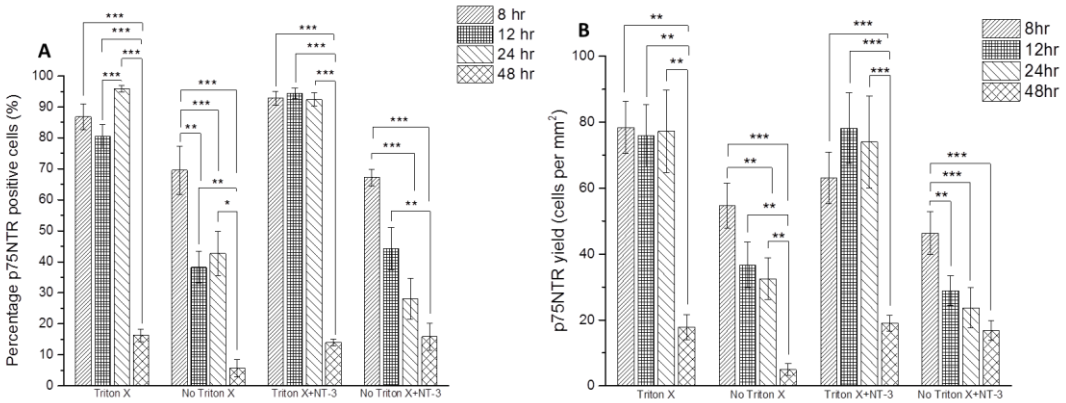

Figure 4.7: Quantification of p75NTR protein expression. Cells that labelled positive for p75NTR in all staining conditions were quantified and plotted. Cells were quantified for the proportion of p75NTR positive cells (A) and the total yield of p75NTR positive cells (B). The 48 hour point was significantly lower in positive p75NTR cells than the other time points in both percentage positive and yield for every condition (one-way ANOVA, Bonferroni post-hoc, $p<0.001$). Data are means ± SEM, n=3.

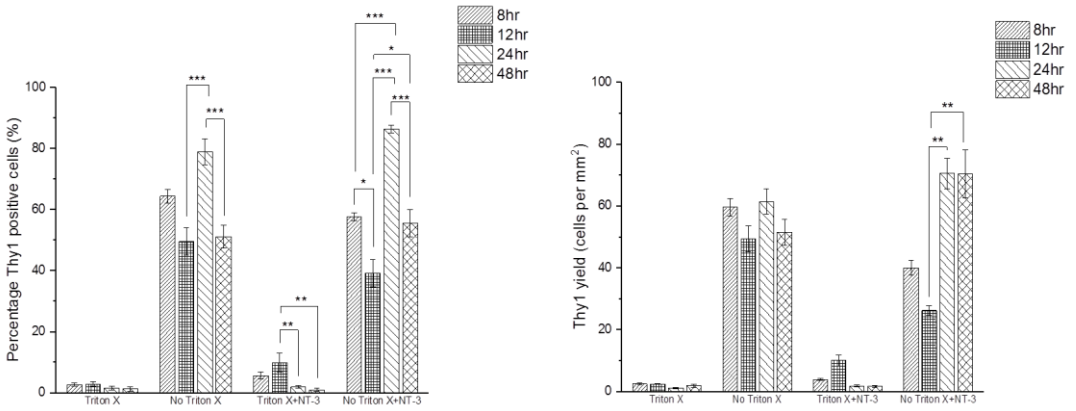

Figure 4.8: Quantification of Thy1 protein expression. Cells that labelled positive for Thy1 in all staining conditions were quantified and plotted. Cells were quantified for the proportion of Thy1 positive cells (A) and the total yield of Thy1 positive cells (B). Thy1.1 appears to switch on and off during culture time. When Triton X was used, the expression of Thy1 was lost, whereas when the cell membrane is left intact, the expression was able to be detected. Data are means ± SEM, n=3.

From this work, it was observed that p75NTR is not a stable marker to characterise OECs as it decreases over time in culture. When the OECs were plated onto new culture plates, p75NTR expression was around 90% over the first 24 hours. After this time, p75NTR was downregulated.

Thy1 is also a marker whose expression fluctuates over time in culture. This further impedes accurate characterisation of OECs and potentially "contaminating" fibroblastic cells. In addition to this, if Triton X is used to permeabilise cells, the Thy1 signal decreases. The knowledge gained in this work was applied to subsequent experiments by characterising Thy1 marker expression over a longer time course without using Triton X permeabilisation.

4.3.3 Expression of Identity Markers after six days in culture

Building on the knowledge gained in Section 4.3.2, the MACS purification experiment was repeated and cell populations were characterised at both 24 and 48 hours post-processing and in the presence and absence of Triton X permeabilisation (p75NTR characterised in the presence and Thy1 in the absence of Triton X). The aim of this experiment was to increase the accuracy of the characterisation of the purified populations.

4.3.3.1 Experimental Overview

PA5 cells were cultured on laminin coated flasks in the presence of NT-3. The staining was carried out at 24 and 48 hours post-plating and labelling was performed both with and without Triton X permeabilisation.

4.3.3.2 Results and Discussion

The ICC micrographs obtained from this experiment (Figure 4.9) and the quantification (Figure 4.10-Figure 4.11) revealed that the p75NTR signal decreased after 24 hours, which was consistent with Figure 4.6. Fewer cells express p75NTR in the retained fraction in the absence of Triton X permeabilisation (63.6±13.5% at 24 hours) compared with cells in the pre-purified (93.6±2.1% at 24 hours) and eluted fractions (91.8±3.9% at 24 hours). This may indicate that the cells in the retained fraction express comparatively more of its p75NTR intracellularly as opposed to on the surface compared with the eluted and pre-purified fractions.

Thy1 labelling intensity was sharper without Triton X permeabilisation, confirming previous data. Previously, in Figure 4.6, Thy1 was observed in the retained fraction, although not to the same degree as was obtained with flow cytometry. There was also a lack of strong Thy1 expression in the pre-purified population. When Triton X was excluded from the staining protocol, higher levels of Thy1 expression were observed (63.9±3.2% at 24 hours in the pre-purified fraction and 75.2±11.1% at 24 hours in the retained fraction), correlating with the flow cytometry data. Therefore, from this experiment a more accurate picture of cell marker characteristics that corresponds with flow cytometry data was obtained.

From quantification in Figure 4.10, expression of Thy1 cells in the eluted fraction was significantly lower (9.9±8.5% at 24 hours without Triton X permeabilisation), compared with the retained (75.2±11.1 at 24 hours without Triton X permeabilisation) and pre-purified fractions (63.9±3.2% at 24 hours without Triton X permeabilisation) indicating the purification was successful (one-way ANOVA, Bonferroni post-hoc, $p<0.001$). No patterns were observed when the cells were treated with Triton X, most likely due to the small values obtained due to the permeabilisation destroying the ability to detect Thy1.
Figure 4.9-Figure 4.11 also documents the expression of S100β and Fn. No significant difference between the three conditions was observed. The only observation in the ICC was

that the S100β expression appeared to be stronger and more cytoplasmic in the pre-purified and retained fraction as was previously observed in Figure 4.6. This was postulated to be related to the dose dependent nature of S100β (Sandrin and Cosset, 2006). At 48 hours, S100β expression was stronger in all three conditions which indicates upregulation taking place.

Examination of how Triton X permeabilisation changes S100β and Fn detection was not carried out as it is well documented that S100β is an intracellular marker found in the cytoplasm (Chong, 2016, Jin et al., 2014) and that Fn is expelled into the extracellular matrix space (Wang and Ni, 2016, Tom et al., 2004, Liu et al., 2010, Ramón-Cueto and Nieto-Sampedro, 1992). If no Triton X permeabilisation was used prior to S100β detection, no signal would be observed (Chong, 2016, Jin et al., 2014). Conversely, when Triton X permeabilisation is used when detecting Fn, there is no difference in detection levels (Wang and Ni, 2016, Tom et al., 2004, Liu et al., 2010, Ramón-Cueto and Nieto-Sampedro, 1992).

In Figure 4.10 all cells were 100% positive for both S100β and Fn. When this was interpreted alongside yield values, this allowed differences in the population numbers to be observed. As the populations have the same purity, the difference in yield can be used as an estimate of total cell number. The pre-purified fraction at both time points and with both markers had the highest yield (237.7±37.1 S100β positive cells/mm^2 compared with 153.4±21.3 S100β positive cells/mm^2 for the retained fraction and 107.8±17.9 S100β positive cells/mm^2 for the eluted fraction, all at 24 hours). This indicates that the cells in the pre-purified fraction have a higher proliferation rate and this advantage remains for the first 48 hours. After 48 hours the difference in yield between the pre-purified and eluted fractions was significant (239.1±38.5 S100β positive cells/mm^2 pre-purified fraction and 107.9±18.0 S100β positive cells/mm^2 eluted fraction, one-way ANOVA, Bonferroni post-hoc, $p<0.05$). This could be due to the pre-purified and retained fractions containing Thy1 positive cells which may include fibroblasts which have a faster attachment and higher proliferation rate. Further work needs to be done to understand the true identity of these cells.

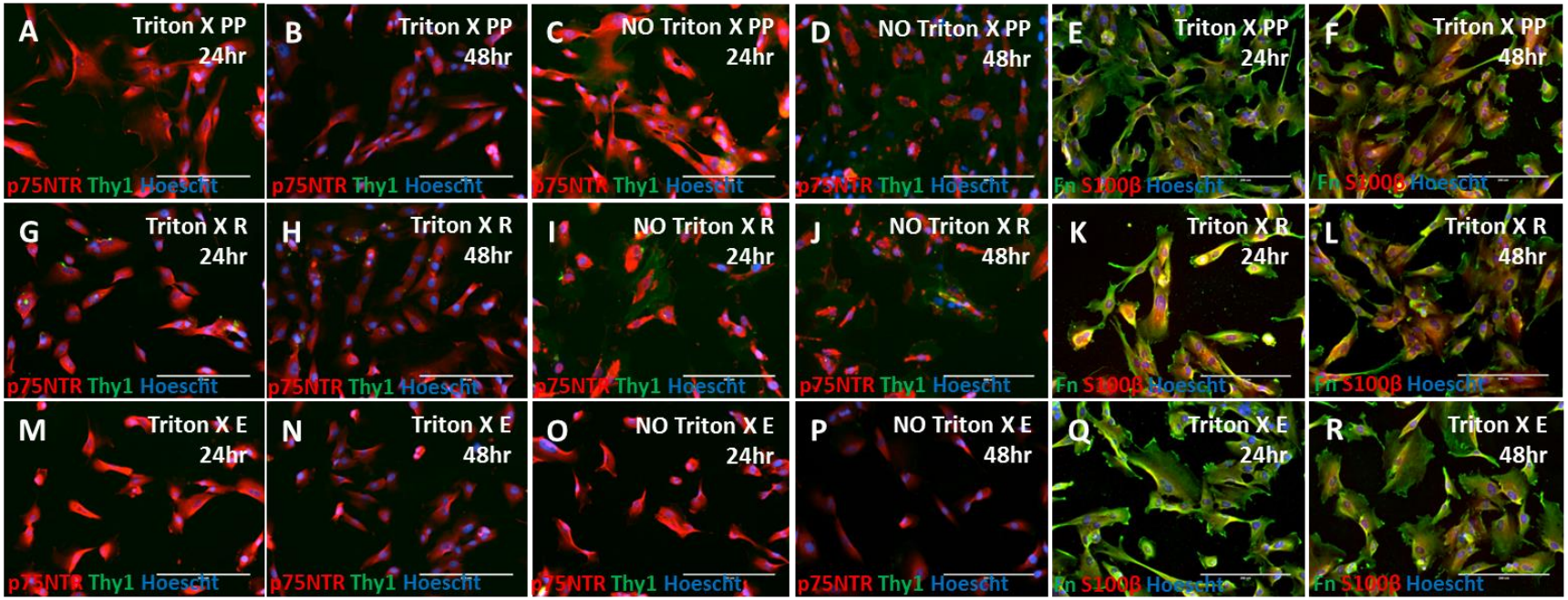

Figure 4.9: Fluorescent micrographs of time point staining of PA5 cell population after MACS purification. From the previous work it was determined that differences occurred depending on the staining conditions and the time at which the cells were fixed. To improve the detection method for p75NTR and Thy1, cells were fixed at 24 and 48 hours and stained with and without Triton X permeabilisation to ensure the best representation of the population was attained. Cells were also stained for S100β and Fn. There did not appear to be a difference in p75NTR, S100β and Fn expression (A-R) between the three populations. There was a significant difference observed when Triton X was used to detect Thy1. Without Triton X, Thy1 can be seen to be present in the pre-purified and retained fractions (C, D, I and J), but absent in the eluted fraction (O and P). The scale bar represents 200µm.

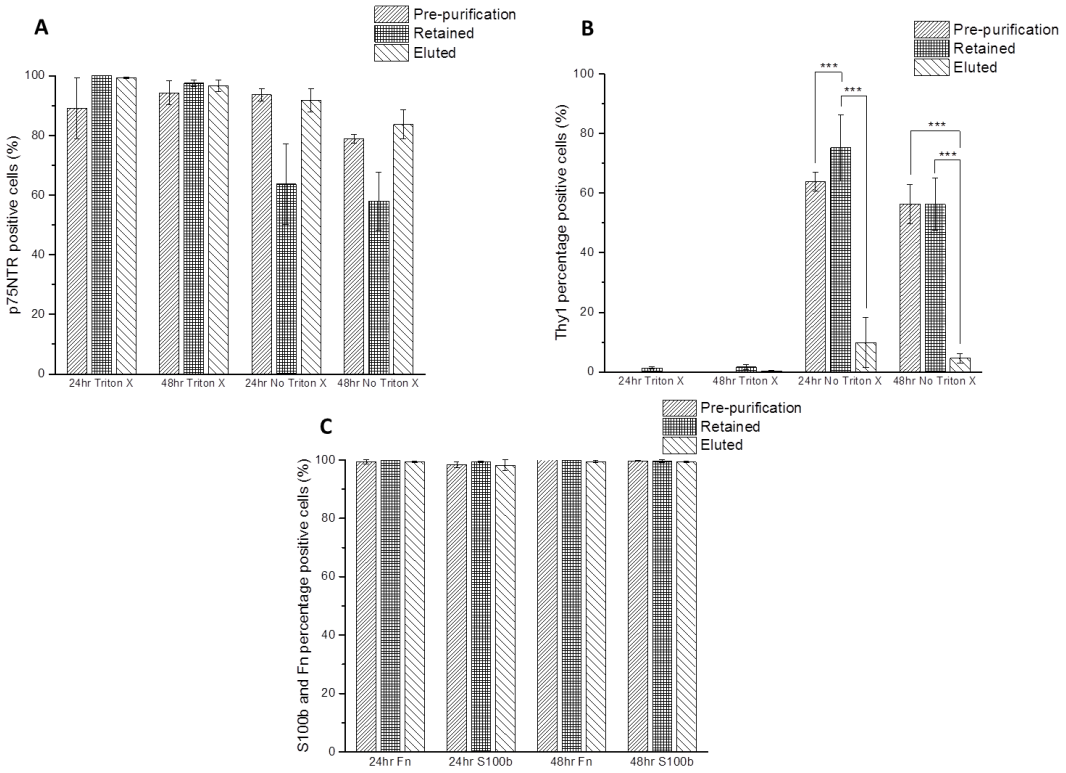

Figure 4.10: Quantification of time point characterisation of MACS purified PA5 population protein expression. Cells that were positive for p75NTR (A), Thy1 (B), S100β and Fn (C) were quantified using ImageJ. These graphs show the percentage of positive cells for each marker. Although p75NTR was not present to the same extend in the retained fraction, this was not found to be statistically significant (one-way ANOVA, Bonferroni post-hoc, $p<0.05$) (A). The presence of Thy1 was found to be significantly lower in the eluted fraction at both 24 and 48 hours when staining was completed without the use of Triton X permeabilisation (one-way ANOVA, Bonferroni post-hoc, $p<0.001$) (B). The effect of two time points did not change the levels of Fn and S100β expression (C). Data are means ± SEM, n=3.

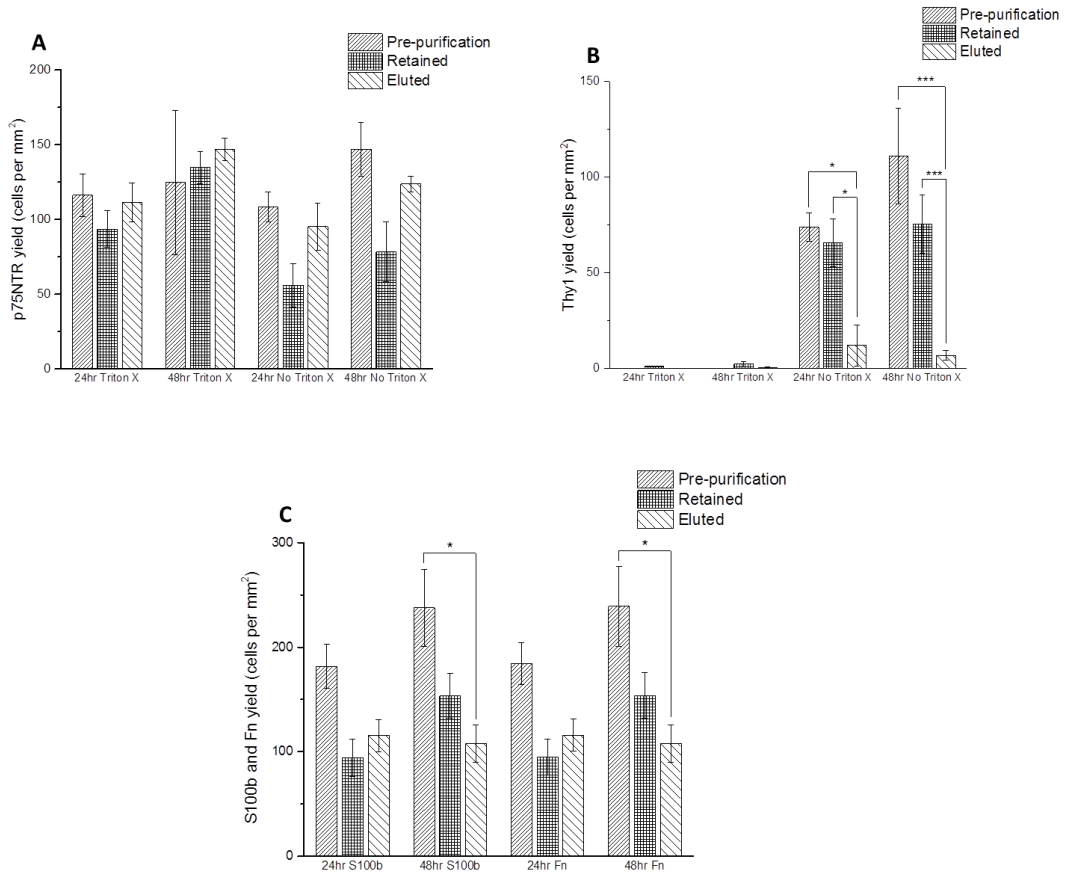

Figure 4.11: Quantification of time point characterisation of purified PA5 population yield. Cells that were positive for p75NTR (A), Thy1 (B), S100β, and Fn (C) were quantified using ImageJ. These graphs show the total yield of positive cells for each marker. There were no significantly different results for p75NTR (A). Thy1 was statistically different in the eluted fraction compared with retained and pre-purification fractions without Triton X permeabilisation (B). For S100β and Fn yields, at the 48 hour time point, the eluted fraction was statistically lower than the pre-purification fraction (C). Data are means ± SEM, n=3.

As with Section 4.3.1, differences in morphology were observed in the ICC staining in Figure 4.9. The eluted cells formed a more rounded morphology, whereas the pre-purified and retained fractions adopted morphologies that were more elongated. This morphological difference was quantified using p75NTR positive cells and the macro described in Section 2.3.2. The distributions generated are plotted in Figure 4.12.

At 24 and 48 hours, the histogram for the circularity of the pre-purified cells (Figure 4.12A, B), did not change over time and this was validated by the lack of significance in comparing these two distributions (Kolmogorov-Smirnov). Significant differences existed between the pre-purified fraction (at 24 and 48 hours) and the eluted and retained fractions (both at 24 hours) (Kolmogorov-Smirnov, $p<0.001$). These morphological differences may be indicative of different cell populations being present. The distribution of the retained cells at 24 hours

(Figure 4.12C) was significantly different to the one at 48 hours (Figure 4.12D) and it can be seen shifting to the left and obtaining a sharper peak. This may be due to the cells requiring time to attach and requiring time to adopt their morphology or morphology related cell signalling.

The distribution for the eluted fraction at 24 hours (Figure 4.12E) quantifies the more enlarged morphology observed in Figure 4.9 with a uniform distribution occurring with values from 0.2-0.6 all giving similar numbers of cells. After a further 24 hours, this fraction exhibits a shift to the left with cells with circularities over 0.6 forming the tail. This shift occurs slower than those by pre-purified and retained fractions. This could be due to the cells taking longer to attach and adapt to their surroundings, or because this sub-population does not usually form spindle shaped cells. Further observation over longer periods of time would be required to determine which one of these hypotheses is correct.

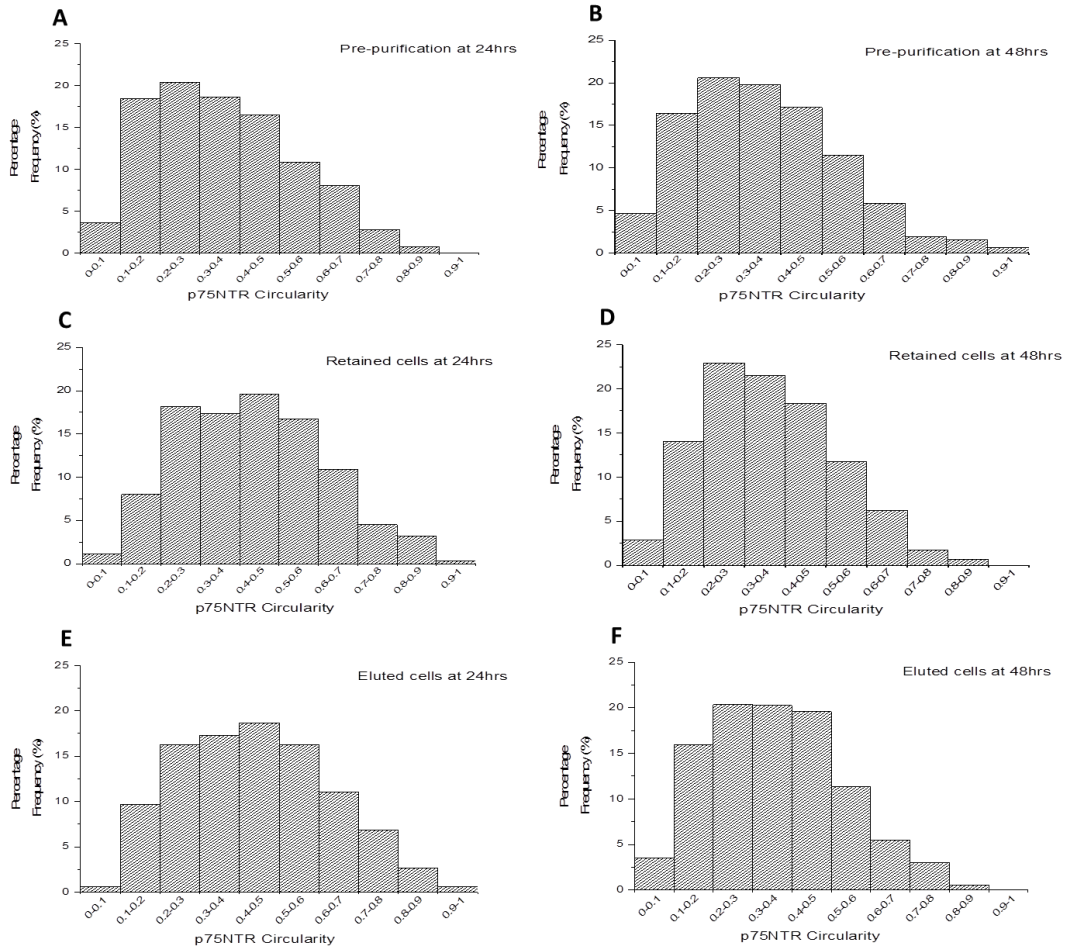

Figure 4.12: p75NTR circularity of time point MACS purification populations. Cells that were positive for p75NTR in each purified fraction at 24 and 48 hours were analysed for circularity using the ImageJ macro. This data was organised and graphed as a distribution for percentage frequency in each interval. From these distributions it was observed that the pre-purified population (A, B) retained a left shifted distribution, whereas the retained and eluted cells (C-F) had a more centred distribution with the exception of retained cells at 48 hours (D) which had a larger left shift. This data was analysed at n=3.

By removing Triton X from the ICC protocol, this allowed counts of Thy1 positive cells to reach similar levels to the flow cytometry in Section 4.3.1. Improving the confidence in the positive ICC results increases the confidence that the negative result in the eluted fraction is truly negative. There were more cells present in the pre-purified fraction compared to the other fractions as determined by the proportions and yields of S100β and Fn staining. After 48 hours cells in the eluted fraction were still Thy1 negative and starting to adopt a more enlarged morphology. To further understand these populations, it was decided to culture them for six days to examine how protein expression and morphology changes over a more prolonged period of time.

4.3.4 Characterisation of Purified PA5 cells after six days in culture

Thy1 positive cells were immunodepleted from the culture using MACs purification and the populations were initially characterised up to 48 hours after purification. The aim of the next experiment was to further characterise the purified cell populations after extended culture duration. This was carried out by culturing the cells for six days after purification.

4.3.4.1 Experimental Overview

Previously cells were purified and fixed for staining within 48 hours of the purification. In this time it could be seen that the eluted fraction was negative for Thy1 and differences in morphology were observed. In order to obtain a better understanding of these populations the cells from the eluted and retained fraction were cultured on laminin coated flasks in the presence of NT-3 for 6 days before being fixed and stained using ICC. Cells were fixed at 24 hours, 48 hours, day 5 and day 6 to ensure a 24 hour time difference existed between the 'pre' and 'post' conditions and that Thy1 expression would be able to be observed. As in the previous experiment, Thy1 was stained without Triton X permeabilisation.

4.3.4.2 Results and Discussion

It was observed that p75NTR signal reduces over time in both the retained and eluted cell populations (97.5±1.3% and 93.8±2.4% respectively at 24 hours, down to 18.9±4.2% and 13.8±11.7 at day 6, all with Triton X permeabilisation, Figure 4.13-Figure 4.14). Quantification of p75NTR yield (Figure 4.14C, D) needs to be interpreted carefully as the seeding density of the culture was different for 24/48 hours compared to 5/6 days. Only comparison within these time frames can be carried out. This was done due to the time the eluted fraction took to attach. In order to have a stable culture to stain after 24 hours, the seeding density was 12,000 cells/cm^2. A lower seeding density (6000 cells/cm^2) can be used for staining after 5 days as the cells have enough time to attach and establish a culture.

The proportions of p75NTR positive cells do not exhibit any significant differences between the Thy1 positive and negative fractions (97.5±1.3% for the Thy1 positive fraction, and 93.8±2.4% for the Thy1 negative fraction, at 24 hours with Triton X permeabilisation, Figure 4.15) which implies the OECs co-expressed p75NTR and Thy1. Significance exists between the 24/48 hour values and 5/6 day values in most cases (one-way ANOVA, Bonferroni post-

hoc, $p<0.01$). From the proportion of p75NTR positive cells, even in the absence of Triton X, the expression of p75NTR can be seen to dramatically decrease over time in culture (32.5±8.2% at 24 hours down to 3.5±1.6% at day 6 for the retained fraction, Figure 4.14). This is in line with results obtained in Section 4.3.2 and Section 4.3.3.

When the results for p75NTR expression for Triton X and no Triton X were examined, it was observed that with Triton X permeabilisation, the retained fractions exhibited higher levels of p75NTR expression (97.5±1.3% at 24 hours versus 93.8±2.4% for the eluted fraction). When Triton X permeabilisation was removed from the staining protocol, the eluted fraction in most instances displayed higher proportions/yields of p75NTR positive cells (56.8±9.7% at 24 hours versus 32.5±8.2% for the retained fraction). This indicates that the eluted fraction was expressing more p75NTR on the surface of the cell compared with the retained fraction. By expressing p75NTR on the surface, this may imply that the use of this protein is more active. The significance of this expression requires further investigation into the relationship between OEC behaviour, function and p75NTR expression.

The effect of Triton X on the Thy1 signal was repeated and in the retained fraction it can be seen to vary in strength over 24 hours intervals (24-48 hours and 5-6 days). At 24 and 48 hours, the eluted fraction can be seen to be devoid of Thy1 positive cells. The key observation from this experiment was that Thy1 turns back on in the Thy1 negative fraction. At 5 and 6 days, Thy1 can be observed in the eluted fraction (54.3±7.1% at day 6) and although it does not reach the same proportion as the retained fraction (68.7±16.6% at day 6), it is clearly present.

This upregulation of Thy1 expression shows that the cells have received signals that have resulted in Thy1 being turned back on in this population. When cells expressingThy1 were removed, the population switched this marker back on and re-established the balance. As OECs also express other adhesion proteins (Josvay et al., 2014) such as Fn (Ramon-Cueto et al., 1993, Kawaja et al., 2009), it would be beneficial to knock out Thy1 in order to determine whether Thy1 is needed for attachment. It may be that OECs use several different adhesion molecules and can attach using other molecules such as Fn if Thy1 is not available. Further work would be required in this area.

These data shows removing Thy1 from the population was not an efficient long term solution. Although the purification may be removing fibroblasts from the polyclonal population, the removal of Thy1 does not ensure that the cells in the negative fraction do not express Thy1. Thy1 was previously observed to change with time in culture (Section 4.3.2), however, it can be seen from this work that when the population had no Thy1 expressed after 48 hours, the cells were able to upregulate this marker and turn it back on.

Figure 4.16 displays the quantification of S100β staining. The expression of S100β decreases over time (52.8±23.9% at 24 hours compared to 14.0±4.1% at day 5 in the retained fraction, Figure 4.16A) and also exhibits large error bars. The reason for this variation where little has been seen before has not been identified. From this data, not only does p75NTR decrease in signal, but so does S100β. Further investigation would be useful to determine whether this downregulation is linked or whether they have been influenced by separate factors. p75NTR is associated with cell cycle and cell density (Kendall et al., 2002, Erck et al., 1998) whereas S100β acts in a dose dependent manner (Steiner et al., 2007, Gilquin et al., 2010) so it may be that these have coincided as opposed to being related to a common source.

Fn staining was not quantified in this experiment due to the inability to identify the cell responsible for the expression at days 5 and 6. Fn was strongly expressed and the extracellular nature of this marker can be observed as initially it was associated with specific cells. By 5 days, Fn had spread throughout the entire well and it was too challenging to identify where the expression originated.

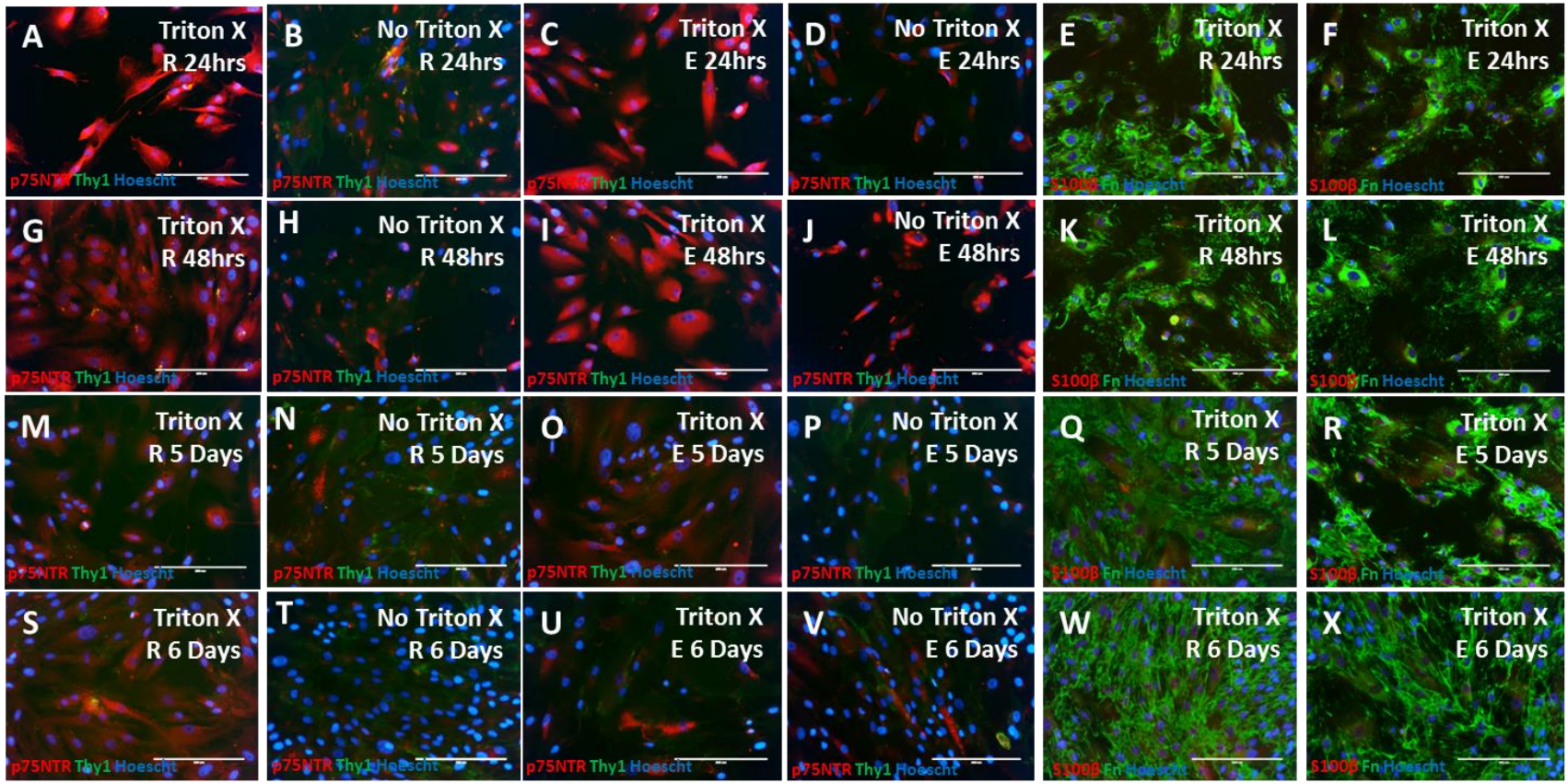

Figure 4.13: Fluorescent micrographs of extended time point staining of PA5 cell population after MACS purification. To determine if removing Thy1 influenced the growth and behaviour of the cells, PA5s were purified using MACS and cultured for 6 days. Cells were stained at 24 hour intervals. p75NTR and Thy1 staining was carried out with and without Triton X permeabilisation. p75NTR decreased in expression over time up to six days and detection was best with Triton X permeabilisation (A-D, G-J, M-P and S-V). Thy1 was detected in the retained fraction without Triton X permeabilisation at 24/48 hours (B and H) but not in the eluted fraction (D and J). The use of Triton X permeabilisation decreased the detection of Thy1 (A-D, G-J, M-P and S-V). After 5/6 in culture Thy1 expression increased in the eluted fraction (P and V).By 5 days, Fn can be found in the majority of the well plate (E-F, K-L, Q-R, W-X). The scale bar represents 200µm.

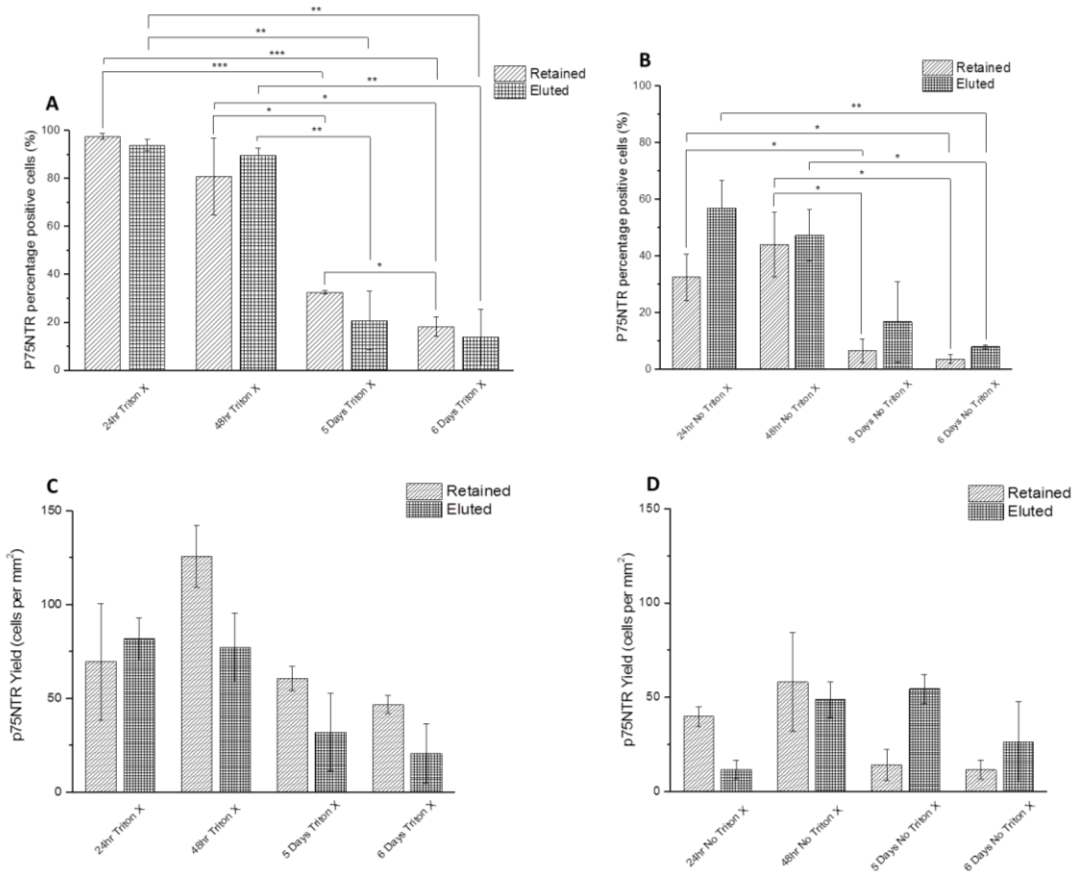

Figure 4.14: Quantification of extended time point p75NTR staining of MACS PA5 purification. p75NTR was quantified using the proportion of positive cells observed (A, B) and the total yield (C, D). Statistical tests were carried out by comparing the retained time points to each other (for example retained at 24 hours compared to retained at 48 hours) using one-way ANOVA. The eluted and retained fractions were compared to each other within the same time point using the Shapiro-Wilk test and then either the Tukey test (normally distributed data) or the Kruskal Wallis test (non-normally distributed data). The number of p75NTR positive cells detected significantly decreased from 24/48 hours to 5/6 days (A, B, one-way ANOVA, Bonferroni post-hoc, *p<0.05, **p<0.01, ***p<0.001). Yield graphs need to be interpreted carefully as the starting density at 24/48 hours was different to the cells that were plated for 5/6 days. This means the bars can only be compared within these two conditions. Data are means ± SEM, n=3.

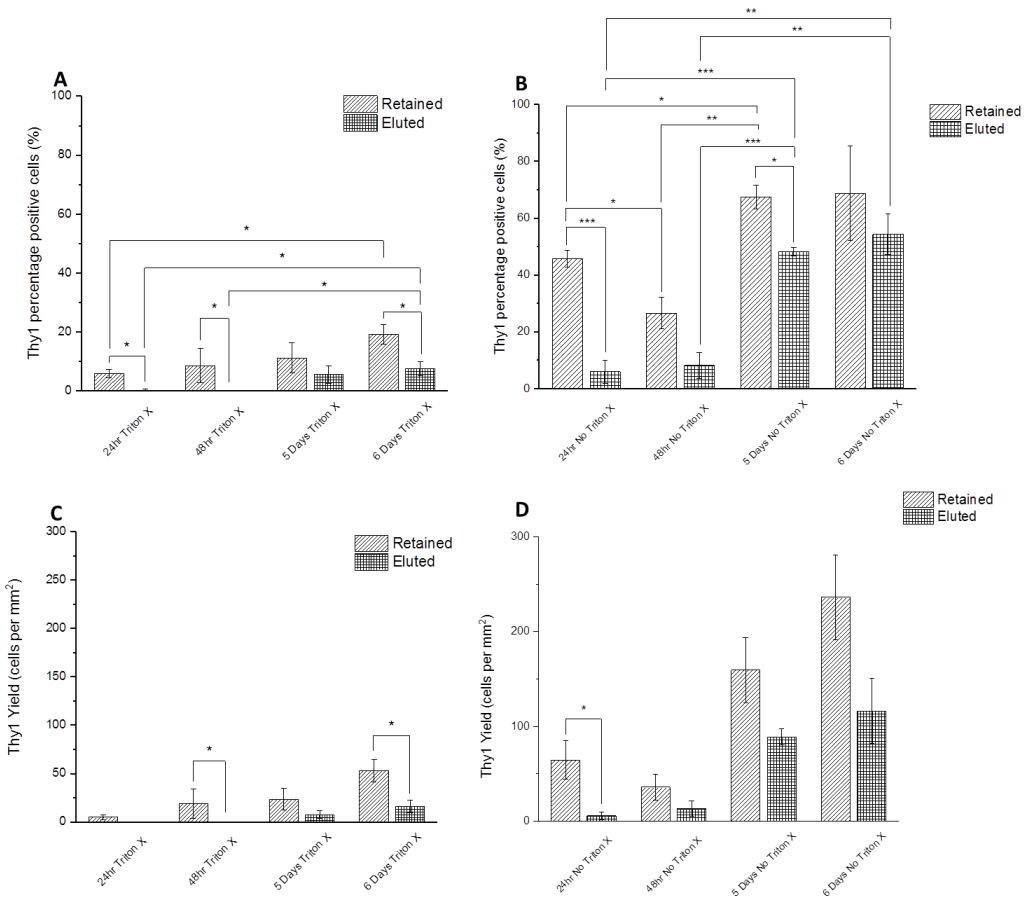

Figure 4.15: Quantification of extended time point Thy1 staining of MACS PA5 purification. Thy1 was quantified using the proportion of positive cells observed (A, B) and the total yield (C, D). When the cells were stained with Triton X permeabilisation, the number of positive cells detected was very low and no significance existed between conditions (A and C). In conditions stained without Triton X permeabilisation (B and D), it was observed that the eluted fraction started with significantly lower Thy1 positive cells (Tukey test, *p<0.05, **p<0.01, ***p<0.001). As the length of time in culture increased, the number of positive Thy1 cells in the eluted fraction increased. Due to the difference in seeding densities, the yield increase from 24/48 hours to 5/6 days cannot be tested for significance. Data are means ± SEM, n=3.

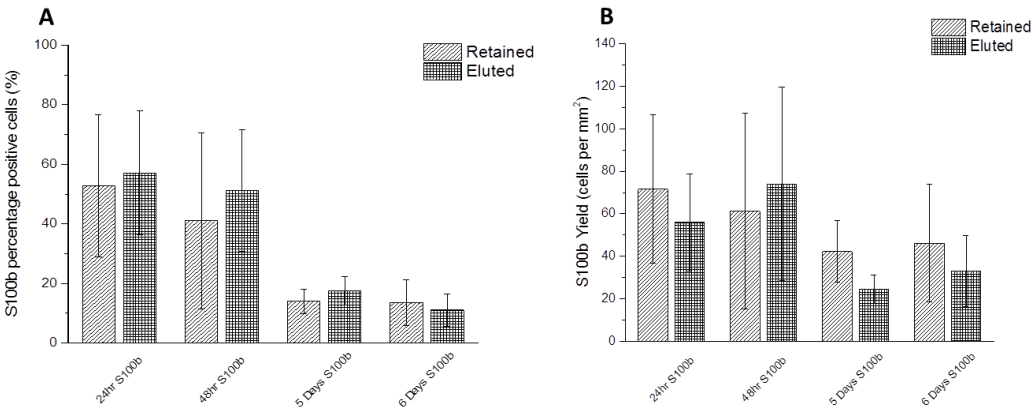

Figure 4.16: Quantification of extended time point S100β staining of MACS PA5 purification. Results were separated into individual markers and staining conditions in order to get a full view of the patterns that emerged. S100β was quantified using the proportion of positive cells observed (A) and the total yield (B). The staining for S100β generated large standard errors (A and B) and due to this, there was no significance found in these staining conditions. Yield needs to be considered carefully due to the different seeding densities used. Data are means ± SEM, n=3.

As in previous experiments, the morphology of the cells was examined using p75NTR positive cells and the macro developed (Section 2.3.2). The distributions generated are visualised in Figure 4.17. The immediate observation was that although the distributions for eluted and retained cells both start in different places with different distribution shapes, by 6 days in culture, the cells exhibited similar morphologies. When this was examined in parallel with Thy1 expression, it is possible that the purification has separated two sub-populations of OECs. After time in culture there is communication between the cells that re-establish the balance of the sub-populations. This implies that the population is able to determine the proportion of cells it requires to express certain proteins. Although the cultures do not reach the same levels as each other after 6 days in culture, the pattern is towards achieving this. It has been hypothesised in the past that there are two sub-populations that carry out different aspects of the neural regeneration (Chen et al., 2014, Hayat et al., 2003). This data would indicate that when part of this population is removed, the population is able to adapt to these changes by changing part of its population to ensure it has the required proportion to carry out its function. Alternatively it could be linked to proliferation and the adhesion properties of Thy1 (Saalbach et al., 2005, Kisselbach et al., 2009) and expression changes as the proliferative rate changes over time.

OECs have long been known to be plastic in regards to their morphology and expression (Chuah and Au, 1993, Barnett and Riddell, 2004). From this data it seems that not only are they able to change their morphology and expression, but also that they are sensitive to missing parts of the population and respond accordingly. Although cells were purified and Thy1 positive cells were removed from the population, the negative population had over 54.3±7.1% of cells expressing Thy1 after 6 days in culture. It appears to be a repeated requirement that the significance of the markers expressed by OECs need further examination so the population can be understood in more detail. Only once this understanding of the markers is attained, can the true significance of these markers and their expression be interpreted.

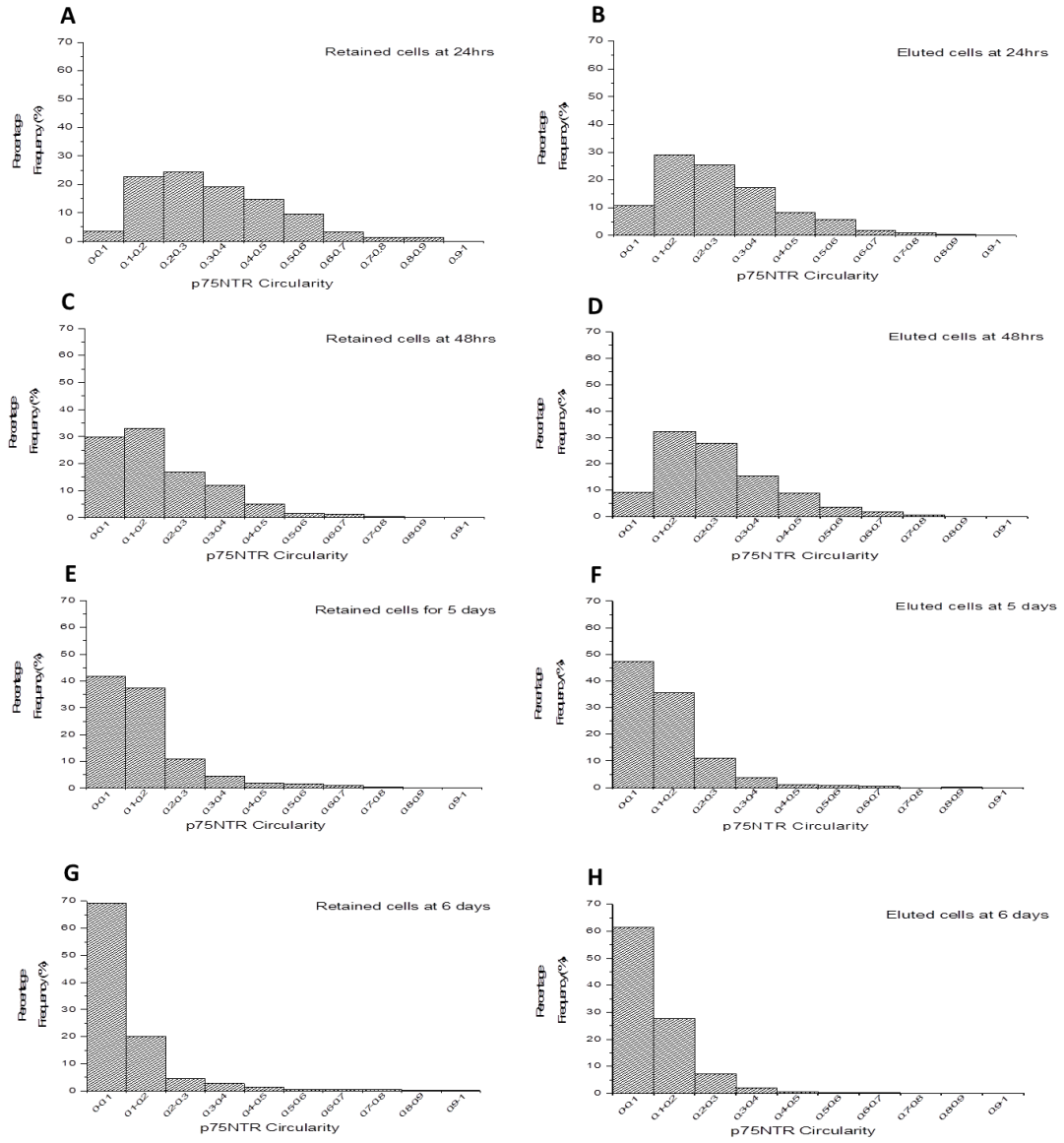

Figure 4.17: Cell circularity of MACS purified populations during extended culture. Morphology was analysed using p75NTR positive cells for these conditions. Images from each time point were analysed using the ImageJ macro which calculated the circularity of the positive cells. This data was organised and graphed as a distribution for percentage frequency in each interval. Cells got more spindle shaped with time in culture. For both retained and eluted fractions, they followed the same pattern, starting with a reasonable peak and left shifted distribution initially (A-D). After 5-6 days however, the peak becomes very sharp and virtually all the cells have a circularity less than 0.4 (E-H). In terms of difference between retained and eluted fraction, they both seem to follow the same pattern although the retained fraction appears to achieve a faster left shift which can be observed after 48 hours (C and D). This data was analysed at n=3.

4.4 Conclusions

p75NTR and Thy1 expression were examined in PA5 cell culture and it was found that p75NTR is downregulated over time in culture whereas Thy1 changes in time, though not in a set direction. Moreover, when processing cells for immunolabelling, introduction of a permeabilisation step using Triton X, prevented the detection of Thy1. A more optimal

labelling protocol was identified for the detection of Thy1. It can be concluded that Triton X should not be used as a permeabilisation agent. Using MACS to immunodeplete Thy1 positive cells ultimately does not prevent loss of p75NTR immunolabelling over time, nor does it prevent an increase in Thy1 expression. Therefore, p75NTR can be considered a transient marker and cells can express both p75NTR and Thy1.

A limitation of this study was that only ICC was used as a method of quantification. Western blots were investigated, however, we were unable to capture the presence of Thy1 using this method. The use of PCR or FACS to further quantify the results would strengthen this study.

5.0 The impact of different bioprocess parameters on OEC support of neuronal function

In this chapter, a neural cell line was cultured with OECs in a range of different conditions previously described in Chapters 3 and 4. The goal was to identify how these different conditions, that were shown to influence OEC marker expression, impacted on the resultant ability of OECs to support neuronal functional behaviour. Success was quantified by measuring the length of neurites and normalising this against the number of neurons and neurites. Initially NG108-15 neurons were co-cultured with PA5 cells on laminin and feeders in standard and HuG418-conditioned media (Section 5.3.1) to determine whether high levels of S100β correlated with longer neurite extension. Neurons were then co-cultured on PA5 cells, which exhibited different levels of p75NTR, to investigate whether the active expression of p75NTR correlated to the amount of support the PA5 cells provided to neurons (Section 5.3.2). Thy1 immunodepletion was carried out following the same method in Section 4.3.1 and neurons were co-cultured on pre-purified, eluted and retained fractions in order to examine the effect of the OEC sub-populations (Section 5.3.3). Finally, conditioned media was taken from PA5 cells at time points correlating with high and low p75NTR expression and compared against co-culture to identify if trophic support was responsible for the effect PA5 has on neurons as opposed to cell contact (Section 5.3.4).

5.1 Introduction

In Chapters 3 and 4, the focus was on optimising the culture of rat and human OECs to minimise contaminating cell types and maximise the expression of p75NTR. Although expression of p75NTR is agreed in the literature to be a positive marker for OECs and populations with high levels of p75NTR expression are considered to have high OEC purity (Franssen et al., 2007, Barnett and Riddell, 2004, Boyd et al., 2003, Guerout et al., 2011, Pellitteri et al., 2010, Sonigra et al., 1999), this does not necessarily relate to the ability of OECs to restore function (Radtke et al., 2010). The conditions explored in Chapters 3 and 4 were replicated during co-culture with neural NG108-15 cells to determine if these conditions were optimal for neuronal regeneration.

Neurons are formed of axons, dendrites, synapses and the cell body. Neurites extend out of the neuron body and form the axon or differentiate into dendrites. Axons are responsible for the intracellular transfer of information over long distances, whereas the dendrites receive information from other neurons. Dendrites are able to transmit information via electrical signals, but their main role is receiving information. Neurites elongate and form synapses at their termination point (Levitan and Kaczmarek, 2015).

When examining the potential function of neurons, the number and length of neurites were measured (Lozano et al., 1995, Mitchell et al., 2007, Rossi et al., 2010, Efthymiou et al., 2014) and normalised against the number of neurons. Reporting results in this way has been found to correlate with functional recovery observed in transplanted animals (Rossi et al., 2010). Measurements were carried out using the NeuronJ plugin for ImageJ.

NG108-15 (Sigma-Aldrich, UK), as reported in Section 2.1.5, is a hybrid cell line created by the fusion of mouse neuroblastoma and rat glioma (Klee and Nirenberg, 1974). NG108-15s are commonly used for functional assays as they mimic naturally occurring motor neurons (Jiang et al., 2003) that are present in the spinal cord (Maynard et al., 1997).

5.2 Aim and Hypothesis

The aim of this chapter was to determine whether PA5 cells under the range of conditions tested in previous chapters could promote neurite extension in NG108-15 when the conditions favoured p75NTR and S100β expression. It was hypothesised that neuronal functional responses would be enhanced when higher p75NTR/S100β expression was observed or when Thy1 was immunodepleted.

5.3 Results

5.3.1 Functional responses of neuronal cells to OECs when cultured with difference ECM and culture media conditions

PA5 cells were cultured on Ms3T3 and laminin with and without HuG418 CM (10,000 cells/cm^2). After 5 days of culture, NG108-15 neurons (500 cells/cm^2) were plated on top of the PA5 cells for a further 5 days of culture. The aim of this experiment was to quantify the neuronal behaviour and determine whether the conditions linked with the highest and lowest S100β expression gave the highest and lowest score for neuronal behaviour respectively. NG108-15s were cultured in the absence of PA5s as the negative control.

5.3.1.1 Experimental Overview

In Section 3.3.5, optimum conditions for PA5 culture were determined to be laminin and standard media supplemented with NT-3. The least favourable conditions were Ms3T3 feeders with HuG418 CM. Laminin coated flasks with HuG418 CM were used as a midpoint. As a negative control, NG108-15 neurons were cultured in the absence of PA5s for all three matrix/media combinations. Although NT-3 supplementation was determined to be beneficial to PA5 culture, it was not used in this experiment. This was in order to be able to identify patterns related to standard media and CM and the substrate. The addition of NT-3 would have added an extra variable which would have complicated data interpretation. PA5 cells were characterised in the same way as in Section 3.3.5 with ICC using antibodies against S100β and Fn.

It was determined in our laboratory that 5 days of co-culture is optimal for observing enhanced neurite outgrowth compared with 3 days of co-culture (Georgiou et al., 2017). After 5 days of co-culture, cells were labelled with antibodies against βIII-tubulin. Neuron number, neurite number and neurite length were quantified using the NeuronJ plugin in ImageJ (Meijering et al., 2004). Neurites were traced and measured within the software and exported to Microsoft Excel for analysis.

5.3.1.2 *Results and Discussion*

To ensure comparability with previous experiments (Section 3.3.4-3.3.5) PA5 cells were fixed and stained after 5 days for S100β and Fn. From the fluorescent micrographs obtained (Figure 5.1) and quantification (Figure 5.2), it was found that laminin with standard media gave the highest level of S100β staining (31.8±4.7%, 75.4±7.1 cells/mm^2), followed by laminin with CM (21.8±1.6%, 46.6±11.9 cells/mm^2) and Ms3T3s with CM (20.9±6.4%, 34.4±4.9 cells/mm^2). This quantification was necessary to ensure that any conclusions that were drawn from the neuronal behaviour could be linked to cell populations expressing different levels of S100β.

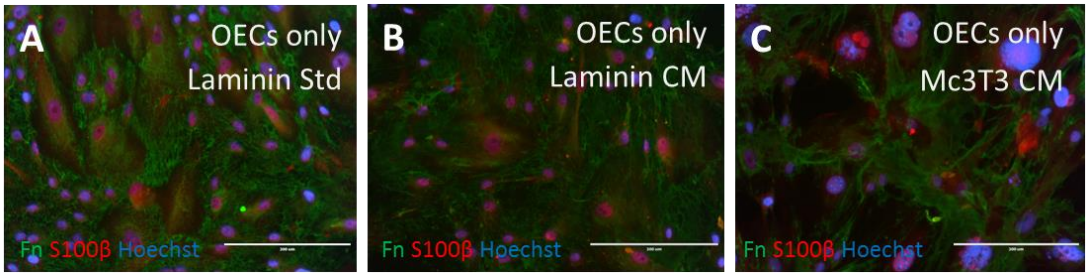

Figure 5.1: Fluorescent micrographs of OECs cultured in isolation for 5 days. OECs cultured in isolation were fixed and stained at day 5 for Fn and S100β to ensure the cells were behaving in a similar way as seen previously (Section 3.3.4-3.3.5). All three conditions had levels of S100β present, however, laminin conditions (A, B) produced higher levels of S100β than OECs cultured on mouse feeders (C). The scale bar represents 200μm.

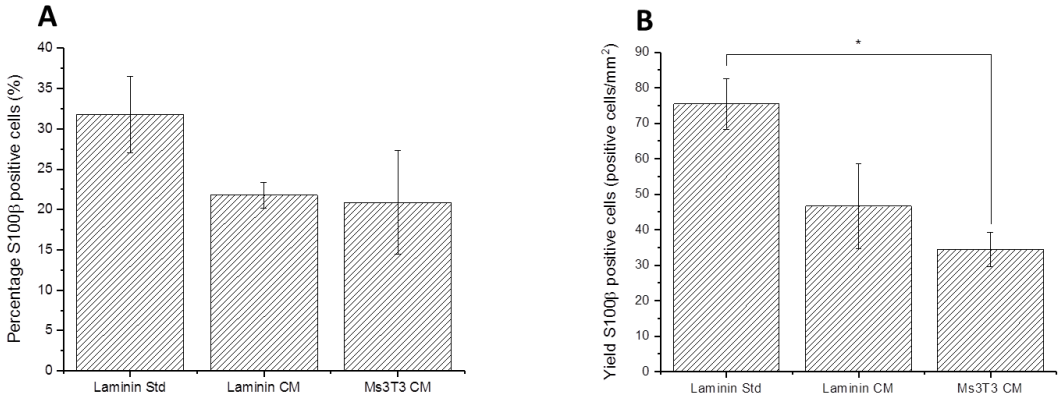

Figure 5.2: Quantification of S100β positive cells at day 5 on OEC only conditions. PA5s were fixed and stained for S100β after 5 days to ensure the behaviour of the cells was the same as had been observed previously. This was quantified by the percentage of cells positive for S100β and the total yield of these positive cells. Data are means ± SEM, n=3.

Figure 5.3 shows phase contrast images taken two days after neurons were plated. OECs were plated on their own to ensure they behaved in the same way as seen previously (Section 3.3.4-3.3.5). The phase contrast images show that the neurons attached and were

viable. OECs plated in isolation reached a higher level of confluency on laminin than on Ms3T3 feeders (as seen previously in Section 3.3.4-3.3.5).

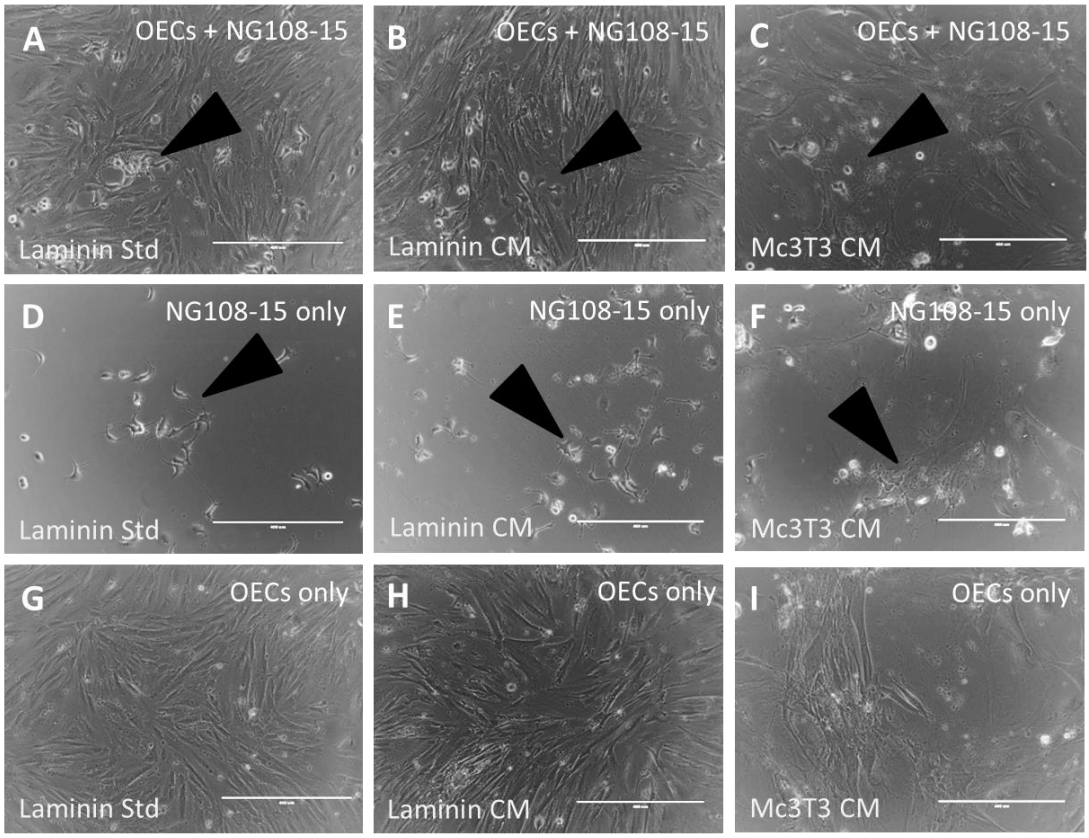

Figure 5.3: Phase contrast images of OECs and NG108-15s cultured in different matrix and media conditions. Images were captured two days after NG108-15s were plated onto the appropriate conditions and seven days after the OECs had been plated. From these images it was possible to identify the NG108-15s as identified by the arrows (A-F) that were starting to grow. It was observed that the laminin conditions have a higher confluency of OECs compared with the Ms3T3 feeders (A, B, C, G, H and I). The scale bar represents 400µm.

After 5 days of co-culture, the cells were fixed and stained for βIII-tubulin and p75NTR. The results of this staining and quantification are presented in Figure 5.4 and Figure 5.5. Neurite outgrowth in cultured neurons is considered an indication of neuro-regenerative potential (Lozano et al., 1995, Encinas et al., 2000, Lehmann et al., 1999, Fournier et al., 2002, Simpson et al., 2001) and therefore neurite outgrowth was quantified to compare the cultures. Neurite number and length were normalised to the number of neurites and neurons. This was done in order to take the average length of each neurite produced by each neuron and to determine any patterns that existed with the number of neurites produced by neurons.

Cells co-cultured on laminin with standard media had a higher number of neurites with longer extensions (Figure 5.4). Cells co-cultured on laminin and feeders with CM did not perform as well as cells cultured with standard media. No difference was observed between the neuron only conditions on the different matrices for all measurements. This indicates that the neurons were responding to the PA5s as opposed to the culture conditions (matrix and media).

The conditions cultured with OECs performed best in regards to average neurite length (Figure 5.5A, one-way ANOVA, Bonferroni post-hoc, $p<0.001$). Although co-culture on laminin with standard media performed better than those co-cultured with CM (49.7±3.7µm versus 40.4±1.6µm), this did not result in any significant difference.

When the neurite length per neuron was examined (Figure 5.5B), the co-culture on laminin with standard media showed significantly longer neurites per neuron (76.0±11.2µm) compared with every other condition (43.6±5.5µm on laminin with CM and 41.0±10.6µm on Ms3T3 with CM, one-way ANOVA, Bonferroni post-hoc, $p<0.01$). All conditions without OECs performed similarly to each other (22.8±2.4µm, 17.8±2.3µm and 17.9±1.1µm on laminin with standard media, laminin with CM and Ms3T3 with CM respectively).

Finally the number of neurites extended by each neuron was plotted (Figure 5.5C). This revealed a similar pattern to Figure 5.5B where the co-culture on laminin with standard media produced more neurites per neuron (1.54±0.20) than the majority of the other conditions (one-way ANOVA, Bonferroni post-hoc, $p<0.001$) with the exception of co-culture on laminin with CM (1.08±0.14). Collectively, these data show that the matrix and media condition that gave the highest S100β expression in OECs resulted in the best neuronal growth support.

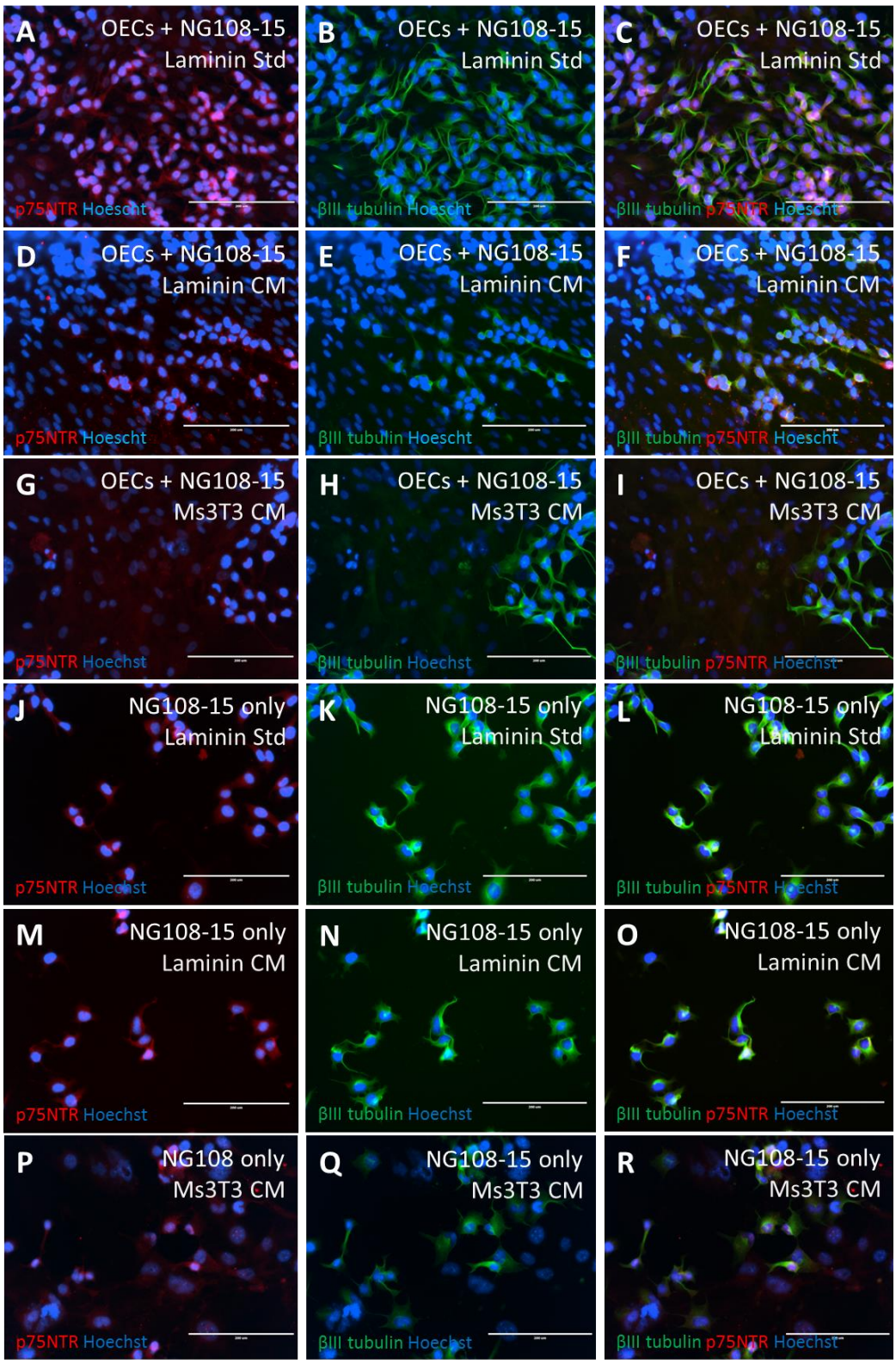

Figure 5.4: Fluorescent micrographs of NG108-15 cells grown on laminin and Ms3T3 feeders with either standard media or conditioned media. Cells were fixed and stained for βIII-tubulin (green) and p75NTR (red), using Hoechst as a nuclear stain. It was observed that there were more neurons and neurites present in the conditions with OEC co-culture (A-I) compared with the conditions with only NG108-15 cells present (J-R). In addition to this, neurites were longest when the NG108-15s were grown with OECs on laminin with standard media (A-C) which was the best performing condition previously for S100β expression. The scale bar represents 200μm.

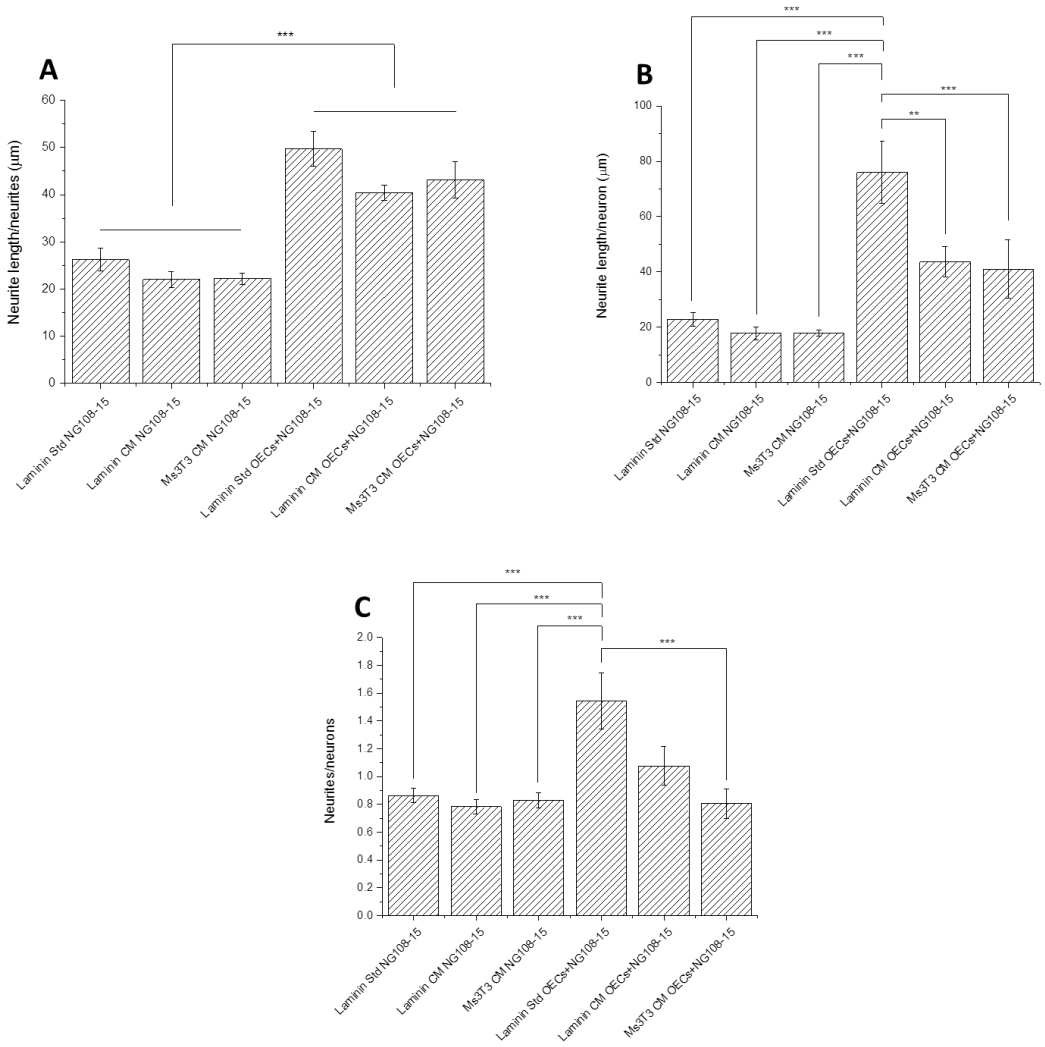

Figure 5.5: Quantification of neurites and neurons in OEC co-culture on laminin and Ms3T3 feeders with standard and CM. The fluorescent micrographs were quantified using positive βIII tubulin staining. Neurites were counted and measured using NeuronJ (ImageJ plugin). Neurites and their length were normalised against the number of neurons and neurites. When neurite length/neurite was quantified (A), it was found that the conditions with OECs had significantly longer neurites (one-way ANOVA, Bonferroni post-hoc, p<0.001). In between OEC conditions and NG108-15 conditions, however, no significance was found. Co-culture with OECs in standard media conditions on laminin significantly outperformed all other conditions in regard to neurite length/neuron (B) and this pattern was repeated when neurites/neurons was examined (C, one-way ANOVA, Bonferroni post-hoc,**p<0.01, *** p<0.001). Data are means ±SEM, n=3.

The formation of neurites from neurons is vital to the functionality and development of the nervous system (Lai et al., 2013). From these results, it can be seen that co-culture on laminin with standard media was the condition that provided the most support to the development of neurons in regards to the longest average neurite. In the absence of co-culture, the development of neurons was not well supported and as a result shorter neurites were observed. Previously in Section 3.3.4-3.3.5, it was found that laminin with standard media was a promising condition for OEC proliferation and S100β expression. This suggests that when OECs are expressing higher levels of S100β they are able to provide

better support to neurons. When S100β expression was lower, the presence of the OECs was still able to benefit the neurons.

When Schwann cells support peripheral nerve repair, it has been observed that an upregulation of S100β leads to identification of so called 'reactive' Schwann cells which were responsible for axonal sprouting (Son et al., 1996). If OECs follow a similar behavioural pattern, it could be that the conditions with higher S100β are more capable of allowing axonal sprouting and therefore result in increased neurite numbers.

It has been observed in several studies that laminin is an extracellular matrix that is able to stimulate rapid neurite growth and has been directly linked to neurite outgrowth in vitro (Menager et al., 2004, Chen et al., 2007, Kuhn et al., 1995). Studies have also shown that enhanced neurite outgrowth and preferred attachment was observed when neurons from the CNS were plated on laminin (Liesi et al., 1984) and it is thought that the presence of laminin starts to create a more permissible environment for axonal extension (di Summa et al., 2013). The hostile environment present after SCI is a key part of why nerve regeneration does not happen spontaneously (Ahuja et al., 2017, Hagg and Oudega, 2006, Franssen et al., 2007). There was no significant difference observed between neurons cultured in isolation on laminin and on Ms3T3 feeders. This suggests there is more to the interaction than the preference for laminin. The combined effect of the favourable matrix and support cells could explain why laminin with standard media was the highest performing condition.

CM collected from HuG418 had a lesser effect on the average neurite length per neuron (Figure 5.5B) compared to standard media. This may be initially related to the lower S100β expression in the OECs in this condition. It would indicate that the CM from HuG418 does not have any beneficial soluble paracrine factors for the neurons. This lack of factors and therefore interaction between these two populations is not necessarily unexpected as although studies have shown a benefit in transplantation with a mixed population of OECs and fibroblasts (Keyvan-Fouladi et al., 2003, Ramón-Cueto et al., 2000, Raisman and Li, 2007, Teng et al., 2008), it has been under the understanding that the fibroblasts support the OECs not the neurons. Fibroblasts have not been pursued as a cell therapy option for nerve regeneration and they are not believed to have specific properties that enhance the function of neurons (Pizzi and Crowe, 2006, Kisselbach et al., 2009). Therefore standard

media resulting in longer neurites than conditioned media can be seen as an expected output.

5.3.2 Functional response of neuronal cells to OECs with different time-dependent p75NTR expression levels

PA5 cells (10,000 cells/cm^2) were cultured on laminin with NT-3 for 24 hours and 5 days. NG108-15 neurons (500 cells/cm^2) were plated on top of the OECs at these two time points and cultured for a further 5 days. The aim of this experiment was to determine if an increase in p75NTR expression related to an increase in neurite extension. NG108-15 cells were cultured in the absence of PA5 cells as the negative control.

5.3.2.1 Experimental Overview

p75NTR has been extensively used as a putative marker for OECs in literature (Franssen et al., 2007, Barnett and Riddell, 2004, Boyd et al., 2003, Guerout et al., 2011, Pellitteri et al., 2010, Sonigra et al., 1999). Little work has been done, however, to relate the presence of this marker to OEC function (Chen et al., 2009). In Section 4.3.2, it was found that p75NTR expression decreases over time in culture. Initially expression was found to be high but, after 48 hours, it declined rapidly and was significantly lower after 5 days. In order to determine if the expression of p75NTR had any relation to neuronal behaviour, NG108-15 cells (500 cells/cm^2) were plated onto PA5s (10,000 cells/cm^2) at high (24 hours) and low (5 days) levels of p75NTR expression. NG108-15s were cultured for 5 days after plating and NG108-15s were plated in isolation as a negative control.

As in Section 5.3.1, neuron number, neurite number and length were quantified using the NeuronJ plugin in for ImageJ. Cells were characterised using p75NTR to confirm the same staining pattern occurred as previously observed (Section 4.3.2-4.3.3). βIII-tubulin was used to label the neurons.

5.3.2.2 Results and Discussion

Initially cells were fixed and labelled for p75NTR to confirm the expression pattern was the same as previously observed in Section 4.3.2 and 4.3.3. From these images and quantification (Figure 5.6-Figure 5.7), it was determined that p75NTR expression was

significantly higher at 24 hours (96.8±1.2%) compared to 5 days (31.0±4.8%, one-way ANOVA, Bonferroni post-hoc, p<0.001).

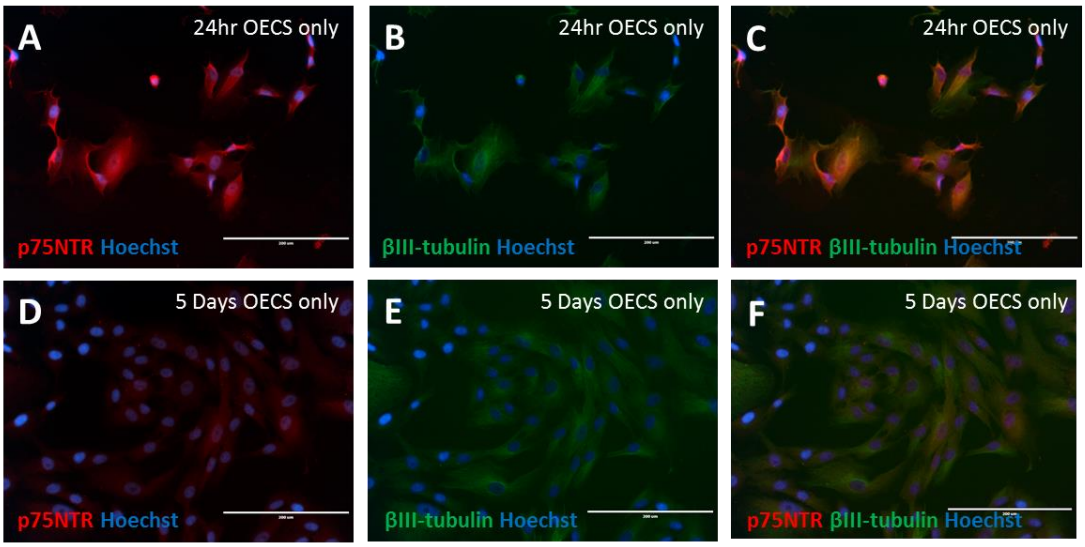

Figure 5.6: Fluorescent micrographs validating p75NTR expression over time. Cells were fixed and stained for βIII-tubulin (green) and p75NTR (red), using Hoechst as a nuclear stain. It was observed that higher p75NTR expression was exhibited after 24 hours (A) compared to 5 days in culture (D). The scale bar represents 200µm.

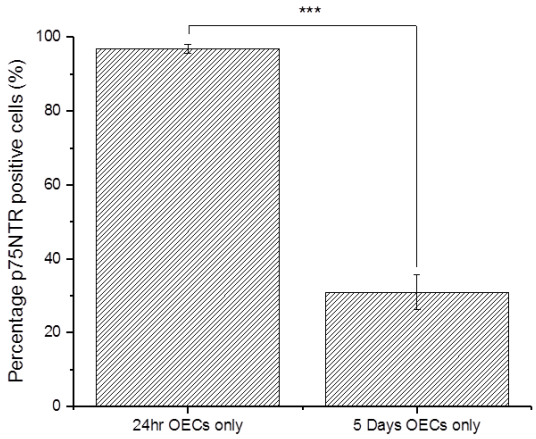

Figure 5.7: Quantification of p75NTR positive cells at 24 hours and 5 days for OEC only conditions. PA5s were fixed and stained for p75NTR after 5 days to ensure the behaviour of the cells was the same as had been observed previously. This work validated the previous findings that, at 24 hours, OECs express significantly higher levels of p75NTR than at 5 days (one-way ANOVA, Bonferroni post-hoc, p<0.001). Data are means ±SEM, n=3.

Phase contrast images of the cells in culture were taken two days after NG108-15 neurons were plated. From these images (Figure 5.8) it can be observed that the NG108-15s have attached and in the conditions with OECs (Figure 5.8C and Figure 5.8D) can be seen to be

forming colonies. When the neurons were cultured in isolation (Figure 5.8E and Figure 5.8F) the neurons do not appear to form obvious colonies.

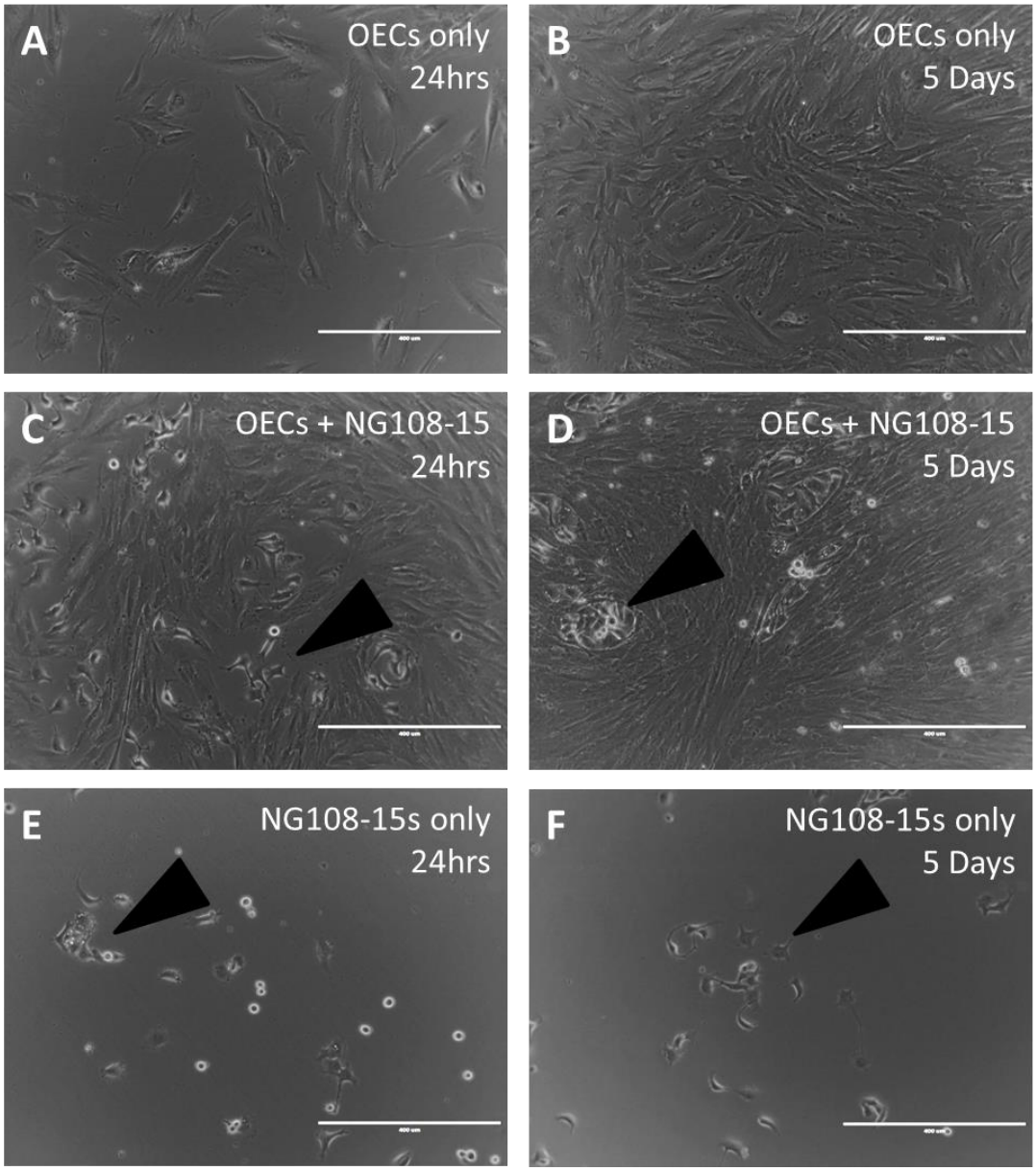

Figure 5.8: Phase contrast images of OECs and NG108-15s cultured at different levels of p75NTR expression. These images with NG108-15s were taken two days after NG108-15s were plated on the appropriate conditions and the images of 'OECs only' were when NG108-15s were plated onto these conditions. The NG108-15s are identified by the arrows. From these images it was observed that the NG108-15s on OECs (C, D) have more neurons which were also communicated with each other more compared with those grown in isolation (E, F). The scale bar represents 400μm.

Neurons were cultured for 5 days and fixed and stained to detect p75NTR and βIII-tubulin. From the ICC micrographs and quantification (Figure 5.9-Figure 5.10) it can be determined that, as previously reported in Section 5.3.1, neurons cultured in isolation showed few

neurite extensions (Figure 5.9E, K) and neurons co-cultured with OECs showed longer neurite extensions (Figure 5.9B, H).

When neurite length/neurite and neurite length/neuron was considered, neurons co-cultured with OECs from 24 hours after plating had significantly longer neurites (48.8±1.7µm and 39.2±2.8µm for neurite length/neurite and neurite length/neuron respectively) than every other condition (one-way ANOVA, Bonferroni post hoc, $p<0.001$). In addition to this, neurons co-cultured with OECs 5 days after plating had significantly longer neurites (32.6±1.5µm and 21.9±1.7µm for neurite length/neurite and neurite length/neuron respectively) than conditions where neurons were cultured in isolation (23.0±1.0µm and 14.2±1.0µm for neurite length/neurite and neurite length/neuron respectively, one-way ANOVA, Bonferroni post hoc, $p<0.05$ (*), $p<0.01$ (**), $p<0.001$ (***)). This validates the conclusion drawn from Section 5.3.1 that OECs have a beneficial impact on neurite extension.

In Figure 5.10C, only a small difference was observed between conditions in regard to neurites/neuron. The same pattern was observed with co-culture at high levels of p75NTR (24 hours) providing the highest ratio (0.80±0.05), followed by co-culture at low levels of p75NTR (5 days, 0.68±0.05) and finally neurons cultured in isolation (0.63±0.04 for the 24 hours condition and 0.61±0.05 for the 5 day condition). Despite this pattern, the only significance found was between co-culture at 24 hours and neurons cultured in isolation (one-way ANOVA, Bonferroni post-hoc, $p<0.01$).

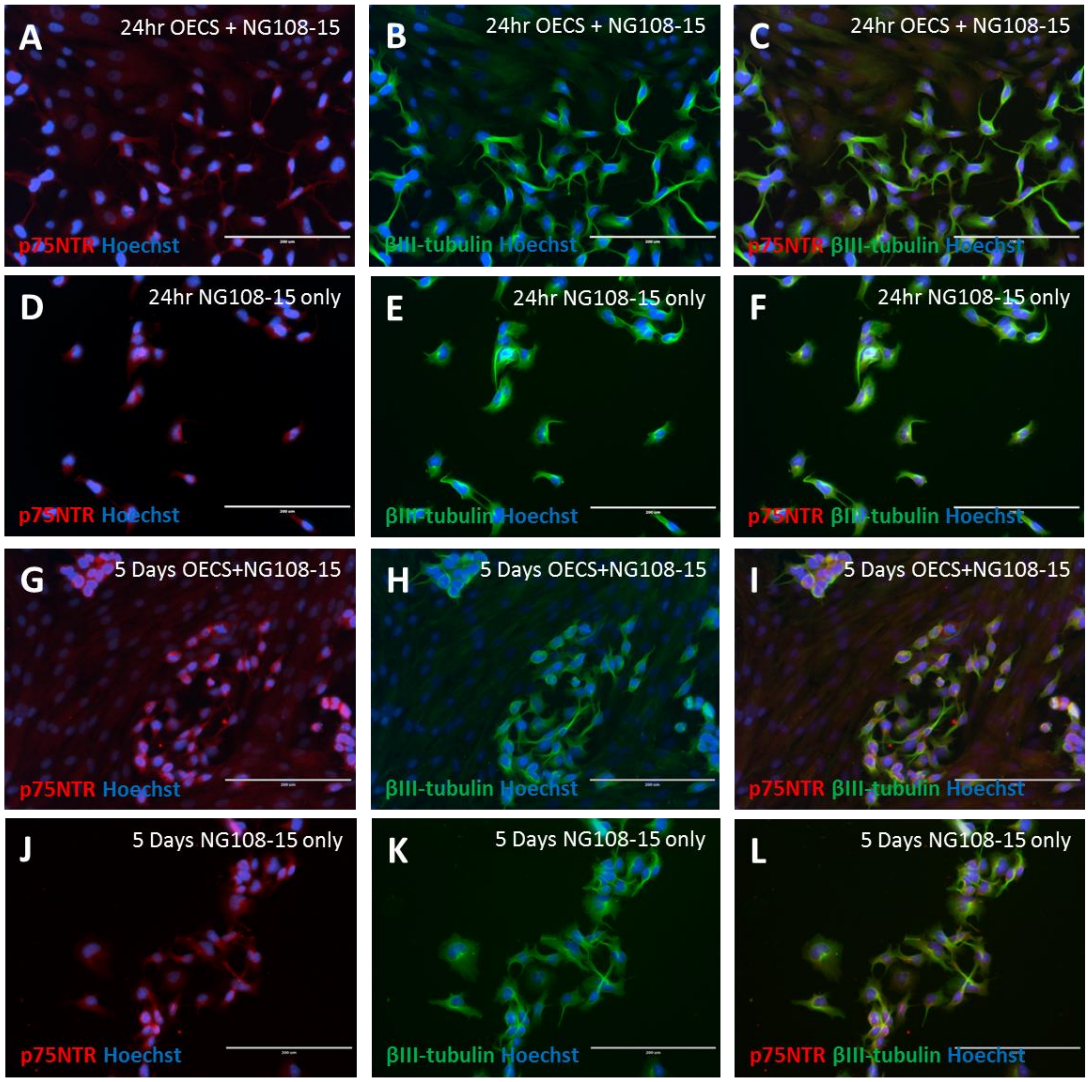

Figure 5.9: Fluorescent micrographs of NG108-15 cells grown on OECs at different levels of p75NTR expression. Cells were fixed and stained for βIII-tubulin (green) and p75NTR (red), using Hoechst as a nuclear stain. Neurons plated on OECs after 24 hours (A-C) as opposed to plated after 5 days (G-I), showed not only more extensions from the neuron body, but longer extensions. Both conditions with OECs (A-C, G-I), were always better in terms of neuronal behaviour compared with neurons grown in isolation (D-F, J-L). The scale bar represents 200µm.

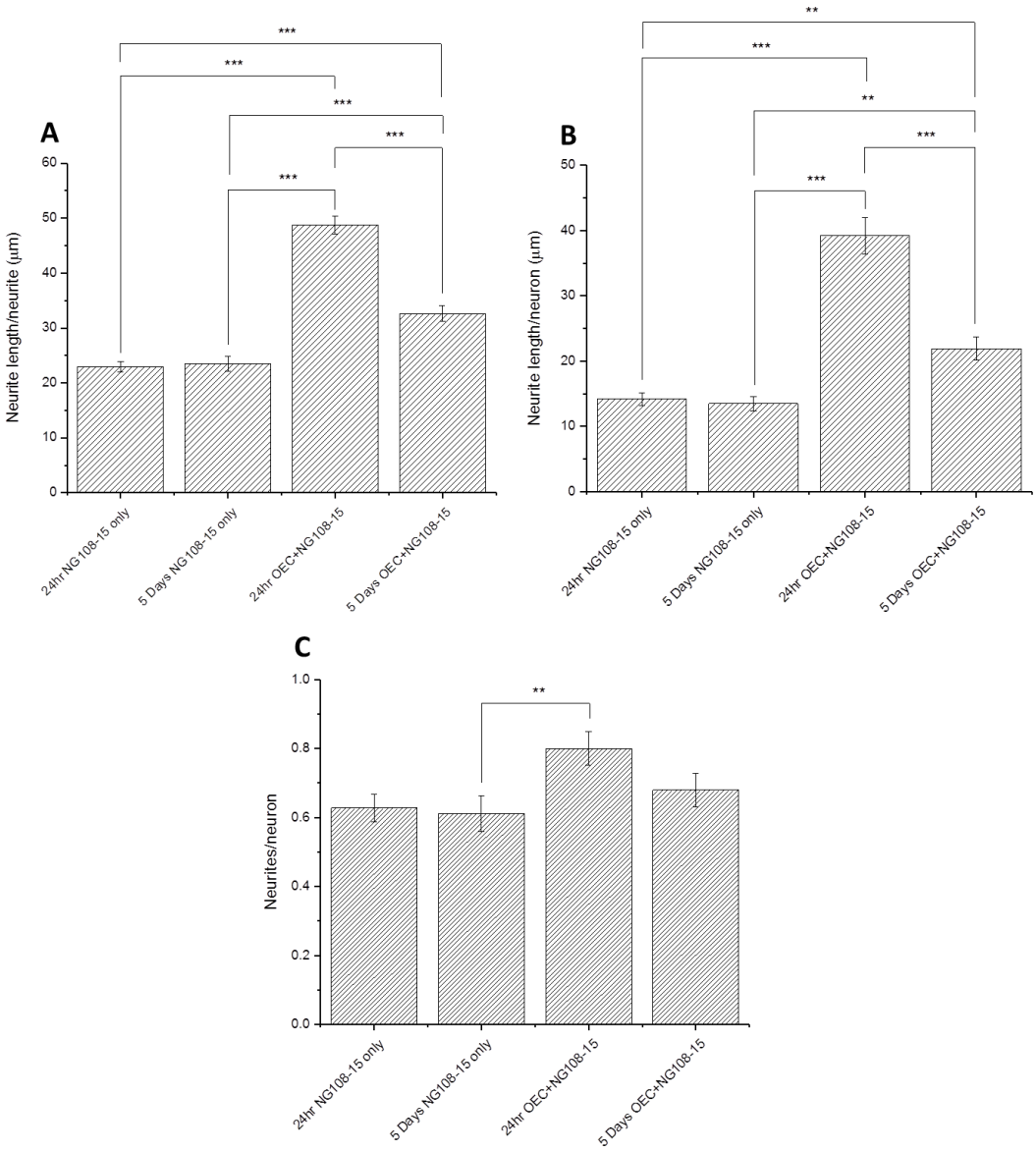

Figure 5.10: Quantification of NG108-15 neurites and neuron number cultured on OECs at different levels of p75NTR expression. The fluorescent micrographs were quantified using positive βIII tubulin staining. Neurites were counted and measured using NeuronJ (ImageJ plugin). Neurites and their length were normalised against the number of neurons and neurites. When neurite length/neurite was quantified (A), it was observed that conditions with OECs had significantly longer neurites per neuron (one-way ANOVA, Bonferroni post-hoc, $p<0.001$). In addition to this, neurons co-cultured at 24 hours had significantly longer neurites per neuron compared with those co-cultured at 5 days (one-way ANOVA, Bonferroni post-hoc, $p<0.001$). When the neurite length/neuron was plotted (B), this followed the same trend as observed with neurite length/neurite (A). Finally the number of neurites/neuron was considered (C) where the same downward trend was observed. Data are means ± SEM, n=3.

Studies conducted on neurons have found that p75NTR expression encourages neurite outgrowth (Chen et al., 2009). This may be related to the system Schwann cells use to encourage neurite outgrowth in the PNS. Schwann cells have been observed to upregulate p75NTR after peripheral nerve injury (Wei et al., 2007) and that axons rely on the factors provided by Schwann cells (Mirsky et al., 2002). It could be that OECs operate in a similar

way and their interaction with neurons follows similar patterns. This recognition by NG108-15s of higher p75NTR expression could prompt neurons to start extending and developing (Fawcett and Keynes, 1990).

p75NTR is the receptor to nerve growth factor (NGF) (Woodhall et al., 2001) and it has been observed that high levels of NGF promote survival of sympathetic neurons which are the autonomic neurons found in the spinal cord (Davies et al., 1993, Lai et al., 2013, Simpson et al., 2001). The interaction between the receptor and the growth factor could have significant implications for the improvement seen. OECs not only express p75NTR, they also express NGF (Woodhall et al., 2001). As reported in the previous paragraph, axons rely on paracrine factors from Schwann cells (Mirsky et al., 2002). One of these factors is NGF. It is accepted that Schwann cells transfer NGF to the growing or regenerating axons in the PNS. This signals the axon to elongate and Schwann cells are the trophic source of NGF for neurons after peripheral nerve injury (Woodhall et al., 2001). OECs in their behaviour and protein expression are indiscernible from Schwann cells (with the exception of astrocyte interaction) and therefore could behave in a parallel way in the CNS (Yang et al., 2014, Orbay et al., 2015, Tong et al., 2010, Niapour et al., 2010, Wen et al., 2012, Mahapatra et al., 2009, Kawaja et al., 2009).

From this work it can be reported that a higher level of p75NTR expression in OECs coincides with longer neurites in co-culture. Whether this can be put down to the p75NTR expression itself or soluble paracrine factors that are secreted when p75NTR expression is occurring is currently unknown. This will be the focus of further work carried out in Section 5.3.4.

When this data is examined alongside the data obtained in Section 5.3.1, it indicates that high levels of p75NTR and S100β expression can be used as indicators for OEC subtypes that are better able to aid neuron growth.

5.3.3 Functional response of neuronal cells to OECs with different Thy1 expression levels

PA5 cells were purified using the MACS technology described in Section 4.3.1.1. A sample of PA5 cells was taken and plated before purification took place and the two purified populations were also plated on laminin coated well plates and cultured in the presence of

NT-3. After 24 hours, NG108-15 neurons were plated on top of the PA5 cells and cultured for 5 days. The aim of this experiment was to determine whether the Thy1 negative fraction of the population gave enhanced neuronal behaviour compared with the Thy1 positive and original population. NG108-15 neurons were cultured in the absence of PA5 cells as the negative control.

5.3.3.1 Experimental Overview

PA5s were purified (see Section 4.3.1) and fully characterised (see Section 4.3.4). This purification removed Thy1 expressing cells from the population and both the negative and positive populations were cultured. It was found in Section 4.3.1 that the purification process was efficient for removing Thy1 from the population although in Section 4.3.4 it was observed that Thy1 turned back on after 5 days in culture.

NG108-15s were plated on the Thy1 negative and positive fractions and a sample from the pre-population after 24 hours. As in Section 5.3.1 and Section 5.3.2, NG108-15s were plated at 500 cells/cm^2 and co-cultured for 5 days. Cells were labelled with Thy1 to validate the purification and βIII-tubulin to label the neurons. NeuronJ (plugin for ImageJ) was used to measure the neurites extended.

5.3.3.2 Results and Discussion

Cells were plated and fixed for 24 and 48 hours and stained to detect Thy1. Triton X permeabilisation was excluded from the staining protocol and cells were stained at 24 hour intervals to allow for the transient nature of the protein.

It can be determined from the ICC images and quantification, as previously reported in Section 4.3.3, the purification removed Thy1 from the cell population (Figure 5.11-Figure 5.12). The retained (Thy1 positive) fraction had a high level of Thy1 reactivity (70.8±3.0% at 24 hours), the eluted fraction (Thy1 negative) showed a lack of Thy1 positive staining (11.2±3.0% at 24 hours) and the difference between the two was significant (one-way ANOVA, Bonferroni post-hoc, p<0.001). Although the retained fraction showed higher proportions and yields (83.9±0.5%, 104.4±12.3 cells/mm^2 at 24 hours) than the pre-purified fraction (70.8±3.0%, 66.2±7.8 cells/mm^2 at 24 hours), this was not significant (Figure 5.12).

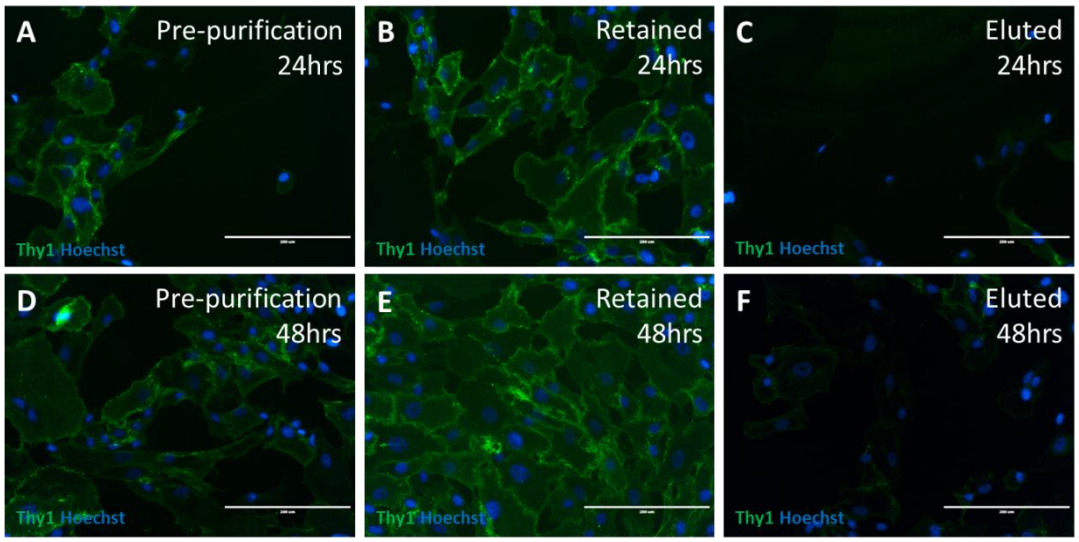

Figure 5.11: Fluorescent micrographs validating the MACS purification process. ICC was carried out on the original population as well as the Thy1 positive (retained) and negative (eluted) in order to validate the purification. Cells were fixed and stained at 24 and 48 hours in the absence of Triton X. It was observed that the original population (A and D) had a high level of Thy1 reactivity which was further enhanced in the retained fraction (B and E). Eluted cells (C and F) were found to be nearly completely negative for Thy1 showing the purification process was successful. The scale bar represents 200µm.

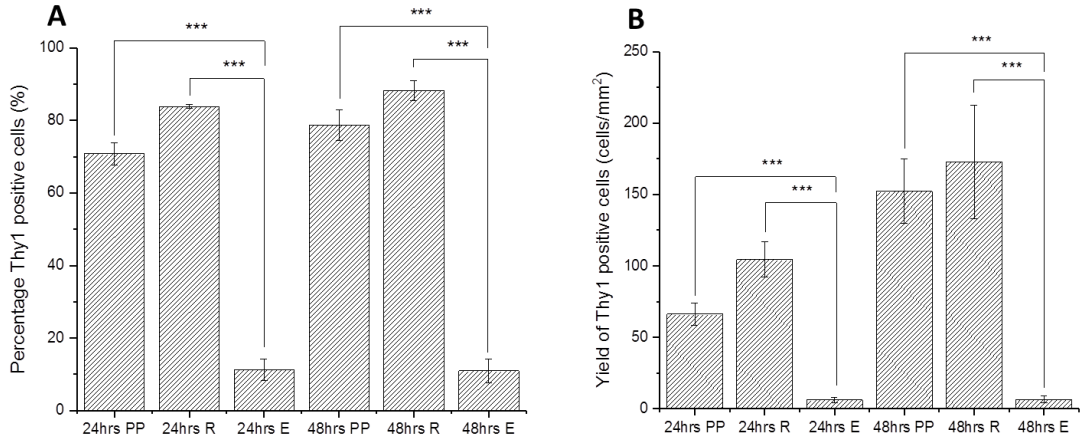

Figure 5.12: Quantification of Thy1 staining before and after MACS purification. The fluorescent micrographs in Figure 5.11 were quantified for Thy1 positive cells. The proportion and yield of Thy1 positive cells were significantly lower in the eluted fraction compared with the pre-purified and retained fractions (one-way ANOVA, Bonferroni post-hoc, $p<0.001$). It was observed that a higher proportion of Thy1 positive cells was found in the retained fraction. Data are means ±SEM, n=3.

Phase images were taken two days after NG108-15s were plated onto the conditions (Figure 5.13). Despite the PA5 cells being seeded at identical seeding densities, the eluted (Thy1 negative) cells had a much lower attached cell density. This was observed in Section 4.3.1 where the yield for all markers was significantly lower for the eluted fraction. As

discussed in Chapter 4.0, the removal of Thy1 may be inhibiting the ability of the cells to attach and therefore a decrease in cell attachment can be observed.

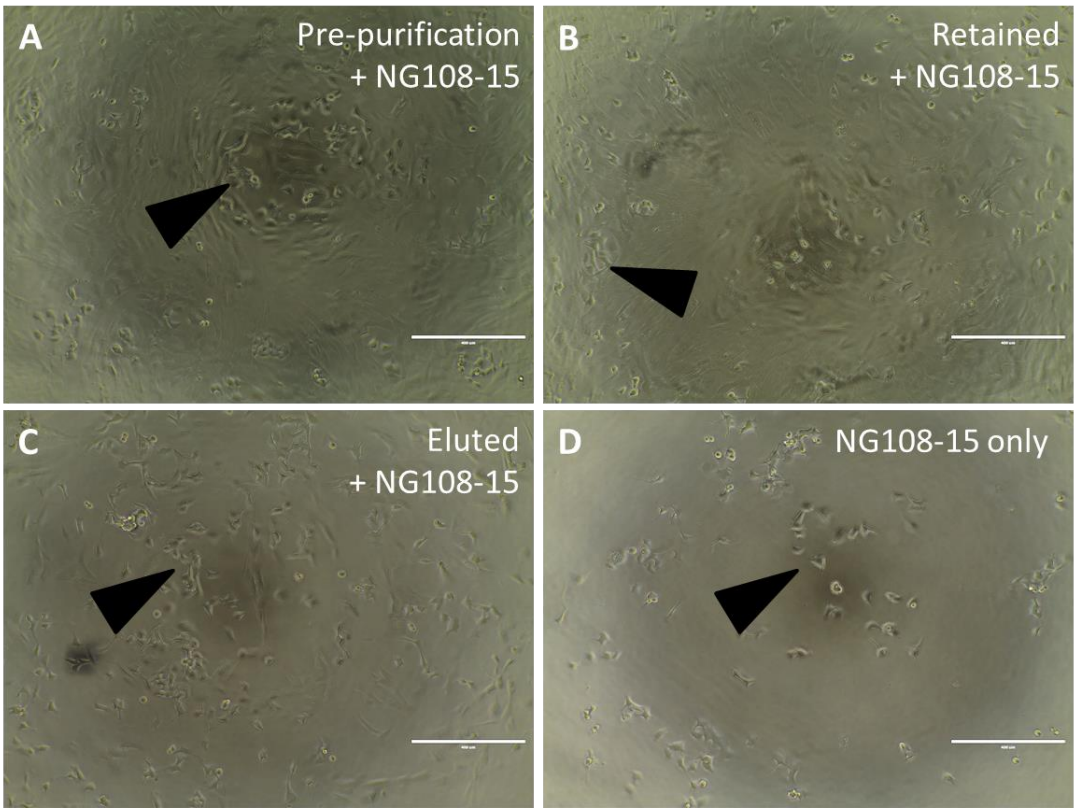

Figure 5.13: Phase contrast images of OECs and NG108-15s cultured on OECs before and after purification process. These images were taken two days after NG108-15s were plated on the appropriate conditions and the NG108-15s are identified by the arrows. From these images it can be observed that there were a higher number of OECs present in the pre-purified and retained fractions (A, B) than were present in the eluted fraction (C). The neurons cultured in isolation were observed to have attached (D). The scale bar represents 400µm.

After 5 days of neuronal culture, the cells were fixed and stained for p75NTR and βIII-tubulin. The micrographs show that the pre-purified population of PA5s were able to support the neurons better than those cultured in isolation (Figure 5.14) as previously observed in Section 5.3.1-5.3.2. This was further confirmed in the quantification (Figure 5.15)

The average neurite lengths (Figure 5.14-Figure 5.15A) between the three PA5 fractions were significantly different to the neurons alone (16.9±0.8µm, one-way ANOVA, Bonferroni post-hoc, p<0.001), however no difference was observed between these fractions. The average neurite length in the pre-purified fraction (30.1±0.7µm) was slightly lower than the retained (31.4±0.8µm) and eluted fractions (31.3±1.0µm), but no significance was found.

Differences in the PA5 fractions were detectable when comparing the neurite length per neuron (Figure 5.14, Figure 5.15B). Although the average neurite length was similar, examining the length of neurites per neuron showed the pre-purified fraction had significantly shorter neurites per neuron (19.4±1.0µm) compared with the eluted (30.4±1.9µm) and retained fractions (27.8±2.0µm, one-way ANOVA, Bonferroni post-hoc, $^{**}p<0.01$, $^{***}p<0.001$). All PA5 conditions were significantly better than neurons on their own (10.0±1.1µm, one-way ANOVA, Bonferroni post-hoc, $p<0.001$).

This pattern was repeated when comparing the number of neurites per neuron (Figure 5.14, Figure 5.15C). The neurons cultured in isolation provided the lowest ratio (0.53±0.05), followed by the pre-purified fraction (0.65±0.03) and then the retained and eluted fractions giving similar values (0.88±0.05 and 0.98±0.06 respectively). The eluted fraction showed a tendency to give a higher ratio than the retained fraction, however, this was not significant. This pattern was seen in all three graphs where the eluted appears to be slightly, although not obviously, better at supporting neuronal growth than the retained fraction.

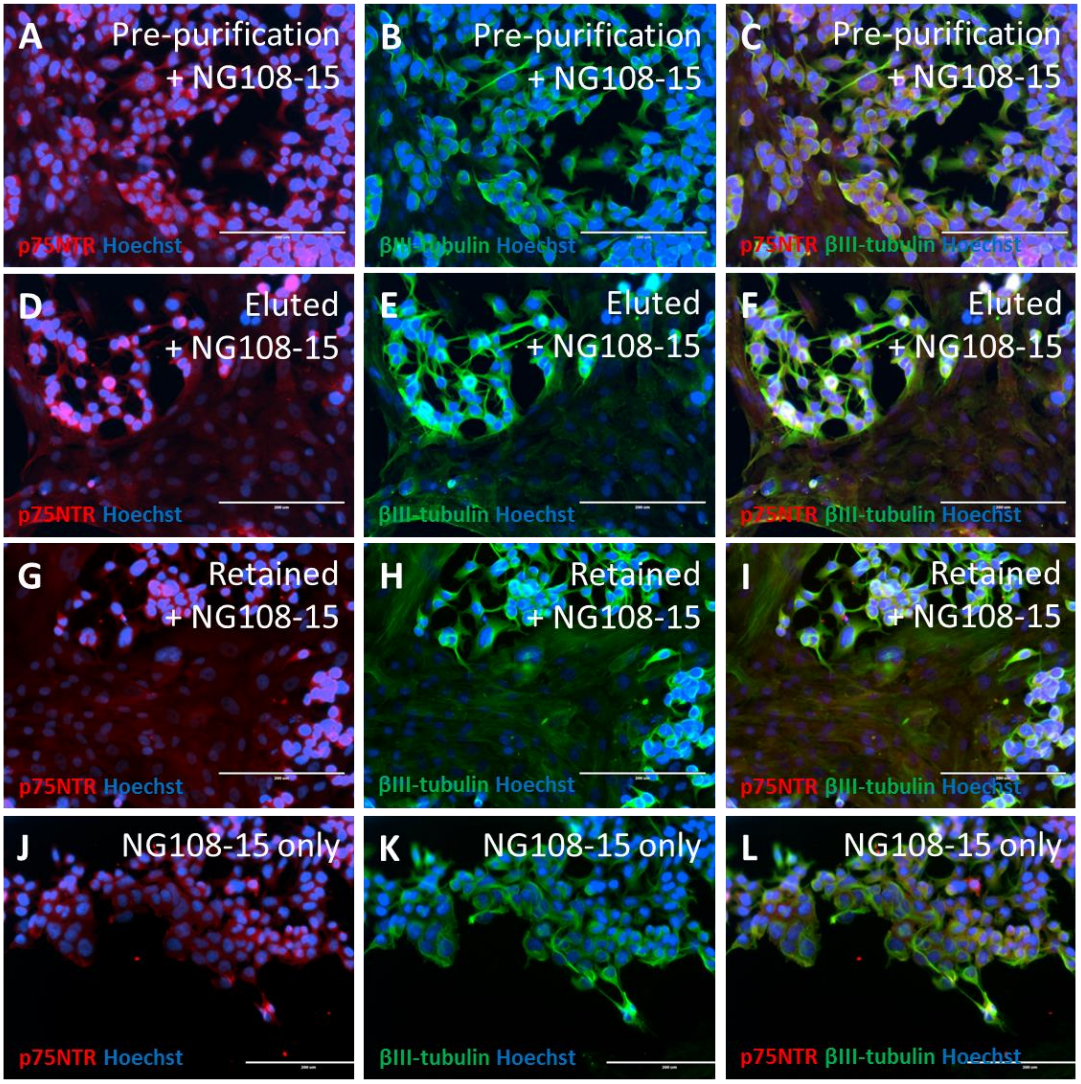

Figure 5.14: Fluorescent micrographs of NG108-15 cells grown on OECs before and after purification process. Cells were fixed and stained for βIII-tubulin (green) and p75NTR (red), using Hoechst as a nuclear stain. It was observed that neurons were positive for p75NTR (A, D, G and J) and the expression of p75NTR in OECs fades over time (A, D, G and J). In relation to neuron behaviour, it was observed that neurons on OECs (B, E and H) extend more and longer neurites than neurons cultured in isolation (K). In regards to the different purification populations, the pre-purified fraction (B) performed the worst out of the OEC co-culture populations. Between the eluted and retained fractions, the eluted fraction (E) appeared to lead to longer extensions than the retained fraction (H). The scale bar represents 200µm.

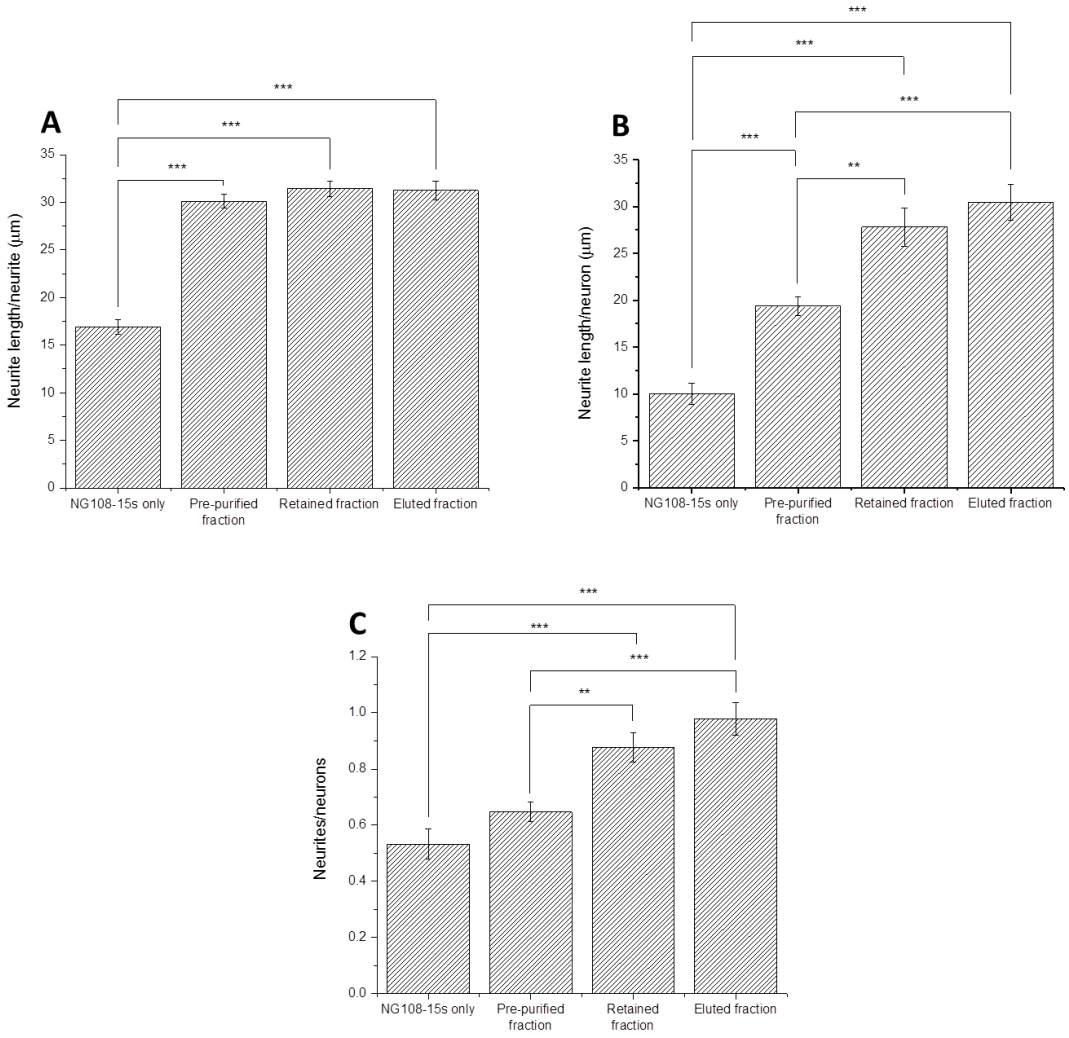

Figure 5.15: Quantification of NG108-15 cells cultured on OECs before and after purification process. The fluorescent micrographs were quantified using positive βIII tubulin staining. Neurites were counted and measured using NeuronJ (ImageJ plugin). Neurites and their length were normalised against the number of neurons and neurites. When neurite length/neurite was quantified (A), the OEC populations led to significantly longer neurites per neurite compared with neurons cultured in isolation (one-way ANOVA, Bonferroni post-hoc, $p<0.001$). No significance was found between the pre-purified fraction, eluted and retained fractions. When the neurite length/neuron (B) was considered, significance was found between every conditioned except the retained and eluted fractions (one-way ANOVA, Bonferroni post-hoc, $^{**}p<0.01$, $^{***}p<0.001$). This pattern was repeated when the number of neurites per neurons (C) was examined. Pre-purified cells were out performed by the eluted and retained fractions. Data are means ±SEM, n=3.

This work suggests that neurite elongation is not a function of Thy1 expression as previous experiments in Section 4.3.2 and Section 4.3.4 found that p75NTR and S100β expression did not change between these populations. When OEC populations with high and low Thy1 expression were co-cultured with neurons, there was no significant difference observed between the two conditions but differences did exist when the Thy1 population was mixed. The Thy1 purification therefore must have prompted a more significant change in the population to explain this behaviour.

The concept of lateral inhibition was investigated to determine if this phenomenon can be applied to this situation. This is a regulatory mechanism that controls cell fate and enables differential activation in neighbouring cells to generate different cell types (Guisoni et al., 2017, Sancho et al., 2015, Kim et al., 2014). Lateral inhibition is linked to the receptor Notch and its membrane bound ligand Delta. Delta activates Notch in neighbouring cells and once Notch is activated, it reduces the ability of the cell to signal through Delta. This leads to a state of mutual repression which is eventually broken and leads to neighbouring cells taking different fates (Guisoni et al., 2017, Nikolaou et al., 2009). It is a phenomenon observed in tissue stem cells (Sancho et al., 2015), Schwann cell development (Miller et al., 2016) and is known to exist in the olfactory system, although not necessarily in OECs (McIntyre and Cleland, 2016, Miller et al., 2016).

It is an accepted idea that the OEC population is made up of sub-populations (Hayat et al., 2003, Ramón-Cueto and Nieto-Sampedro, 1992) and therefore it is possible that these sub-populations come about via lateral inhibition (Sancho et al., 2015). In the pre-purified (mixed) population, lateral inhibition could be occurring which limits the ability of the OECs to completely fulfil their potential. Once these cells are separated, they have dedicated to a set fate so lateral inhibition is no longer able to impact differentiation (Guisoni et al., 2017). If both sub-populations are equally capable of supporting neurite extension, this would explain why they perform better when they are separated as lateral inhibition is not preventing some of the potential function. In Section 4.3.4, the two populations appeared to become more similar over time and therefore in order to fully understand the population present, daughter cells should be tracked and characterised. It could be that the daughter cells that are produced are capable of introducing lateral inhibition and therefore it could enter back into the population which is why the populations start to revert to their original state. Additionally, staining for activated Notch1 in the PA5 population would show whether the Notch-Delta pathway is active (Guisoni et al., 2017, Nikolaou et al., 2009, Sancho et al., 2015).

5.3.4 Functional response of NG108-15 neurons co-cultured with OECs and conditioned media collected during high and low p75NTR expression

Previously (Section 5.3.2), NG108-15s were cultured on OECs with different levels of p75NTR expression. From this it was found that OECs with higher levels of p75NTR expression gave better support to the neurons in terms of neurite extension. CM was

collected from PA5s during high and low p75NTR expression and cultured with NG108-15s to observe any effects of soluble trophic factors. The aim of this experiment was to determine if soluble paracrine signalling was responsible for the increased neurite length observed during co-culture. NG108-15 cells were cultured in the absence of PA5 cells as the negative control.

5.3.4.1 Experimental Overview

PA5 cells (10,000 cells/cm^2) were cultured on laminin with NT-3 for 24 hours and 5 days. NG108-15 neurons (500 cells/cm^2) were plated on top of the OECs at these two time points and cultured for a further 5 days. CM was collected after 24 hours and 5 days, spun at 400g for 5 minutes and added at a 1:1 ratio with fresh media. All the conditions run in Section 5.3.2 were run in parallel for comparison.

5.3.4.2 Results and Discussion

As in Section 4.3.2 and 5.3.2, expression of p75NTR in the OEC population decreased over time from 24 hours (98.8±0.4%) to 5 days (22.7±7.9%). This decrease can be observed from the ICC staining (Figure 5.16) and quantification (Figure 5.17).

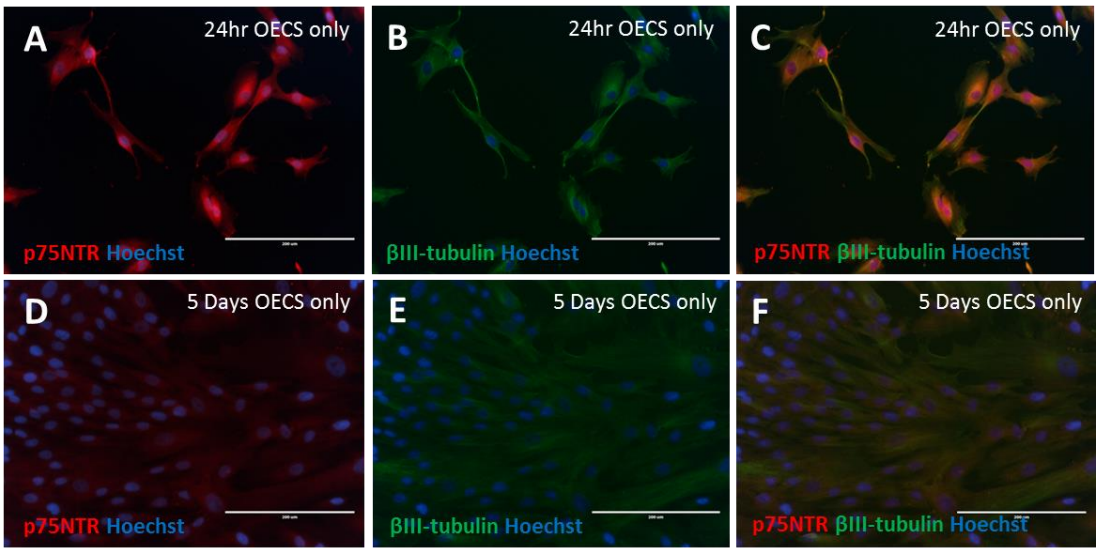

Figure 5.16: Fluorescent micrographs validating p75NTR expression over time. Cells were fixed and stained for βIII-tubulin (green) and p75NTR (red), using Hoechst as a nuclear stain. It was observed that higher p75NTR expression was present after 24 hours (A) compared to 5 days in culture (D). This validates previous work on the expression of p75NTR (Section 4.3.2). The scale bar represents 200µm.

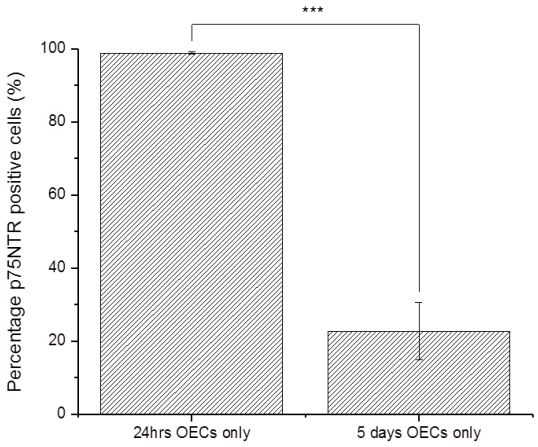

Figure 5.17: Quantification of p75NTR positive cells at 24 hours and day 5 on OEC only conditions. OECs were fixed and stained for p75NTR after 5 days to ensure the behaviour of the cells was the same as had been observed previously. This work validated what was seen before which was that at 24 hours, OECs express significantly higher p75NTR than at 5 days (one-way ANOVA, Bonferroni post-hoc, $p<0.01$). Data are means ± SEM, n=3.

Phase contrast images of the cells were taken two days after NG108-15 plating (Figure 5.18). For the 'OECs only' condition, the images were taken before the cells were fixed for staining at 24 hours and 5 days respectively. From these images it was observed that neurons attached faster to the conditions with OECs. Neurons cultured in isolation only had a small population present after two days in culture with no interaction between the neurons occurring. When the neurons were cultured with CM from OECs cultured for 24 hours, it was observed that a higher level of attachment occurred compared with the neurons in standard media. In addition to this, interaction between the neurons was able to be observed in the CM condition. Neurons cultured in the presence of CM from OECs cultured for 5 days appeared to have a higher attachment rate, however, minimal interaction between the neurons was observed. This indicated CM from OECs with a high level of p75NTR expression was beneficial to NG108-15 survival, proliferation and extension and this can be observed after only two days in culture.

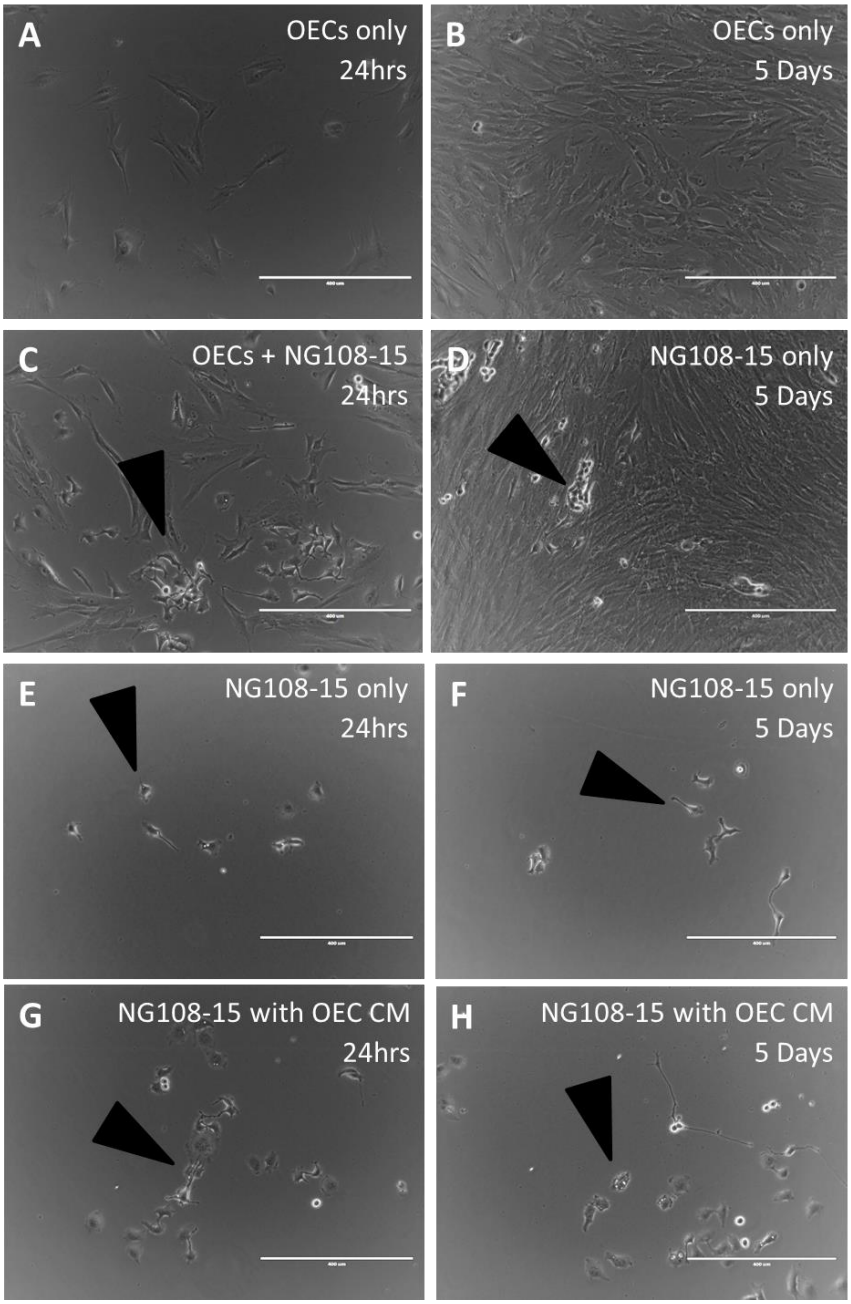

Figure 5.18: Phase contrast images of OECs and NG108-15s cultured at different levels of p75NTR expression in different media conditions. These images with NG108-15s were taken two days after NG108-15s were plated on the appropriate conditions. The NG108-15s are identified by the arrows. The images of 'OECs only' were taken the day NG108-15s were plated onto these conditions. From these images it can be determined that NG108-15s on OECs (C, D) have more neurons compared with those cultured in isolation (E-H). In addition to this, there appeared to be more neurons when NG108-15s were plated on a 24 hour old OEC culture (C) compared with a 5 day old OEC culture (D). Neurons cultured with CM showed higher survival as well as obvious neurite outgrowth after just two days compared with neurons in isolation. The scale bar represents 400μm.

To build on the work that was completed in Section 5.3.2, CM was collected from the OECs at 24 hours and 5 days, spun at 400g for 5 minutes and added at a 1:1 ratio with fresh media to neurons cultured in isolation. Neurons cultured with PA5s or in isolation for 5

days were fixed, stained for p75NTR and βIII-tubulin (Figure 5.19) and quantified (Figure 5.20).

When the neurite length was normalised against the number of neurites or the number of neurons (Figure 5.20), a pattern emerged. Co-culture at 24 hours gave significantly longer neurites (30.6±0.6µm neurite length/neurite) than other conditions tested (one-way ANOVA, Bonferroni post-hoc, $p<0.001$). As with Section 5.3.2, although co-culture with OECs at 5 days (19.3±0.8µm neurite length/neurite) did not encourage neurite extension to the same extent as co-culture at 24 hours, the neurites were longer than those cultured in isolation with standard media (15.0±0.7µm and 14.8±0.8µm neurite length/neurite at 24 hours and 5 days respectively). The longer neurite extensions measured in the CM conditions, (21.7±0.8µm and 18.2±1.0µm neurite length/neurite for 24 hours and 5 days respectively) compared to neurons cultured in isolation, suggests that CM from OECs was beneficial to neurons in culture. However, culturing neurons with OEC CM did not allow the neurons to reach the same level of extension as co-culture. This indicates OECs may be providing more than trophic factors. CM taken at 24 hours (21.7±0.8µm neurite length/neurite) allowed neurites to extend further than those cultured alone (15.0±0.7µm neurite length/neurite), although the neurites were significantly shorter than those in co-culture (30.6±0.6µm neurite length/neurite, one-way ANOVA, Bonferroni post-hoc, $p<0.001$). Conversely, CM taken at 5 days (18.2±1.0µm neurite length/neurite) performed slightly better than neurons in isolation (14.8±0.8µm neurite length/neurite) but no significant difference was found between the CM and co-culture conditions (19.3±0.8µm neurite length/neurite).

When the neurites per neuron were compared (Figure 5.19-Figure 5.20), trends were more difficult to observe (as was found in Sections 5.3.1-3). The same pattern seems to occur, although not as distinct. This indicated the culture conditions have a larger influence on the length of the neurites extended as opposed to the number of neurites extended. This may be because, in the time frame investigated, neurons are unlikely to put out several neurites and were more likely to send out one or two to explore the culture environment before dedicating to migration (Lozano et al., 1995, Encinas et al., 2000, Lehmann et al., 1999, Fournier et al., 2002, Simpson et al., 2001). If co-culture was carried out for longer, a more stark difference may be able to be observed.

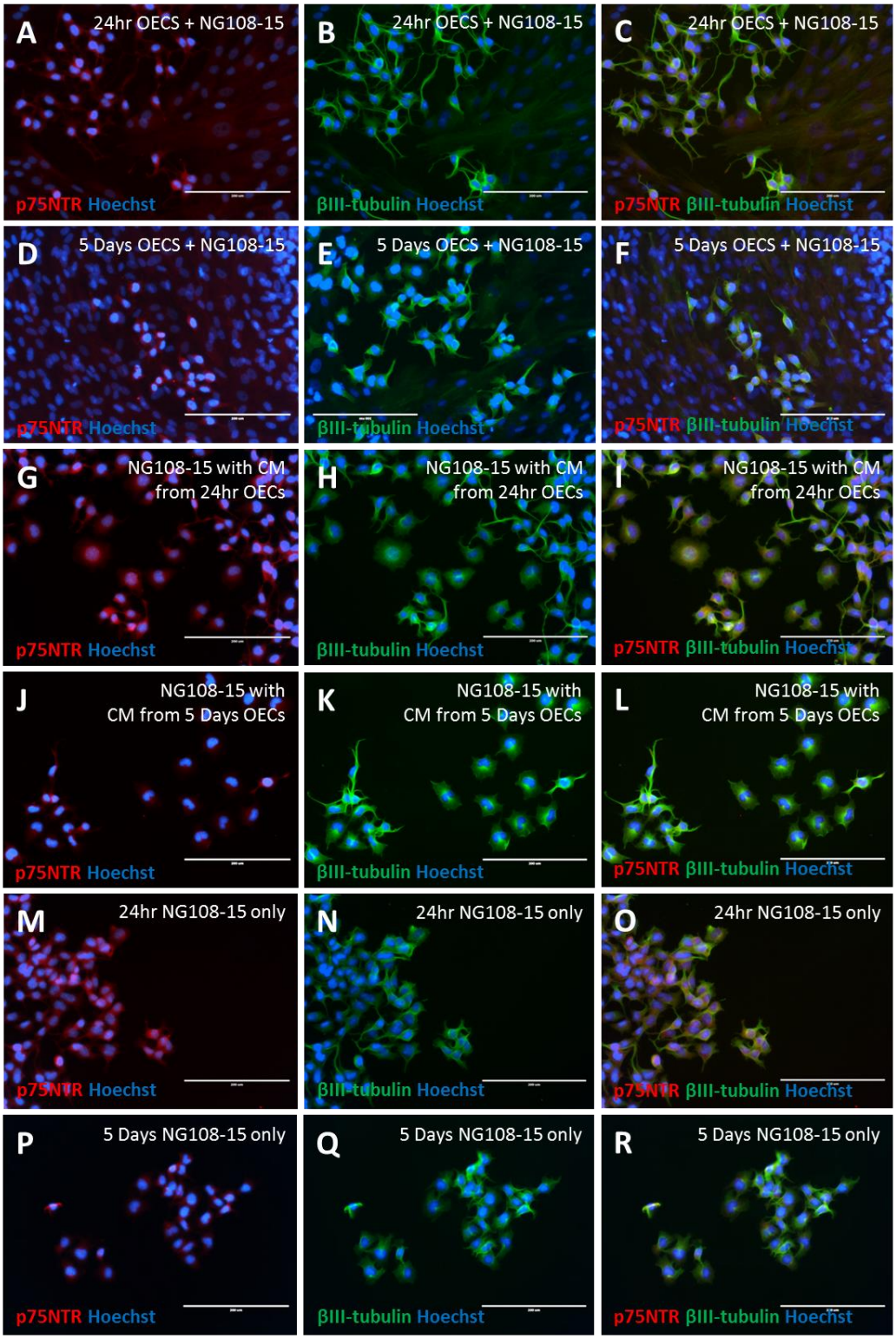

Figure 5.19: Fluorescent micrographs of NG108-15 cells grown on OECs at different levels of p75NTR expression in different media conditions. Cells were fixed after 5 days of neuronal culture. More neurite extensions were observed when the neurons were cultured in conditions of high p75NTR expression (A-C) compared with those cultured in conditions of low p75NTR expression (D-F). Additionally, when neurons were cultured in isolation (M-R) very few neurite extensions were observed. When neurons were cultured with CM from OECs with high p75NTR expression (G-I), there were more neurites than those cultured in isolation (M-R), although not as many as co-culture (A-C). However, when neurons were cultured with CM from OECs with low p75NTR expression (J-L), although an improvement over neurons cultured alone was observed (M-R), there was no obvious difference between the CM (J-L) and co-culture conditions (D-F). The scale bar represents 200µm.

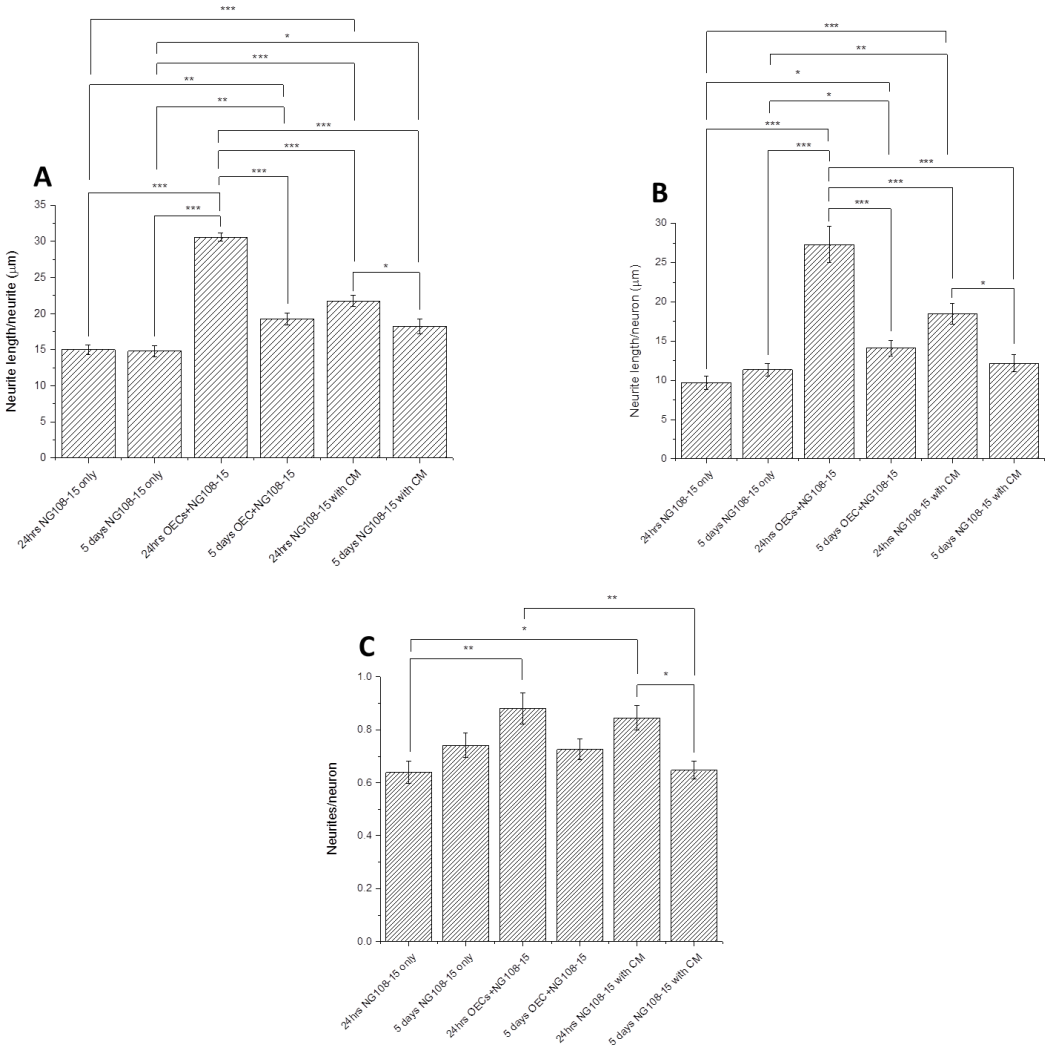

Figure 5.20: Quantification of NG108-15 neurites and neuron number cultured on OECs at different levels of p75NTR expression in different media conditions. The number of neurites and their lengths were quantified from the fluorescent images using positive βIII-tubulin staining. Neurites were counted and measured using NeuronJ (ImageJ plugin). When the neurite length/neurite (A) and neurite length/neuron (B) were considered, a similar pattern was observed. Co-culture with neurons at 24 hours was significantly better than all other conditions (one-way ANOVA, Bonferroni post-hoc, $p<0.001$), followed by neurons cultured with CM from the 24 hour condition. The neurons co-cultured with OECs at 5 days and CM from the 5 day condition performed better than the negative controls (NG108-15s only), although these two conditions behaved in a similar way. Neurites/neuron (C) showed a less distinguishable pattern. Data are means ± SEM, n=3.

PA5 CM was seen to have a positive effect on neurite extension. During periods of high p75NTR expression, CM did not modify neurite behaviour as much as during low p75NTR expression. This could be due to a difference in soluble factors secreted by OECs between these two periods. Another option that needs to be considered is related to the observation that high p75NTR expression occurs in the first 24 hours. CM collected during this time may have fewer soluble factors as the media was only in contact with the OECs

for 24 hours and for around one third of this time, the cells were attaching. This may change the soluble factors given out by the cells as they are focusing on attachment as opposed to proliferation.

CM collected at 5 days, and therefore during low p75NTR expression, resulted in the same degree of neurite extension as co-culture at 5 days (19.3±0.8µm and 18.2±1.0µm neurite length/neurite respectively). The CM collected at 5 days was in contact with the PA5 cells for 48 hours and the cells were close to confluency. If the factors are produced uniformly, each cell would produce half of the factors of cells at 24 hours, so there would be significantly more factors in the CM at 5 days. However, the expression pattern depends on the factor and factors can be expressed in a variety of ways and patterns. Although this could explain why CM was not as effective as co-culture at 24 hours while both co-culture and CM give similar results at 5 days, more research would need to go into the factors present and their expression patterns to identify whether this is possible. CM collected at 24 hours provided longer neurites than conditions associated with 5 days, although this was never significant. This could be due to the change in CM components in this time as there may be more molecules secreted by cells but fewer that actively promote neuron elongation.

Following on the assumption explored in Section 5.3.1-5.3.3, that OECs may have a similar behavioural pattern to Schwann cells, it would be expected that CM from OECs have a positive impact on neurite extension. The effect of Schwann cell CM on neurite extension has been investigated extensively in literature and it has been shown by several researchers that trophic factors (such as NGF, NT-3 and BDNF) derived from Schwann cells are vital to axon development and neurite extension (Mirsky et al., 2002, Fawcett and Keynes, 1990, Grinspan et al., 1996, Ceci et al., 2014, Lai et al., 2013, Cao and Shoichet, 2003). When there is an inadequate level of growth factors such as NGF, neurite extension is not observed. Schwann cells have been observed to provide NGF for neurons which signals the regenerating axons to elongate and it is accepted that Schwann cells provide necessary trophic support for neuron regeneration (Vickland et al., 1991). In addition to this, it has been observed that Schwann cells derive trophic factors from PNS neurons reinforcing the idea that there is a strong reciprocal trophic interactions occurring in neuron regeneration (Grinspan et al., 1996, Ceci et al., 2014).

During Section 5.3.1 CM collected from HuG418 was examined on its ability to modify neurite behaviour. It was found to not be beneficial for neurite extension. In this section, it was found that CM from PA5s positively influences neuron development. This indicates that differences exist between the CM and either components in HuG418 CM are detrimental to neurite elongation, or beneficial molecules are present in PA5 CM.

NGF, NT-3 and BDNF have been observed to increase axonal elongation in vitro and in vivo (Lai et al., 2013, Encinas et al., 2000, Simpson et al., 2001). These are factors that have been shown to be expressed by OECs (Woodhall et al., 2001, Chen et al., 2007). As such, these factors could be responsible for the longer neurites observed. In order to fully understand the interaction occurring between the OECs and neurons, the PA5 CM would need to be studied to determine the components present and identify any differences that exist between the CM at 24 hours and 5 days. It would be beneficial to identify the components in HuG418 CM to understand why this did not aid neurite elongation. This is part of the focus of future study covered in Section 6.2.

5.4 Conclusions

Conditions that were found in previous chapters to result in the highest p75NTR expression levels in OEC lines also correlated with the best neural cell responses of NG108-15 cells when co-cultured with OECs under the same conditions.

Therefore OECs were most supportive of neurite extension at 24 hours (high p75NTR expression) compared to 5 days (low p75NTR expression) and HuG418 CM did not positively impact on neurite elongation. PA5 CM collected during periods of high p75NTR expression gave longer extensions than neurons cultured in isolation in standard media, which suggests that trophic signalling is occurring between the OECs and the neurons.

When Thy1 was immunodepleted, there was no significant difference between the neurons and neurites co-cultured with Thy1 negative and positive fractions. Both of these conditions outperformed the pre-purified population in regards to neurite extension. This may be due to lateral inhibition, which is a subject for further research.

Overall, this work revealed that the expression of p75NTR and S100β was a reliable indicator of the level of neurite extension that occurred during PA5 co-culture with NG108-15 cells.

Additional quantification with techniques such as PCR or western blots would have been beneficial in this work to track the extent of p75NTR and Thy1 expression during co-culture. Another limitation of this study is that no function was tested, only the neurite extensions were quantified. This work would be strengthened by staining for myelin and using imaging techniques such as electron microscopy to determine the presence of myelin sheaths. These ideas will be discussed in more detail in Section 6.2.

6.0 Conclusions and Future Work

6.1 Concluding Remarks

A major challenge in developing a successful cell therapy for SCI is the lack of understanding of the most promising cell type to date, the olfactory ensheathing cell. The inherent plasticity of these cells, along with variability in cell yield and growth potential has made these a challenging cell type to characterise. Their ability to support neuronal regeneration from the PNS to the CNS has made them a promising candidate for a SCI cell therapy and in order to translate them into clinic, OECs need to be better understood and characterised in terms of identity marker expression and potency. This thesis explored culture conditions that can be used to increase the expression of key OEC markers p75NTR and S100β.

The initial objective was to examine whether fibroblast feeders could support the proliferation and expression of key markers of OEC^Rs. Feeders have been used to support stem cell cultures (Richards et al., 2002, Simon et al., 2005, Fong and Bongso, 2006) and fibroblasts isolated from the human olfactory mucosa were immobilised and cultured with OEC^Rs. It was found that although human mucosal fibroblasts were able to enhance the expression of p75NTR (Section 3.3.1) and encourage a more spindle-like morphology (Kawaja et al., 2009, Pellitteri et al., 2010, Fraher, 2000, Alexander et al., 2002), this enhancement was not unique to olfactory-specific fibroblasts, as mouse embryonic fibroblasts yielded similar improvement. Moreover, CM derived from the human fibroblasts which resulted in increased expression of undesirable marker Thy1.1. A key observation from this set of work was the lack of translation of results from OEC^Rs to OEC^Hs. It was found that OEC^Hs did not behave in the same way as OEC^Rs and therefore care has to be taken when undertaking fundamental studies with animal models as this work may not directly translate. Laminin was the best condition for OEC^Hs in terms of S100β expression, however, mouse feeders (Ms3T3) produced the most clinically relevant results for rat OECs.

Once the OEC^H cell line was generated in the laboratory, work with rat tissue ceased and focus was translated to the human lines. The OEC^H cell line PA5 was subject to further studies that examined the pattern of p75NTR and Thy1 expression. Time point experiments

ran from 8 hours up to 6 days and it was found that p75NTR turned off over time in culture, which is thought to be a response to the increasing cell density. Thy1 was observed to vary in expression levels over time when stained in the absence of Triton X permeabilisation. The expression pattern could be due to its role in cell adhesion. Both of these studies showed that identifying cell populations using these two markers needed to be carried out with caution as the time of staining as well as the methods used have a significant effect on the protein expression observed.

MACS technology was used to purify the population by immunodepleting cells that were Thy1 positive. This was an effective tool to remove Thy1 positive cells from the population, however, after 6 days in culture, the Thy1 negative fraction was observed to contain significant levels of Thy1 positive cells. Whether this was due to cells upregulating expression or because the daughter cells produced expressed Thy1 was not able to be determined and this is the focus of some of the future work which is discussed in Section 6.2.

In order to validate the optimum conditions identified in Chapters 3 and 4, PA5 cells were co-cultured with NG108-15 neurons. This was carried out to determine whether improved expression of p75NTR and S100β were relevant indicators of the functional capability of the PA5 OECs. The experimental output from these studies was the length of the neurites extended which was normalised against the number of neurites and neurons. Literature indicates that reporting neurite output in this way correlates to functional recovery observed in transplanted animals (Rossi et al., 2010). Neurons were cultured in isolation to ensure that any improvement that was observed could be related to the presence of the PA5 cells. In the work carried out, neurons that were cultured alone showed minimal ability to extend neurites of a significant length. Conditions that gave a higher level of p75NTR or S100β expression (laminin with standard media after 24 hours, Section 5.3.1-5.3.2) were found to result in neurons with significantly longer neurites than those that were cultured in less favourable conditions for these proteins (Ms3T3 feeders with CM and at 5 days of PA5 culture, Section 5.3.1-5.3.2). This was thought to be related to trophic factors secreted by the PA5 cells as is seen with Schwann cells in peripheral nerve repair (Mirsky et al., 2002, Woodhall et al., 2001). This was investigated by culturing NG108-15 neurons in isolation with CM from the PA5 cells during high and low points of p75NTR expression (Section 5.3.4). It was found that the presence of PA5 CM resulted in longer neurites than those

cultured in standard media. CM from high p75NTR expression (24 hours) did not achieve as promising results as co-culture at 24 hours, however, CM from low p75NTR expression (5 days) gave similar neurite lengths to co-culture at 5 days. It is thought this is due to the limited time PA5 cells have to excrete factors during the first 24 hours of culture as well as the trophic factors present at these different times. Further investigation is required to characterise this relationship which is outlined in Section 6.2.

The relationship between Thy1 and neurite outgrowth was not straightforward. Thy1 removal and enrichment gave longer neurite extensions than the original mixed population, but were not significant from each other. The separation of the sub-populations allowed the OECs to better support neuronal development which was not the expected result. It is thought this may be related to the phenomenon of lateral inhibition although there is minimal literature that has observed this in OECs (Miller et al., 2016). Characterisation of the two sub-populations and detection of Notch/Delta signalling would help to fully explain the results observed.

The work carried out in this thesis has identified methods to increase the expression of key OEC markers p75NTR and S100β and related this to their ability to aid neuron development. Key observations from this work include; OEC rat models are not necessarily appropriate for scale up to human OEC studies, p75NTR expression decreases over time in culture, Thy1 expression changes during time in culture and needs to be detected without the use of Triton X, removal of Thy1 from OEC culture is not a long term solution to dividing sub-populations, and higher p75NTR and S100β expression in the conditions investigated translates to more numerous and longer neurites.

6.2 Recommendations for Future Work

This thesis identified culture conditions that enhance expression of putative OEC markers p75NTR and S100β which in turn results in improved functional responses of neurons. However, further work is needed, examples of which are outlined here.

Limitations of the current work are that for the most part, this study has focused on a single candidate OEC^{H} cell line (PA5) and although a study conducted with PA7 found similar results for matrix and media conditions (Section 3.3.4), these cell populations were

both isolated from the human mucosa. It would be beneficial to carry out these experiments with other mucosa and bulb cell lines to determine if the results obtained are particular to mucosa cells, the individual from whom the cells were isolated from or if these results can be translated to OECs from both sources. Any differences observed would help further the understanding of how OECs lend themselves to neural regeneration. The natural variation between different human donors is a problem that has not been solved (Kachramanoglou et al., 2013) and although the work in this thesis has focused on cell lines that would be an allogeneic cell therapy, identification of why differences occur in samples could provide insight with which to develop an autologous cell therapy.

One area of future work would be to expand the purified cell sub-populations from Section 4.3.1 to determine if they re-acquire a mix of phenotypes as seen in the start population. Insights from this thesis reveal that Thy1 was detected in the Thy1 negative fraction after 5 days (Section 4.3.4) and it would be beneficial to assess whether the cells restore this balance after prolonged culture or whether these populations remain separate entities. These purified samples could be co-cultured with NG108-15s after several passages to determine whether serial passaging after purification significantly impacts the ability of PA5s to encourage neurite outgrowth and help characterise whether the cells revert to a mixed population. ICC detecting proteins other than Thy1 would be useful although in this study no differences were observed. This study would be further strengthened by examining the potential of lateral inhibition as a regulatory mechanism of cell phenotype in this population. This work could be carried out by staining with an antibody against activated Notch1 which detects the N-terminal sequence. Literature has shown that positive staining for Notch1 suggests the Notch pathway is active (Miller et al., 2016). If the Notch pathway is active, this is indicative of Notch/Delta signalling which controls lateral inhibition (Guisoni et al., 2017, Nikolaou et al., 2009, Sancho et al., 2015) and therefore positive staining can be used to determine whether lateral inhibition is occurring. Confirmation of lateral inhibition in this cell population could explain why the purified sub-populations support neuron development better than the mixed population.

Another area of work could address furthering our understanding of how OECs support neural regeneration. One approach could be to use knock-out technology such as siRNA to silence p75NTR. The work in this thesis revealed that during periods of high p75NTR expression, PA5 cells are better able to support neurite elongation compared with periods

of low p75NTR expression (Section 5.3.2, 5.3.4). By knocking out expression of p75NTR, it would be possible to determine whether it is critical for supporting neural regeneration. Similarly, knockout of Thy1 expression could yield further insight, as elevated Thy1 seems to correlate with a less regenerative phenotype. After purification Thy1 negative cells initially appeared more enlarged (Section 4.3.4) although they became more elongated with time in culture, which coincided with an increase in Thy1 expression. Attachment was delayed and doubling time was increased. Knockout of Thy1 would help relate expression to cell characteristics such as proliferation rate, attachment and morphology.

Application of time-lapse fluorescence microscopy could be used to monitor p75NTR and Thy1 expression over time using live staining techniques. If p75NTR expression is related to cell density, a decrease in p75NTR expression would be observed over time in culture. Live staining of cells plated at different densities would determine whether the decrease in p75NTR expression is related to time or cell density. If Thy1 expression is related to adhesion, the proliferation rate of cell populations and the expression of Thy1 would be able to be linked through this method. Further understanding of the relationship between p75NTR and neurite extension could also be monitored using time lapse microscopy in co-culture work. It could help track whether expression levels from OECs influences the direction and rate of neurite extension.

Further insight could be gained by examining the components of the CM collected from PA5s expressing high or low levels of p75NTR expression. Studies of Schwann cells revealed that they produce several trophic factors necessary for the development of axons (Mirsky et al., 2002, Fawcett and Keynes, 1990, Grinspan et al., 1996, Ceci et al., 2014, Lai et al., 2013, Cao and Shoichet, 2003). In the current study it was found that CM collected from the PA5 populations supported neuronal function. Identifying the factors present in the CM and relating them to the trophic requirements of neurons would help explain how OECs support neural regeneration. It would be beneficial to carry out a Design of Experiments approach using trophic factors identified to determine if the benefits of OECs can be achieved with appropriate media composition. Neurons that have been severed during an SCI find themselves in an unfavourable environment that does not provide neurons with the conditions required for regeneration (Barnett and Riddell, 2007, Ramer et al., 2005, Carwardine et al., 2016). It could be that the presence of specific factors that are present in

OEC culture could suitably modify this environment so the neurons are able to proliferate, migrate and reconnect with their original targets (Ramer et al., 2005).

In this thesis the functional ability of PA5s to support neuronal regeneration has been characterised *in vitro*. To advance the work towards clinic, animal models need to be undertaken to address regeneration and myelination of neurons which is the key functional response required in SCI repair. A study carried out by Ravasi (2013) looked at the myelination ability of MSCs by carrying out co-culture for two weeks with MSCs and dorsal root ganglia neurons. After this time, the cultures were characterised using immunofluorescence, western blot and ELISA to identify the presence of myelin proteins MBP (myelin basic protein) and Connexin 32. In addition to this, electron microscopy was used to visualise any myelin sheaths present (Ravasi et al., 2013). PA5 and NG108-15 co-culture would be stained for MBP and Connexin 32, and imaged to determine the level of myelin sheath formation. The restoration of the myelin sheath is a key factor in restoring function in SCI. Without the myelin sheath, the neurons are unable to send electrical impulse and communicate with the body (Franssen et al., 2007, Levitan and Kaczmarek, 2015). If the ability of the cells to myelinate neurons can be linked to expression of p75NTR or S100β, this would provide a valuable predictive tool for translating 2D cell culture to transplantation.

7.0 References

AHUJA, C. S., WILSON, J. R., NORI, S., KOTTER, M. R. N., DRUSCHEL, C., CURT, A. & FEHLINGS, M. G. 2017. Traumatic spinal cord injury. 3**,** 17018.

ALBERTS, B., JOHNSON, A., LEWIS, J., RAFF, M., ROBERTS, K. & WALTER, P. 2002. *Molecular Biology of the Cell,* New York, Garland Science.

ALEXANDER, C. L., FITZGERALD, U. F. & BARNETT, S. C. 2002. Identification of growth factors that promote long-term proliferation of olfactory ensheathing cells and modulate their antigenic phenotype. *Glia,* 37**,** 349-64.

AMBROGINI, P., LATTANZI, D., CIUFFOLI, S., AGOSTINI, D., BERTINI, L., STOCCHI, V., SANTI, S. & CUPPINI, R. 2004. Morpho-functional characterization of neuronal cells at different stages of maturation in granule cell layer of adult rat dentate gyrus. *Brain Research,* 1017**,** 21-31.

ANDERSON, K. D., GUEST, J. D., DIETRICH, W. D., BARTLETT, B. M., DIDIDZE, M., GREEN, B. A., KHAN, A., PEARSE, D. D., WIDERSTROM-NOGA, E., WOOD, P., LEVI, A. D., ANDERSON, K. D., GUEST, J. D., DIETRICH, W. D., BARTLETT, B. M., DIDIDZE, M., GREEN, B. A., PEARSE, D. D., WIDERSTROM-NOGA, E., WOOD, P., LEVI, A. D., GUEST, J. D., DIETRICH, W. D., BARTLETT, B. M., PEARSE, D. D., WIDERSTROM-NOGA, E., DIETRICH, W. D., BARTLETT, B. M., DIETRICH, W. D., BARTLETT, B. M., GREEN, B. A., DIETRICH, W. D., BARTLETT, B. M., KHAN, A., PEARSE, D. D., CURIEL, R., GREEN, B. A., LEVI, A. D., GREEN, B. A., WIDERSTROM-NOGA, E., PEARSE, D. D., WIDERSTROM-NOGA, E. & SARAF-LAVI, E. 2017. Safety of Autologous Human Schwann Cell Transplantation in Subacute Thoracic Spinal Cord Injury. *J Neurotrauma,* 34**,** 2950-2963.

APPARELYZED. 2015. *Spinal Cord Injury Statistics* [Online]. Available: http://www.apparelyzed.com/statistics.html [Accessed 12/09/2016 2016].

BABIARZ, J., KANE-GOLDSMITH, N., BASAK, S., LIU, K., YOUNG, W. & GRUMET, M. 2011. Juvenile and adult olfactory ensheathing cells bundle and myelinate dorsal root ganglion axons in culture. *Exp Neurol,* 229**,** 72-9.

BARBACID, M. 1994. The Trk family of neurotrophin receptors. *J. Neurobiol.,* 25**,** 1386-403.

BARNETT, S. C. & CHANG, L. 2004. Olfactory ensheathing cells and CNS repair: going solo or in need of a friend? *Trends in Neurosciences,* 27**,** 54-60.

BARNETT, S. C. & RIDDELL, J. S. 2004. Olfactory ensheathing cells (OECs) and the treatment of CNS injury: advantages and possible caveats. *J Anat,* 204**,** 57-67.

BARNETT, S. C. & RIDDELL, J. S. 2007. Olfactory ensheathing cell transplantation as a strategy for spinal cord repair--what can it achieve? *Nat Clin Pract Neurol,* 3**,** 152-61.

BARNETT, S. C. & ROSKAMS, A. J. 2008. Olfactory ensheathing cells: Isolation and culture from the neonatal oflactory bulb. *Methods Mol. Biol. (Totowa, NJ, U. S.),* 438**,** 85-94.

BECTON, D. A. C. 2015. BD Accuri C6 Flow Cytometer Technical Specifications. *In:* BIOSCIENCES, B. (ed.).

BIANCO, J. I., PERRY, C., HARKIN, D. G., MACKAY-SIM, A. & FERON, F. 2004. Neurotrophin 3 promotes purification and proliferation of olfactory ensheathing cells from human nose. *Glia,* 45**,** 111-23.

BISSON, F., PAQUET, C., BOURGET, J.-M., ZANIOLO, K., ROCHETTE, P. J., LANDREVILLE, S., DAMOUR, O., BOUDREAU, F., AUGER, F. A., GUÉRIN, S. L. & GERMAIN, L. 2015. Contribution of Sp1 to Telomerase Expression and Activity in Skin Keratinocytes Cultured With a Feeder Layer. *Journal of Cellular Physiology,* 230**,** 308-317.

BLESCH, A. & TUSZYNSKI, M. H. 2003. Cellular GDNF delivery promotes growth of motor and dorsal column sensory axons after partial and complete spinal cord transections and induces remyelination. *J. Comp. Neurol.,* 467**,** 403-417.

BLUMENTHAL, J., COHEN-MATSLIAH, S. I. & LEVENBERG, S. 2013. Olfactory Bulb-Derived Cells Seeded on 3D Scaffolds Exhibit Neurotrophic Factor Expression and Pro-Angiogenic Properties. *Tissue Engineering Part A,* 19**,** 2284-2291.

BORDEAUX, J., WELSH, A. W., AGARWAL, S., KILLIAM, E., BAQUERO, M. T., HANNA, J. A., ANAGNOSTOU, V. K. & RIMM, D. L. 2010. Antibody validation. *BioTechniques,* 48**,** 197-209.

BOYD, J. G., DOUCETTE, R. & KAWAJA, M. D. 2005. Defining the role of olfactory ensheathing cells in facilitating axon remyelination following damage to the spinal cord. *FASEB J.,* 19**,** 694-703.

BOYD, J. G., SKIHAR, V., KAWAJA, M. & DOUCETTE, R. 2003. Olfactory ensheathing cells: historical perspective and therapeutic potential. *Anat Rec B New Anat,* 271**,** 49-60.

BRADBURY, E. J., KHEMANI, S., VON, R., KING, PRIESTLEY, J. V. & MCMAHON, S. B. 1999. NT-3 promotes growth of lesioned adult rat sensory axons ascending in the dorsal columns of the spinal cord. *Eur J Neurosci,* 11**,** 3873-83.

BRAMLETT, H. M. & DIETRICH, W. D. 2007. Progressive damage after brain and spinal cord injury: pathomechanisms and treatment strategies. *In:* JOHN, T. W. & ANDREW, I. R. M. (eds.) *Progress in Brain Research.* Elsevier.

BREGMAN, B. S., MCATEE, M., DAI, H. N. & KUHN, P. L. 1997. Neurotrophic Factors Increase Axonal Growth after Spinal Cord Injury and Transplantation in the Adult Rat. *Experimental Neurology,* 148**,** 475-494.

BUBELINY, P. 2013. A note on the biasedness and unbiasedness of two-sample Kolmogorov–Smirnov test. *Statistics & Risk Modeling with Applications in Finance and Insurance.*

BUSH, T. G., PUVANACHANDRA, N., HORNER, C. H., POLITO, A., OSTENFELD, T., SVENDSEN, C. N., MUCKE, L., JOHNSON, M. H. & SOFRONIEW, M. V. 1999. Leukocyte infiltration, neuronal degeneration, and neurite outgrowth after ablation of scar-forming, reactive astrocytes in adult transgenic mice. *Neuron,* 23**,** 297-308.

CAO, L., LIU, L., CHEN, Z.-Y., WANG, L.-M., YE, J.-L., QIU, H.-Y., LU, C.-L. & HE, C. 2004. Olfactory ensheathing cells genetically modified to secrete GDNF to promote spinal cord repair. *Brain,* 127**,** 535-49.

CAO, L., ZHU, Y.-L., SU, Z., LV, B., HUANG, Z., MU, L. & HE, C. 2007. Olfactory ensheathing cells promote migration of Schwann cells by secreted nerve growth factor. *Glia,* 55**,** 897-904.

CAO, X. & SHOICHET, M. S. 2003. Investigating the synergistic effect of combined neurotrophic factor concentration gradients to guide axonal growth. *Neuroscience,* 122**,** 381-389.

CARWARDINE, D., WONG, L.-F., FAWCETT, J. W., MUIR, E. M. & GRANGER, N. 2016. Canine olfactory ensheathing cells from the olfactory mucosa can be engineered to produce active chondroitinase ABC. *J. Neurol. Sci.,* 367**,** 311-318.

CECI, M. L., MARDONES-KRSULOVIC, C., SÁNCHEZ, M., VALDIVIA, L. E. & ALLENDE, M. L. 2014. Axon-Schwann cell interactions during peripheral nerve regeneration in zebrafish larvae. *Neural Development,* 9**,** 22.

CHEN, C. R., KACHRAMANOGLOU, C., LI, D. Q., ANDREWS, P. & CHOI, D. 2014. Anatomy and Cellular Constituents of the Human Olfactory Mucosa: A Review. *Journal of Neurological Surgery Part B-Skull Base,* 75**,** 293-300.

CHEN, Y., ZENG, J., CHEN, Y., WANG, X., YAO, G., WANG, W., QI, W. & KONG, K. 2009. Multiple roles of the p75 neurotrophin receptor in the nervous system. *J. Int. Med. Res.,* 37**,** 281-288.

CHEN, Z.-L., YU, W.-M. & STRICKLAND, S. 2007. Peripheral regeneration. *Annu. Rev. Neurosci.,* 30**,** 209-233.
CHENG, L., ESCH, F. S., MARCHIONNI, M. A. & MUDGE, A. W. 1998. Control of Schwann cell survival and proliferation: autocrine factors and neuregulins. *Mol. Cell. Neurosci.,* 12**,** 141-156.
CHOI, D., LI, D. Q., LAW, S., POWELL, M. & RAISMAN, G. 2008. A prospective observational study of the yield of olfactory ensheathing cells cultured from biopsies of septal nasal mucosa. *Neurosurgery,* 62**,** 1140-1144.
CHONG, Z. Z. 2016. S100B raises the alert in subarachnoid hemorrhage. *Rev. Neurosci. (Berlin, Ger.),* 27**,** 745-759.
CHUAH, M. I. & AU, C. 1993. Cultures of ensheathing cells from neonatal rat olfactory bulbs. *Brain Res,* 601**,** 213-20.
COSGAYA, J. M., CHAN, J. R. & SHOOTER, E. M. 2002. The Neurotrophin Receptor p75NTR as a Positive Modulator of Myelination. *Science,* 298**,** 1245.
CUMMING, G., FIDLER, F. & VAUX, D. L. 2007. Error bars in experimental biology. *J. Cell Biol.,* 177**,** 7-11.
DAVIES, A. M., LEE, K.-F. & JAENISCH, R. 1993. p75-Deficient trigeminal sensory neurons have an altered response to NGF but not to other neurotrophins. *Neuron,* 11**,** 565-574.
DI SUMMA, P. G., KALBERMATTEN, D. F., RAFFOUL, W., TERENGHI, G. & KINGHAM, P. J. 2013. Extracellular Matrix Molecules Enhance the Neurotrophic Effect of Schwann Cell-Like Differentiated Adipose-Derived Stem Cells and Increase Cell Survival Under Stress Conditions. *Tissue Engineering. Part A,* 19**,** 368-379.
DIAZ, E. & MORALES, H. 2016. Spinal Cord Anatomy and Clinical Syndromes. *Semin Ultrasound CT MR,* 37**,** 360-71.
DIETZ, V. & CURT, A. 2006. Neurological aspects of spinal-cord repair: promises and challenges. *The Lancet Neurology,* 5**,** 688-694.
DODSON, B. P. & LEVINE, A. D. 2015. Challenges in the translation and commercialization of cell therapies. *BMC Biotechnology,* 15**,** 1-15.
DORON-MANDEL, E., FAINZILBER, M. & TERENZIO, M. 2015. Growth control mechanisms in neuronal regeneration. *FEBS Lett.,* 589**,** 1669-1677.
DOUCETTE, R. 1990. Glial influences on axonal growth in the primary olfactory system. *Glia,* 3**,** 433-49.
DOUCETTE, R. 1993. Glial cells in the nerve fiber layer of the main olfactory bulb of embryonic and adult mammals. *Microsc Res Tech,* 24**,** 113-30.
DOUCETTE, R. & DEVON, R. 1995. Elevated intracellular levels of cAMP induce olfactory ensheathing cells to express GAL-C and GFAP but not MBP. *Glia,* 13**,** 130-40.
EBEL, C., BRANDES, G., RADTKE, C., ROHN, K. & WEWETZER, K. 2013. Clonal In Vitro Analysis of Neurotrophin Receptor p75-Immunofluorescent Cells Reveals Phenotypic Plasticity of Primary Rat Olfactory Ensheathing Cells. *Neurochem. Res.,* 38**,** 1078-1087.
EFTHYMIOU, A., SHALTOUKI, A., STEINER, J. P., JHA, B., HEMAN-ACKAH, S. M., SWISTOWSKI, A., ZENG, X., RAO, M. S. & MALIK, N. 2014. Functional screening assays with neurons generated from pluripotent stem cell–derived neural stem cells. *Journal of biomolecular screening,* 19**,** 32-43.
EGELHOFER, T. A., MINODA, A., KLUGMAN, S., LEE, K., KOLASINSKA-ZWIERZ, P., ALEKSEYENKO, A. A., CHEUNG, M.-S., DAY, D. S., GADEL, S., GORCHAKOV, A. A., GU, T., KHARCHENKO, P. V., KUAN, S., LATORRE, I., LINDER-BASSO, D., LUU, Y., NGO, Q., PERRY, M., RECHTSTEINER, A., RIDDLE, N. C., SCHWARTZ, Y. B., SHANOWER, G. A., VIELLE, A., AHRINGER, J., ELGIN, S. C. R., KURODA, M. I., PIRROTTA, V., REN, B., STROME, S., PARK, P. J., KARPEN, G. H., HAWKINS, R. D. & LIEB, J. D. 2011. An

assessment of histone-modification antibody quality. *Nat Struct Mol Biol,* 18**,** 91-93.
ENCINAS, M., IGLESIAS, M., LIU, Y., WANG, H., MUHAISEN, A., CENA, V., GALLEGO, C. & COMELLA, J. X. 2000. Sequential treatment of SH-SY5Y cells with retinoic acid and brain-derived neurotrophic factor gives rise to fully differentiated, neurotrophic factor-dependent, human neuron-like cells. *J. Neurochem.,* 75**,** 991-1003.
ERCK, C., MEISINGER, C., GROTHE, C. & SEIDL, K. 1998. Regulation of nerve growth factor and its low-affinity receptor (p75NTR) during myogenic differentiation. *Journal of cellular physiology,* 176**,** 22-31.
ESLAMINEJAD, M. B., NADRI, S. & HOSSEINI, R. H. 2007. Expression of Thy 1.2 surface antigen increases significantly during the murine mesenchymal stem cells cultivation period. *Dev., Growth Differ.,* 49**,** 351-364.
FAULKNER, J. & KEIRSTEAD, H. S. 2005. Human embryonic stem cell-derived oligodendrocyte progenitors for the treatment of spinal cord injury. *Transplant Immunology,* 15**,** 131-142.
FAWCETT, J. & KEYNES, R. J. 1990. Peripheral nerve regeneration. *Annual review of neuroscience,* 13**,** 43-60.
FAWCETT, J. W. & ASHER, R. A. 1999. The glial scar and central nervous system repair. *Brain Research Bulletin,* 49**,** 377-391.
FERON, F., PERRY, C., COCHRANE, J., LICINA, P., NOWITZKE, A., URQUHART, S., GERAGHTY, T. & MACKAY-SIM, A. 2005. Autologous olfactory ensheathing cell transplantation in human spinal cord injury. *Brain,* 128**,** 2951-60.
FONG, C.-Y. & BONGSO, A. 2006. Derivation of human feeders for prolonged support of human embryonic stem cells. *Methods Mol Biol,* 331**,** 129-35.
FOURNIER, A. E., GOULD, G. C., LIU, B. P. & STRITTMATTER, S. M. 2002. Truncated soluble Nogo receptor binds Nogo-66 and blocks inhibition of axon growth by myelin. *J. Neurosci.,* 22**,** 8876-8883.
FRAHER, J. P. 2000. The transitional zone and CNS regeneration. *J Anat,* 196 (Pt 1)**,** 137-58.
FRANCESCHINI, I. A. & BARNETT, S. C. 1996. Low-affinity NGF-receptor and E-N-CAM expression define two types of olfactory nerve ensheathing cells that share a common lineage. *Dev. Biol.,* 173**,** 327-43.
FRANKLIN, R. J. M. 2002. Remyelination of the demyelinated CNS: the case for and against transplantation of central, peripheral and olfactory glia. *Brain Research Bulletin,* 57**,** 827-832.
FRANKLIN, R. J. M. & BARNETT, S. C. 1997. Do olfactory glia have advantages over Schwann cells for CNS repair? *J. Neurosci. Res.,* 50**,** 665-672.
FRANSSEN, E. H. P., DE, B. F. M. & VERHAAGEN, J. 2007. Olfactory ensheathing glia: their contribution to primary olfactory nervous system regeneration and their regenerative potential following transplantation into the injured spinal cord. *Brain Res Rev,* 56**,** 236-58.
FROSTICK, S. P., YIN, Q. & KEMP, G. J. 1998. Schwann cells, neurotrophic factors, and peripheral nerve regeneration. *Microsurgery,* 18**,** 397-405.
GALOW, A.-M., REBL, A., KOCZAN, D., BONK, S. M., BAUMANN, W. & GIMSA, J. 2017. Increased osteoblast viability at alkaline pH in vitro provides a new perspective on bone regeneration. *Biochemistry and Biophysics Reports,* 10**,** 17-25.
GARCÍA-ESCUDERO, V., GARCÍA-GÓMEZ, A., LANGA, E., MARTÍN-BERMEJO, M. J., RAMÍREZ-CAMACHO, R., GARCÍA-BERROCAL, J. R., MORENO-FLORES, M. T., ÁVILA, J. & LIM, F. 2012. Patient-derived olfactory mucosa cells but not lung or skin fibroblasts mediate axonal regeneration of retinal ganglion neurons. *Neuroscience Letters,* 509**,** 27-32.

GARCIA-SEGURA, L. M. & MELCANGI, R. C. 2006. Steroids and glial cell function. *Glia,* 54**,** 485-98.

GE, L., LIU, K., LIU, Z. & LU, M. 2016. Co-transplantation of autologous OM-MSCs and OM-OECs: a novel approach for spinal cord injury. *Rev Neurosci,* 27**,** 259-70.

GEORGIOU, M., WOOD, R., PEREZ ESTEBAN, P., NEVES DOS REIS, J., MASON, C., LI, D., LI, Y., CHOI, D. & WALL, I. 2017. Optimization of bioprocessing strategies to enhance the challenging isolation of neuro-regenerative cells. *[Unpublished Manuscript]*.

GILQUIN, B., CANNON, B. R., HUBSTENBERGER, A., MOULOUEL, B., FALK, E., MERLE, N., ASSARD, N., KIEFFER, S., ROUSSEAU, D. & WILDER, P. T. 2010. The calcium-dependent interaction between S100B and the mitochondrial AAA ATPase ATAD3A and the role of this complex in the cytoplasmic processing of ATAD3A. *Molecular and cellular biology,* 30**,** 2724-2736.

GOMEZ, V. M., AVERILL, S., KING, V., YANG, Q., DONCEL, P. E., CHACON, S. C., WARD, R., NIETO-SAMPEDRO, M., PRIESTLEY, J. & TAYLOR, J. 2003. Transplantation of olfactory ensheathing cells fails to promote significant axonal regeneration from dorsal roots into the rat cervical cord. *J Neurocytol,* 32**,** 53-70.

GONG, Q., BAILEY, M. S., PIXLEY, S. K., ENNIS, M., LIU, W. & SHIPLEY, M. T. 1994. Localization and regulation of low affinity nerve growth factor receptor expression in the rat olfactory system during development and regeneration. *J. Comp. Neurol.,* 344**,** 336-48.

GONG, Q. & SHIPLEY, M. T. 1996. Expression of extracellular matrix molecules and cell surface molecules in the olfactory nerve pathway during early development. *J. Comp. Neurol.,* 366**,** 1-14.

GOODMAN, S. L., DEUTZMANN, R. & VON DER MARK, K. 1987. Two distinct cell-binding domains in laminin can independently promote nonneuronal cell adhesion and spreading. *J. Cell Biol.,* 105**,** 589-98.

GORRIE, C. A., HAYWARD, I., CAMERON, N., KAILAINATHAN, G., NANDAPALAN, N., SUTHARSAN, R., WANG, J., MACKAY-SIM, A. & WAITE, P. M. E. 2010. Effects of human OEC-derived cell transplants in rodent spinal cord contusion injury. *Brain Res.,* 1337**,** 8-20.

GRANGER, N., BLAMIRES, H., FRANKLIN, R. J. M. & JEFFERY, N. D. 2012. Autologous olfactory mucosal cell transplants in clinical spinal cord injury: a randomized double-blinded trial in a canine translational model. *Brain,* 135**,** 3227-3237.

GRANGER, N., FRANKLIN, R. J. M. & JEFFERY, N. D. 2014. Cell Therapy for Spinal Cord Injuries: What Is Really Going on? *Neuroscientist*.

GREAT BRITAIN, H. O. S. & OFFICE, G. B. H. 2000. *Animals (Scientific Procedures) Act 1986: Guidance on the Operation of the Animals (Scientific Procedures) Act 1986*, Stationery Office.

GRINSPAN, J. B., MARCHIONNI, M. A., REEVES, M., COULALOGLOU, M. & SCHERER, S. S. 1996. Axonal interactions regulate Schwann cell apoptosis in developing peripheral nerve: neuregulin receptors and the role of neuregulins. *J. Neurosci.,* 16**,** 6107-6118.

GUDINO-CABRERA, G. & NIETO-SAMPEDRO, M. 1996. Ensheathing cells: Large scale purification from adult olfactory bulb, freeze-preservation and migration of transplanted cells in adult brain. *Restor Neurol Neurosci,* 10**,** 25-34.

GUEROUT, N., PAVIOT, A., BON-MARDION, N., DUCLOS, C., GENTY, D., JEAN, L., BOYER, O. & MARIE, J.-P. 2011. Co-transplantation of olfactory ensheathing cells from mucosa and bulb origin enhances functional recovery after peripheral nerve lesion. *PLoS One,* 6**,** e22816.

GUISONI, N., MARTINEZ-CORRAL, R., GARCIA-OJALVO, J. & DE NAVASCUÉS, J. 2017. Diversity of fate outcomes in cell pairs under lateral inhibition. *Development,* 144**,** 1177-1186.

GWAK, Y. S., KANG, J., UNABIA, G. C. & HULSEBOSCH, C. E. 2012. Spatial and temporal activation of spinal glial cells: Role of gliopathy in central neuropathic pain following spinal cord injury in rats. *Experimental Neurology,* 234**,** 362-372.

HAGG, T. & OUDEGA, M. 2006. Degenerative and spontaneous regenerative processes after spinal cord injury. *J Neurotrauma,* 23**,** 264-80.

HAHN, C.-G., HAN, L.-Y., RAWSON, N. E., MIRZA, N., BORGMANN-WINTER, K., LENOX, R. H. & ARNOLD, S. E. 2005. In vivo and in vitro neurogenesis in human olfactory epithelium. *J Comp Neurol,* 483**,** 154-63.

HAO, Y. & COLLINS, C. 2017. Intrinsic mechanisms for axon regeneration: insights from injured axons in Drosophila. *Current Opinion in Genetics & Development,* 44**,** 84-91.

HAYAT, S., THOMAS, A., AFSHAR, F., SONIGRA, R. & WIGLEY, C. B. 2003. Manipulation of olfactory ensheathing cell signaling mechanisms: effects on their support for neurite regrowth from adult CNS neurons in coculture. *Glia,* 44**,** 232-41.

HIGGINSON, J. R. & BARNETT, S. C. 2011. The culture of olfactory ensheathing cells (OECs)—a distinct glial cell type. *Experimental Neurology,* 229**,** 2-9.

HOLZAPFEL, B. M., WAGNER, F., MARTINE, L. C., REPPENHAGEN, S., RUDERT, M., SCHUETZ, M., DENHAM, J., SCHANTZ, J.-T. & HUTMACHER, D. W. 2016. Tissue engineering and regenerative medicine in musculoskeletal oncology. *Cancer and Metastasis Reviews***,** 1-13.

HOSOYA, A., NAKAMURA, H., NINOMIYA, T., YOSHIBA, K., YOSHIBA, N., NAKAYA, H., WAKITANI, S., YAMADA, H., KASAHARA, E. & OZAWA, H. 2006. Immunohistochemical Localization of α-Smooth Muscle Actin During Rat Molar Tooth Development. *Journal of Histochemistry and Cytochemistry,* 54**,** 1371-1378.

HU, J.-J., SUN, C., LAN, L., CHEN, Y.-W. & LI, D.-G. 2010. Therapeutic effect of transplanting β2m-/Thy1+ bone marrow-derived hepatocyte stem cells transduced with lentiviral-mediated HGF gene into CCl4,-injured rats. *J. Gene Med.,* 12**,** 244-254.

HUANG, Z.-H., WANG, Y., CAO, L., ZHU, Y.-L., CHEN, Y.-Z., YUAN, X.-B. & HE, C. 2008. Migratory properties of cultured olfactory ensheathing cells by single-cell migration assay. *Cell research,* 18**,** 479-490.

IMAIZUMI, T., LANKFORD, K. L., BURTON, W. V., FODOR, W. L. & KOCSIS, J. D. 2000. Xenotransplantation of transgenic pig olfactory ensheathing cells promotes axonal regeneration in rat spinal cord. *Nat. Biotechnol.,* 18**,** 949-953.

IMAIZUMI, T., LANKFORD, K. L., WAXMAN, S. G., GREER, C. A. & KOCSIS, J. D. 1998. Transplanted olfactory ensheathing cells remyelinate and enhance axonal conduction in the demyelinated dorsal columns of the rat spinal cord. *J Neurosci,* 18**,** 6176-85.

IMITOLA, J., RADDASSI, K., PARK, K. I., MUELLER, F.-J., NIETO, M., TENG, Y. D., FRENKEL, D., LI, J., SIDMAN, R. L., WALSH, C. A., SNYDER, E. Y. & KHOURY, S. J. 2004. Directed migration of neural stem cells to sites of CNS injury by the stromal cell-derived factor 1α/CXC chemokine receptor 4 pathway. *Proceedings of the National Academy of Sciences,* 101**,** 18117-18122.

ISHIHARA, M., MOCHIZUKI-ODA, N., IWATSUKI, K., KISHIMA, H., OHNISHI, Y.-I., MORIWAKI, T., UMEGAKI, M. & YOSHIMINE, T. 2014. Primary olfactory mucosal cells promote axonal outgrowth in a three-dimensional assay. *J. Neurosci. Res.,* 92**,** 847-855.

ISHII, K., NAKAMURA, M., DAI, H., FINN, T. P., OKANO, H., TOYAMA, Y. & BREGMAN, B. S. 2006. Neutralization of ciliary neurotrophic factor reduces astrocyte production from transplanted neural stem cells and promotes regeneration of corticospinal tract fibers in spinal cord injury. *J. Neurosci. Res.,* 84**,** 1669-1681.

JAHED, A., ROWLAND, J. W., MCDONALD, T., BOYD, J. G., DOUCETTE, R. & KAWAJA, M. D. 2007. Olfactory ensheathing cells express smooth muscle α-actin in vitro and in vivo. *Journal of Comparative Neurology,* 503**,** 209-223.

JANI, H. R. & RAISMAN, G. 2004. Ensheathing cell cultures from the olfactory bulb and mucosa. *Glia,* 47**,** 130-7.

JIANG, J. X., CHOI, R. C., SIOW, N. L., LEE, H. H., WAN, D. C. & TSIM, K. W. 2003. Muscle Induces Neuronal Expression of Acetylcholinesterase in Neuron-Muscle Co-culture TRANSCRIPTIONAL REGULATION MEDIATED BY cAMP-DEPENDENT SIGNALING. *Journal of Biological Chemistry,* 278**,** 45435-45444.

JIN, X., CHEN, Z., LIU, X., LIANG, B., ZHANG, H. & ZHANG, Z. 2014. The expression of endothelial barrier antigen (EBA) and S100B in the rat parietal cortex following brain irradiation. *Brain Res.,* 1558**,** 84-89.

JIN, Y., FISCHER, I., TESSLER, A. & HOULE, J. D. 2002. Transplants of Fibroblasts Genetically Modified to Express BDNF Promote Axonal Regeneration from Supraspinal Neurons Following Chronic Spinal Cord Injury. *Experimental Neurology,* 177**,** 265-275.

JOSVAY, K., WINTER, Z., KATONA, R. L., PECZE, L., MARTON, A., BUHALA, A., SZAKONYI, G., OLAH, Z. & VIZLER, C. 2014. Besides neuro-imaging, the Thy1-YFP mouse could serve for visualizing experimental tumours, inflammation and wound-healing. *Sci. Rep.,* 4**,** 6776.

KACHRAMANOGLOU, C., LAW, S., ANDREWS, P., LI, D. & CHOI, D. 2013. Culture of Olfactory Ensheathing Cells for Central Nerve Repair: The Limitations and Potential of Endoscopic Olfactory Mucosal Biopsy. *Neurosurgery,* 72**,** 170-178.

KANG, K. N., KIM, D. Y., YOON, S. M., LEE, J. Y., LEE, B. N., KWON, J. S., SEO, H. W., LEE, I. W., SHIN, H. C., KIM, Y. M., KIM, H. S., KIM, J. H., MIN, B. H., LEE, H. B. & KIM, M. S. 2012. Tissue engineered regeneration of completely transected spinal cord using human mesenchymal stem cells. *Biomaterials,* 33**,** 4828-4835.

KAWAJA, M. D., BOYD, J. G., SMITHSON, L. J., JAHED, A. & DOUCETTE, R. 2009. Technical strategies to isolate olfactory ensheathing cells for intraspinal implantation. *J Neurotrauma,* 26**,** 155-77.

KENDALL, S. E., GOLDHAWK, D. E., KUBU, C., BARKER, P. A. & VERDI, J. M. 2002. Expression analysis of a novel p75NTR signaling protein, which regulates cell cycle progression and apoptosis. *Mechanisms of Development,* 117**,** 187-200.

KEYVAN-FOULADI, N., LI, Y. & RAISMAN, G. 2002. How do transplanted olfactory ensheathing cells restore function? *Brain Res Brain Res Rev,* 40**,** 325-7.

KEYVAN-FOULADI, N., RAISMAN, G. & LI, Y. 2003. Functional repair of the corticospinal tract by delayed transplantation of olfactory ensheathing cells in adult rats. *J. Neurosci.,* 23**,** 9428-9434.

KIGERL, K. A., DE RIVERO VACCARI, J. P., DIETRICH, W. D., POPOVICH, P. G. & KEANE, R. W. 2014. Pattern recognition receptors and central nervous system repair. *Experimental Neurology,* 258**,** 5-16.

KIM, H.-S., JUN SONG, X., DE PAIVA, C. S., CHEN, Z., PFLUGFELDER, S. C. & LI, D.-Q. 2004. Phenotypic characterization of human corneal epithelial cells expanded ex vivo from limbal explant and single cell cultures. *Experimental Eye Research,* 79**,** 41-49.

KIM, T.-H., LI, F., FERREIRO-NEIRA, I., HO, L.-L., LUYTEN, A., NALAPAREDDY, K., LONG, H., VERZI, M. & SHIVDASANI, R. A. 2014. Broadly permissive intestinal chromatin underlies lateral inhibition and cell plasticity. *Nature,* 506**,** 511-515.

KISSELBACH, L., MERGES, M., BOSSIE, A. & BOYD, A. 2009. CD90 Expression on human primary cells and elimination of contaminating fibroblasts from cell cultures. *Cytotechnology,* 59**,** 31-44.

KLEE, W. A. & NIRENBERG, M. 1974. A Neuroblastoma × Glioma Hybrid Cell Line with Morphine Receptors. *Proceedings of the National Academy of Sciences,* 71**,** 3474-3477.

KOZAK, L. P., EPPIG, J. J., DAHL, D. & BIGNAMI, A. 1978. Enhanced neuronal expression in reaggregating cells of mouse cerebellum cultured in the presence of poly-L-lysine. *Dev. Biol.,* 64**,** 252-64.

KRUDEWIG, C., DESCHL, U. & WEWETZER, K. 2006. Purification and in vitro characterization of adult canine olfactory ensheathing cells. *Cell Tissue Res.,* 326**,** 687-696.

KUEH, J. L.-L., RAISMAN, G., LI, Y., STEVENS, R. & LI, D. 2011. Comparison of bulbar and mucosal olfactory ensheathing cells using FACS and simultaneous antigenic bivariate cell cycle analysis. *Glia,* 59**,** 1658-1671.

KUHN, T. B., SCHMIDT, M. F. & KATER, S. B. 1995. Laminin and Fibronectin Guideposts signal sustained but opposite effects to passing growth cones. *Neuron,* 14**,** 275-85.

LAI, P.-L., NAIDU, M., SABARATNAM, V., KAH HUI, W., DAVID, P., KUPPUSAMY, U. R., ABDULLAH, N. & ABD MALEK, S. N. 2013. *Neurotrophic Properties of the Lion's Mane Medicinal Mushroom, Hericium erinaceus (Higher Basidiomycetes) from Malaysia*.

LAKATOS, A., SMITH, P. M., BARNETT, S. C. & FRANKLIN, R. J. M. 2003. Meningeal cells enhance limited CNS remyelination by transplanted olfactory ensheathing cells. *Brain,* 126**,** 598-609.

LEE, M. K., TUTTLE, J. B., REBHUN, L. I., CLEVELAND, D. W. & FRANKFURTER, A. 1990. The expression and posttranslational modification of a neuron-specific β-tubulin isotype during chick embryogenesis. *Cell Motil. Cytoskeleton,* 17**,** 118-32.

LEHMANN, M., FOURNIER, A., SELLES-NAVARRO, I., DERGHAM, P., SEBOK, A., LECLERC, N., TIGYI, G. & MCKERRACHER, L. 1999. Inactivation of Rho signaling pathway promotes CNS axon regeneration. *J. Neurosci.,* 19**,** 7537-7547.

LEVITAN, I. B. & KACZMAREK, L. K. 2015. *The neuron : cell and molecular biology*, New York : Oxford University Press.

LI, X., LIU, S., ZHAO, Y., LI, J., DING, W., HAN, S., CHEN, B., XIAO, Z. & DAI, J. 2016. Training Neural Stem Cells on Functional Collagen Scaffolds for Severe Spinal Cord Injury Repair. *Adv. Funct. Mater.,* 26**,** 5835-5847.

LI, Y., DECHERCHI, P. & RAISMAN, G. 2003a. Transplantation of olfactory ensheathing cells into spinal cord lesions restores breathing and climbing. *J. Neurosci.,* 23**,** 727-731.

LI, Y., FIELD, P. M. & RAISMAN, G. 1997. Repair of adult rat corticospinal tract by transplants of olfactory ensheathing cells. *Science (Washington, D. C.),* 277**,** 2000-2002.

LI, Y., FIELD, P. M. & RAISMAN, G. 1998. Regeneration of adult rat corticospinal axons induced by transplanted olfactory ensheathing cells. *J. Neurosci.,* 18**,** 10514-10524.

LI, Y., FIELD, P. M. & RAISMAN, G. 2005. Olfactory ensheathing cells and olfactory nerve fibroblasts maintain continuous open channels for regrowth of olfactory nerve fibres. *Glia,* 52**,** 245-51.

LI, Y. & RAISMAN, G. 1994. Schwann cells induce sprouting in motor and sensory axons in the adult rat spinal cord. *J Neurosci,* 14**,** 4050-63.

LI, Y., SAUVE, Y., LI, D., LUND, R. D. & RAISMAN, G. 2003b. Transplanted olfactory ensheathing cells promote regeneration of cut adult rat optic nerve axons. *J. Neurosci.,* 23**,** 7783-7788.

LIESI, P., DAHL, D. & VAHERI, A. 1984. Neurons cultured from developing rat brain attach and spread preferentially to laminin. *J. Neurosci. Res.,* 11**,** 241-51.

LIMA, C., PRATAS-VITAL, J., ESCADA, P., HASSE-FERREIRA, A., CAPUCHO, C. & PEDUZZI, J. D. 2006. Olfactory Mucosa Autografts in Human Spinal Cord Injury: A Pilot Clinical Study. *The Journal of Spinal Cord Medicine,* 29**,** 191-203.

LIU, Y., TAN, B., WANG, L., LONG, Z., LI, Y., LIAO, W. & WU, Y. 2015. Endogenous neural stem cells in central canal of adult rats acquired limited ability to differentiate into neurons following mild spinal cord injury. *Int. J. Clin. Exp. Pathol.,* 8**,** 3835-3842.

LIU, Y., TENG, X., YANG, X., SONG, Q., LU, R., XIONG, J., LIU, B., ZENG, N., ZENG, Y., LONG, J., CAO, R., LIN, Y., HE, Q., CHEN, P., LU, M. & LIANG, S. 2010. Shotgun proteomics and network analysis between plasma membrane and extracellular matrix proteins from rat olfactory ensheathing cells. *Cell Transplant,* 19**,** 133-46.

LOZANO, A. M., SCHMIDT, M. & ROACH, A. 1995. A convenient in vitro assay for the inhibition of neurite outgrowth by adult mammalian CNS myelin using immortalized neuronal cells. *Journal of Neuroscience Methods,* 63**,** 23-28.

LU, P., JONES, L. L., SNYDER, E. Y. & TUSZYNSKI, M. H. 2003. Neural stem cells constitutively secrete neurotrophic factors and promote extensive host axonal growth after spinal cord injury. *Exp. Neurol.,* 181**,** 115-129.

LU, P. J., L.L., TUSZYNSKI, M.H. 2005. BDNF-expressing marrow stromal cells support extensive axonal growth at sites of spinal cord injury. *Experimental Neurology,* 191**,** 344-360.

LU, P. J., L.L., TUSZYNSKI, M.H. 2007. Axon regeneration through scars and into sites of chronic spinal cord injury. *Experimental Neurology,* 203**,** 8-21.

LU, R., BIAN, F., LIN, J., SU, Z., QU, Y., PFLUGFELDER, S. C. & LI, D.-Q. 2012. Identification of human fibroblast cell lines as a feeder layer for human corneal epithelial regeneration. *PLoS One,* 7**,** e38825.

MACKAY-SIM, A. & CHUAH, M. I. 2000. Neurotrophic factors in the primary olfactory pathway. *Progress in Neurobiology,* 62**,** 527-559.

MAHAPATRA, S., MEHTA, H., WOO, S. B. & NEET, K. E. 2009. Identification of critical residues within the conserved and specificity patches of nerve growth factor leading to survival or differentiation. *J Biol Chem,* 284**,** 33600-13.

MARTIN-ZANCA, D., HUGHES, S. H. & BARBACID, M. 1986. A human oncogene formed by the fusion of truncated tropomyosin and protein tyrosine kinase sequences. *Nature (London),* 319**,** 743-8.

MAYNARD, F. M., BRACKEN, M. B., CREASEY, G., DITUNNO, J. F., DONOVAN, W. H., DUCKER, T. B., GARBER, S. L., MARINO, R. J., STOVER, S. L. & TATOR, C. H. 1997. International standards for neurological and functional classification of spinal cord injury. *Spinal cord,* 35**,** 266-274.

MCINTYRE, A. B. & CLELAND, T. A. 2016. Biophysical constraints on lateral inhibition in the olfactory bulb. *Journal of neurophysiology,* 115**,** 2937-2949.

MCTIGUE, D. M., HORNER, P. J., STOKES, B. T. & GAGE, F. H. 1998. Neurotrophin-3 and brain-derived neurotrophic factor induce oligodendrocyte proliferation and myelination of regenerating axons in the contused adult rat spinal cord. *J. Neurosci.,* 18**,** 5354-5365.

MEIJERING, E., JACOB, M., SARRIA, J. C., STEINER, P., HIRLING, H. & UNSER, M. 2004. Design and validation of a tool for neurite tracing and analysis in fluorescence microscopy images. *Cytometry Part A,* 58**,** 167-176.

MELO, F. R., BRESSAN, R. B., FORNER, S., MARTINI, A. C., RODE, M., DELBEN, P. B., RAE, G. A., FIGUEIREDO, C. P. & TRENTIN, A. G. 2017. Transplantation of Human Skin-Derived Mesenchymal Stromal Cells Improves Locomotor Recovery After Spinal Cord Injury in Rats. *Cellular and Molecular Neurobiology,* 37**,** 941-947.

MENAGER, C., ARIMURA, N., FUKATA, Y. & KAIBUCHI, K. 2004. PIP3 is involved in neuronal polarization and axon formation. *J Neurochem,* 89**,** 109-18.

MENEZES, K., NASCIMENTO, M. A., GONCALVES, J. P., CRUZ, A. S., LOPES, D. V., CURZIO, B., BONAMINO, M., LACERDA DE MENEZES, J. R., BOROJEVIC, R., ROSSI, M. I. D. & COELHO-SAMPAIO, T. 2014. Human mesenchymal cells from adipose tissue deposit

laminin and promote regeneration of injured spinal cord in rats. *PLoS One,* 9**,** e96020/1-e96020/15, 15 pp.
MICHEL, M. C., WIELAND, T. & TSUJIMOTO, G. 2009. How reliable are G-protein-coupled receptor antibodies? *Naunyn-Schmiedeberg's Archives of Pharmacology,* 379**,** 385-388.
MILLER, S. R., PERERA, S. N., BENITO, C., STOTT, S. R. W. & BAKER, C. V. H. 2016. Evidence for a Notch1-mediated transition during olfactory ensheathing cell development. *Journal of Anatomy,* 229**,** 369-383.
MILTENYI, S., MÜLLER, W., WEICHEL, W. & RADBRUCH, A. 1990. High gradient magnetic cell separation with MACS. *Cytometry,* 11**,** 231-238.
MIRONOV, V., VISCONTI, R. P. & MARKWALD, R. R. 2004. What is regenerative medicine? Emergence of applied stem cell and developmental biology. *Expert Opin Biol Ther,* 4**,** 773-81.
MIRSKY, R., JESSEN, K. R., BRENNAN, A., PARKINSON, D., DONG, Z., MEIER, C., PARMANTIER, E. & LAWSON, D. 2002. Schwann cells as regulators of nerve development. *Journal of Physiology-Paris,* 96**,** 17-24.
MITCHELL, P., HANSON, J., QUETS-NGUYEN, A., BERGERON, M. & SMITH, R. 2007. A quantitative method for analysis of in vitro neurite outgrowth. *Journal of neuroscience methods,* 164**,** 350-362.
MORRISON, E. E. & COSTANZO, R. M. 1992. Morphology of olfactory epithelium in humans and other vertebrates. *Microsc Res Tech,* 23**,** 49-61.
MOTHE, A. J. & TATOR, C. H. 2013. Review of transplantation of neural stem/progenitor cells for spinal cord injury. *International Journal of Developmental Neuroscience,* 31**,** 701-713.
NAMIKI, J., KOJIMA, A. & TATOR, C. H. 2000. Effect of brain-derived neurotrophic factor, nerve growth factor, and neurotrophin-3 on functional recovery and regeneration after spinal cord injury in adult rats. *J Neurotrauma,* 17**,** 1219-31.
NASH, H. H., BORKE, R. C. & ANDERS, J. J. 2001. New method of purification for establishing primary cultures of ensheathing cells from the adult olfactory bulb. *Glia,* 34**,** 81-7.
NASH, H. H., BORKE, R. C. & ANDERS, J. J. 2002. Ensheathing cells and methylprednisolone promote axonal regeneration and functional recovery in the lesioned adult rat spinal cord. *J. Neurosci.,* 22**,** 7111-7120.
NATIONAL SPINAL CORD INJURY CENTER 2006. National Spinal Cord Injury Statistical Center Fact Sheet.
NIAPOUR, A., KARAMALI, F., KARBALAIE, K., KIANI, A., MARDANI, M., NASR-ESFAHANI, M. H. & BAHARVAND, H. 2010. Novel method to obtain highly enriched cultures of adult rat Schwann cells. *Biotechnol. Lett.,* 32**,** 781-786.
NIKOLAOU, N., WATANABE-ASAKA, T., GERETY, S., DISTEL, M., KOSTER, R. W. & WILKINSON, D. G. 2009. Lunatic fringe promotes the lateral inhibition of neurogenesis. *Development (Cambridge, U. K.),* 136**,** 2523-2533.
NOE, M. 1972. The Calculation of Distributions of Two-Sided Kolmogorov-Smirnov Type Statistics. *The Annals of Mathematical Statistics,* 43**,** 58-64.
NOVIKOVA, L. N., LOBOV, S., WIBERG, M. & NOVIKOV, L. N. 2011. Efficacy of olfactory ensheathing cells to support regeneration after spinal cord injury is influenced by method of culture preparation. *Experimental Neurology,* 229**,** 132-142.
O'LEARY, M. T. & BLAKEMORE, W. F. 1997. Oligodendrocyte precursors survive poorly and do not migrate following transplantation into the normal adult central nervous system. *Journal of Neuroscience Research,* 48**,** 159-167.
O'MALLEY, A. M., SHANLEY, D. K., KELLY, A. T. & BARRY, D. S. 2014. Towards an understanding of semaphorin signalling in the spinal cord. *Gene,* 553**,** 69-74.

OMAR, M., BOCK, P., KREUTZER, R., ZIEGE, S., IMBSCHWEILER, I., HANSMANN, F., PECK, C.-T., BAUMGAERTNER, W. & WEWETZER, K. 2011. Defining the morphological phenotype: 2',3'-cyclic nucleotide 3'-phosphodiesterase (CNPase) is a novel marker for in situ detection of canine but not rat olfactory ensheathing cells. *Cell Tissue Res.,* 344**,** 391-405.

OMAR, M., HANSMANN, F., KREUTZER, R., KREUTZER, M., BRANDES, G. & WEWETZER, K. 2013. Cell Type- and Isotype-Specific Expression and Regulation of β-Tubulins in Primary Olfactory Ensheathing Cells and Schwann Cells In Vitro. *Neurochem. Res.,* 38**,** 981-988.

OPRYCH, K., COTFAS, D., CHOI, D. & CHOI, D. 2016. Common olfactory ensheathing glial markers in the developing human olfactory system. *Brain Struct Funct*.

ORBAY, H., LITTLE, C. J., LANKFORD, L., OLSON, C. A. & SAHAR, D. E. 2015. The Key Components of Schwann Cell-like Differentiation Medium and their Effects on Gene Expression Pattern of Adipose-Derived Stem Cells. *Ann. Plast. Surg.,* 74**,** 584-588.

PARK, W. B., KIM, S. Y., LEE, S. H., KIM, H.-W., PARK, J.-S. & HYUN, J. K. 2010. The effect of mesenchymal stem cell transplantation on the recovery of bladder and hindlimb function after spinal cord contusion in rats. *BMC Neuroscience,* 11**,** 119.

PELLITTERI, R., SPATUZZA, M., STANZANI, S. & ZACCHEO, D. 2010. Biomarkers expression in rat olfactory ensheathing cells. *Front Biosci (Schol Ed),* 2**,** 289-98.

PETERSEN, M. J., KAPLAN, J., JORGENSEN, C. M., SCHMIDT, L. A., LI, L., MORGAN, J. R., KWAN, M. K. & KRUEGER, G. G. 1995. Sustained production of human transferrin by transduced fibroblasts implanted into athymic mice: A model for somatic gene therapy. *J. Invest. Dermatol.,* 104**,** 171-6.

PIXLEY, S. K. 1992. The olfactory nerve contains two populations of glia, identified both in vivo and in vitro. *Glia,* 5**,** 269-84.

PIZZI, M. A. & CROWE, M. J. 2006. Transplantation of fibroblasts that overexpress matrix metalloproteinase-3 into the site of spinal cord injury in rats. *J Neurotrauma,* 23**,** 1750-65.

POLLOCK, K., STROEMER, P., PATEL, S., STEVANATO, L., HOPE, A., MILJAN, E., DONG, Z., HODGES, H., PRICE, J. & SINDEN, J. D. 2006. A conditionally immortal clonal stem cell line from human cortical neuroepithelium for the treatment of ischemic stroke. *Experimental Neurology,* 199**,** 143-155.

PRASAD, B. M., HOLLINS, B. & LAMBERT, N. A. 2010. Methods to detect cell surface expression and constitutive activity of GPR6. *Methods in enzymology,* 484**,** 179-195.

PROWSE, A. B. J., MCQUADE, L. R., BRYANT, K. J., MARCAL, H. & GRAY, P. P. 2007. Identification of Potential Pluripotency Determinants for Human Embryonic Stem Cells Following Proteomic Analysis of Human and Mouse Fibroblast Conditioned Media. *J. Proteome Res.,* 6**,** 3796-3807.

PUGDEE, K., SHIBATA, Y., YAMAMICHI, N., TSUTSUMI, H., YOSHINARI, M., ABIKO, Y. & HAYAKAWA, T. 2007. Gene expression of MC3T3-E1 cells on fibronectin-immobilized titanium using tresyl chloride activation technique. *Dental materials journal,* 26**,** 647-655.

RADTKE, C., AKIYAMA, Y., BROKAW, J., LANKFORD, K. L., WEWETZER, K., FODOR, W. L. & KOCSIS, J. D. 2004. Remyelination of the nonhuman primate spinal cord by transplantation of H-transferase transgenic adult pig olfactory ensheathing cells. *FASEB J.,* 18**,** 335-337, 10.1096/fj.03-0214fje.

RADTKE, C., LANKFORD, K. L., WEWETZER, K., IMAIZUMI, T., FODOR, W. L. & KOCSIS, J. D. 2010. Impaired spinal cord remyelination by long-term cultured adult porcine olfactory ensheathing cells correlates with altered in vitro phenotypic properties. *Xenotransplantation,* 17**,** 71-80.

RAISMAN, G. 2007. Repair of spinal cord injury by transplantation of olfactory ensheathing cells. *Comptes Rendus Biologies,* 330**,** 557-560.
RAISMAN, G., CARLSTEDT, T., CHOI, D. & LI, Y. 2011. Clinical prospects for transplantation of OECs in the repair of brachial and lumbosacral plexus injuries: opening a door. *Exp Neurol,* 229**,** 168-73.
RAISMAN, G. & LI, Y. 2007. Repair of neural pathways by olfactory ensheathing cells. *Nat. Rev. Neurosci.,* 8**,** 312-319.
RAMER, L. M., AU, E., RICHTER, M. W., LIU, J., TETZLAFF, W. & ROSKAMS, A. J. 2004. Peripheral olfactory ensheathing cells reduce scar and cavity formation and promote regeneration after spinal cord injury. *The Journal of Comparative Neurology,* 473**,** 1-15.
RAMER, L. M., RAMER, M. S. & STEEVES, J. D. 2005. Setting the stage for functional repair of spinal cord injuries: a cast of thousands. *Spinal Cord,* 43**,** 134-61.
RAMÓN-CUETO, A. & AVILA, J. 1998. Olfactory ensheathing glia: properties and function. *Brain Research Bulletin,* 46**,** 175-187.
RAMÓN-CUETO, A., CORDERO, M. I., SANTOS-BENITO, F. F. & AVILA, J. 2000. Functional Recovery of Paraplegic Rats and Motor Axon Regeneration in Their Spinal Cords by Olfactory Ensheathing Glia. *Neuron,* 25**,** 425-435.
RAMÓN-CUETO, A. & NIETO-SAMPEDRO, M. 1992. Glial cells from adult rat olfactory bulb: Immunocytochemical properties of pure cultures of ensheathing cells. *Neuroscience,* 47**,** 213-220.
RAMON-CUETO, A., PEREZ, J. & NIETO-SAMPEDRO, M. 1993. In vitro enfolding of olfactory neurites by p75 NGF receptor positive ensheathing cells from adult rat olfactory bulb. *Eur J Neurosci,* 5**,** 1172-80.
RAVASI, M., SCUTERI, A., PASINI, S., BOSSI, M., RODRIGUEZ MENENDEZ, V., MAGGIONI, D. & TREDICI, G. 2013. Undifferentiated MSCs are able to myelinate DRG neuron processes through p75. *Exp. Cell Res.,* 319**,** 2989-2999.
RAYNALD, LI, Y., YU, H., HUANG, H., GUO, M., HUA, R., JIANG, F., ZHANG, K., LI, H., WANG, F., LI, L., CUI, F. Z. & AN, Y. 2016. The hetero-transplantation of human bone marrow stromal cells carried by hydrogel unexpectedly demonstrates a significant role in the functional recovery in the injured spinal cord of rats. *Brain Res.,* 1634**,** 21-33.
RICHARDS, M., FONG, C.-Y., CHAN, W.-K., WONG, P.-C. & BONGSO, A. 2002. Human feeders support prolonged undifferentiated growth of human inner cell masses and embryonic stem cells. *Nat. Biotechnol.,* 20**,** 933-936.
RICHTER, M. W., FLETCHER, P. A., LIU, J., TETZLAFF, W. & ROSKAMS, A. J. 2005. Lamina propria and olfactory bulb ensheathing cells exhibit differential integration and migration and promote differential axon sprouting in the lesioned spinal cord. *J. Neurosci.,* 25**,** 10700-10711.
ROCKEY, D. C., WEYMOUTH, N. & SHI, Z. 2013. Smooth muscle α actin (Acta2) and myofibroblast function during hepatic wound healing. *PloS one,* 8**,** e77166.
RODRIGUEZ, J. P., COULTER, M., MIOTKE, J., MEYER, R. L., TAKEMARU, K. I. & LEVINE, J. M. 2014. Abrogation of β-Catenin signaling in oligodendrocyte precursor cells reduces glial scarring and promotes axon regeneration after CNS injury. *Journal of Neuroscience,* 34**,** 10285-10297.
ROLOFF, F., ZIEGE, S., BAUMGARTNER, W., WEWETZER, K. & BICKER, G. 2013. Schwann cell-free adult canine olfactory ensheathing cell preparations from olfactory bulb and mucosa display differential migratory and neurite growth-promoting properties in vitro. *BMC Neuroscience,* 14**,** 141.

RONAGHI, M., ERCEG, S., MORENO-MANZANO, V. & STOJKOVIC, M. 2010. Challenges of stem cell therapy for spinal cord injury: human embryonic stem cells, endogenous neural stem cells, or induced pluripotent stem cells? *Stem Cells,* 28**,** 93-9.

ROSSI, S. L., NISTOR, G., WYATT, T., YIN, H. Z., POOLE, A. J., WEISS, J. H., GARDENER, M. J., DIJKSTRA, S., FISCHER, D. F. & KEIRSTEAD, H. S. 2010. Histological and functional benefit following transplantation of motor neuron progenitors to the injured rat spinal cord. *PloS one,* 5**,** e11852.

RUBIN, H. 1966. A substance in conditioned medium which enhances the growth of small numbers of chick embryo cells. *Experimental Cell Research,* 41**,** 138-148.

RUBIO, M.-P., MUNOZ-QUILES, C. & RAMON-CUETO, A. 2008. Adult olfactory bulbs from primates provide reliable ensheathing glia for cell therapy. *Glia,* 56**,** 539-51.

RUITENBERG, M. J., VUKOVIC, J., SARICH, J., BUSFIELD, S. J. & PLANT, G. W. 2006. Olfactory Ensheathing Cells: Characteristics, Genetic Engineering, and Therapeutic Potential. *Journal of Neurotrauma,* 23**,** 468-478.

SAALBACH, A., WETZEL, A., HAUSTEIN, U.-F., STICHERLING, M., SIMON, J. C. & ANDEREGG, U. 2005. Interaction of human Thy-1 (CD 90) with the integrin αvβ3 (CD51/CD61): an important mechanism mediating melanoma cell adhesion to activated endothelium. *Oncogene,* 24**,** 4710-4720.

SAKAMOTO, K. & KADOMATSU, K. 2017. Mechanisms of axon regeneration: The significance of proteoglycans. *Biochimica et Biophysica Acta (BBA) - General Subjects*.

SANCHO, R., CREMONA, C. A. & BEHRENS, A. 2015. Stem cell and progenitor fate in the mammalian intestine: Notch and lateral inhibition in homeostasis and disease. *EMBO Rep.,* 16**,** 571-581.

SANDRIN, V. & COSSET, F.-L. 2006. Intracellular versus cell surface assembly of retroviral pseudotypes is determined by the cellular localization of the viral glycoprotein, its capacity to interact with Gag, and the expression of the Nef protein. *Journal of Biological Chemistry,* 281**,** 528-542.

SEKHON, L. H. & FEHLINGS, M. G. 2001. Epidemiology, demographics, and pathophysiology of acute spinal cord injury. *Spine (Phila Pa 1976),* 26**,** S2-12.

SETOGUCHI, T., NAKASHIMA, K., TAKIZAWA, T., YANAGISAWA, M., OCHIAI, W., OKABE, M., YONE, K., KOMIYA, S. & TAGA, T. 2004. Treatment of spinal cord injury by transplantation of fetal neural precursor cells engineered to express BMP inhibitor. *Experimental Neurology,* 189**,** 33-44.

SHAFFER, J. P. 1995. Multiple hypothesis testing. *Annual review of psychology,* 46**,** 561.

SIDDIQUE, R. & THAKOR, N. 2014. Investigation of nerve injury through microfluidic devices. *Journal of The Royal Society Interface,* 11**,** 20130676.

SIMON, C., ESCOBEDO, C., VALBUENA, D., GENBACEV, O., GALAN, A., KRTOLICA, A., ASENSI, A., SANCHEZ, E., ESPLUGUES, J., FISHER, S. & PELLICER, A. 2005. First derivation in Spain of human embryonic stem cell lines: use of long-term cryopreserved embryos and animal-free conditions. *Fertil Steril,* 83**,** 246-9.

SIMPSON, P. B., BACHA, J. I., PALFREYMAN, E. L., WOOLLACOTT, A. J., MCKERNAN, R. M. & KERBY, J. 2001. Retinoic acid-evoked differentiation of neuroblastoma cells predominates over growth factor stimulation: an automated image capture and quantitation approach to neuritogenesis. *Anal. Biochem.,* 298**,** 163-169.

SKALLI, O., PELTE, M. F., PECLET, M. C., GABBIANI, G., GUGLIOTTA, P., BUSSOLATI, G., RAVAZZOLA, M. & ORCI, L. 1989. Alpha-smooth muscle actin, a differentiation marker of smooth muscle cells, is present in microfilamentous bundles of pericytes. *Journal of Histochemistry & Cytochemistry,* 37**,** 315-321.

SMITH, P. M., LAKATOS, A., BARNETT, S. C., JEFFERY, N. D. & FRANKLIN, R. J. M. 2002. Cryopreserved Cells Isolated from the Adult Canine Olfactory Bulb Are Capable of

Extensive Remyelination Following Transplantation into the Adult Rat CNS. *Experimental Neurology,* 176**,** 402-406.

SOFRONIEW, M. V. 2005. Reactive astrocytes in neural repair and protection. *Neuroscientist,* 11**,** 400-407.

SON, Y.-J., TRACHTENBERG, J. T. & THOMPSON, W. J. 1996. Schwann cells induce and guide sprouting and reinnervation of neuromuscular junctions. *Trends in Neurosciences,* 19**,** 280-285.

SONIGRA, R. J., BRIGHTON, P. C., JACOBY, J., HALL, S. & WIGLEY, C. B. 1999. Adult rat olfactory nerve ensheathing cells are effective promoters of adult central nervous system neurite outgrowth in coculture. *Glia,* 25**,** 256-69.

STEINER, J., BERNSTEIN, H.-G., BIELAU, H., BERNDT, A., BRISCH, R., MAWRIN, C., KEILHOFF, G. & BOGERTS, B. 2007. Evidence for a wide extra-astrocytic distribution of S100B in human brain. *BMC Neuroscience,* 8**,** 2.

STEPHENS, P., GENEVER, P. G., WOOD, E. J. & RAXWORTHY, M. J. 1997. Integrin receptor involvement in actin cable formation in an in vitro model of events associated with wound contraction. *The International Journal of Biochemistry & Cell Biology,* 29**,** 121-128.

TABAKOW, P., JARMUNDOWICZ, W., CZAPIGA, B., FORTUNA, W., MIEDZYBRODZKI, R., CZYZ, M., HUBER, J., SZAREK, D., OKUROWSKI, S., SZEWCZYK, P., GORSKI, A. & RAISMAN, G. 2013. Transplantation of Autologous Olfactory Ensheathing Cells in Complete Human Spinal Cord Injury. *Cell Transplantation,* 22**,** 1591-1612.

TABAKOW, P., RAISMAN, G., FORTUNA, W., CZYZ, M., HUBER, J., LI, D., SZEWCZYK, P., OKUROWSKI, S., MIEDZYBRODZKI, R., CZAPIGA, B., SALOMON, B., HALON, A., LI, Y., LIPIEC, J., KULCZYK, A. & JARMUNDOWICZ, W. 2014. Functional Regeneration of Supraspinal Connections in a Patient With Transected Spinal Cord Following Transplantation of Bulbar Olfactory Ensheathing Cells With Peripheral Nerve Bridging. *Cell Transplantation,* 23**,** 1631-1655.

TECHANGAMSUWAN, S., KREUTZER, R., KREUTZER, M., IMBSCHWEILER, I., ROHN, K., WEWETZER, K. & BAUMGAERTNER, W. 2009. Transfection of adult canine Schwann cells and olfactory ensheathing cells at early and late passage with human TERT differentially affects growth factor responsiveness and in vitro growth. *J. Neurosci. Methods,* 176**,** 112-120.

TENG, X., NAGATA, I., LI, H.-P., KIMURA-KURODA, J., SANGO, K., KAWAMURA, K., RAISMAN, G. & KAWANO, H. 2008. Regeneration of nigrostriatal dopaminergic axons after transplantation of olfactory ensheathing cells and fibroblasts prevents fibrotic scar formation at the lesion site. *J. Neurosci. Res.,* 86**,** 3140-3150.

TETZLAFF, W., OKON, E. B., KARIMI-ABDOLREZAEE, S., HILL, C. E., SPARLING, J. S., PLEMEL, J. R., PLUNET, W. T., TSAI, E. C., BAPTISTE, D., SMITHSON, L. J., KAWAJA, M. D., FEHLINGS, M. G. & KWON, B. K. 2011. A systematic review of cellular transplantation therapies for spinal cord injury. *J Neurotrauma,* 28**,** 1611-82.

THURET, S., MOON, L. D. F. & GAGE, F. H. 2006. Therapeutic interventions after spinal cord injury. *Nat. Rev. Neurosci.,* 7**,** 628-643.

TODARO, G. J. & GREEN, H. 1963. QUANTITATIVE STUDIES OF THE GROWTH OF MOUSE EMBRYO CELLS IN CULTURE AND THEIR DEVELOPMENT INTO ESTABLISHED LINES. *The Journal of Cell Biology,* 17**,** 299-313.

TOM, V. J., DOLLER, C. M., MALOUF, A. T. & SILVER, J. 2004. Astrocyte-associated fibronectin is critical for axonal regeneration in adult white matter. *J. Neurosci.,* 24**,** 9282-9290.

TOME, M., SILAJDZIC, E., SANTOS-SILVA, A. & BARNETT, S. C. 2007. Calponin is expressed by subpopulations of connective tissue cells but not olfactory ensheathing cells in the neonatal olfactory mucosa. *BMC Neurosci.,* 8**,** No pp. given.

TONG, L., JI, L., WANG, Z., TONG, X., ZHANG, L. & SUN, X. 2010. Differentiation of neural stem cells into Schwann-like cells in vitro. *Biochemical and Biophysical Research Communications,* 401**,** 592-597.

TORIGOE, K., TANAKA, H.-F., TAKAHASHI, A., AWAYA, A. & HASHIMOTO, K. 1996. Basic Behavior of Migratory Schwann Cells in Peripheral Nerve Regeneration. *Experimental Neurology,* 137**,** 301-308.

ULRICH, R., IMBSCHWEILER, I., KALKUHL, A., LEHMBECKER, A., ZIEGE, S., KEGLER, K., BECKER, K., DESCHL, U., WEWETZER, K. & BAUMGARTNER, W. 2014. Transcriptional profiling predicts overwhelming homology of Schwann cells, olfactory ensheathing cells, and Schwann cell-like glia. *Glia,* 62**,** 1559-81.

VAN DEN POL, A. N. & SANTARELLI, J. G. 2003. Olfactory ensheathing cells: time lapse imaging of cellular interactions, axonal support, rapid morphologic shifts, and mitosis. *J Comp Neurol,* 458**,** 175-94.

VICKLAND, H., WESTRUM, L. E., KOTT, J. N., PATTERSON, S. L. & BOTHWELL, M. A. 1991. Nerve growth factor receptor expression in the young and adult rat olfactory system. *Brain Res.,* 565**,** 269-79.

VINCENT, A. J., WEST, A. K. & CHUAH, M. I. 2005. Morphological and functional plasticity of olfactory ensheathing cells. *J Neurocytol,* 34**,** 65-80.

WALL, I. B., TOLEDO, G. S. & JAT, P. S. 2016. Recent advances in conditional cell immortalization technology. *Cell & Gene Therapy Insights,* 2**,** 391-396.

WALLQUIST, W., PATARROYO, M., THAMS, S., CARLSTEDT, T., STARK, B., CULLHEIM, S. & HAMMARBERG, H. 2002. Laminin chains in rat and human peripheral nerve: distribution and regulation during development and after axonal injury. *J. Comp. Neurol.,* 454**,** 284-293.

WANG, Y. & NI, H. 2016. Fibronectin maintains the balance between hemostasis and thrombosis. *Cell. Mol. Life Sci.,* 73**,** 3265-3277.

WATSON, KAYALIOGLU, G., PAXINOS, G. & WATSON, C. 2008. *Spinal Cord*.

WEI, Y., WANG, N., LU, Q., ZHANG, N., ZHENG, D. & LI, J. 2007. Enhanced protein expressions of sortilin and p75NTR in retina of rat following elevated intraocular pressure-induced retinal ischemia. *Neurosci. Lett.,* 429**,** 169-174.

WEN, X., LIU, L., DENG, M., ZHANG, L., LIU, R., XING, Y., ZHOU, X. & NIE, X. 2012. Characterization of p75+ ectomesenchymal stem cells from rat embryonic facial process tissue. *Biochemical and Biophysical Research Communications,* 427**,** 5-10.

WEWETZER, K., RADTKE, C., KOCSIS, J. & BAUMGARTNER, W. 2011. Species-specific control of cellular proliferation and the impact of large animal models for the use of olfactory ensheathing cells and Schwann cells in spinal cord repair. *Exp Neurol,* 229**,** 80-7.

WILLERTH, S. M. & SAKIYAMA-ELBERT, S. E. 2008. Cell therapy for spinal cord regeneration. *Advanced Drug Delivery Reviews,* 60**,** 263-276.

WOJTOWICZ, A. M., OLIVEIRA, S., CARLSON, M. W., ZAWADZKA, A., ROUSSEAU, C. F. & BAKSH, D. 2014. The importance of both fibroblasts and keratinocytes in a bilayered living cellular construct used in wound healing. *Wound Repair and Regeneration,* 22**,** 246-255.

WOODHALL, E., WEST, A. K. & CHUAH, M. I. 2001. Cultured olfactory ensheathing cells express nerve growth factor, brain-derived neurotrophic factor, glia cell line-derived neurotrophic factor and their receptors. *Molecular Brain Research,* 88**,** 203-213.

WU, J., SONG, W., ZHU, H., NIU, Z., MU, H., LEI, A., YANG, C., PENG, S., LI, X., LI, G. & HUA, J. 2013a. Enrichment and characterization of Thy1-positive male germline stem cells (mGSCs) from dairy goat (Capra hircus) testis using magnetic microbeads. *Theriogenology,* 80**,** 1052-1060.

WU, X., BOLGER, W. E. & ANDERS, J. J. 2013b. Fibroblasts isolated from human middle turbinate mucosa cause neural progenitor cells to differentiate into glial lineage cells. *PLoS One,* 8**,** e76926.

XU, X. M., GUÉNARD, V., KLEITMAN, N., AEBISCHER, P. & BUNGE, M. B. 1995. A Combination of BDNF and NT-3 Promotes Supraspinal Axonal Regeneration into Schwann Cell Grafts in Adult Rat Thoracic Spinal Cord. *Experimental Neurology,* 134**,** 261-272.

YAN, H., BUNGE, M. B., WOOD, P. M. & PLANT, G. W. 2001. Mitogenic response of adult rat olfactory ensheathing glia to four growth factors. *Glia,* 33**,** 334-42.

YANG, H., HE, B. R. & HAO, D. J. 2014. Biological Roles of Olfactory Ensheathing Cells in Facilitating Neural Regeneration: A Systematic Review. *Molecular Neurobiology***,** 1-12.

YOSHIHARA, H., SHUMSKY, J. S., NEUHUBER, B., OTSUKA, T., FISCHER, I. & MURRAY, M. 2006. Combining motor training with transplantation of rat bone marrow stromal cells does not improve repair or recovery in rats with thoracic contusion injuries. *Brain research,* 1119**,** 65-75.

YU, F., HSIEH, W.-S., PETERSSON, F., YANG, H., LI, Y., LI, C., LOW, S. W., LIU, J., YAN, Y., WANG, D.-Y. & LOH, K. S. 2014. Malignant cells derived from 3T3 fibroblast feeder layer in cell culture for nasopharyngeal carcinoma. *Exp. Cell Res.,* 322**,** 193-201.

YUI, S., ITO, D., FUJITA, N. & NISHIMURA, R. 2011. Effects of fibroblasts derived from the olfactory bulb and nasal olfactory mucosa on proliferation of olfactory ensheathing cells harvested from the olfactory bulb. *J Vet Med Sci,* 73**,** 133-7.

ZHANG, M.-L., ZHANG, X.-J., KANG, J., ZHANG, H.-J., CHEN, X.-L., LIU, N., LIU, S.-Q., MA, W.-D., ZHANG, G.-X. & ZHU, L. 2017. Matrine promotes NT3 expression in CNS cells in experimental autoimmune encephalomyelitis. *Neuroscience Letters,* 649**,** 100-106.

ZHOU, H.-L., ZHANG, X.-J., ZHANG, M.-Y., YAN, Z.-J., XU, Z.-M. & XU, R.-X. 2016. Transplantation of Human Amniotic Mesenchymal Stem Cells Promotes Functional Recovery in a Rat Model of Traumatic Spinal Cord Injury. *Neurochemical Research,* 41**,** 2708-2718.

ZIEGE, S., BAUMGARTNER, W. & WEWETZER, K. 2013. Toward defining the regenerative potential of olfactory mucosa: establishment of Schwann cell-free adult canine olfactory ensheathing cell preparations suitable for transplantation. *Cell Transplant,* 22**,** 355-67.

ZOLLINGER, A. J. & SMITH, M. L. 2016. Fibronectin, the extracellular glue. *Matrix Biol.***,** Ahead of Print.

8.0 Appendix One

8.1 Circularity Macro

As described in Section 2.3.2, a macro was written in ImageJ to automate the process to measure the circularity and number of cells in the field. It is written below.

```
//run("Threshold...");
//untick brightness on Threshold
//Adjust brightness on Threshold
//Adjust 'hue' on threshold to get the correct selection
run("Set Measurements...", "area mean standard modal min centroid center perimeter bounding fit shape feret's integrated median skewness kurtosis area_fraction stack redirect=None decimal=3");
run("Analyze Particles...", "size=100-4000 show=Outlines display exclude clear add");
run("Distribution...", "parameter=Circ. automatic");

k= 0;
 while (k<=nResults-1) {
m=getResult("Circ.",k);
print(m);
 k = k + 1;
 }

//log prints off the circularities which can be exported to excel for analysis
//ImageJ prints off its own distribution, which although works, gives different intervals for each image analysed so is
//unsuitable for comparison work
//Roi Manager and the output image allows the circularity of each image to be tracked.
//If the programme is selecting cells which are too small/too large, adjust the line which states size=100-4000 as appropriate
```

8.2 Flow cytometry for LD column

In Section 4.3, LS columns were used to purify the OEC population. According to the recommendation from MACS, an LD column was used to purify the PA7 OEC population. The output from the flow cytometer is visualised in Figure A8.1. This shows the unsuccessful results from the LD column where the population starts at 86.2% Thy1 negative (Figure A8.1B) and after purification is 88.8% Thy1 negative (Figure A8.1C). The population that is supposed to be positive for Thy1 is only 0.3% positive (Figure A8.1D) after the LD purification. In Section 4.3, Figure 4.2 shows that the population can be

successfully purified using LS columns. For this reason, the LS column was used for the experiments described in Chapter 4.

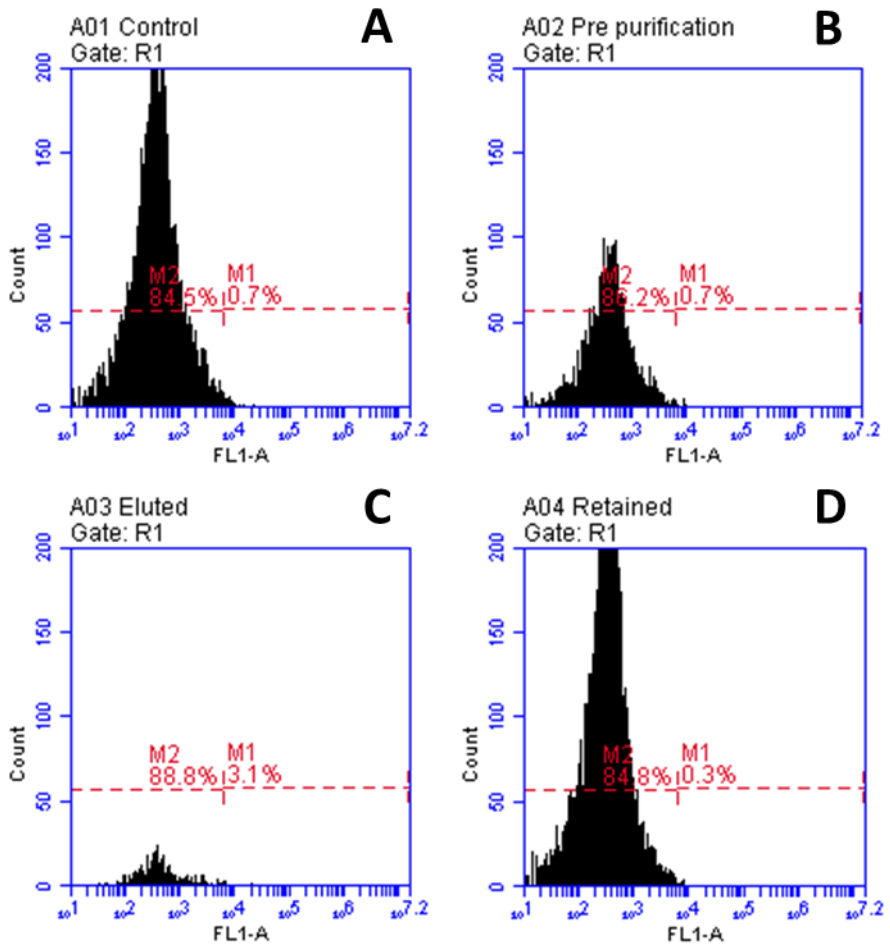

Figure A8.1: Flow cytometry graph output from BD Accuri™ C6 flow cytometer from purification with LD column. The PA7 cell line was purified using an MACS LD column. From the output graphs it can be seen that the Thy1 negative fraction starts at 0.7% positive (B) and increases to 3.1% (C). This is effectively no increase at all and is not an efficient method to decrease the proportion of Thy1 positive cells. From these results, it was decided to continue with the LS column and the purification can be seen to have been successful in Figure 4.2.